PUBLISHER :

Address of Publisher & Editor's Office :

GDAŃSK UNIVERSITY
OF TECHNOLOGY
Faculty
of Ocean Engineering
& Ship Technology

ul. Narutowicza 11/12
80-952 Gdańsk, POLAND
tel.: +48 58 347 13 66
fax : +48 58 341 13 66
e-mail : office.pmr@pg.gda.pl

Account number :
BANK ZACHODNI WBK S.A.
I Oddział w Gdańsku
41 1090 1098 0000 0000 0901 5569

Editorial Staff :
Kazimierz Kempa Editor in Chief
e-mail : kkempa@pg.gda.pl
Przemysław Wierzchowski Scientific Editor
e-mail : e.wierzchowski@chello.pl
Jan Michalski Editor for review matters
e-mail : janmi@pg.gda.pl
Tadeusz Borzęcki Editor for international relations
e-mail : tadbor@pg.gda.pl
Piotr Bzura Managing Editor
e-mail : pbzura@pg.gda.pl
Cezary Spigarski Computer Design
e-mail : biuro@oficynamorska.pl

Domestic price :
single issue : 20 zł

Prices for abroad :
single issue :
- in Europe EURO 15
- overseas US$ 20

ISSN 1233-2585

POLISH MARITIME RESEARCH

in internet

www.bg.pg.gda.pl/pmr/pmr.php

POLISH MARITIME RESEARCH

No 4(58) 2008 Vol 15

CONTENTS

The papers published in this issue have been reviewed by:
Prof. J. Badura ; Prof. A. Balawender ; Prof. A. Brandowski
Prof. M. Hann ; Prof. G. Kosman ; Assoc. Prof. K. Kosowski
Prof. W. Precht ; Prof. I. N. Semenov ; Prof. Z. Walczyk

Editorial

POLISH MARITIME RESEARCH is a scientific journal of worldwide circulation. The journal appears as a quarterly four times a year. The first issue of it was published in September 1994. Its main aim is to present original, innovative scientific ideas and Research & Development achievements in the field of :

Engineering, **Computing & Technology**, **Mechanical Engineering**,

which could find applications in the broad domain of maritime economy. Hence there are published papers which concern methods of the designing, manufacturing and operating processes of such technical objects and devices as : ships, port equipment, ocean engineering units, underwater vehicles and equipment as well as harbour facilities, with accounting for marine environment protection.
The Editors of POLISH MARITIME RESEARCH make also efforts to present problems dealing with education of engineers and scientific and teaching personnel. As a rule, the basic papers are supplemented by information on conferences , important scientific events as well as cooperation in carrying out international scientific research projects.

Scientific Board

POLISH MARITIME RESEARCH 4(58) 2008 Vol 15; pp. 3-11
10.2478/v10012-007-0090-1

Functional model of river-sea ships operating in European system of transport corridors

Part II
Methods of determination of design assumptions for river-sea ships operating in European system of transport corridors, according to their functional model

Magdalena Kaup, Ph. D.
Szczecin University of Technology

ABSTRACT

This paper presents continuation of the research on the functional model of river-sea ships operating in European system of transport corridors. It deals with a set of methods of determination of design assumptions for river-sea ships. Relevant calculations were performed on the basis of a future network of European routes for operating the river-sea ships within EU system of water transport corridors, in which rates of cargo flows and lengths of particular routes as well as their mathematical model were taken into account. In consequence, technical assumptions for designing the fleet of river-sea ships to be operated in European system of water transport corridors, were obtained.

Keywords: European system of transport, river-sea ships, river-sea transport system, water transport

INTRODUCTION

Every floating unit is designed and used to fulfill a shipping task attributed to it. Depending on a given shipping task such shipping strategy, out of various transport possibilities, can be selected which will ensure best features and profits. In Part I (3/2008 PMR) of the paper the graphical and mathematical model for analyzing the functioning of fleet of river-sea ships (shortly marked SRM) was presented. From the investigations a determination model of design assumptions for river-sea ships has been obtained. In this part of the paper are presented results of investigations of the functional model of river-sea ships, performed for the proposed system of European transport corridors.

AREA OF INVESTIGATIONS OF THE FUNCTIONAL MODEL OF RIVER-SEA SHIPS

The first step of proceeding with the functional model is to form databases of:

- ⇨ geography of cargo flows in Europe
- ⇨ geography of waterways and transport corridors intended for river-sea navigation in Europe.

By making use of information on export and import of particular European countries it is possible to elaborate rates and directions of cargo flows realized in the frame of the EU.

In Fig. 1 graphical illustration is presented of cargo flows structure in Europe, which will be used for analysis of the functional model.

To the next database for the functional model, collected information on European inland waterways network and sea routes was introduced. On their basis the future network of European water transport corridors to be used by river-sea ships was elaborated (Fig. 2). On the network today existing connections of inland waterways widened by sea route sections, are shown. Also, are there indicated the lacking connections and those necessary to be extended, which could supplement the existing network after introduction of certain changes to internal and external factors. Moreover, distances between ports in [km] as well as rates of cargo flows running within the network are given in [mln t/year]. The performed analysis showed that rates of the cargo flows possible to be shipped by the SRM fleet constitute 7-10 % of the total rate of cargo flow running along a given route. The SRM fleet effectiveness will be respectively higher at greater cargo flow rates. Some cargo flows have been attributed to river-sea routes by shifting them from other transport branches in compliance with EU policy guidelines for the transport services sector.

Only one, the most representative port of each country was indicated on the map because the rates of cargo flows were elaborated by using the data distinguished only by the names of the countries, with the exception of Poland, Slovakia

and Germany for which also the lacking connections very important for further development of the countries, were shown.

Fig. 1. Directions and rates of cargo flows in 25 EU countries, candidate countries, EFTA countries and Russia – current state (2007).

The elaborated databases made it possible:

- to elaborate the system of European river-sea transport corridors for which different variants of the SRM fleet functioning were calculated
- to adjust parameters of the river-sea ships both to rates of cargo flows and dimensions of waterways.

DETERMINATION OF DESIGN ASSUMPTIONS FOR RIVER-SEA SHIPS OPERATING IN THE SYSTEM OF EUROPEAN TRANSPORT CORRIDORS

The crucial aim of the functional model is to determine design assumptions for structure of the RSM fleet intended for operating in the system of European transport corridors. The determination process consists of the following phases:

Phase I. The determination of effective operation limits for the SRM fleet.

Phase II. The analysis of the obtained results and determination of design assumptions for the RSM fleet structure.

Phase III. The correction of the design assumptions.

The procedure of determination of design assumptions for structure of the RSM fleet operating in the system of European transport corridors, based on the functional model, was carried out in accordance with the algorithm presented in Fig. 3.

Within the functional model of the SRM fleet, the assumptions were made as to:

- decision variables
- limitations
- choice criteria.

on the basis of the parameters of:

- possible shipping routes
- present rates and directions of cargo flows as well as probability of their changes
- groups of shipping tasks, strategies and schemes of functioning the river-sea ships.

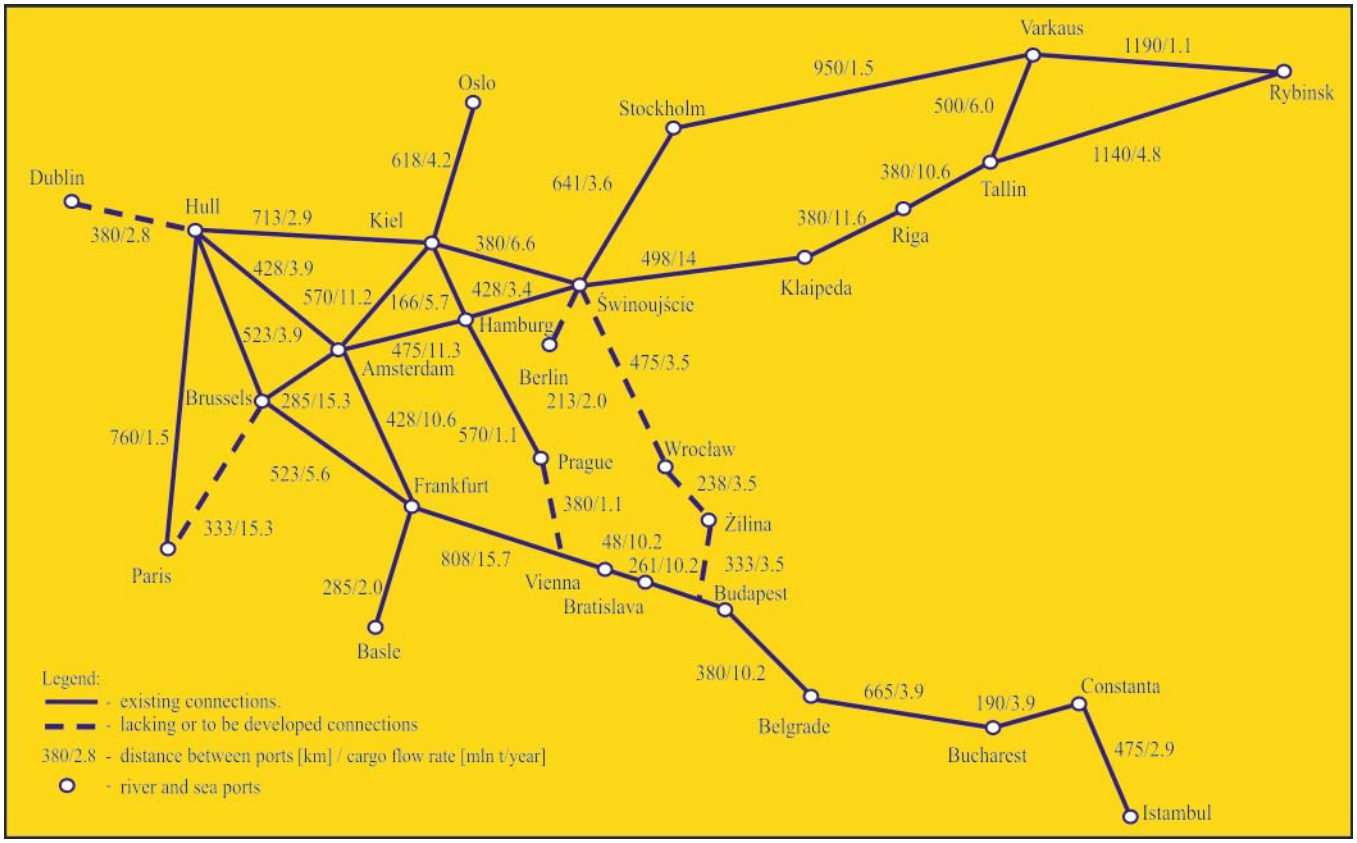

Fig. 2. Future system of European water transport corridors intended for operation of fleet of river-sea ships.

Results obtained from the investigation of the functional model should satisfy all demands of cargo senders. The algorithm of effectiveness of functioning the river-sea ships in the system of European transport corridors is presented in Fig. 4.

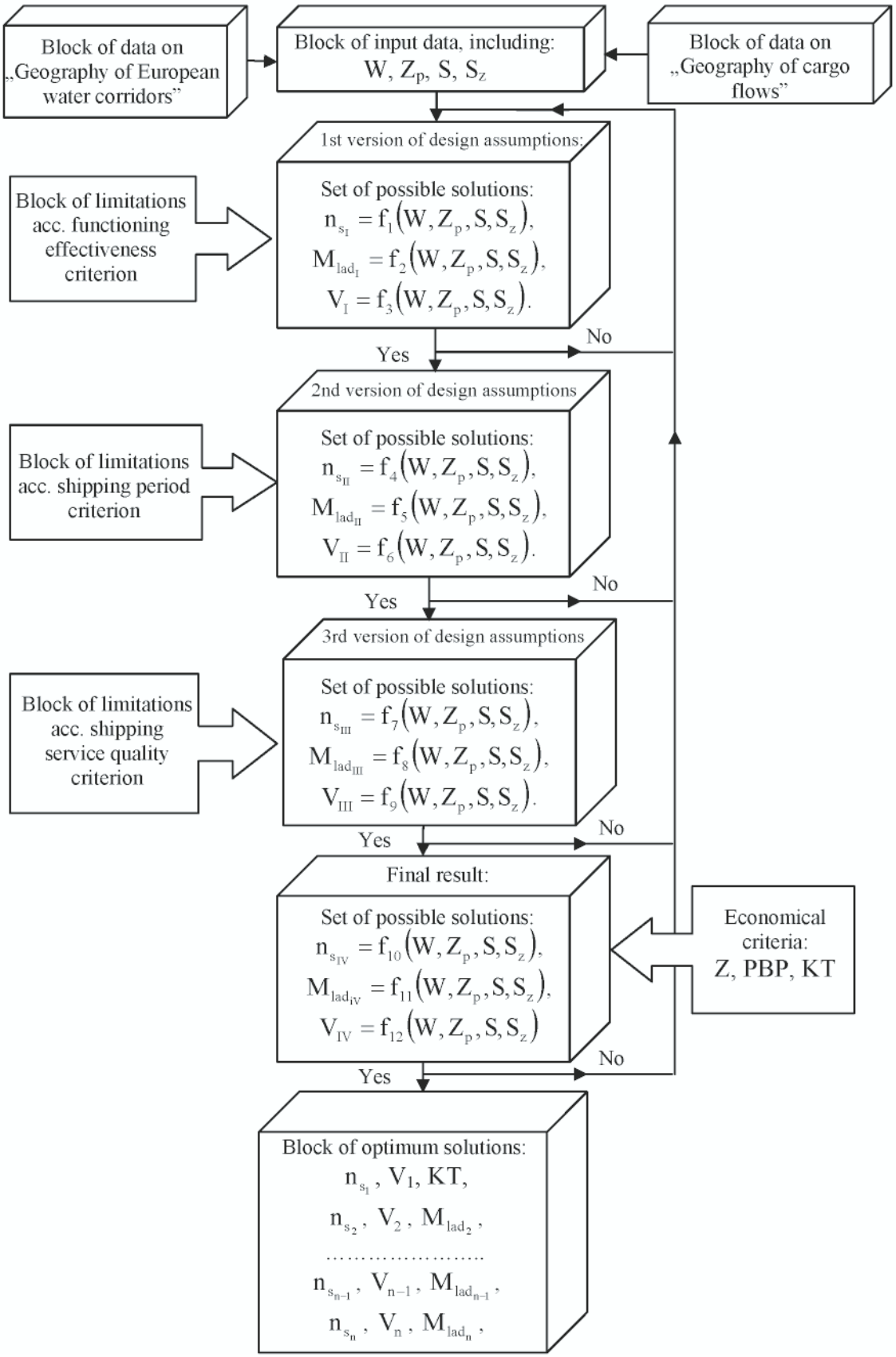

Fig. 3. *Algorithm for determining the design assumptions of the SRM fleet intended for operating in the system of European water transport corridors.*

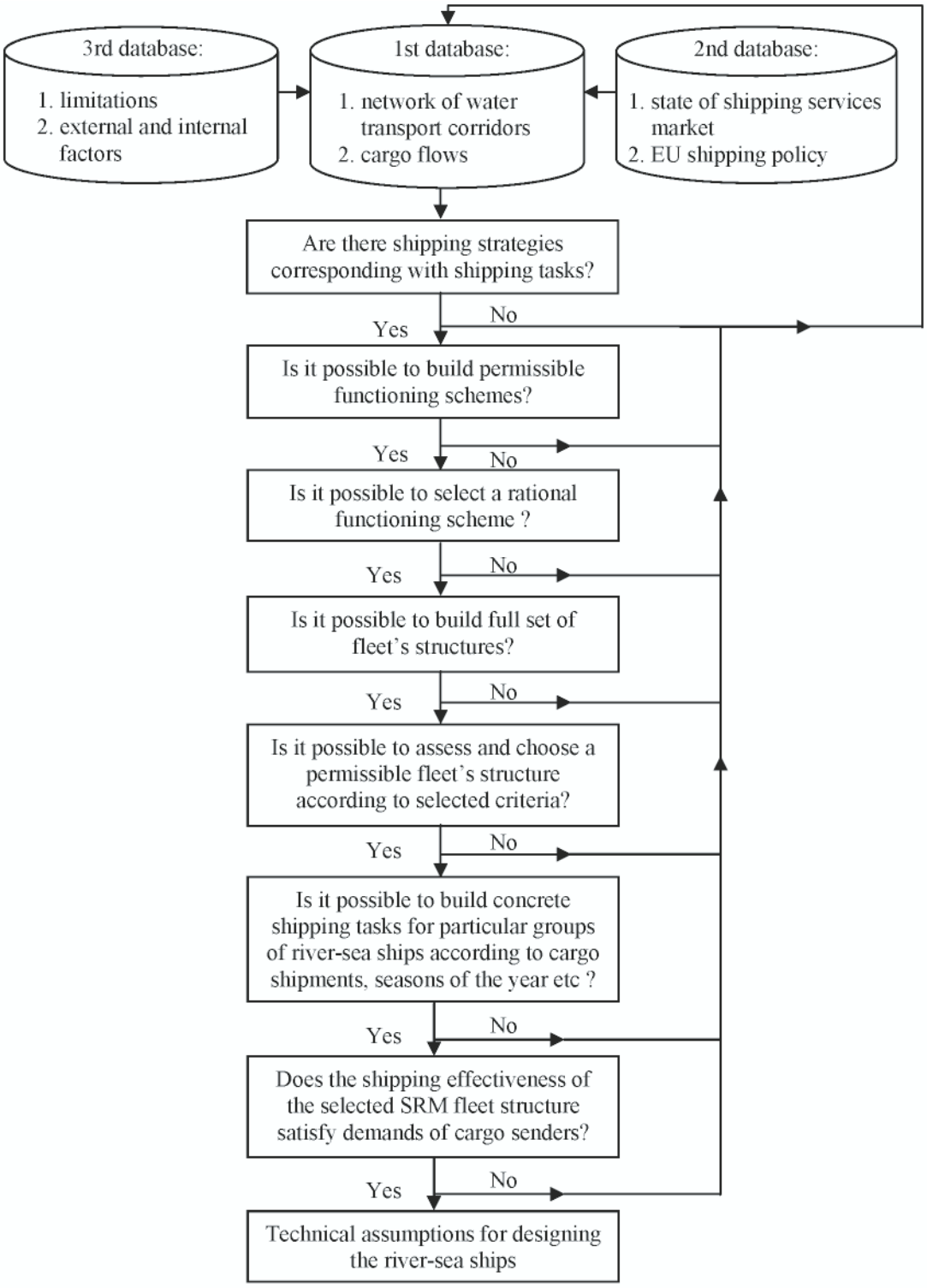

Fig. 4. *Algorithm for assessing the shipping effectiveness of river-sea ships operating in the system of European water transport corridors*

DETERMINATION OF BOUNDARIES OF AREAS OF EFFECTIVE FUNCTIONING THE SRM FLEET

The first phase of the determination of design assumptions for structure of the SRM fleet intended for operating in the system of European transport corridors is to determine number of the ships depending on their speed and cargo carrying capacity. To this end, after performed analysis 10 corridors (Tab. 1) were selected out of the future European network of water transport corridors shown in Fig. 4, for which calculations according to the functional model were performed and their results analysed.

Tab. 1. European river-sea transport corridors

Route	Corridor parameters
From west to east	
Corridor 1. Dublin – Hull – Amsterdam – Frankfurt – Vienna – Bratislava – – Budapest – Belgrade – Bucharest – Constanta – Istambul	S = 4063 [km] W = 7.43 [mln t/year]
Corridor 2. Dublin – Hull – Brussels – Frankfurt – Vienna – Bratislava – – Budapest – Belgrade – Bucharest – Constanta – Istambul	S = 4253 [km] W = 7.90 [mln t/year]
Corridor 3. Dublin - Hull – Kiel – Świnoujście – Klaipeda – Riga –Tallin – Rybinsk	S = 3871 [km] W = 7.61 [mln t/year]
Corridor 4. Dublin – Hull – Kiel – Świnoujście – Stockholm – Varkaus – Rybinsk	S = 4254 [km] W = 3.083 [mln t/year]
Corridor 5. Paris – Brussels – Amsterdam – Hamburg – Świnoujście – Stockholm – Varkaus – Rybinsk	S = 4302 [km] W = 7.36 [mln t/year]
Corridor 6. Paris – Brussels – Amsterdam – Hamburg – Świnoujście – Klaipeda – Riga –Tallin – Rybinsk	S = 3919 [km] W = 10.79 [mln t/year]
From north to south	
Corridor 7. Stockholm – Świnoujście – Wrocław – Zilina – Budapest	S = 1687 [km] W = 3.53 [mln t/year]
Corridor 8. Oslo – Kiel – Hamburg – Prague – Vienna	S = 1734 [km] W = 3.03 [mln t/year]
Corridor 9. Oslo – Kiel – Amsterdam – Frankfurt – Basle	S = 1901 [km] W = 7.00 [mln t/year]
Corridor 10. Hull – Paris	S = 760 [km] W = 1.50 [mln t/year]

where:
S – assumed length of shipping route [km]
W – assumed cargo flow rate [mln t/year].

The following assumptions were made to determine limits of the effective functioning of the SRM fleet:

Assumption 1

As the river-sea ships belong to those of relatively small deadweight and speed (resulting from various limitations from the side of waterways and amount of available cargo shipments) the following values of particular parameters were taken for the calculations:

$$8 \leq V \leq 20 \text{ [km/h]} \quad (1)$$

$$1000 \leq M_{lad} \leq 3500 \text{ [t]} \quad (2)$$

Assumption 2

Inland sections of the river-sea corridors are led along 4th class waterways.

Assumption 3

Cargo flow rate in a given corridor is equal to the mean value of its components.

Assumption 4

In the end terminals 100 % of cargo is unloaded, and in intermediate ports – 30% of it.

The second phase of the determination of design assumption for the SRM fleet intended for operating in the system of European water transport corridors was to determine such values of ship speed and cargo carrying capacity for which the capital return period PBP would be as short as possible. To this end, on the basis of Eq. (3) the required cargo shipping capability of the SRM fleet for particular variants of the corridors was determined under assumption that the designed structure of the fleet satisfies demands of the cargo flows (Eq. 4).

$$PBP = KI / Z \quad (3)$$

$$\sum_i E_i \geq W \quad (4)$$

where:
KI – investment cost of river-sea ship [mln €/year]
Z – profitability of river-sea ship [mln €/year]
W – assumed cargo flow rate [mln t/year]
$\sum_i E_i$ – functional effectiveness (shipping capability) of the SRM fleet [mln t/year].

The last phase of the determination of tasks for the SRM fleet was to select their optimum variants and to determine influence of selected market factors (fuel price, freight rate) on the return period of the capital invested in the SRM fleet.

RESULTS OF THE INVESTIGATIONS

On the basis of the functional model of river-sea ships, presented in Part I (PMR 3/2008) of this paper, relevant calculations were performed to obtain design assumptions for the river-sea ships depending on length of a given corridor and its parameters as well as values of cargo flow rates. Below are given the example calculation results which made achieving rational solutions possible.

To determine searched decision variables the following values were assumed:

- in order to check conditions of the mathematical functional model of river-sea ship:
  - assumed period of repairs, inspections etc of river-sea ship: t_{rm} = 30 [days]
  - assumed cargo handling capacity of port: Z_p = 2400 [t/day].

- in order to determine the economic criteria:
  - for determination of the invested capital return period:
    - yearly interest rate of credit: i = 0.04 [%]
    - credit payback period: e = 7 [years]
  - for determination of current expenditures:
    - unit shipping rate: $f_{r,i}$ = 0.013 [€/t*km]
    - number of months of labour of one member of crew of river-sea ship: k_1 = 10 [month]
    - coefficient of repair and maintenance cost of river-sea ship: k_2 = 0.025 [-]
    - assumed fuel price: C_{pal} = 492 [€/t]
    - assumed specific fuel oil consumption during voyage: h^j_{pal} = 220 [g/kWh]
    - assumed calculation factor: q = 1.10 [-]
    - assumed port charge: β = 0.1 [€/t]
    - assumed cargo handling charge: χ = 0.02 [€/t]
    - mean monthly wage of one crew member of river-sea ship: w = 4000 [€]
    - required number of crew members: n_{zal} = 10 [persons].

On the basis of the performed analysis, assumed values and simplifying assumptions, results of the calculations for particular European water transport corridors were obtained. Three of the calculated variants are presented below.

Variant 1. Corridor: Dublin – Hull – Amsterdam – Frankfurt – Vienna – Bratislava – Budapest – Belgrade – Bucharest – Constanta – Istambul

Tab. 2. *Minimum number of ships necessary to cope with rate of cargo flow along the proposed river-sea corridor no. 1 [units]*

W = 7.43 [mln t /year]											
V [km/h]	M_{lad_i} [t], i = 1÷11										
	1000	1250	1500	1750	2000	2250	2500	2750	3000	3250	3500
8	513	419	357	312	279	253	232	215	200	188	178
10	419	344	294	258	232	211	194	180	169	159	151
12	357	294	253	223	200	183	169	158	148	140	133
14	312	258	223	197	178	163	151	141	133	126	121
16	279	232	200	178	161	148	138	129	122	116	111
18	253	211	183	163	148	137	127	120	113	108	104
20	232	194	169	151	138	127	119	112	107	102	98

Tab. 3. *Yearly profit per one ship operating in the proposed river-sea corridor no. 1 [mln €/year]*

W = 7.43 [mln t /year]											
V [km/h]	M_{lad_i} [t], i = 1÷11										
	1000	1250	1500	1750	2000	2250	2500	2750	3000	3250	3500
8	-0.08	0.17	0.40	0.61	0.81	0.99	1.15	1.30	1.43	1.55	1.65
10	0.20	0.56	0.84	1.10	1.33	1.54	1.73	1.90	2.05	2.18	2.30
12	0.47	0.93	1.26	1.55	1.82	2.05	2.26	2.45	2.61	2.76	2.88
14	0.73	1.28	1.65	1.97	2.27	2.52	2.75	2.95	3.12	3.27	3.40
16	0.98	1.61	2.02	2.37	2.68	2.96	3.20	3.40	3.58	3.73	3.86
18	1.21	1.93	2.36	2.74	3.07	3.36	3.61	3.82	4.00	4.16	4.28
20	1.44	2.24	2.69	3.09	3.44	3.73	3.99	4.21	4.39	4.54	4.67

Tab. 4. *Capital return period for the proposed river-sea corridor no. 1 [years]*

W = 7.43 [mln t /year]											
V [km/h]	M_{lad_i} [t], i = 1÷11										
	1000	1250	1500	1750	2000	2250	2500	2750	3000	3250	3500
8	-	35.97	15.58	10.54	8.28	7.02	6.22	5.68	5.31	5.04	4.85
10	23.32	10.73	7.41	5.89	5.04	4.50	4.13	3.88	3.70	3.57	3.47
12	10.14	6.44	4.96	4.17	3.69	3.38	3.16	3.01	2.90	2.83	2.78
14	6.57	4.67	3.78	3.28	2.96	2.75	2.60	2.50	2.43	2.38	2.35
16	4.92	3.70	3.09	2.73	2.50	2.35	2.24	2.17	2.12	2.09	2.07
18	3.96	3.09	2.63	2.36	2.18	2.07	1.98	1.93	1.89	1.87	1.87
20	3.33	2.67	2.31	2.09	1.95	1.86	1.79	1.75	1.73	1.72	1.71

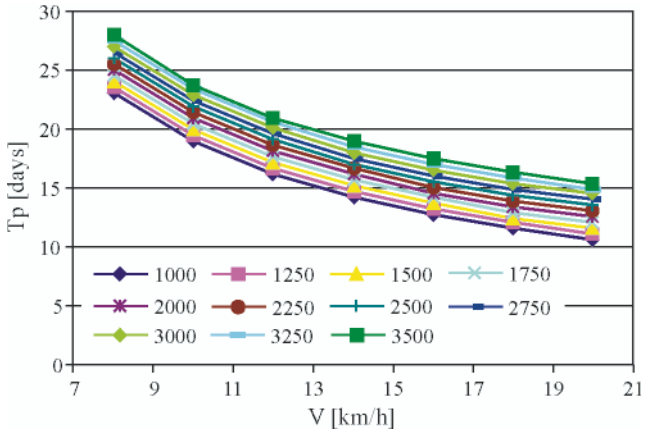

Fig. 5. *Shipping period in function of ship speed in the proposed river-sea corridor no. 1*

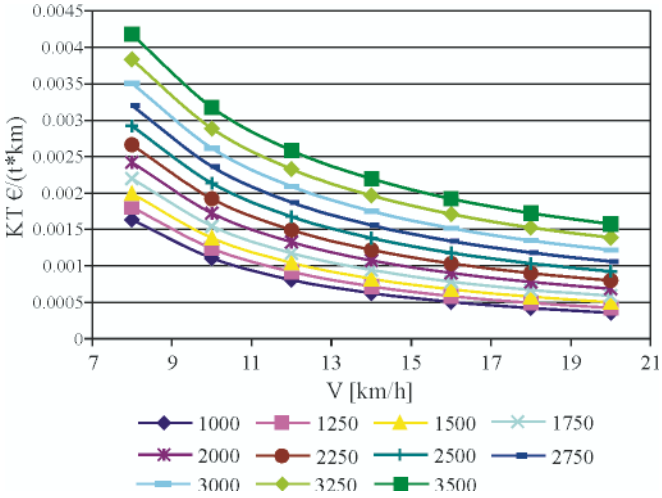

Fig. 6. *Unit shipping cost in function of ship speed in the proposed river-sea corridor no. 1*

Variant 4. Corridor: Dublin – Hull – Kiel – Świnoujście – Stockholm – Varkaus – Rybinsk

Tab. 5. *Minimum number of ships necessary to cope with rate of cargo flow along the proposed river-sea corridor no.4 [units]*

W = 3.08 [mln t /year]											
V [km/h]	M_{lad_i} [t], i = 1÷11										
	1000	1250	1500	1750	2000	2250	2500	2750	3000	3250	3500
8	218	177	150	130	116	105	95	88	82	77	72
10	177	144	123	107	95	86	79	73	68	64	61

W = 3.08 [mln t /year]											
V [km/h]	M_{lad_i} [t], i = 1÷11										
	1000	1250	1500	1750	2000	2250	2500	2750	3000	3250	3500
12	150	123	105	92	82	74	68	63	59	56	53
14	130	107	92	81	72	66	61	56	53	50	47
16	116	95	82	72	65	59	55	51	48	45	43
18	105	86	74	66	59	54	50	47	44	42	40
20	95	79	68	61	55	50	47	44	41	39	37

Tab. 6. *Yearly profit per one ship in the proposed river-sea corridor no.4 [mln €/year]*

W = 3.08 [mln t /year]											
V [km/h]	M_{lad_i} [t], i = 1÷11										
	1000	1250	1500	1750	2000	2250	2500	2750	3000	3250	3500
8	-0.02	0.22	0.45	0.66	0.87	1.05	1.24	1.41	1.56	1.71	1.84
10	0.28	0.57	0.86	1.12	1.36	1.60	1.81	2.01	2.20	2.37	2.53
12	0.56	0.92	1.25	1.56	1.84	2.11	2.35	2.58	2.79	2.98	3.16
14	0.85	1.25	1.63	1.97	2.29	2.58	2.85	3.11	3.33	3.54	3.74
16	1.12	1.57	1.99	2.37	2.72	3.04	3.33	3.60	3.84	4.06	4.26
18	1.39	1.88	2.33	2.74	3.12	3.46	3.77	4.06	4.31	4.54	4.75
20	1.64	2.18	2.66	3.11	3.50	3.86	4.19	4.48	4.75	4.98	5.20

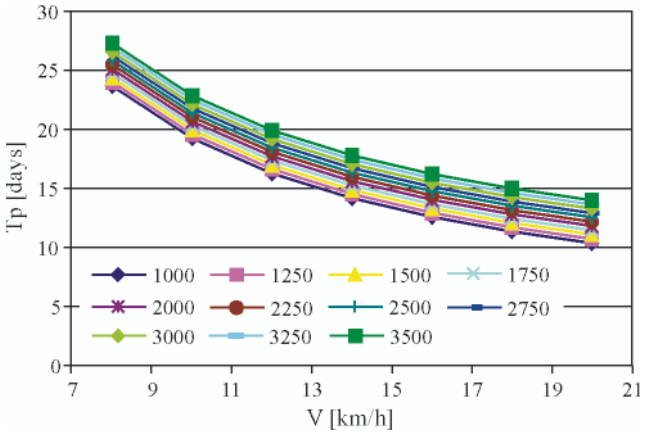

Fig. 7. *Shipping period in function of ship speed in the proposed river-sea corridor no.4.* **Source**: the author's elaboration

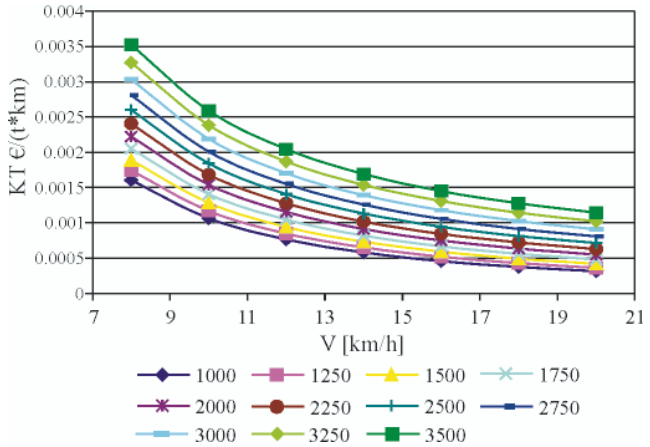

Fig. 8. *Unit shipping cost in function of ship speed in the proposed river-sea corridor no.4.* **Source**: the author's elaboration

Tab. 7. *Capital return period for the proposed river-sea corridor no. 4 [years]*

W = 3.08 [mln t /year]											
V [km/h]	M_{lad_i} [t], i = 1÷11										
	1000	1250	1500	1750	2000	2250	2500	2750	3000	3250	3500
8	-	23.09	11.78	8.26	6.54	5.54	4.88	4.42	4.09	3.84	3.64
10	17.28	8.72	6.12	4.86	4.13	3.66	3.32	3.08	2.90	2.76	2.65
12	8.45	5.46	4.19	3.50	3.07	2.77	2.56	2.41	2.29	2.20	2.13
14	5.65	4.01	3.22	2.76	2.47	2.26	2.11	2.00	1.92	1.85	1.80
16	4.28	3.20	2.64	2.30	2.08	1.92	1.81	1.73	1.66	1.61	1.58
18	3.46	2.67	2.25	1.99	1.81	1.69	1.60	1.53	1.48	1.44	1.42
20	2.92	2.31	1.97	1.76	1.61	1.51	1.44	1.39	1.34	1.32	1.29

Variant 10. Corridor: Hull - Paris

Tab. 8. *Minimum number of ships necessary to cope with rate of cargo flow along the proposed river-sea corridor no. 10 [units]*

W = 1.50 [mln t /year]											
V [km/h]	M_{lad_i} [t], i = 1÷11										
	1000	1250	1500	1750	2000	2250	2500	2750	3000	3250	3500
8	22	18	16	14	13	12	11	11	10	10	9
10	18	16	14	12	11	11	10	9	9	9	8
12	16	14	12	11	10	9	9	9	8	8	8
14	14	12	11	10	9	9	8	8	8	7	7
16	13	11	10	9	9	8	8	7	7	7	7
18	12	11	9	9	8	8	7	7	7	7	6
20	11	10	9	8	8	7	7	7	7	6	6

Tab. 9. *Yearly profit per one ship in the proposed river-sea corridor no. 10 [mln /year]*

W = 1.50 [mln t /year]											
V [km/h]	M_{lad_i} [t], i = 1÷11										
	1000	1250	1500	1750	2000	2250	2500	2750	3000	3250	3500
8	-0.28	-0.15	-0.07	0.00	0.04	0.07	0.08	0.07	0.04	0.00	-0.05
10	-0.07	0.08	0.18	0.25	0.29	0.32	0.32	0.30	0.27	0.23	0.17
12	0.13	0.28	0.39	0.47	0.51	0.53	0.53	0.51	0.46	0.41	0.34
14	0.29	0.46	0.58	0.66	0.71	0.72	0.71	0.68	0.63	0.56	0.49
16	0.46	0.63	0.76	0.83	0.88	0.88	0.87	0.83	0.77	0.70	0.61
18	0.61	0.79	0.91	0.99	1.02	1.03	1.00	0.96	0.89	0.82	0.72
20	0.75	0.93	1.05	1.13	1.15	1.15	1.13	1.07	1.00	0.91	0.81

Tab. 10. *Capital return period for the proposed river-sea corridor no. 10 [years]*

W = 1.50 [mln t /year]											
V [km/h]	M_{lad_i} [t], i = 1÷11										
	1000	1250	1500	1750	2000	2250	2500	2750	3000	3250	3500
8	-	-	-	-	-	-	-	-	-	-	-
10	-	-	29.72	21.83	19.08	18.31	18.76	20.35	23.42	29.08	-

W = 1.50 [mln t /year]											
V [km/h]	M_{lad_i} [t], i = 1÷11										
	1000	1250	1500	1750	2000	2250	2500	2750	3000	3250	3500
12	-	18.07	13.43	11.66	11.00	10.95	11.37	12.24	13.68	15.97	19.75
14	16.05	10.82	9.00	8.26	8.02	8.12	8.49	9.13	10.12	11.58	13.81
16	10.41	7.92	6.94	6.55	6.47	6.62	6.96	7.49	8.27	9.38	11.00
18	7.85	6.36	5.75	5.53	5.53	5.69	6.01	6.48	7.14	8.06	9.37
20	6.40	5.38	4.97	4.84	4.89	5.06	5.36	5.79	6.38	7.18	8.30

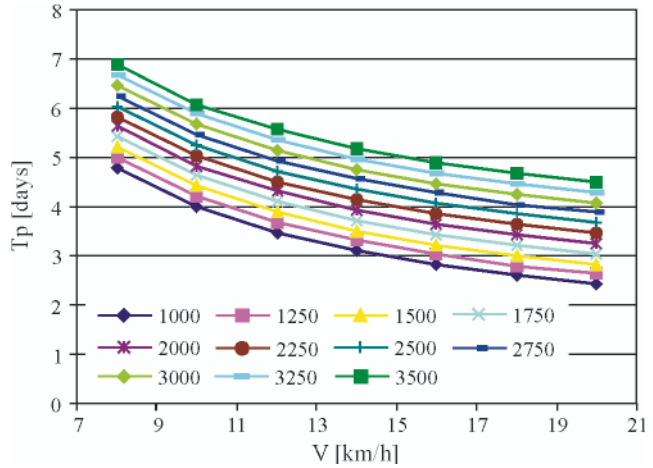

Fig. 9. *Shipping period in function of ship speed in the proposed river-sea corridor no. 10*

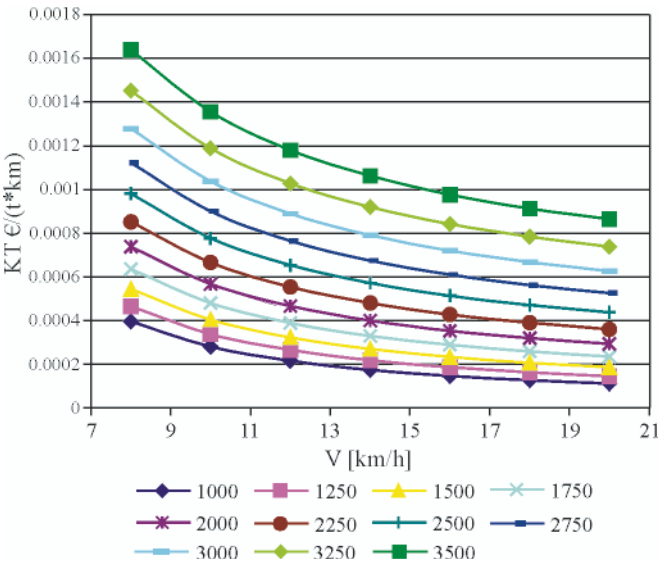

Fig. 10. *Unit cost in function of ship speed in the proposed river-sea corridor no. 10*

CONCLUSIONS

In the above presented tables is shown the influence of the SRM fleet's speed and deadweight on limits of areas of permissible solutions for the fleet of such ships necessary for servicing the analyzed cargo flows. The following parameters have significant impact on number of the ships:

- length of shipping route
- cargo handling capacity of ports.

On the basis of the investigations performed for 10 proposed river-sea corridors the rational variants of the SRM fleet with a view of economic criteria were achieved (Fig. 11).

The performed simulation investigations made it possible to draw the following conclusions:

- In the case of the shortest routes a weak dependence of necessary number of ships on their cargo carrying capacity can be observed.
- For the longest routes a significant decrease of number of necessary ships along with increasing their cargo carrying capacity can be observed.

The main aim of shipowner is to find ways for reaching possibly large profits at possibly low investment outlays. However to predict either short- or long- term costs and profits for river-sea ships is difficult. This is caused by changeability of main cost-generating factors which mainly depend on situation on the market and are very hard to be predicted for whole ship service period.

In this work the influence of fuel oil cost and freight rate on capital return period for 10 optimum solutions of the functional model of the SRM fleet was analyzed. It was assumed that changes in fuel oil price and freight rate amount to 15%. The performed investigations made it possible to draw the following conclusions:

- the fuel oil price change within 15% range does not influence the capital return period significantly
- further increase of the fuel oil price results in an insignificant increase of the capital return period
- the freight rate change very much influences the capital return period, resulting either in its lengthening or shortening, that was shown in Fig. 12.

The analysis performed by means of the elaborated functional model of river-sea ships intended for operating in the system of European water transport corridors can be concluded by the following statements:

- The direct cargo shipping on sea-river or river-sea routes makes it possible to achieve some profits which lead to:
  - decreased investment outlays by about 8÷14 % (due to a lower number of ships by a better usage of their cargo shipping capability resulting from elimination of ship lying periods in intermediate ports)
  - decreased cargo handling costs even by 30% (due to elimination of intermediate ports).
- The analysis of the functional model of river-sea ships with taking into account relevant limitations and criteria makes it possible to obtain a set of the best solutions which can increase profits of ship operators on the water transport market by 3 ÷ 7 %, or avoid choice of an unprofitable variant.
- Regardless of physical and geographical limitations associated with a navigation region the task assigned to a given ship and its parameters are important.
- The neglecting of the functional model can result in an incorrect adjustment of number of ships, their speed and deadweight values to traffic capacity of river-sea routes and - in consequence - capital return periods longer even several times.
- Investigations with the use of the functional model make it possible to increase the probability of compatibility of ship design assumptions with real state of transport market, at least by 21 ÷ 28 %, as it results from the performed transport development prediction up to 2015 and 2030. It can be stated that the neglecting of the predictions would result in a proportional incompatibility of ship design assumptions with real state of transport market.

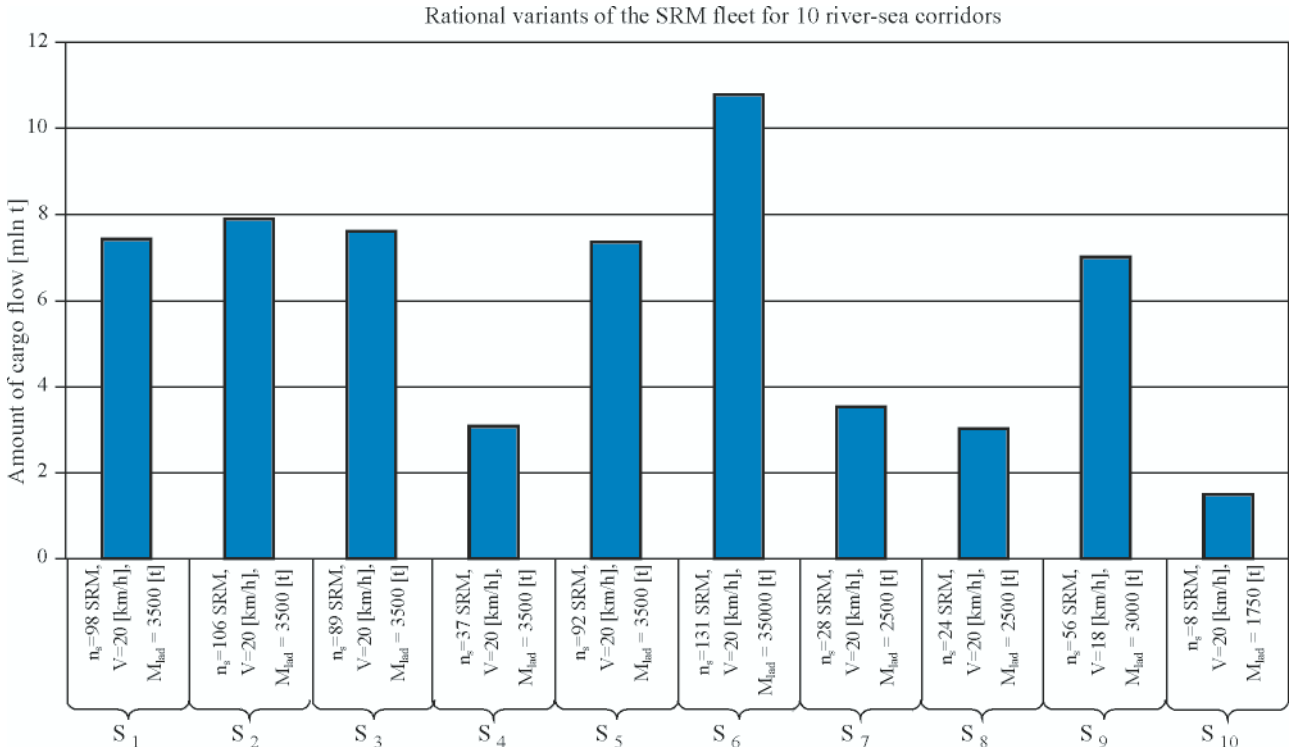

Fig. 11. *Rational variants of SRM fleet for particular shipping corridors with a view of economic criteria*

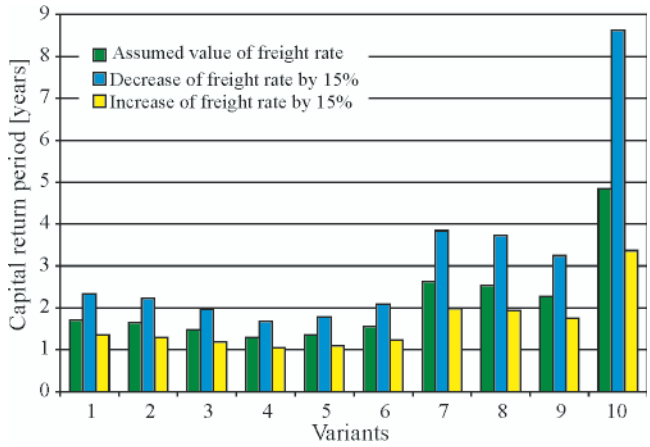

Fig. 12. *Influence of freight rate change on capital return period*

BIBLIOGRAPHY

1. Charlier J. & Ridolfi G.: *Intermodal transportation in Europe: of modes, corridors and nodes*. Maritime Policy and Management, 21 (3), 1994
2. Kaup M.: *Importance of river-sea fleet for development of the Baltic Sea region* (in Polish). Materials of 2nd International Scientific Conference on „ Operation of the Polish Liner and Ferry Fleet in 2004", Szczecin 2004
3. Kaup M., Kaup J.: *Design model of river-sea ships operating on European waterways*. Marine Technology Transactions, Vol.16, Polish Academy of Sciences – Branch in Gdańsk, Gdańsk 2005
4. Kaup M.: *Functional model of river-sea ships operating in European system of transport corridors. Part I. Methods used to elaborate functional models of river-sea ships operating in European system of transport corridors.* Polish Maritime Research, 3/2008 (57), Vol. 15, Gdańsk, 2008, p. 3-11
5. Kreutzberger I.E.: *Innovative networks and new-generation terminals for intermodal transport*, 1999
6. Tarnowski W.: *CAD CAM computer aiding. Essentials of technical design* (in Polish). Scientific Technical Publishers (Wydawnictwo Naukowo-Techniczne), Warszawa 1997.

CONTACT WITH THE AUTHOR

Magdalena Kaup, Ph. D.
Faculty of Marine Technology
Szczecin University of Technology
AL. Piastów 41,
71-065 Szczecin, POLAND
e-mail: mkaup@ps.pl
phone: (091) 449 - 47 - 50

POLISH MARITIME RESEARCH 4(58) 2008 Vol 15; pp. 12-16
10.2478/v10012-007-0091-0

Multihull vessel excitations in stochastic formulation

Agnieszka Królicka, M. Sc.
Gdansk University of Technology

ABSTRACT

The article analyses excitations of a multihull vessel using stochastic formulation. The excitations which make the vessel move come from the motion of sea waves and the action of wind. The sea undulation has most frequently the form of irregular waves, and that is why it is assumed in many studies of sea-going vessel dynamics that the undulation process has probabilistic nature. In the article the dynamics of a multihull vessel is analysed using a linear model on which an irregular wave acts. It was assumed that the examined object interacts with the head sea, and for this wave a set of state equations was derived. The head sea provokes symmetric movements of the object, i.e. surge, heave and pitch.

Keywords: excitations, multihull vessel, stochastic formulation, the motion of sea waves, vessel

INTRODUCTION

The motion of a vessel is mainly provoked by the excitations coming from sea waves. The nature of the wind undulation, along with difficulties in determining precisely the initial conditions for the motion of sea waves, are the reasons why the dynamics of the sea waves can be only modelled within the framework of the stochastic theory [6,7]. The basic quantity in the stochastic theory of sea motion is the function $\eta(x, y, t)$ which characterises the altitude of the sea surface with respect to the undisturbed reference state. The function $\eta(x, y, t)$ is a random function of time and position [1]. Probabilistic properties of this function are partially derived based on the results of measurements and partially from the hydrodynamic theory of waves. It is usually assumed in dynamic analyses that the process of sea undulation is stationary, ergodic, and Gaussian [8]. These assumptions facilitate developing mathematical models, and their effect can be assessed via identification and estimation. At those assumptions, the process $\eta(x, y, t)$ is characterised for an arbitrary fixed point (x, y) by the spectral density $g_\eta(\omega)$. Having known the spectral density of the Gaussian random function $\eta(x, y, t)$, for instance, we can find the wave time scale T_s and height h_s. The time scale is defined as the average time between successive instants at which the average calm sea level is exceeded, while the wave height represents the expected value equal to one third of the highest wave height.

The dynamic model comprises a deterministically defined non-deformable object which is subject to the action of a wave, the state of which is described in stochastic formulation. The forces which act on the multihull vessel come from irregular waves.

WAVE-EXCITED MULTIHULL VESSEL MOVEMENTS

For the vessel treated as a rigid object moving at constant speed v and arbitrary angle with respect to the direction of sea waves, its movements can be described by the mathematical model having the form a set of second-order differential equations (1). Local movements of the object around its equilibrium position are its response to the excitations coming from sea undulation.

If the model of the dynamic system is a linear model of a vessel, then the equations [5]:

$$\sum_{i,j=1}^{6} I_{ij}\eta_i + B_{ij}\eta_i + C_{ij}\eta_i = F_i(t) \qquad (1)$$

where:

- $I = M + A$ – inertia matrix
- M – elements of generalised mass matrix for the construction
- A – elements of hydrodynamic mass- added mass matrix
- B – hydrodynamic damping matrix
- C – hydrostatic stiffness matrix
- η – generalised displacement vector
- F(t) – vector of exciting forces and moments,

can be analysed as a set of two uncoupled groups of mutually coupled equations. We assume the existence of the coupling via linear and nonlinear damping coefficients and hydrostatic elasticity coefficients.

In our analyses the examined object is idealised as the linear dynamic system with six degrees of freedom, which are:

- longitudinal oscillation (surge) - η_1
- transverse oscillation (sway) - η_2
- heaving - η_3
- rolling - η_4
- pitching - η_5
- yawing - η_6

The coordinate system fixed to the catamaran is shown in Fig. 1.

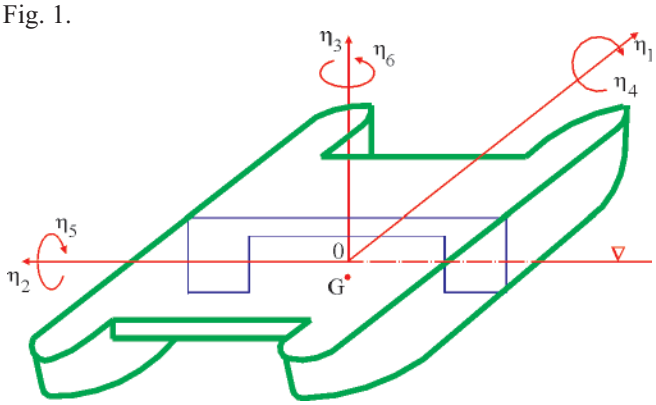

Fig. 1. *Scheme of the physical model of the catamaran*

The first group of equations comprises symmetric (longitudinal) movements, which include: η_1 - linear longitudinal moments (surging), η_3 - linear vertical movements (heave) and η_5 -angular longitudinal movements (pitch).

The second group comprises the equations which describe antisymmetric (transverse) movements, including: η_2 - transverse linear movements (swaying), η_4 - transverse angular movements (rolling), and η_6 - horizontal angular movements (yawing).

In our final discussion we will neglect η_1 - linear longitudinal movements (surging), which are usually analysed using models with one degree of freedom. Consequently, in our case the mathematical model consists of 5 differential equations.

Our goal is to derive stochastic differential equations. Therefore in order to simplify the division of movements, let us introduce new variables given by the relation (2):

$$\begin{Bmatrix} \eta_1 \\ \eta_3 \\ \eta_5 \\ \eta_2 \\ \eta_4 \\ \eta_6 \end{Bmatrix} = \begin{Bmatrix} z_1 \\ z_2 \\ z_3 \\ z_4 \\ z_5 \\ z_6 \end{Bmatrix} \tag{2}$$

For the symmetric and antisymmetric movements selected by us the developed set of differential equations (1) takes the form:

$$\begin{cases} (M_{33}+A_{33})\ddot{z}_2 + (M_{35}+A_{35})\ddot{z}_3 + B_{33}\dot{z}_2 + B_{35}\dot{z}_3 + C_{33}z_2 + C_{35}z_3 = F_3 \\ (M_{23}+A_{23})\ddot{z}_2 + (M_{25}+A_{25})\ddot{z}_3 + B_{23}\dot{z}_2 + B_{25}\dot{z}_3 + C_{23}z_2 + C_{25}z_3 = F_2 \end{cases}$$

$$\begin{cases} (M_{42}+A_{42})\ddot{z}_4 + (M_{44}+A_{44})\ddot{z}_5 + (M_{46}+A_{46})\ddot{z}_6 + B_{42}\dot{z}_4 + B_{44}\dot{z}_5 + B_{46}\dot{z}_6 + C_{42}z_4 + C_{44}z_5 + C_{46}z_6 = F_4 \\ (M_{52}+A_{52})\ddot{z}_4 + (M_{54}+A_{54})\ddot{z}_5 + (M_{56}+A_{56})\ddot{z}_6 + B_{52}\dot{z}_4 + B_{54}\dot{z}_5 + B_{56}\dot{z}_6 + C_{52}z_4 + C_{54}z_5 + C_{56}z_6 = F_5 \\ (M_{62}+A_{62})\ddot{z}_4 + (M_{64}+A_{64})\ddot{z}_5 + (M_{66}+A_{66})\ddot{z}_6 + B_{62}\dot{z}_4 + B_{64}\dot{z}_5 + B_{66}\dot{z}_6 + C_{62}z_4 + C_{64}z_5 + C_{66}z_6 = F_6 \end{cases} \tag{3}$$

Having solved this set of equations we get the solutions for acceleration coordinates $\ddot{z}_2$ and $\ddot{z}_3$ for symmetric movements, and $\ddot{z}_4$, $\ddot{z}_5$, $\ddot{z}_6$ for antisymmetric movements (see the scheme shown in Fig. 2).

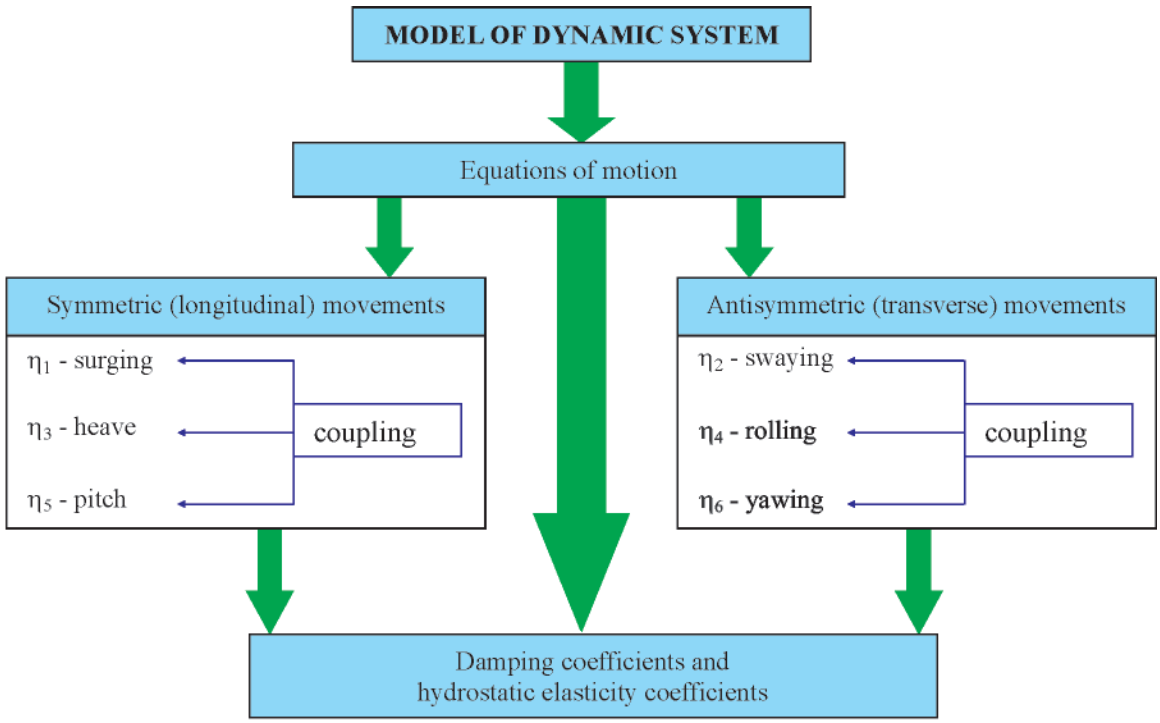

Fig. 2. *Schematic division of multihull vessel motion equations in the linear model of the dynamic system*

Constructional aspects (symmetry) of multihull vessels make it possible to analyse group-coupled movements of the vessel, thus reducing the number of state variables in the equations.

EXTERNAL RANDOM EXCITATIONS

Exciting forces

Fig. 3 shows a sequence of actions aiming at the assessment of the generalised exciting forces.

The exciting forces come from the water undulation and the diffraction of waves, consequently they can be presented as functions of the wave velocity potential φ_W and the diffraction potential φ_D [10]:

$$\vec{F}_m = -i\rho\omega \int_S \vec{n}_m(\phi_W + \phi_D)dS \tag{4}$$

where:

$\vec{F}_m$ for m = 1, 2, 3 – orthogonal projections of the external forces

$\vec{F}_m$ for m = 4, 5, 6 – orthogonal projections of the vector of moments of the external forces

S – catamaran's wetted surface

$\vec{n}_m$ – unit vectors in the direction perpendicular to surface S for m = 1, 2, 3, 4, 5, 6.

The process F(t) in the equation (1) can be presented as a multidimensional homogeneous Markov process which corresponds to the vector $Y(y_1, y_2, \ldots y_n)$ in the phase space, where Y = F(t).

If we assume that the excitation F(t) has the form

$$F(t) = \sum_0^3 (a_i y_1^i + b_i y_2^i) = F(y_1, y_2, y_3, y_4)$$

then we arrive at the stochastic differential equation in the form:

- for symmetric movements:

$$\begin{aligned} y_1 &= F_2(t) \\ \dot{y}_1 &= y_2 \\ \dot{y}_2 &= y_3 \\ \dot{y}_3 &= -S_{02} - S_{12}y_1 - S_{22}y_2 - S_{32}y_3 + W_2(t) \\ y_4 &= F_3(t) \\ \dot{y}_4 &= y_5 \\ \dot{y}_5 &= y_6 \\ \dot{y}_6 &= -S_{03} - S_{13}y_1 - S_{23}y_2 - S_{33}y_3 + W_3(t) \end{aligned} \tag{5}$$

- for antisymmetric movements:

$$\begin{aligned} y_1 &= F_4(t) \\ \dot{y}_1 &= y_2 \\ \dot{y}_2 &= y_3 \\ \dot{y}_3 &= -S_{04} - S_{14}y_1 - S_{24}y_2 - S_{34}y_3 + W_4(t) \\ y_4 &= F_5(t) \\ \dot{y}_4 &= y_5 \\ \dot{y}_5 &= y_6 \\ \dot{y}_6 &= -S_{05} - S_{15}y_1 - S_{25}y_2 - S_{35}y_3 + W_5(t) \\ y_7 &= F_6(t) \\ \dot{y}_7 &= y_8 \\ \dot{y}_8 &= y_9 \\ \dot{y}_9 &= -S_{06} - S_{16}y_1 - S_{26}y_2 - S_{36}y_3 + W_6(t) \end{aligned} \tag{6}$$

where:

W – "white noise"

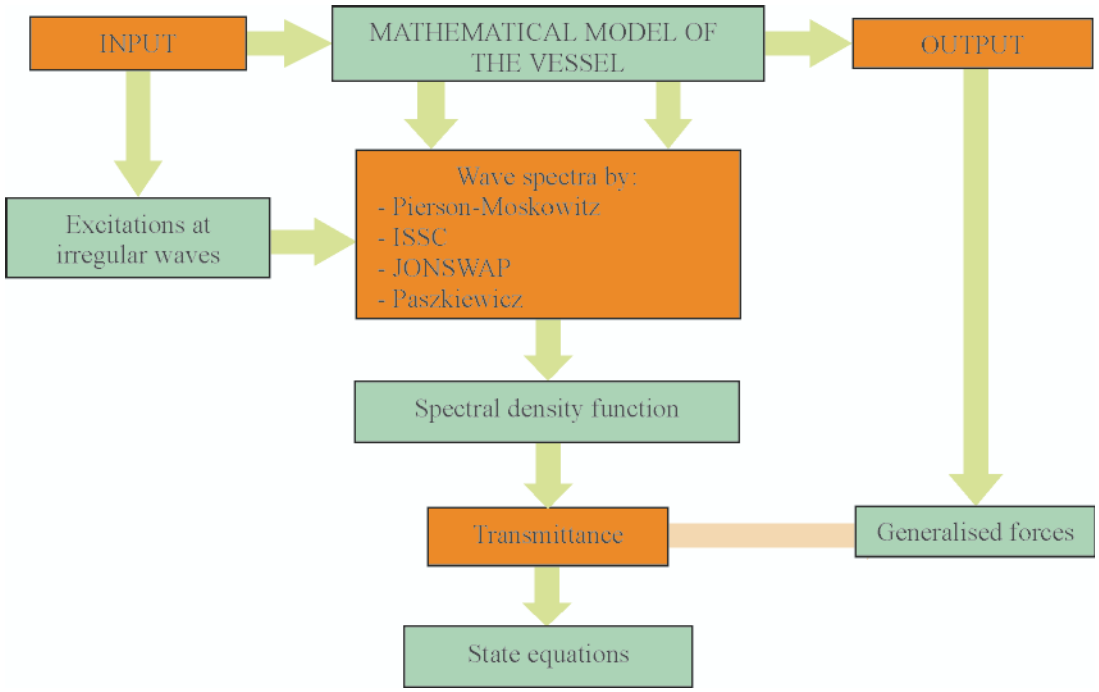

Fig. 3. *Schematic procedure for determining the exciting forces in the mathematical model*

S_i – coefficients of linear filters (determined from the correlation function of the excitation, or from its spectral density).

Using relevant linear filters we replace the "white noise" process, for which the spectral density is constant, with the densities corresponding to different wave spectra.

Deriving the set of state equations

State equations are one of possible ways in which the mathematical model of a dynamic system can be represented. The system output for time t_n depends not only on the system input at time t_n, but also on past inputs at all times $t_i (t_i < t_n)$.

An alternative method of describing the dynamic system to that represented by the state equations is the transmittance, which assumes that the initial state is equal to zero.

The operator transmittance, also referred to as the transfer function G(s), is the ratio of the Laplace transforms of the system's output and input signals when the initial conditions are equal to zero. The transmittance describes general stationary characteristics of the linear system with one input and one output, irrelevant of the type of excitation. For systems described by linear differential equations with constant coefficients, the transmittance is a rational function of the complex variable **s** and can be presented using the ratio of two polynomials (10).

When deriving the set of state equations we adopt the following assumptions:

- ☆ the resultant movement of the object on an irregular wave is the superposition of its movements on regular waves
- ☆ only the head sea effect is taken into account, and it is the source of the following movements: η_1 - surge, η_3 - heave and η_5 - pitch.

With the use of the equation (1), the wave-excited motion of an object is given by the following state equation:

$$I\ddot{\eta} + B\dot{\eta} + C\eta = F_w \tag{7}$$

where :

$$\left.\begin{aligned} \dot{P} &= Q \\ \dot{Q} &= -I^{-1}B\dot{\eta} - I^{-1}C\eta + I^{-1}F_w \end{aligned}\right\} \tag{8}$$

I, B, C – matrices 3x3

$$P = \begin{Bmatrix} \eta_1 \\ \eta_3 \\ \eta_5 \end{Bmatrix},\ Q = \begin{Bmatrix} \dot{\eta}_1 \\ \dot{\eta}_3 \\ \dot{\eta}_5 \end{Bmatrix},\ F_w = \begin{Bmatrix} F_1 \\ F_3 \\ F_5 \end{Bmatrix} \tag{9}$$

- ☆ it is assumed that the response, in the form of generalised forces Fi = (i = 1, 3, 5), to the excitation coming from the wave of the height ξ(t) can be approximated by the system whose transmittance has the form:

$$\frac{F(s)}{\xi(s)} = \frac{b_0 s^2 + b_1 s + b_2}{s^2 + a_1 s + a_2} \tag{10}$$

where:
$F(F_1, F_3, F_5)$,
$b_0(b_{01}, b_{03}, b_{05})$, $b_1(b_{11}, b_{13}, b_{15})$, $b_2(b_{21}, b_{23}, b_{25})$,
$a_1(a_{11}, a_{13}, a_{15})$, $a_2(a_{21}, a_{23}, a_{25})$.

The relation (10) can be written using the following set of state equations:

$$\left.\begin{aligned} \dot{f}_1 &= F - h_0\xi \\ \dot{f}_2 &= \dot{F} - h_0\dot{\xi} - h_1\xi \end{aligned}\right\} \tag{11}$$

$$\left.\begin{aligned} \dot{f}_1 &= f_2 + h_1\xi \\ \dot{f}_2 &= -a_2 f_1 - a_1 f_2 + h_2\xi \end{aligned}\right\} \tag{12}$$

where:
h_0, h_1, h_2 - constants defined by coefficients in equation (10)
$f_1(f_{11}, f_{13}, f_{15})$, $f_2(f_{21}, f_{23}, f_{25})$,
$h_0(h_{01}, h_{03}, h_{05})$, $h_1(h_{11}, h_{13}, h_{15})$, $h_2(h_{21}, h_{23}, h_{25})$.

To obtain the random process of wave height ξ(t) (irregular wave), well-known energy spectra (wave spectra) of the wave which approaches the object are to be used:

$$\phi_{\xi\xi}(\omega) = \begin{cases} -\text{Pierson Moskowitz spectrum, for instance} \\ -\text{ISSC spectrum, for instance} \end{cases} \tag{13}$$

We approximate the selected spectrum using the spectral density function in the form:

$$g(\omega) = \frac{c\omega^2}{\omega^4 - 2v\omega_0^2\omega^2 + \omega_0^4} \tag{14}$$

Then, we introduce the shape filter making use of the following assumptions:

- ⇨ In the two spectra (13) and (14) the maxima take place at the same frequency and are the same in magnitude
- ⇨ $\int_0^\infty \phi_{\xi\xi}(\omega)d\omega = \int_0^\infty g(\omega)d\omega$
- ⇨ The wave height processes are generated by the transmittance G(s). If the so-called "white noise" is at input, then it is a so-called shape filter. Transmittance G(s) is given by the formula [9]:

$$G(s) = \frac{a_0 s}{s^2 + a_1 s + a_2} \tag{15}$$

The relation (15) corresponds to the following set of state equations:

$$\left.\begin{aligned} g_1 &= \xi \\ g_2 &= \dot{\xi} - a_0 W \end{aligned}\right\} \tag{16}$$

$$\left.\begin{aligned} \dot{g}_1 &= g_2 + a_0 W \\ \dot{g}_2 &= -a_2 g_1 - a_1 g_2 - a_0 a_1 W \end{aligned}\right\} \tag{17}$$

where:
W – "white noise".

CONCLUSIONS

In the stochastic process of undulation, linear filters can be applied for irregular undulation in long time intervals. These filters are to be worked out in such a way that the parametric excitations generated by the wave can be described using basic spectra of Pierson-Moskowitz, ISSC, Jonswap, Striekałow-Massel or Paszkiewicz type.

The most frequently used wave spectra (in the dimensionless form - after parametrisation) are given by the following formula:

$$F = \frac{S_\eta(\omega)}{h_{1/3}^2 T_k} \tag{18}$$

where:
$S_\eta(\omega)$ – one-dimensional spectral density function
T_k – time periods
h – wave height.

An important stage in stochastic undulation modelling is selecting the parameters which describe the phenomenon and finding unique relations between wind parameters and undulation parameters.

The main conclusions which can be formulated based on the data presented in the article are the following:

- For both the wave spectrum, and the spectral density function, the maximum takes place at the same frequency and is the same in magnitude.
- The values of the integrals in the infinite interval for the wave spectrum and the spectral density function are equal to each other.
- After deriving the set of state equations, the further goal will be working out and solving Itô equations for symmetric movements.
- In order to obtain the final set of equations we have to determine coefficients in the equation $\dot{X} = \tilde{A}X + \tilde{B}W$, which will be done as part of future continuation of the subject matter presented here.

BIBLIOGRAPHY

1. Davis M.R.: Holloway D.S. and Watson N.L., *Dynamic wave loads on a high speed catamaran ferry fitted with t-foils and stern tabs*. Transactions of the Royal Institution of Naval Architects, International Journal of Maritime Engineering, Vol.148, Part A1, 1-16, 2006
2. Gichman I.I.: Skorochod A.W., *Introduction to the theory of stochastic processes* (in Polish). Warsaw 1968
3. Gutowski R.: *Ordinary differential equations* (in Polish), Warsaw 1971
4. Kang D., Hasegawa K., *Prediction method of hydrodynamic forces acting on the hull of a blunt-body ship in the even keel condition*. Journal of Marine Science and Technology, Vol. 12, Number 1, 1-14, 2007.
5. Królicka A.: *Stochastic approach to the dynamics of a linear floating object*. Marine Technology Transactions-Vol.17, pp.121-130, Gdańsk 2006.
6. Rumianowski A.: *Studying the dynamics of selected marine floating objects* (in Polish). Gdańsk 2003
7. Rumianowski A.: *Stochastic approach to the dynamics of marine floating objects*. Marine Technology Transactions-Vol.17, pp. 155-165, Gdańsk 2006
8. Sobczyk K.: *Stochastic differential equations* (in Polish). Warsaw 1996
9. Sobczyk K.: Spencer Jr.,B.F., *Stochastic models of material fatigue* (in Polish). Wydawnictwa Naukowo-Techniczne, Warsaw 1996
10. Trębacki K., Królicka A.: *External loads for multihull watercraft*. Vibrations in physical systems, Vol.XXIII-pp 371-376, Poznań 2008.

CONTACT WITH THE AUTHOR

Agnieszka Królicka, Ms. C.
Faculty of Ocean Engineering
and Ship Technology,
Gdańsk University of Technology
Narutowicza 11/12
80-952 Gdańsk, POLAND
e-mail : krag@pg.gda.pl
phone:(058) 347-11-46

Photo: Cezary Spigarski

POLISH MARITIME RESEARCH 4(58) 2008 Vol 15; pp. 17-20
10.2478/v10012-007-0092-z

Experimental research on hydroelastic behaviour of a tank model subdivided into liquid-filled compartments

Kazimierz Trębacki, Ph. D.
Gdansk University of Technology

ABSTRACT

The research was performed with the use of plexiglass models subdivided into 12 separate compartments. The compartments can be filled with a liquid. The model was excited to vibrations within a given frequency band by means of an exciter and accelerations were measured in selected points of the model. During measurement series oscillograms were obtained for various filling states at continuously changing range of measured frequencies. The oscillograms obtained for free vibrations measured on liquid-filled tank models were then processed. Results of the model tests were compared with those theoretically calculated for simple cases of tank-liquid system. The simple cases were used to test correctness of the elaborated computational program for determining hydrodynamic loads applied to tank walls. The application program for determining hydrodynamic internal loads was elaborated. Also, the influence of liquid filling state on values of loading, accelerations and wall deformations was demonstrated.

Keywords: vibrations, hydroelasticity, modelling, ship tanks for liquid

INTRODUCTION

The research concerns an internal hydroelasticity problem and is devoted to experimental vibration tests on a model of liquid – filled tank. It constitutes a continuation of other work where motion of liquid inside the tank has been taken into account. The research deals with transverse vibrations in vertical plane of the liquid - filled deformable tank. Oscillograms were obtained for dry model (free of liquid) as well as the model fully filled with liquid. Next, the oscillograms were processed with respect to vibration of the model within the measuring frequency range.

CHOICE OF A KIND OF ANALYSIS

The crucial problem in measuring is to determine a kind of frequency analysis which fits the best to a character of vibrations to be measured. Generally, signals which contain discrete frequency components, signals of vibrations which occur in extremely unfavourable conditions as well as spectral density measurements are most correctly analyzed by narrow-band filters of a constant bandwidth, whereas broad – spectrum vibrations including system's resonance are analyzed best by means of filters of a constant relative bandwidth.

Choice of analyzed bandwidth is a compromise between required accuracy and duration time of analysis – generally, the smaller bandwidth the longer time necessary to ensure a reasonable accuracy. Application of a real-time analyzer would reduce duration time of the analysis to a minimum but its dynamic range is usually somewhat smaller than that of other kinds of frequency analyzers.

Another choice is also possible: in which case to use a linear mode of frequency tuning, and when logarithmic one. The linear frequency tuning is more favourable when harmonic components of a given frequency are searched for; in the remaining cases application of the logarithmic frequency tuning is more favourable.

To the analysis with constant relative bandwidth the logarithmic frequency tuning is always applied.

The relative bandwidth is defined by the following formula:

$$f_w = \frac{f_g - f_d}{f_o} \tag{1}$$

where:
f_g – upper band frequency
f_d – lower band frequency
f_o – mid-frequency calculated as the mean geometrical value of lower and upper frequencies:

$$f_o = \sqrt{f_d} \cdot f_g \tag{2}$$

The relative bandwidth of analyzers is of a value within the range from 1 % to 23 %. In the logarithmic tuning their bandwidth is constant and in the linear tuning their bandwidth is proportional to the mid-frequency:

$$B = n\%\, f_o \tag{3}$$

Constant frequency bandwidth analyzers have the following bandwidths: 3.16 Hz, 10 Hz, 31.6 Hz, 100 Hz, 316 Hz i 1000 Hz. In the linear tuning widths of the bands are constant, and in the logarithmic one their widths decrease in a logarithmic scale along with frequency increasing.

CHOICE OF MEASUREMENT PARAMETERS

Accuracy of measurement results depends on an assumed period of the averaging of speed of recorder tape tracking and strip velocity (of recorder response), width of a measured band and filter response time.

For instance, too short averaging time would not ensure statistically reliable samples of random signal, and too small writting velocity would cause that recording pen would fall behind with appropriate changing the signal, and this way its ups and downs could be lost. A longer averaging time would give a statistically better accuracy, but of course time of analysis would be longer. Excessively large writting speed can often lead to an undesirable fluctuation of a recorded signal level, which otherwise could be damped. As time of analysis and its accuracy are mutually conflicting it should be carefully considered which aspect is more important in a considered case.

In order to reduce the measurement amplitude accuracy of ±1 dB and frequency shift by ¼ filter band, the following procedure should be assumed in determining the measurement parameters.

The filter bandwidth B and filter response time T_R are mutually dependent according to the following formula:

$$B\,T_R \approx 1 \tag{4}$$

The filter response time T_R determines the filter tuning time T_D:

$$T_D \geq 4T_R \tag{5}$$

From the formulas (4) and (5) the relation between the bandwidth of analyzed frequencies and the tuning time of the bands is achieved:

$$B\,T_D \geq 4 \tag{6}$$

From the relation (6) results that if to extend bandwidth of analyzed frequency the filter tuning time can be shortened at the same measurement accuracy maintained, and this way the whole measurement process can be accelerated.

For random signals the following should be assumed to obtain the accuracy of ±1.5 dB:

$$B\,T_D \geq 10 \tag{7}$$

and to obtain the accuracy of ±0.6 dB:

$$B\,T_D \geq 50$$

The signal averaging time can be determined by using the following formula:

$$T_A \leq \tfrac{1}{2}T_D \tag{8}$$

There are available ready-to-use diagrams from which the tuning time T_D, signal averaging time T_A, and tuning rate $S = B/T_D$ can be promptly determined for measurements of both determinate and random signals.

MEASURING SYSTEM

Schematic diagram of the measuring system is presented in Fig. 1.

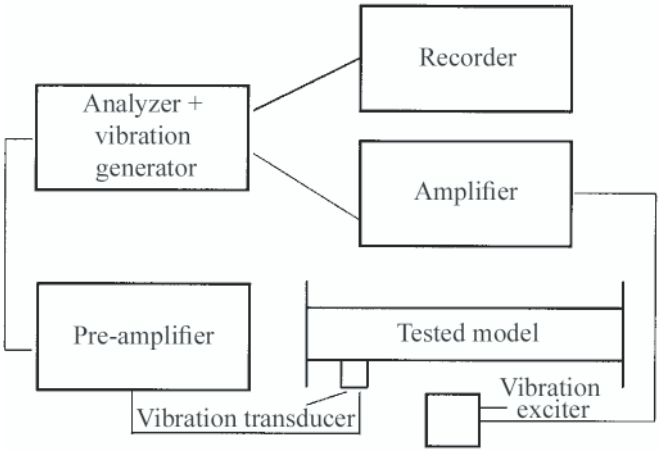

Fig. 1. *Schematic diagram of measuring system*

The measuring system consists of 2010 Brüel-Kjaer analyzer fitted with beat-frequency generator. Measurements of vibrations at a given frequency is synchronized with that excited.

The so generated signal is transmitted to the amplifier. The amplified signal is transmitted from the amplifier to the electrodynamic exciter of vibrations. The exciter's core connected with the model by means of a clamping ring, excites the model to vibrations in the frequency band of 63 Hz ÷ 6300 Hz.

Vibration accelerations are measured by means of 4324 Brüel-Kjaer piezo-electric transducer. The signal is transferred to 2625 Brüel-Kjaer pre-amplifier, and next to the 2010 analyzer. The so measured quantities expressed in g – units are then saved by using a recorder.

MODEL OF TANK SUBDIVIDED INTO COMPARTMENTS

The model was made of 2 mm plexiglass plates. Its dimensions were: 1340 mm in length, 204 mm in breadth and 120 mm in depth. The model was subdivided by a few transverse bulkheads and one longitudinal bulkhead in its plane of symmetry. This way 12 compartments were formed. The model was rigidly connected with a structure made of 200x70x8 channel bar and loaded by metal plates. The full weight of the model fixing structure amounted to about 200kG. The model was fastened to the metal structure by means of thirteen M12 bolts.

The model and the way of its fastening is presented in Fig. 2 and Photos 1 and 2.

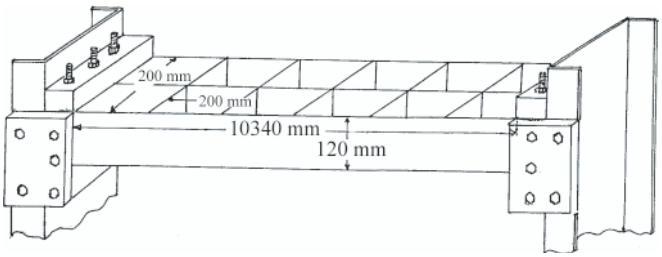

Fig. 2. *Draft of the model and way of its fastening*

MEASUREMENTS CARRIED OUT ON THE TANK MODEL AND THEIR RESULTS

The measurements were performed in three characteristic points: 1 – in the middle of the side bulkhead of the first compartment counting from the model mid-length; 2 – in the middle of the bottom of the same compartment; 3 – in the

connection of the compartments 170 mm distant from the mid-length (see Fig. 2 – shaded compartment).

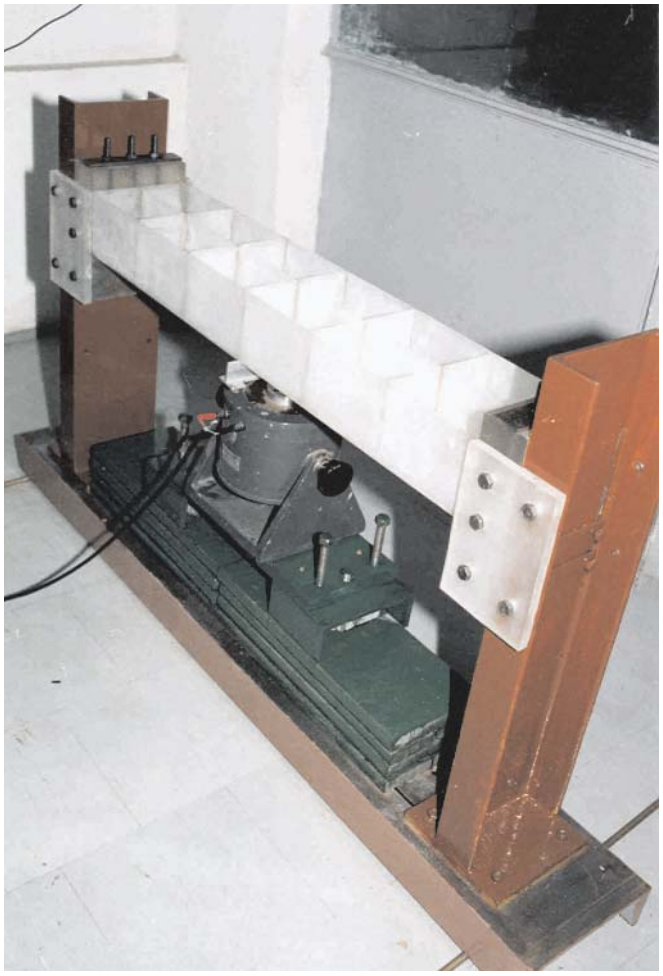

Photo 1. *Overall view of the testing installation*

Photo 2. *The tested model connected with vibration exciter*

The measurements were performed for the empty model and that with all the compartments filled with water. The influence of the water on vibration damping is shown in Fig. 3 through 8. In each case the amplification of the exciter fixed by means of the clamping ring in the middle of the model,

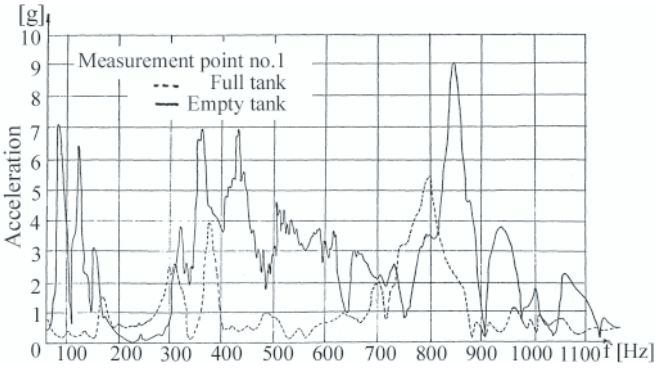

Fig. 3. *Run of vibrations at the measuring point 1*

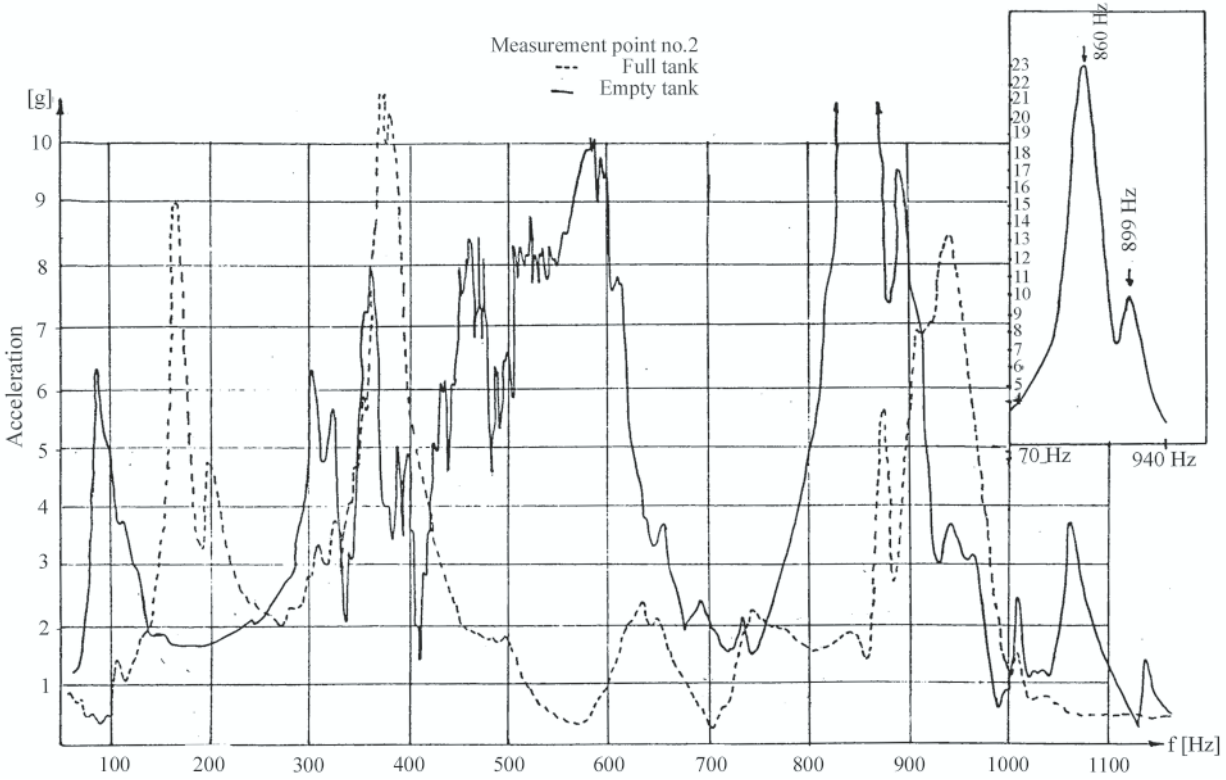

Fig. 4. *Run of vibrations at the measuring point 2*

was the same. Comparing the vibrations in the points 1, 2 and 3 one can state that character of the vibrations in the points 1 and 2 decisively differ from those in the point 3. The form of vibration spectrum in the points 1 and 2 of the empty model is influenced mainly by excitation of the bulkheads considered as plates, especially in the frequency range from 300 Hz to700 Hz. The vibrations became damped after filling the tank with water. To determine vibration resonance frequency of the model considered as a beam the diagrams shown in Fig. 7 and 8 should be compared.

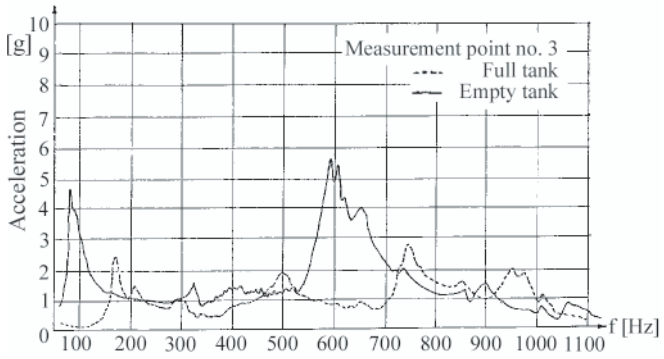

Fig. 5. *Run of vibrations at the measuring point 3*

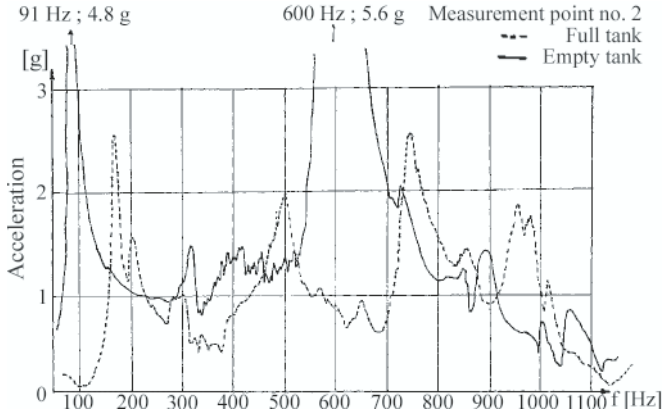

Fig. 6. *Vibration spectrum at the measuring point no. 2*

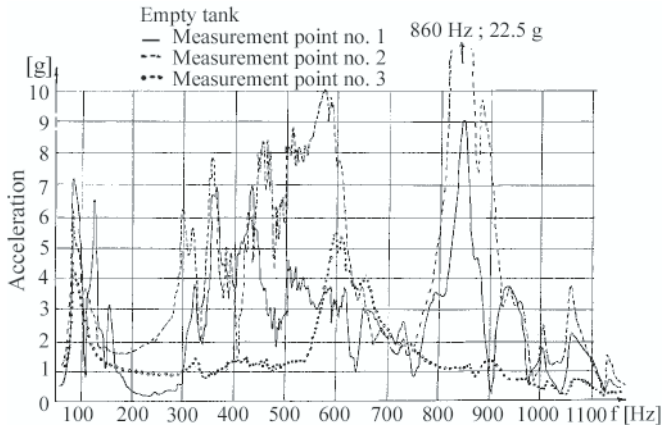

Fig. 7. *Comparison of vibration characteristics for empty tank*

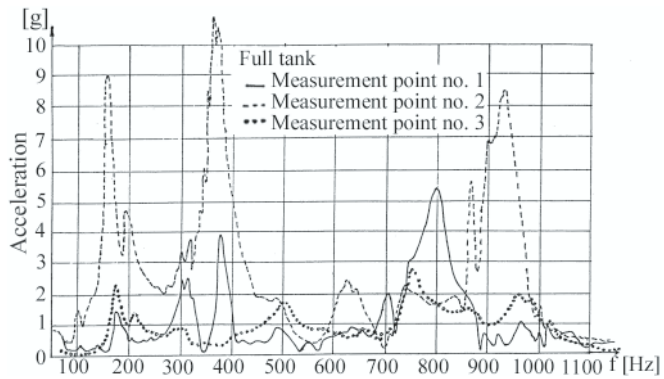

Fig. 8. *Comparison of vibration characteristics for tank full of liquid*

The measuring system used for the above presented measurements has been already described. To recording of their results a compensatory recorder of Carl Zeiss Jena was applied. Result analysis was carried out for frequencies linearly selected from the range of 60 Hz ÷ 1100 Hz, and for 10 Hz filtering band (Photo 2).

CONCLUSION

The performed work makes it possible to verify theoretical analysis by means of results of experimental tests on laboratory models. The results may be useful for designers constructors and users of ship and offshore structures in sea conditions.

NOMENCLATURE

B – filter width
f_d – lower band frequency
f_g – upper band frequency
f_o – mid- frequency of band
P – recorder tape stracking speed
S – tuning rate
T_A – averaging time
T_D – filter tuning time
T_R – filter response time

BIBLIOGRAPHY

1. Bathe K.J.: *Finite Element Procedure in Engineering Analysis*. Prentice Hall, New Jersey, 1982
2. Roliński Y.: *Resistance extensometry* (in Polish).WNT (Scientific Technical Publishing House), Warsaw 1981
3. Styburski W.: *Extensometric transducers* (in Polish). WNT (Scientific Technical Publishing House), Warsaw 1971
4. Trębacki K.: *Hydrodynamic loads on ship and offshore structures filled with liquid* (in Polish), Part I and II, Research reports No. 52/99 and 53/99, Faculty of Ocean Engineering and Ship Technology, Gdańsk University of Technology, Gdańsk 1999
5. Trębacki K.: *Free vibrations of a deformable tank filled with liquid* (in Polish). Technika Morska (Marine Technology), Vol. I, p. 173-192, Polish Academy of Sciences, Gdańsk 1989
6. Trębacki K.: *Selected problems of hydroelastic behaviour of tanks filled with liquid* (in Polish). Research report No.14/02/ BW, Faculty of Ocean Engineering and Ship Technology, Gdańsk University of Technology, Gdańsk 2002
7. Zienkiewicz O.C., Bettes P.: *Fluid-structure dynamic interaction and wave forces. An introduction to numerical treatment*. Int. J. for Num. Meth. in Eng., 13, 1, 1-76, 1978.

CONTACT WITH THE AUTHOR

Kazimierz Trębacki, Ph. D.
Faculty of Ocean Engineering
and Ship Technology
Gdansk University of Technology
Narutowicza 11/12
80-952 Gdansk, POLAND
e-mail : katre@pg.gda.pl

POLISH MARITIME RESEARCH 4(58) 2008 Vol 15; pp. 21-29
10.2478/v10012-007-0093-y

Graphical presentation of the power of energy losses and power developed in the elements of hydrostatic drive and control system

Part II

Rotational hydraulic motor speed parallel throttling control and volumetric control systems

Zygmunt Paszota, Prof.
Gdansk University of Technology

ABSTRACT

Paper presents graphical interpretation of the power of energy losses in the hydrostatic drive and control system elements and also of the power developed by those elements. An individual system fed by a constant capacity pump, where rotational hydraulic motor speed control is effected by a parallel throttling control system, is analyzed and also a system with the rotational hydraulic motor speed volumetric control by a variable capacity pump, an individual system with a rotational hydraulic motor volumetric speed control by means of a simultaneous change of the pump capacity per one revolution and change of the motor capacity per one revolution, the system operating at the constant pressure in the pump discharge conduit equal to the nominal pressure of the system: $p_{P2} = p_n$ and central system (with situated in parallel and simultaneously operating motors) with volumetric speed control of each rotational hydraulic motor by a motor secondary circuit assembly, the system fed by a pump with variable capacity per one shaft revolution fitted with pressure regulator $p_{P2} = p_n$.

Keywords: hydrostatic drive and control system, power of energy losses, energy efficiency

SYSTEM OF THE MOTOR SPEED PARALLEL THROTTLING CONTROL

Fig. 14 presents the areas of power of energy losses occurring in the elements of **an individual system fed by a constant capacity pump, where rotational hydraulic motor speed control is effected by a parallel throttling control system**. The parallel throttling control assembly may have a form of a set throttling valve (Fig. 15a) or a set 2 – way regulator (Fig. 15b) placed at the pump discharge conduit branch.

The use of a constant capacity pump (Q_P = cte) in a motor speed parallel throttling control system is a necessary condition from the point of view of achieving a relatively precise change of the flow intensity Q_M towards the motor and the change of motor speed ω_M (n_M) by means of the change of flow intensity Q_0 of the stream controlled by a throttling valve (2 – way flow regulator) and directed to the tank ($Q_P - Q_0 = Q_M$).

The current useful power $P_{Mu} = M_M\ \omega_M$ of the hydraulic motor (independent of the used motor speed control structure), required by the motor driven device (and the same as in the systems shown in Fig. 2, 5, 8 and 11 - PMR 03/2008 Part. I), influences in a different way (than in the series throttling control systems) the structural losses generated in the system.

The current small hydraulic motor loading torque M_M has a direct impact on the lowered level of the pump discharge pressure p_{P2}, the pressure resulting from the decrease Δp_M of pressure in the motor and losses Δp_C of pressure in the system conduits ($p_{P2} = \Delta p_M + \Delta p_C$). In effect, the power ΔP_{stp} of structural pressure losses is reduced to zero ($\Delta P_{stp} = 0$) and the power ΔP_{stv} of structural volumetric losses is clearly smaller than in a system with constant capacity pump feeding the motor speed series throttling control assembly ($\Delta P_{stv} = p_{P2}\ (Q_P - Q_M)$).

In a rotational hydraulic motor, operating in the conditions of parallel throttling speed control, occur power ΔP_{Mm} of mechanical losses, power ΔP_{Mv} of volumetric losses and power ΔP_{Mp} of pressure losses of the values close to powers ΔP_{Mm}, ΔP_{Mv} and ΔP_{Mp}, which would occur in such a motor with the series throttling speed control (with a tendency to slight decrease of the power ΔP_{Mm} of mechanical losses and the power ΔP_{Mv} of volumetric losses, due to decrease of pressure p_{M2} at the motor outlet in the parallel throttling control system).

Power $\Delta P_C = p_C\ Q_M$ of pressure losses in the conduits of the discussed system with parallel throttling control is equal to the power ΔP_C of pressure losses in the above analyzed four systems with the series throttling control.

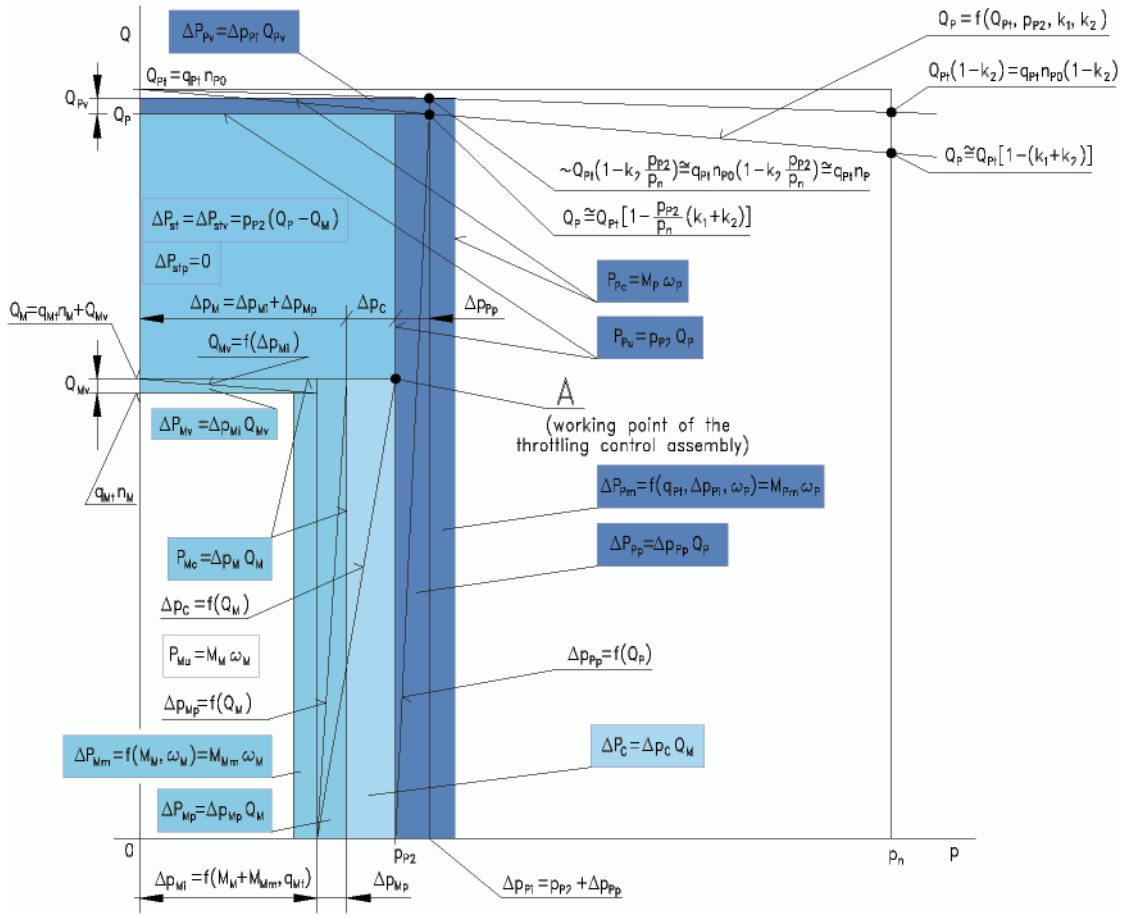

Fig. 14. Graphical interpretation of power losses in a hydrostatic drive and control system elements. Individual system with rotational hydraulic motor speed parallel throttling control fed by a constant capacity pump; the parallel throttling control assembly in the form of: – set throttling valve, – set two-way flow regulator

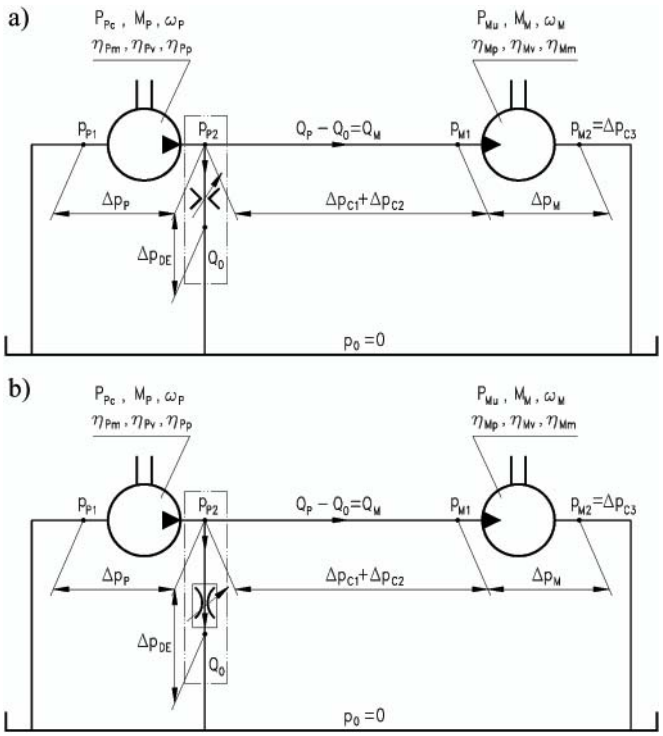

*Fig. 15. Individual system with the rotational hydraulic motor speed parallel throttling control; the throttling control assembly in the form of: **a)** set throttling valve, **b)** set two – way flow regulator*

In the constant capacity pump, due to its operation with the discharge pressure p_{P2} lower than in the series throttling control systems, a slight increase of the power $\Delta P_{Pp} = \Delta p_{Pp}\, Q_P$ of pressure losses occurs, and at the same time clear decrease of the power $\Delta P_{Pv} = \Delta p_{Pi}\, Q_{Pv}$ of volumetric losses and also decrease of the power $\Delta P_{Mp} = M_{Pm}\, \omega_P$ of mechanical losses.

When the hydraulic motor is loaded with small torque M_M, as an effect of decreased power of losses in system elements, the power $P_{Pc} = M_P\, \omega_P$ absorbed by the pump from the drive (electric or internal combustion) motor is also decreased compared with power P_{Pc} absorbed by a constant capacity pump used in the motor speed series throttling control system. With the unchanged hydraulic motor useful power $P_{Mu} = M_M\, \omega_M$, this increases the energy efficiency η of the whole system compared with the efficiency η of a series throttling control system fed by a constant capacity pump.

The discussed structure of a hydraulic system, with a constant capacity pump and with hydraulic motor parallel throttling speed control, may achieve, during the operation with maximum speed ω_{Mmax} (n_{Mmax}) of the controlled motor and in the full range $0 \le M_M \le M_{Mmax}$ of its load, energy efficiency η equal to the total efficiency η of the system with volumetric control of the hydraulic motor speed (with a variable capacity pump).

SYSTEM OF THE MOTOR SPEED VOLUMETRIC CONTROL BY A VARIABLE CAPACITY PUMP

Fig. 16 interprets the areas of power of energy losses in the elements of **a system with the rotational hydraulic motor speed volumetric control by a variable capacity pump**.

The hydraulic motor (with a constant capacity q_{Mt} per one shaft revolution) shaft speed ω_M (n_M) volumetric control by the

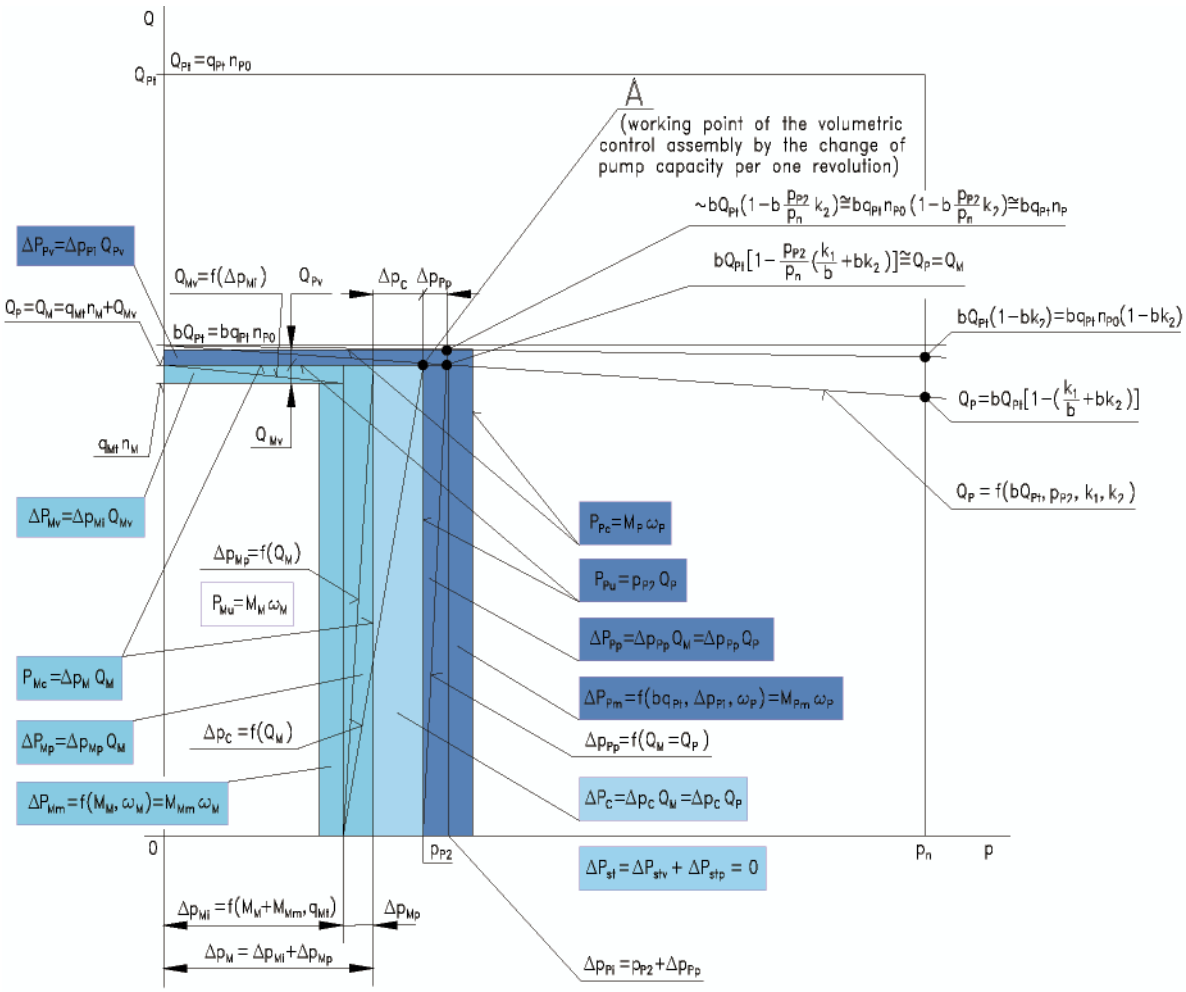

Fig. 16. *Graphical interpretation of power losses in a hydrostatic drive and control system. Individual system with rotational hydraulic motor (with constant capacity per one revolution) speed volumetric control by a pump with variable capacity per one revolution*

change of its capacity Q_M required by the motor, allowing to achieve the speed ω_M (n_M) imposed by the motor driven device, is effected by the change of capacity of the motor feeding pump (Fig. 17).

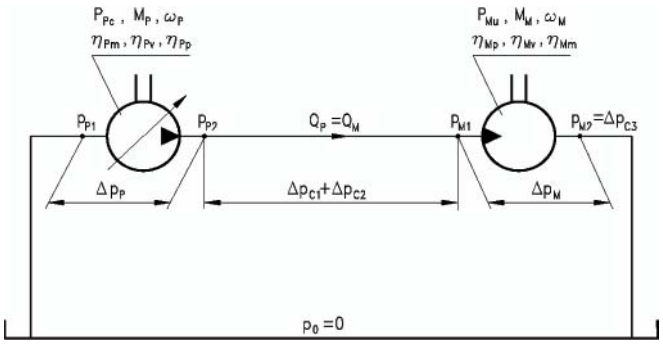

Fig. 17. *Individual system with hydraulic motor speed volumetric control by a variable capacity pump*

The imposed motor speed ω_M (n_M) is obtained by the corresponding pump capacity Q_P ($Q_P = Q_M$). Therefore, eliminated are the structural volumetric losses ($\Delta P_{stv} = 0$) and structural pressure losses ($\Delta P_{stp} = 0$) connected with the hydraulic motor speed throttling control assembly structure.

The current pump discharge pressure p_{P2} results from the sum of current pressure decrease Δp_M required by the driven hydraulic motor and pressure losses Δp_C in the conduit between the pump and motor and in the motor outlet conduit. The maximum limit pressure value p_{P2max} in the pump discharge conduit is determined by the safety valve (closed during the normal pump operation, i.e. in the $0 < p_{P2} \leq p_n$ pressure range) whose opening pressure is higher than the nominal pressure p_n of the system (maximum pressure of continuous system operation).

In a rotational hydraulic motor, operating in a speed ω_M (n_M) control system by a variable capacity pump, occur the same values of power ΔP_{Mm} of mechanical losses, power ΔP_{Mv} of volumetric losses and power ΔP_{Mp} of pressure losses as in the system where the change of speed ω_M (n_M) is controlled by series throttling control assembly and the system is fed by a constant capacity pump. Power ΔP_{Mm} of mechanical losses and ΔP_{Mv} of volumetric losses in the motor are slightly lower than power of those losses that would occur in a motor with the series throttling control system, where the flow is throttled at the motor outlet (the motor outlet pressure p_{M2} is higher).

Power $\Delta P_C = \Delta p_C\, Q_M$ of pressure losses in the conduits of the hydraulic motor speed volumetric system with a variable capacity pump is (with an unchanged motor shaft required speed ω_M (n_M)) equal to the power ΔP_C of losses in the motor speed series or parallel throttling control systems.

In a variable capacity pump feeding the hydraulic motor occurs (with the motor useful power $P_{Mu} = M_M\, \omega_M$ unchanged) decrease of power $\Delta P_{Pp} = \Delta p_{Pp}\, Q_P$ of pressure losses (due to decrease of Δp_{Pp} and Q_P), decrease of power $\Delta P_{Pv} = \Delta p_{Ppi}\, Q_{Pv}$ of volumetric losses (due to decrease of Δp_{Pi} and Q_{Pv}) and decrease of power $\Delta P_{Pm} = M_{Pm}\, \omega_P$ of mechanical losses (due to decrease of M_{Pm} and slight increase of ω_P).

In a volumetric motor (with a constant capacity per one revolution) speed control system (by a variable capacity pump), the sum of current (unchanged in relation to power P_{Mu} in the

above discussed systems) value of hydraulic motor useful power $P_{Mu} = M_M \omega_M$ and of:

- ✶ power $\Delta P_{Mm} = M_{Mm} \omega_M$ of mechanical losses in the motor
- ✶ power $\Delta P_{Mv} = \Delta p_{Mi} Q_{Mv}$ of volumetric losses in the motor
- ✶ power $\Delta P_{Mp} = \Delta p_{Mp} Q_M$ of pressure losses in the motor
- ✶ power $\Delta P_C = \Delta p_C Q_M$ of pressure losses in the hydraulic system connecting conduits
- ✶ power $\Delta P_{Pp} = \Delta p_{Pp} Q_P$ of pressure losses in the pump
- ✶ power $\Delta P_{Pv} = \Delta p_{Pi} Q_{Pv}$ of volumetric losses in the pump
- ✶ power $\Delta P_{Pm} = M_{Pm} \omega_P$ of mechanical losses in the pump

decides that the power $P_{Pc} = M_P \omega_P$ required by the pump from the pump driving (electric or internal combustion) motor is smaller than power P_{Pc} absorbed by the pump in the above discussed systems with the hydraulic motor speed throttling control.

Energy efficiency $\eta = P_{Mu}/P_{Pc}$ of a system with volumetric control by a variable capacity pump is the highest efficiency η amongst the considered systems in the whole range of speed $0 \le \omega_M \le \omega_{Mmax}$ and hydraulic motor load $0 \le M_M \le M_{Mmax}$. However, it has to be noted that the energy advantage of a system with the hydraulic motor speed ω_M (n_M) control by a variable capacity pump over the systems with the motor speed throttling control decreases markedly when the motor speed ω_M approaches ω_{Mmax} and the motor load approaches M_{Mmax}.

SYSTEM OF THE MOTOR SPEED VOLUMETRIC CONTROL BY A VARIABLE CAPACITY PUMP AND A MOTOR WITH VARIABLE CAPACITY PER ONE REVOLUTION, SYSTEM OPERATING AT NOMINAL PRESSURE P_N

Fig. 18 illustrates the areas of power of energy losses in **an individual system with a rotational hydraulic motor volumetric speed control by means of a simultaneous change**

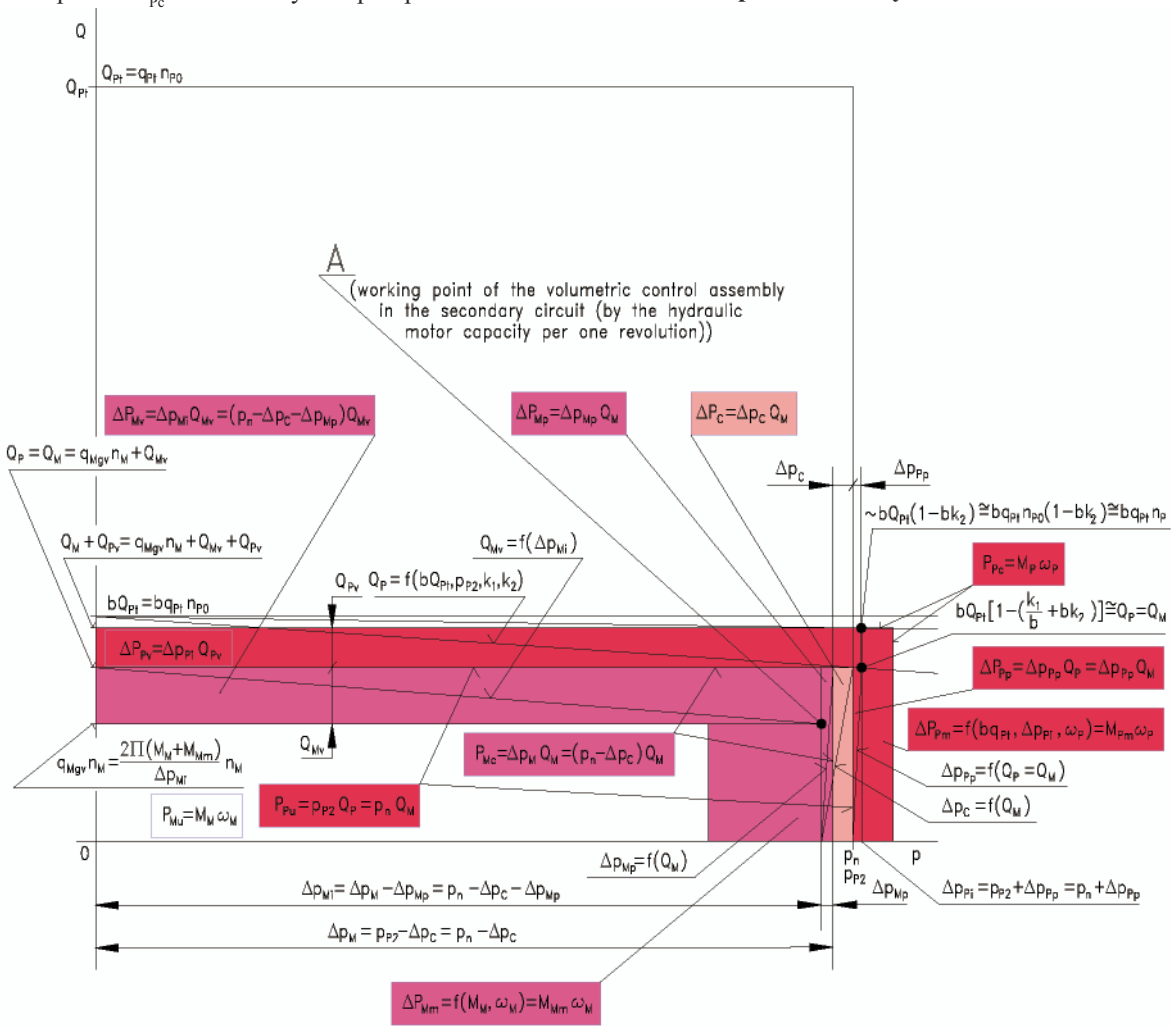

Fig. 18. *Graphical interpretation of power losses in a hydrostatic drive and control system elements:*

– *Individual system with the rotational hydraulic motor speed volumetric control by a pump with variable capacity per one revolution and a motor with variable capacity per one revolution operating at the nominal pressure $p_{P2} = cte \approx p_n$; capacity q_{Mgv} per one motor revolution determines, at a given loading M_M, the nominal pressure in the pump discharge (outlet) conduit: $p_{P2} \approx p_n$, and capacity q_{Pgv} per one pump revolution controls the motor rotational speed n_M*

– *Central system with the rotational hydraulic motor speed volumetric control in the secondary motor circuit, fed by a pump with a variable capacity per one revolution fitted with pressure regulator $p_{P2} = cte = p_n$ (Rexroth conception) – operation with one motor fed; (coefficient "a_1" of the increase of regulator controlled pump pressure: $a_1=0$)*

The Figure demonstrates the system with motor speed volumetric control by the so called secondary motor circuit (adjusting, by the change of capacity q_{Mgv} per one shaft revolution, the pressure decrease Δp_M in the motor to a value $\Delta p_M = p_n - \Delta p_C$, and at the same time setting the motor speed ω_M (n_M) required by the motor driven device); the system is fed by the pump (with variable capacity q_{Pgv} per one shaft revolution) fitted with pressure regulator $p_{P2} = p_n$.

of the pump capacity per one revolution and change of the motor capacity per one revolution, the system operating at the constant pressure in the pump discharge conduit equal to the nominal pressure of the system: $p_{P2} = p_n$.

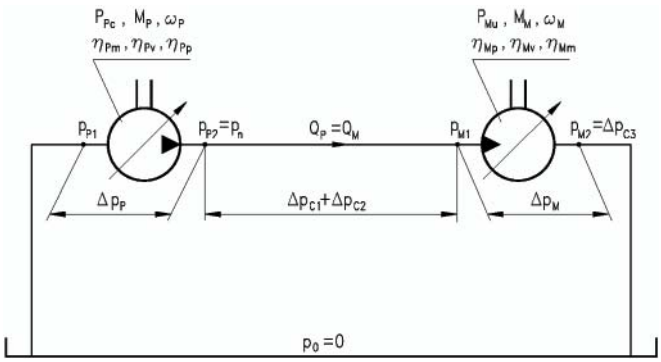

Fig. 19. *Individual system with the rotational hydraulic motor speed volumetric control by means of simul-teneous change of the pump capacity per one revolution and change of the motor capacity per one revolution; system operating at the constant pressure in the pump discharge conduit equal to the system nominal pressure: $p_{P2} = p_n$*

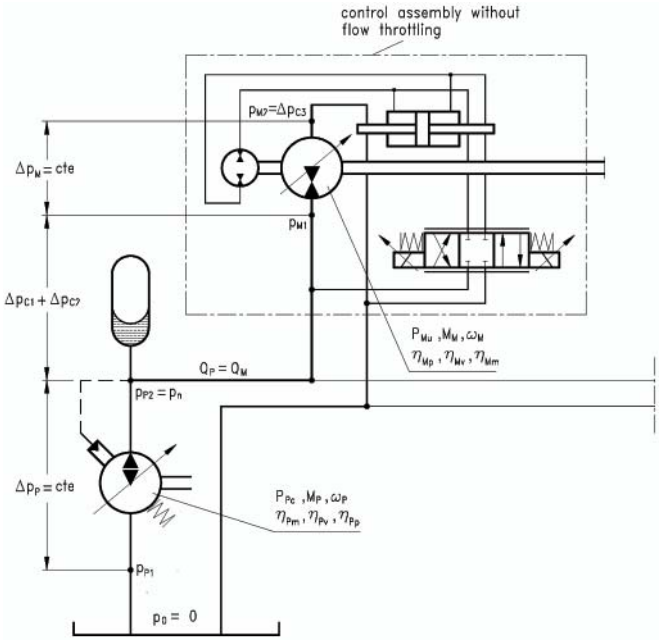

Fig. 20. *Central system, with rotational motors situated in parallel, with volumetric control of each motor speed by a secondary circuit assembly, system fed by a variable capacity pump cooperating with regulator in a constant pressure conditions: $p_{P2} = cte \approx p_n$ (conception of the Rexroth company) – during one motor operation*

This solution allows to use pump useful power P_{Pu} (resulting from a product of pump working pressure p_{P2} equal to the nominal system pressure p_n ($p_{P2} = p_n$) and maximum pump capacity Q_{Pmax} achieved at the coefficient $b = q_{Pgv}/q_{Pt} = 1$ of the change of the pump capacity per one revolution) also during the period of smaller hydraulic motor load (with the torque $M_M < M_{Mmax}$), by an increase of the motor speed ω_M above its nominal speed ω_{Mn} ($\omega_M > \omega_{Mn}$).

Nominal pressure in the pump discharge conduit: $p_{P2} = p_n$, at a given load M_M, is determined by the changing capacity q_{Mgv} per one motor shaft revolution, the motor speed ω_M (n_M) is controlled by the capacity q_{Pgv} per one pomp revolution.

The idea of feeding by one pump (of variable capacity q_{Pgv} per one revolution), at a constant pressure level $p_{P2} = p_n$ in its discharge conduit, of two or more simultaneously operating hydraulic motors (of variable capacity q_{Mgv} per one revolution) has been used by the Rexroth company in the conception of a hydraulic **central system (with situated in parallel and simultaneously operating motors) with volumetric speed control of each rotational hydraulic motor by a motor secondary circuit assembly, the system fed by a pump with variable capacity per one shaft revolution fitted with pressure regulator $p_{P2} = p_n$** (Fig. 20 – central system during one motor operation).

The speed ω_M (n_M) control of each of the simultaneously operating hydraulic motors in the central system by an own secondary circuit assembly consists in a solution where the capacity q_{Mgv} per one revolution adjusts the decrease of pressure Δp_M, required by the motor, to a value $\Delta p_M = p_n - \Delta p_C$ (i.e. to a value equal to the difference of pressure $p_{P2} = p_n$ in the pump discharge conduit and pressure drop Δp_C in the conduits of a system) and, at the same time, the motor speed ω_M (n_M), required by the motor driven device, is controlled by that assembly.

The use of the central system solution with parallelly situated rotational hydraulic motors, where the speed ω_M (n_M) of each motor (driving one of the simultaneously operating devices) is determined by its secondary circuit assembly (structurally connected with the motor), eliminates the need of setting the flow intensity Q_M, directed to each motor, by the throttling control assembly located on the branch to each motor and situated in series with the motor. Therefore, such solution eliminates the power $\Delta P_{stp} = \Delta p_{DE} Q_M$ of the structural pressure losses in the throttling control assembly (in the servo-valve, proportional directional valve, set throttling valve or set two - way flow regulator).

Conditions of work of such central system during feeding of one motor (from the point of view of the power of energy losses in the system) are very similar to the conditions of work of the above described individual system with volumetric control of the pump and motor (with one pump of variable capacity per one shaft revolution driving one hydraulic motor of variable capacity per one shaft revolution), where a constant pressure $p_{P2} = p_n$ in the pump discharge conduit is independent of the current hydraulic motor load M_M. These two systems differ from each other by the size of pump; in the individual system, its nominal capacity Q_{Pn} must provide the required nominal capacity Q_{Mn} of the driven motor; in the central system, the nominal capacity Q_{Pn} of the pump must be greater in order to deliver the flow of an intensity equal to the sum of the required nominal capacities Q_{Mni} of the simultaneously operating and parellelly connected motors.

However, let us assume, in order to compare the power of losses in those two systems of the hydraulic motor volumetric speed control with power of losses in the earlier discussed individual systems, that in both systems (the individual one and the central one feeding one motor) a pump is used with nominal capacity Q_{Pn} required by the nominal capacity Q_{Mn} of the controlled single motor. With such assumption, the conditions of work of both systems and power of energy losses are identical.

Let us consider the areas of power of losses in the elements of a central system according to the Rexroth company conception, with volumetric speed control of each motor by the secondary circuit assembly, the system feeding a single motor.

In a hydraulic motor with variable capacity q_{Mgv} per one shaft revolution, operating at the pressure decrease $\Delta p_M = p_n - \Delta p_C$ (i.e. only slightly lower than the nominal pressure p_n), the useful power $P_{Mu} = M_M \omega_M$ unchanged compared with previous system (Fig. 2, 5, 8, 11 - PMR 03/2008 Part. I, 14 and 16), resulting from the same torque M_M and motor shaft speed ω_M required by the driven device, the areas of power of losses in the motor have different shapes.

The power $\Delta P_{Mm} = M_{Mm}\,\omega_M$ of mechanical losses in the motor depends (apart from ω_M) on the torque M_{Mm} of those losses. Torque M_{Mm} of mechanical losses in the motor practically does not depend on the speed ω_M (n_M) and the current capacity q_{Mgv} per one motor shaft revolution, and depends mainly on the motor loading torque M_M. Therefore, the area of power ΔP_{Mm} of mechanical losses (Fig. 18) is practically the same as the area ΔP_{Mm} in a system with a pump with variable capacity per one revolution driving a motor with constant capacity q_{Mt} per one revolution (Fig. 16), although the shape of area ΔP_{Mm} (like the shape of area $P_{Mu} = M_M\,\omega_M$ of the unchanged useful power), presented on a plane with coordinates (p – pressure, Q – intensity), is different.

Power $\Delta P_{Mv} = \Delta p_{Mi}\,Q_{Mv}$ of volumetric losses in a hydraulic motor, with unchanged (compared with previous system) small motor useful power $P_{Mu} = M_M\,\omega_M$ (mainly at a small load M_M) increases, in the considered system, many-fold compared with power ΔP_{Mv} of volumetric losses in a motor with constant capacity q_{Mt} per one revolution (Fig. 16). This is an effect of simultaneous great increase of pressure decrease Δp_{Mi} in the motor working chambers and of accompanying great increase of intensity Q_{Mv} of the volumetric losses.

In turn, power $\Delta P_{Mp} = \Delta p_{Mp}\,Q_M$ of pressure losses in the motor channels (and in the directional control valve, if there is one), (motor with small instantaneous capacity q_{Mgv} per one shaft revolution) decreases distinctly both as an effect of the decrease of motor capacity Q_M (with unchanged n_M) and an effect of the accompanying decrease of Δp_{Mp}. Therefore, power ΔP_{Mp} of pressure losses in the motor with small capacity q_{Mgv} per one shaft revolution is lower then power ΔP_{Mp} of those losses in a motor with constant capacity q_{Mt} per one revolution (Fig. 16).

However, in an axial piston hydraulic motor with variable capacity q_{Mgv} per one revolution, operating with constant decrease Δp_M of pressure close to the system nominal pressure p_n, the energy gain connected with the smaller power ΔP_{Mp} of pressure losses will be much lower than the energy loss resulting from the increased (compared to a motor with constant capacity q_{Mt} per one revolution – Fig. 16) power ΔP_{Mv} of volumetric losses. In effect, the energy efficiency η_M of a motor operating in such conditions is lower.

Power $\Delta P_C = \Delta p_C\,Q_M$ of pressure losses in the conduits of a system operating with constant pressure $p_{P2} = p_n$ in the pump discharge is smaller than the power ΔP_C of those losses in a system with hydraulic motor with constant capacity q_{Mt} per one revolution. This is an effect of decreased flow intensity Q_M in the conduits. Also pressure losses Δp_C in the conduits are decreased.

From the point of view of power ΔP_C of losses in the connecting conduits, a system with hydraulic motor with variable capacity q_{Mgv} per one revolution, operating at constant pressure $p_{P2} = p_n$ in the pump discharge conduit, has great advantage over the systems with a motor of constant capacity q_{Mt} per one revolution, where the decreased motor loading torque M_M is accompanied by smaller decrease Δp_M of pressure required by the motor and, in effect, lower pressure p_{P2} in the pump discharge conduit ($p_{P2} < p_n$). With longer conduits and at low temperature (greater viscosity) of the working medium (hydraulic oil), the gain from energy savings in the conduits of a system with $p_{P2} = p_n$ may be considerable.

In a variable capacity pump cooperating with a $p_{P2} = p_n$ regulator, its capacity Q_P, with unchanged useful power $P_{Mu} = M_M\,\omega_M$ of the hydraulic motor (controlled by the secondary circuit assembly) driven by the pump is smaller than the capacity Q_P of the pump feeding a hydraulic motor with constant capacity q_{Mt} per one shaft revolution (i.e. in a situation when pressure p_{P2} is smaller than the nominal pressure – $p_{P2} < p_n$ (Fig. 16)). It is also accompanied by the decrease of power $\Delta P_{Pp} = \Delta p_{Pp}\,Q_P$ of pressure losses in the pump channels and the pump directional valve (due to decrease of pump capacity Q_P and decrease of pressure losses Δp_{Pp}).

Power $\Delta P_{Pv} = \Delta p_{Pi}\,Q_{Pv}$ of the pump volumetric losses, with unchanged (compared to the above described systems) small useful power $P_{Mu} = M_M\,\omega_M$ of the motor, increases many – fold, compared with power ΔP_{Pv} of volumetric losses in a variable capacity pump feeding directly a hydraulic motor with constant capacity q_{Mt} per one revolution (when $p_{P2} < p_n$; Fig. 16). Power ΔP_{Pv} of volumetric losses is practically equal to the power ΔP_{Pv} in a pump feeding a system with motor speed throttling control, the pump cooperating also with regulator in a constant pressure system $p_{P2} = p_n$ (although then the pump capacity Q_P is greater (Fig. 8)).

Analysing a pump feeding the hydraulic motor controlled in the secondary circuit (i.e. operating at constant pressure $p_{P2} = p_n$ and capacity Q_P corresponding to the current useful power $P_{Pu} = Q_P\,p_n$ of the pump related to the current useful power $P_{Mu} = M_M\,\omega_M$ of the driven motor) one can find, as the first approximation, that torque $M_{Pi} = \Delta p_{Pi}\,q_{Pgv}/2\Pi$ indicated in its working chambers is of the order of torque M_{Pi} of the variable capacity pump feeding the motor with constant capacity q_{Mt} per one revolution (Fig. 16). This is due to the fact, that with similar current useful power of the pump, for instance two-fold increase Δp_{Pi} of pressure in the pump chamber is accompanied by the nearly two-fold decrease q_{Pgv} of the capacity per one revolution. Therefore, it may be assumed with approximation that torque M_{Pm} of mechanical losses, proportional to the indicated torque M_{Pi} ($M_{Pm} \sim M_{Pi}$), will be similar in both cases. In effect, it may also be assumed, that area $\Delta P_{Pm} = M_{Pm}\,\omega_P$ of the power of mechanical losses in the pump will be similar to the area ΔP_{Pm} of mechanical losses in the pump feeding a system with hydraulic motor with constant capacity q_{Mt} per one revolution (Fig. 16), although the shape of the ΔP_{Pm} field is different .

As in a hydraulic motor controlled by own secondary circuit and operating in a continuous way with the decrease Δp_M of pressure close to the system nominal pressure p_n, the pump operation at the pressure $p_{P2} = p_n$ is connected with the energy gain resulting from the decrease of power $\Delta P_{Pp} = \Delta p_{Pp} Q_P$ of pressure losses in the pump, with a given unchanged useful power $P_{Mu} = M_M\,\omega_M$ of the motor, and with great energy loss connected with the increase of power $\Delta P_{Pv} = Q_{Pv}\,\Delta p_{Pi}$ of volumetric losses in the pump compared with the power of those losses in a variable capacity pump feeding a motor with constant capacity q_{Mt} per one shaft revolution (Fig. 16). With comparable power $\Delta P_{Pm} = M_{Pm}\,\omega_P$ of mechanical losses in the pump working in those two systems (Fig. 16 and 18), the sum of power of losses in the pump working at $p_{P2} = p_n$ is greater and its energy efficiency η_P is lower.

The sum ΔP of power of energy losses in a hydraulic motor with variable capacity q_{Mgv} per one shaft revolution, and in a pump with variable capacity q_{Pgv} per one shaft revolution working in the system with short connecting conduits, with the pump discharge conduit pressure equal to the nominal pressure ($p_{P2} = p_n$), may be, with small motor load M_M (Fig. 18), much greater than the sum ΔP of the power of losses in a system with motor with constant capacity q_{Mt} per one shaft revolution controlled volumetrically by variable capacity pump (Fig. 16).

In the operating conditions of a system with $p_{P2} = p_n$ (p_{P2} independent of the motor load M_M), a system with long connecting conduits (and greater pressure losses Δp_C in the conduits), operating with great viscosity ν of a working medium (hydraulic oil), the sum ΔP of power of losses may appear

smaller than the sum ΔP of losses in a system with motor with constant capacity q_{Mt} per one shaft revolution and with variable capacity pump (Fig. 16). With great oil viscosity, the energy gains connected with decrease of pressure losses in the system elements (mainly in the connecting conduits), achieved in effect of decreasing the intensity $Q_P = Q_M$, may appear great, but the power of volumetric losses ΔP_{Pv} in the pump and ΔP_{My} in the motor will not increase as distinctly as with the smaller viscosity.

CONCLUSIONS

- A diagram of the direction of increase of power stream from the shaft or piston rod of a hydraulic motor to the pump shaft, power increasing as an effect of the imposed power of energy losses in the hydrostatic drive and control elements, is proposed and justified.
- Graphical interpretation of the power of energy losses in the hydrostatic drive and control system elements and also of the power developed by those elements is presented.
- Chapters 2 – 5 (PMR 03/2008, Part. I) illustrate the fields of power ΔP of energy losses in the individual system elements, where the hydraulic motor (with constant capacity per one revolution) speed control is effected by series throttling of the working medium flow in order to obtain the intensity Q_M corresponding to the angular ω_M (rotational n_M) speed required by the motor driven device. The use of a throttling directional valve (servo – valve or proportional directional valve) or else set throttling valve or set two – way flow regulator allows to change the motor speed precisely. A cheaper constant capacity pump may be used as a feeding device in the system with series throttling control, the pump cooperating with the overflow valve or controlled overflow valve, or else a variable capacity pump cooperating with a constant pressure regulator or the *Load Sensing* variable pressure regulator.
  - Chapter 2 presents an individual system of motor speed series throttling control fed by a constant capacity pump cooperating with an overflow valve in constant pressure conditions.
    The required level of nominal pressure p_n of pump operation and the required level of pump theoretical capacity Q_{Pt} during the system operation, as well as the current small loading torque M_M and current small hydraulic motor shaft angular speed ω_M are decisive in that motor speed throttling control structure of temporary power ΔP_{stp} of structural pressure losses and power ΔP_{stv} of structural volumetric losses. This is then accompanied by a very low value of the overall energy efficiency η of the system.
    The power ΔP_{stp} of the structural pressure losses in the throttling control assembly may be reduced almost to zero during the hydraulic motor operation at the maximum shaft load M_{Mmax}.
    The power ΔP_{stv} of the structural volumetric losses in the throttling control assembly may be reduced almost to zero in a situation when the hydraulic motor operates with maximum angular speed ω_{Mmax} (rotational speed n_{Mmax}).
    The hydraulic motor operation with maximum load M_{Mmax} and simultaneous maximum speed $\omega_{Mmax}(n_{Mmax})$ may cause minimization of the power of losses connected with the motor speed throttling control and the sum of energy losses in the system consists of the hydraulic motor losses, the conduit losses and pump losses. The overall system efficiency η reaches then a high value η_{max}, close to the value of energy efficiency η_{max} of a system with the motor speed volumetric control (by a variable capacity pump).
    However, in order to be able, in a system with series throttling control, to load the hydraulic motor with a maximum torque M_{Mmax} close to the maximum load M_{Mmax} of the motor in a system with volumetric speed control, the throttling slot of the throttling proportional control valve (or of the throttling valve) has to be increased to the size requiring a small decrease $\Delta p_{DEmin} \approx 0$ of pressure at the maximum flow intensity $Q_{Mmax} \approx Q_P$.
    On the other hand, in order to be able, in a system with series throttling control, to set, with a throttling proportional control valve or a throttling valve, the maximum intensity $Q_{Mmax} \approx Q_P$, i.e. close to the pump capacity, an overflow valve has to be used in the system to stabilize the pressure level $p_{SP} \approx p_n$ of the pump operation at the flow intensity $Q_P - Q_M \approx 0$ (i.e. close to zero).
  - Chapter 3 presents an individual system of motor speed series throttling control fed by a constant capacity pump cooperating with a controlled overflow valve in variable pressure conditions.
    In effect, when the hydraulic motor is loaded with a small torque M_M, the power $\Delta P_{Pc} = M_P \omega_P$ absorbed by the pump from the drive (electric or internal combustion) motor is also significantly reduced, which, with an unchanged hydraulic motor useful power $P_{Mm} = M_M \omega_M$, increases the overall system energy efficiency η compared with the constant pressure feeding system efficiency η.
    Both structures ($p = cte$ and $p = var$) of the hydraulic motor speed series throttling control, fed by a constant capacity pump, may achieve, during maximum motor load M_{Mmax} and simultaneous maximum speed ω_{Mmax} (n_{Mmax}), the same maximum overall system efficiency η_{max}.
    It is close to the maximum energy efficiency η_{max} of a system with volumetric control (by a variable capacity pump) of hydraulic motor speed. The $p = var$ system becomes then a $p = cte$ system, therefore the operating conditions of both systems are the same and structural losses ΔP_{stp} and ΔP_{stv} in the throttling control assembly may be practically eliminated. However, similarly as in the constant capacity pump system $p = cte$, it requires increased area of the f_{DEmax} slot in the throttling directional control valve (throttling valve) to a size requiring slight pressure decrease $\Delta p_{DEmin} \approx 0$ at the maximum flow intensity $Q_{Mmax} = Q_P$. It requires also the use of a controlled overflow valve stabilizing the value $\Delta p_{SPS} = p_{P2} - p_2 = cte$ also at the flow intensity $Q_P - Q_M \approx 0$ (close to zero) and an overflow valve stabilizing the pressure level $p_{SP} \approx p_n$ at the flow intensity $Q_P - Q_M \approx 0$.
  - Chapter 4 presents an individual system of motor speed series throttling control fed by a variable capacity pump cooperating with regulator in constant pressure conditions.
    The use, as a hydraulic motor series throttling speed control system feeding source, a variable capacity pump with pressure regulator, operating at pressure $p_{P2} = cte \approx p_n$, allows, during the motor run with small speed ω_M (n_M), to reduce significantly the power $P_{Pc} = M_P \omega_P$ absorbed by the pump from the drive electric or internal combustion motor. With the unchanged useful power $P_{Mu} = M_M \omega_M$ of the hydraulic motor, the entire system energy efficiency η is significantly higher compared with efficiency η of

a constant pressure (p = cte) throttling assembly constant capacity pump feeding system.

The considered system may achieve, during the maximum hydraulic motor load M_{Mmax} and in the whole range of the motor speed change $0 \le \omega_M \le \omega_{Mmax}$, the overall efficiency η close to the value of energy efficiency η of a system with the motor speed volumetric control (by a variable capacity pump). The power $\Delta P_{stp} = \Delta p_{DE} Q_M$ of the structural pressure losses is then minimized. It requires, in a system with the hydraulic motor speed series throttling control, an increased area of the f_{DEmax} slot in the throttling directional control valve (or the throttling valve) to a size requiring slight pressure decrease $\Delta p_{DEmin} \approx 0$ at the maximum flow intensity $Q_{Mmax} = Q_{Pmax}$, i.e. equal to the full pump capacity. It requires also correct operation of the pump pressure regulator stabilizing the pump discharge pressure p_{p2} at the level $p_{p2} = cte \approx p_n$ in the whole range $0 \le Q_P \le Q_{Pmax}$ of the pump capacity variation.

In a situation of simultaneous maximum load M_{Mmax} and maximum speed ω_{Mmax} of a hydraulic motor controlled by series throttling, the maximum achievable energy efficiency η_{max} of a system is close to the value η_{max} of a system with hydraulic motor speed volumetric control i.e. directly by a variable capacity pump.

The greatest energy savings in the considered series throttling control system, compared with a series control system fed by a constant pressure constant capacity pump, are obtained during the hydraulic motor operation at small speed ω_M (n_M).

- Chapter 5 presents an individual system of motor speed series throttling control fed by a variable capacity pump cooperating with the *Load Sensing* regulator in variable pressure conditions.

  The use, as a feeding source of the hydraulic motor series throttling speed control system, of a variable capacity pump with the *Load Sensing* regulator operating at a pressure $p_{p2} = \Delta p_{LS} + p_2 \approx \Delta p_{LS} + p_{M1}$, i.e. slightly higher then the current pressure p_{M1} required by the hydraulic motor at its inlet (which is accompanied by decrease to a small value of the power ΔP_{st} of structural energy losses in the throttling control assembly) reduces the sum of power of energy losses in the system to a value only slightly higher then the sum of power of losses in the elements of a system with volumetric control of the motor speed (directly by a variable pump capacity). Power $P_{Pc} = M_P \omega_p$ absorbed by the pump from the electric or internal combustion drive motor is only slightly higher here then the power P_{Pc} of a variable capacity pump directly driving the hydraulic motor.

  The considered LS system operates in the whole range $0 \le M_M \le M_{Mmax}$ of the hydraulic motor load and in the whole range $0 \le \omega_M \le \omega_{Mmax}$ of its speed with the energy efficiency η only slightly lower then the efficiency η of a volumetric control system (directly by a variable capacity pump). The difference between overall efficiencies η of both systems will be inversely dependent on the capability of increase of the area of throttling proportional valve (or throttling valve) slot f_{DEmax}. The increase of f_{DEmax} allows to decrease $\Delta p_{DEmin} \approx 0$ at a maximum flow intensity $Q_{Mmax} = Q_{Pmax}$ (i.e. equal to a full pump capacity). It also requires correct operation of the pump LS regulator adjusting, in the whole range $0 \le Q_P \le Q_{Mmax}$ of the pump capacity, the discharge pressure p_{P2} at the level higher by a value $\Delta p_{LS} = p_{P2} - p_2 = cte$ then the p_2 pressure in the discharge conduit from the throttling proportional control valve (throttling valve) to the hydraulic motor.

- Chapter 6 presents an individual system with motor speed parallel throttling control. The parallel throttling control assembly may have a form of set throttling valve or set two – way flow regulator installed in the pump discharge conduit branch.

  The current useful power $P_{Mu} = M_M \omega_M$ of the hydraulic motor (independent of the used motor speed control structure), required by the motor driven device (and the same as in the systems shown in chapters 2 – 5), influences in a different way (than in the series throttling control systems) the structural losses generated in the system.

  When the hydraulic motor is loaded with small torque M_M, as an effect of decreased power of losses in system elements, the power $P_{Pc} = M_P \omega_P$ absorbed by the pump from the drive (electric or internal combustion) motor is also decreased compared with power P_{Pc} absorbed by a constant capacity pump used in the motor speed series throttling control system. With the unchanged hydraulic motor useful power $P_{Mu} = M_M \omega_M$, this increases the energy efficiency η of the whole system compared with the efficiency η of a series throttling control system fed by a constant capacity pump.

  The discussed structure of a hydraulic system, with a constant capacity pump and with hydraulic motor parallel throttling speed control, may achieve, during the operation with maximum speed ω_{Mmax} (n_{Mmax}) of the controlled motor and in the full range $0 \le M_M \le M_{Mmax}$ of its load, energy efficiency η equal to the total efficiency η of the system with volumetric control of the hydraulic motor speed (with a variable capacity pump).

- Chapter 7 presents an individual system with motor speed volumetric control by a variable capacity pump.

  In a volumetric motor (with a constant capacity per one revolution) speed control system (by a variable capacity pump), the sum of current (unchanged in relation to power P_{Mu} in the above discussed systems) values of: hydraulic motor useful power $P_{Mu} = M_M \omega_M$, power $\Delta P_{Mm} = M_{Mm} \omega_M$ of mechanical losses in the motor, power $\Delta P_{Mv} = \Delta p_{Mi} Q_{Mv}$ of volumetric losses in the motor, power $\Delta P_{Mp} = \Delta p_{Mp} Q_M$ of pressure losses in the motor, power $\Delta P_C = \Delta p_C Q_M$ of pressure losses in the hydraulic system connecting conduits, power $\Delta P_{Pp} = \Delta p_{Pp} Q_P$ of pressure losses in the pump, power $\Delta P_{Pv} = \Delta p_{Pi} Q_{Pv}$ of volumetric losses in the pump, power $\Delta P_{Pm} = M_{Pm} \omega_p$ of mechanical losses in the pump decides that the power $P_{Pc} = M_P \omega_p$ required by the pump from the pump driving (electric or internal combustion) motor is smaller than power P_{Pc} absorbed by the pump in the above discussed systems with the hydraulic motor speed throttling control.

  Energy efficiency $\eta = P_{Mu}/P_{Pc}$ of a system with volumetric control by a variable capacity pump is the highest efficiency η amongst the considered systems in the whole range of speed $0 \le \omega_M \le \omega_{Mmax}$ and hydraulic motor load $0 < M_M \le M_{Mmax}$. However, it has to be noted that the energy advantage of a system with the hydraulic motor speed ω_M (n_M) control by a variable capacity pump over the systems with the motor speed throttling control decreases markedly when the motor speed ω_M approaches ω_{Mmax} and the motor load approaches M_{Mmax}.

- Chapter 8 presents an individual system with motor speed volumetric control by means of a simultaneous change of the pump capacity per one revolution and change of the motor capacity per one revolution, system operating at

a constant pressure in the pump discharge conduit equal to the nominal pressure: $p_{P2} = p_n$.

This solution allows to use pump useful power P_{Pu} (resulting from a product of pump working pressure p_{P2} equal to the nominal system pressure p_n ($p_{P2} = p_n$) and maximum pump capacity Q_{Pmax} achieved at the coefficient $b = q_{Pgv}/q_{Pt} = 1$ of the change of the pump capacity per one revolution) also during the period of smaller hydraulic motor load (with the torque $M_M < M_{Mmax}$), by an increase of the motor speed ω_M above its nominal speed ω_{Mn} ($\omega_M > \omega_{Mn}$).

In a hydraulic motor with variable capacity q_{Mgv} per one shaft revolution, operating at the pressure decrease $\Delta p_M = p_n - \Delta p_C$ (i.e. only slightly lower than the nominal pressure p_n), the useful power $P_{Mu} = M_M \omega_M$ unchanged compared with previous system (chapters 2 – 7), resulting from the same torque M_M and motor shaft speed ω_M required by the driven device, the areas of power of losses in the motor have different shapes.

From the point of view of power ΔP_C of losses in the connecting conduits, a system with hydraulic motor with variable capacity q_{Mgv} per one revolution, operating at constant pressure $p_{P2} = p_n$ in the pump discharge conduit, has great advantage over the systems with a motor of constant capacity q_{Mt} per one revolution, where the decreased motor loading torque M_M is accompanied by smaller decrease Δp_M of pressure required by the motor and, in effect, lower pressure p_{P2} in the pump discharge conduit ($p_{P2} < p_n$). With longer conduits and at low temperature (greater viscosity) of the working medium (hydraulic oil), the gain from energy savings in the conduits of a system with $p_{P2} = p_n$ may be considerable.

The sum ΔP of power of energy losses in a hydraulic motor with variable capacity q_{Mgv} per one shaft revolution and in a pump with variable capacity q_{Pgv} per one shaft revolution working in the system with short connecting conduits, with the pump discharge conduit pressure equal to the nominal pressure ($p_{P2} = p_n$), may be, with small motor load M_M, much greater than the sum ΔP of the power of losses in a system with motor with constant capacity q_{Mt} per one shaft revolution controlled volumetrically by variable capacity pump (chapter 7).

In the operating conditions of a system with $p_{P2} = p_n$ (p_{P2} independent of the motor load M_M), a system with long connecting conduits (and greater pressure losses Δp_C in the conduits), operating with great viscosity ν of a working medium (hydraulic oil), the sum ΔP of power of losses may appear smaller than the sum ΔP of losses in a system with motor with constant capacity q_{Mt} per one shaft revolution and with variable capacity pump. With great oil viscosity, the energy gains connected with decrease of pressure losses in the system elements (mainly in the connecting conduits), achieved in effect of decreasing the intensity $Q_P = Q_M$, may appear great, but the power of volumetric losses ΔP_{Pv} in the pump and ΔP_{Mv} in the motor will not increase as distinctly as with the smaller viscosity.

BIBLIOGRAPHY

1. Paszota Z.: *Aspects énergétiques des transmissions hydrostatiques*, Monograph, 2002
2. Paszota Z.: *Model of losses and efficiency of an energy – saving hydraulic servomechanism system*, Marine Technology Transactions, Polish Academy of Sciences, Branch in Gdansk, Vol. 18, 2007
3. Paszota Z.: *Energy saving in a hydraulic servomechanism system*, Proc. 17th Symposium on Theory and Practice of Shipbuilding in memoriam prof. Leopold Sorta, Opatija, 19 – 21 October 2006
4. Skorek G.: *Energy characteristics of the hydraulic systems with proportionally controlled cylinder fed in a constant or variable pressure* (in Polish), Doctor dissertation, Gdansk University of Technology, continuation
5. Paszota Z.: *Energy Saving in a Hydraulic Servomechanism System – Theory and Examples of Laboratory Verification*, Brodogradnja, Journal of Naval Architecture and Shipbuilding Industry, Vol. 58, No 2, Zagreb, June 2007
6. Paszota Z.: *Hydraulic Servomechanism System. Examples of Reduction of Power Losses in the Variable Pressure Power Supply*, International Scientific – Technical Conference "Hydraulics and Pneumatics'2007", Wrocław, 10 – 12 October 2007
7. Paszota Z.: *Power of energy losses in the hydrostatic drive system elements – definitions, relations, range of changes, energy efficiencies*. Part I – Hydraulic motor. Chapter in the monograph: „*Research, design, production and operation of hydraulic systems*" (in Polish), Andrzej Meder and Adam Klich editors. „Cylinder" Library. Komag Mining Mechanisation Centre, Gliwice 2007
8. Paszota Z.: *Power of energy losses in the hydrostatic drive system elements – definitions, relations, range of changes, energy efficiencies*. Part II – Conduits, throttling control assembly, pump. Chapter in the monograph: „*Research, design, production and operation of hydraulic systems*" (in Polish), Andrzej Meder and Adam Klich editors. „Cylinder" Library. Komag Mining Mechanisation Centre, Gliwice 2007
9. Paszota Z.: *Power of energy losses in the hydrostatic drive system elements – definitions, relations, range of changes, energy efficiencies* (in Polish). Part I – Hydraulic motor. Napędy i sterowanie, scientific monthly, No 11 (103), November 2007
10. Paszota Z.: *Power of energy losses in the hydrostatic drive system elements – definitions, relations, range of changes, energy efficiencies* (in Polish). Part II – Conduits, throttling control assembly, pump. Napędy i sterowanie, scientific monthly, No 12 (104), December 2007
11. Paszota Z.: *Graphical presentation of the power of energy losses and power developed in the elements of hydrostatic drive and control system* (in Polish). Part I – Rotational hydraulic motor speed series throttling control systems. To be presented at the Cylinder'2008 Conference in September 2008
12. Paszota Z.: *Graphical presentation of the power of energy losses and power developed in the elements of hydrostatic drive and control system* (in Polish). Part II – Rotational hydraulic motor speed parallel throttling control and volumetric control systems. To be presented at the Cylinder'2008 Conference in September 2008
13. Paszota Z.: *Graphical presentation of the power of energy losses and power developed in the elements of hydrostatic drive and control system. Part I. Rotational hydraulic motor speed series throttling control systems*. Polish Maritime Research 03/2008

CONTACT WITH THE AUTHOR

Prof. Zygmunt Paszota
Faculty of Ocean Engineering
and Ship Technology
Gdansk University of Technology
Narutowicza 11/12
80-952 Gdansk, POLAND
e-mail: zpaszota@pg.gda.pl

POLISH MARITIME RESEARCH 4(58) 2008 Vol 15; pp. 30-36
10.2478/v10012-007-0094-x

Comparative analysis of energy potential of three ways of configuration of a condenser power plant thermal cycle

Tadeusz Chmielniak, Prof.
The Silesian University of Technology
Piotr Krzyślak, Assoc. Prof.
Gdańsk University of Technology

ABSTRACT

A theoretical, comparative analysis of three configuration ways of a condenser power plant thermal cycle is shown in the work. A new regeneration & separation preheater and its application in a thermal cycle is presented. Results obtained allow to compare all three analysed configurations efficiencies.

Keywords: Comparative analysis of energy, condenser, power plant, thermal cycle, new regeneration, separation preheater

GENERAL

A first stage of evaluation of energetic potential of a given technological proposal is to assign to it an ideal thermal cycle and to assess its efficiency.

Condenser power plants are the most common systems of electric energy production in the whole world. Elementary information how to increase their thermal efficiency is taken from an appropriate to a power plant Clausius-Rankine cycle analysis. An evolution of the cycles has reached a high level of their perfection. It does not mean that their future development is not possible. A discussion on new solutions is necessary.

Main projects lead to increase condenser power plant efficiency focus now on both live steam and feed water parameters increasing i.e. on increasing an average temperature of heat transfer into the cycle [1, 2, 3]. Another direction of the whole installation efficiency increase is an integration of exhaust gases cooling process together with regeneration system (a solution used more commonly in supercritical condenser installations for hard coal and lignites [1, 4]).

In the work three ideal cycles with different regeneration process configuration are to be compared. Appropriate Rankine cycles calculations were performed for water as the cycle medium. Differences in cycles efficiency can be basis for future projects and analyses of a regeneration system assumed in the third cycle variant.

CYCLES ANALYSED

An efficiency potential of a thermal cycle operating within a water steam zone will be compared with three different solutions of the regeneration system.

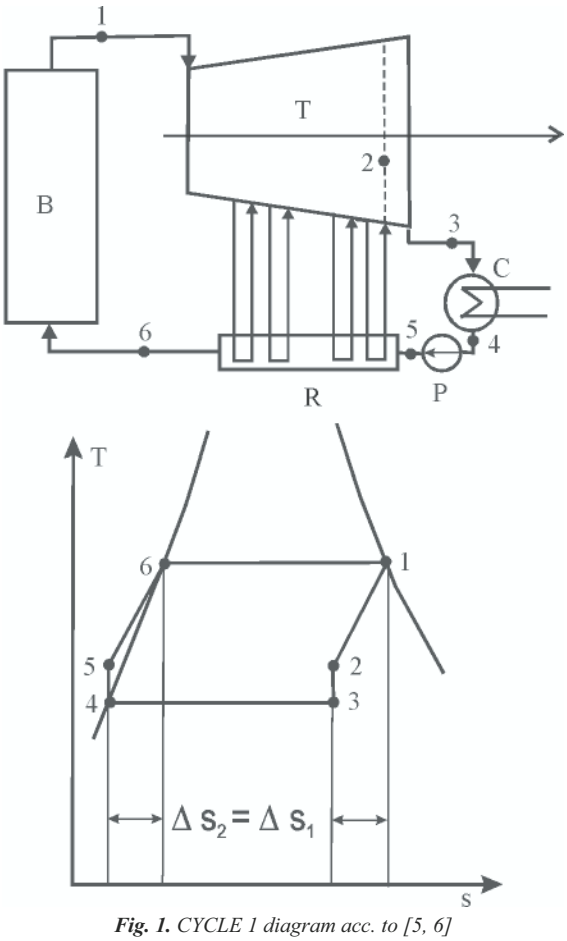

Fig. 1. *CYCLE 1 diagram acc. to [5, 6]*

On Fig. 1 a diagram of an installation is shown to which CYCLE 1 [5, 6] is assigned. Point 1 means live steam parameters. After expansion in the first turbine part steam is directed into regeneration preheaters denominated as R. When the steam gives back a part of its heat into the feed water it is coming back into the turbine flow path for further expansion. Such a process is repeated as many times as is preheaters number in the regeneration system R. The last point where the steam comes back into the regeneration system is denominated with number 2 on Fig. 1. After expansion in the last turbine part the steam flows into a condenser C. That point is denominated as 3. From point 4 a condensate inputs the pump P and with its pressure increased is forced trough regeneration preheaters R and then is introduced into a boiler B. The second part of the Fig. 1 shows the cycle in T-s system. If preheaters number goes to infinity, the analysed cycle efficiency will go to Carnot cycle efficiency [6].

The following assumptions were done while analysing the cycle: expansion and pumping processes are isentropic; the whole expansion process is analysed within a wet steam zone – it comes from the above that steam initial parameters in point 1 are the same as dry saturated steam; heat transfer processes in the boiler and in preheaters R are isobaric. Additionally it is assumed that resistance related to heat transfer in preheaters can be neglected and from that comes that max. temperature the water heated can obtain is equal to saturation temperature of heating steam that is a function of pressure in an extraction the steam is taken from.

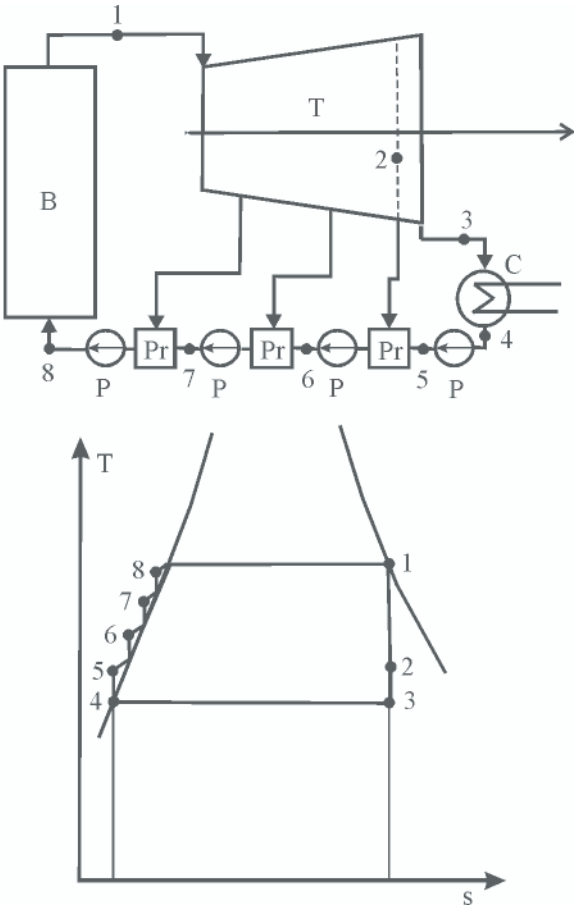

Fig. 2. *CYCLE 2 diagram acc. to [6]*

CYCLE 2 configuration was analysed in [7]. Whereas in the first installation membrane (direct) type preheaters were assumed, in the CYCLE 2 configuration uses no membrane (indirect) ones. The rest of assumptions is the same as for the previous configuration. In the considered configuration a pump operates after each regeneration preheater. It increases the feed water pressure to force the water or into the next preheater either into the boiler.

In CYCLE 1 configuration the medium mass flow rate is the same in each point of the cycle (in the turbine as well). In the second configuration (CYCLE 2) a situation is quite different. A steam taken from turbine extractions does not come back into the flow path but after giving its heat back into preheated water and then condensing it is together with a water flowing into the preheater forced into the next part of the regeneration system. Each next preheater (downstream the water flow) is more loaded than the previous one.

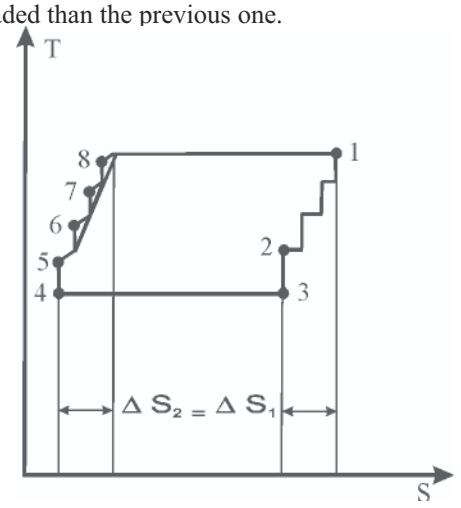

Fig. 3. *Conversions for CYCLE 2 in T-S system*

On Fig. 3 the process is shown on T-S diagram (S - total entropy) taking into account mass flow rate variation. Just like in the CYCLE 1 configuration the cycle efficiency goes to equivalent Carnot cycle efficiency when preheaters number goes to infinity.

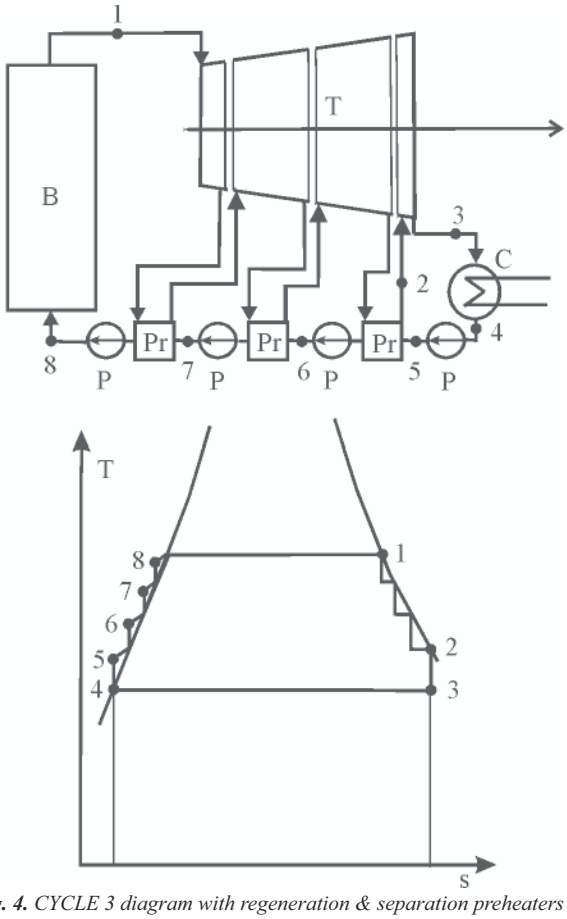

Fig. 4. *CYCLE 3 diagram with regeneration & separation preheaters [8]*

The models of two configurations shown above do not close a list of configurations with efficiency equivalent to Carnot cycle when preheaters number goes to infinity.

A cycle and direct (non membrane) heat preheater of a special type CYCLE 3 [8] were analysed in that work. In that case a regeneration & separation preheater [8] was used that simultaneously preheats feed water and separates moisture from a steam transferred from the preheater into the turbine flow path. A diagram of the cycle with regeneration & separation preheaters as well as processes on T-S diagram are shown on Fig. 4. After expansion in the turbine the steam inputs the preheater where gives its heat back to the feed water; additionally outdropped moisture is separated. For the whole cycle the same simplifying assumptions as for the first and the second configuration can be assumed. On Fig. 5 conception of the regeneration & separation preheater [8] is shown in simplified form.

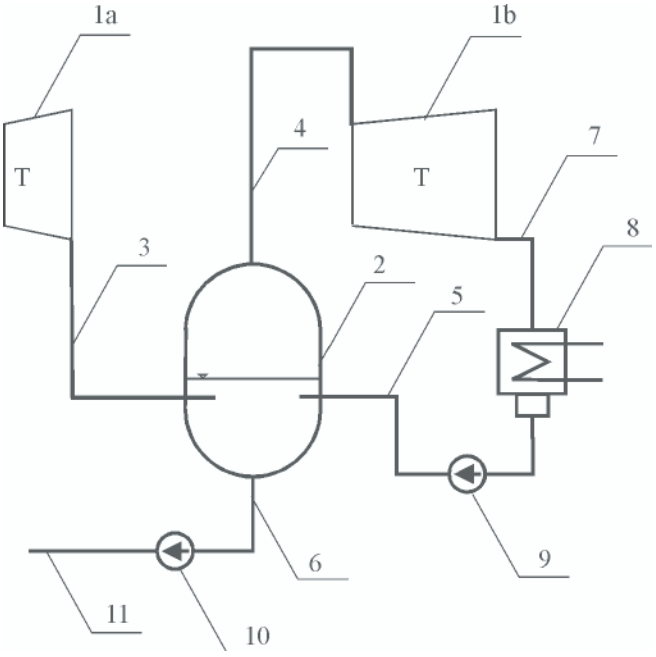

Fig. 5. *Regeneration & separation preheater diagram [8].* ***1a*** *– steam turbine casing,* ***1b*** *– steam turbine next casing,* ***2*** *– regeneration & separation preheater,* ***3*** *– steam exhaust from turbine casing,* ***4*** *– saturated steam extraction from regeneration&speparation preheater into the turbine next casing,* ***5*** *– water into regeneration & separation preheater,* ***6*** *– condensate drain from regeneration & separation preheater, 7 – steam exhaust into condenser,* ***8*** *– steam condenser,* ***9*** *– condensate pump,* ***10*** *– condensate drain pump from regeneration & separation preheater,* ***11*** *– feed water pipeline into the boiler or into regeneration & separation preheaters*

PARAMETRIC AND OPTIMISED CALCULATIONS OF CYCLES

Calculation models

Taking the same assumptions allows to perform a comparative analysis of cycles efficiency for all three chosen configurations with a various regeneration preheaters number. The purpose of the analysis is to check what is a contribution of each preheater in a global effect of efficiency increase as well as to determine the regeneration configuration optimum parameters for assumed preheaters number. The calculation model for the first analysed configuration (CYCLE 1) is described with the following formulas. A single preheater model is shown on Fig. 6.

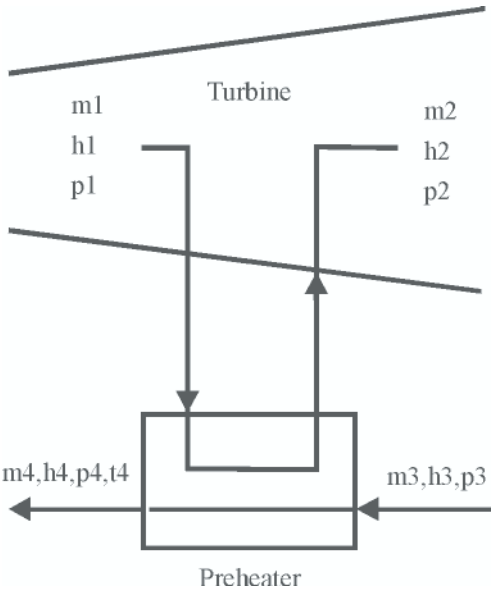

Fig. 6. *Single preheater for CYCLE 1 configuration model*

A mathematic model for that system was assumed as follow:

$$t4 = t_{sat}(p1)$$
$$h4 = h(t4, p3)$$
$$p2 = p1$$
$$m2 = m1$$
$$m4 = m3$$
$$p4 = p3$$
$$h1 - h2 = h4 - h3$$

A final temperature t4 of water preheated is determined as equal to a saturation temperature related to p1 pressure. The last equation describing energy balance makes possible to determine h2 enthalpy of the steam at the preheater outlet. An additional assumption is that heat ambient losses in the whole system can be neglected.

A single preheater model for CYCLE 2 configuration is shown on Fig. 7.

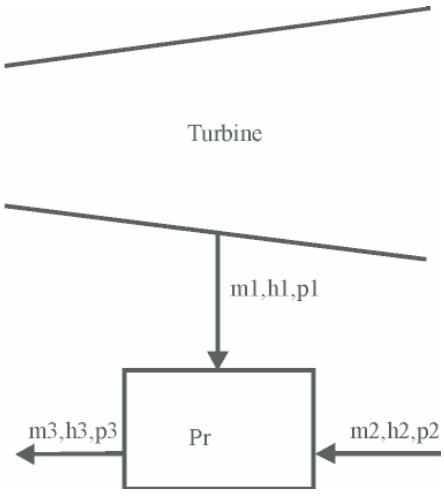

Fig. 7. *Single preheater for CYCLE 2 configuration model*

Processes in direct preheater (no membrane) are described with the following equations:

$$t3 = t_{sat}(p1)$$
$$h3 = h'(t3)$$
$$p3 = p2 = p1$$
$$m3 = m2 + m1$$
$$m3 * h3 = m1*h1 + m2*h2$$

The last equation shows energy balance for direct preheater (no membrane) operates with a steam pressure p1 taken from a given extraction. It allows to calculate a mass flow of steam taken from the turbine extraction necessary to preheat water mass flow m2 up to enthalpy corresponding to boiling water enthalpy h'(t3).

A single preheater simplified model for CYCLE 3 configuration is shown on Fig. 8.

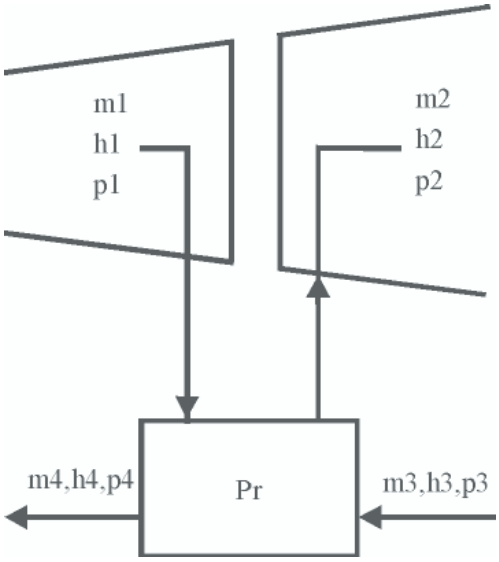

Fig. 8. *Single preheater for CYCLE3 configuration model*

In this case a mathematic model is as follow:

$$t4 = t_{sat}(p1)$$
$$h4 = h'(t4)$$
$$h2 = h''(t4)$$
$$p4 = p3 = p2 = p1$$
$$m3 + m1 = m2 + m4$$
$$m1*h1 + m3*h3 = m2*h2 + m4*h4$$
$$m3 = m2$$

In the regeneration & separation preheater an operating pressure is the same as the pressure in the turbine extraction. The last equation describes a condition that the flow m2 of a steam taken from the preheater has to be the same as a flow m3 of water delivered into the preheater. The equation together with the energy balance one allows to determine both parameters and a mass balance in the cycle analysed.

In the CYCLE1 configuration there is one pump to increase pressure to a value corresponding the live steam pressure. In configurations CYCLE2 and CYCLE3 there are some pumps for each configuration and their number is n+1 where n is regeneration preheaters number. All pumps have isentropic process of pressure increasing assumed that is described with the following equations:

$$\Delta p = p2 - p1$$
$$s1 = s(p1,h1)$$
$$v1 = v(p1,h1)$$
$$s2 = s1$$
$$\Delta h = v1 * \Delta p$$
$$h2 = h1 + \Delta h$$

The equations above allows to estimate water enthalpy rise in the pump while rising pressure from p1 at the pump suction to p2 at the pump discharge.

Turbine internal power is determined wit the following formula:

$$N = \sum_{i=1}^{n+1} m_i * \Delta h_i$$

where:
Δh_i – enthalpy drop in a given stage group
m_i – steam mass flow rate trough that stage group
n – regeneration preheaters number.

Stage group number in analysed configurations is greater by one than preheaters number n. Efficiency comparisons were performed for thermal cycle net efficiency i.e. thermal cycle power was determined as the turbine internal power N decreased by a sum of powers N_{pump} that is need to drive all pumps in the analysed cycle.

$$N_{net} = N - \sum N_{pump}$$

Heat stream inputted into a cycle Q_{in} was determined as a product of a steam in the boiler mass flow rate and steam enthalpy difference at the boiler inlet and outlet. Then the efficiency can be defined with the following formula:

$$\eta = \frac{N_{net}}{Q_{in}} \quad (1)$$

In all calculations water and steam properties were taken in acc. to [9]. For all analysed configurations the live steam pressure was assumed as 120 bar(a) and a pressure in the condenser was assumed as 0.05 bar(a).

Pressures of both live steam and steam in the condenser allow to determine respectively both max. and min. temperatures in the thermal cycle. In that case Carnot cycle efficiency is $\eta_c = 0.488$.

Calculation results

For assumed constant regeneration preheaters number both water preheated in subsequent preheaters and the final preheating temperature of the feed water before the boiler significantly influence on the cycle efficiency. Calculations were performed in variants with feed water into the boiler temperature various. On Fig. 9 results of calculations of CYCLE1 efficiency vs. feed water temperature and number of preheaters n are shown. On Fig. 10 and Fig. 11 similar results for CYCLE2 and CYCLE3 respectively are shown.

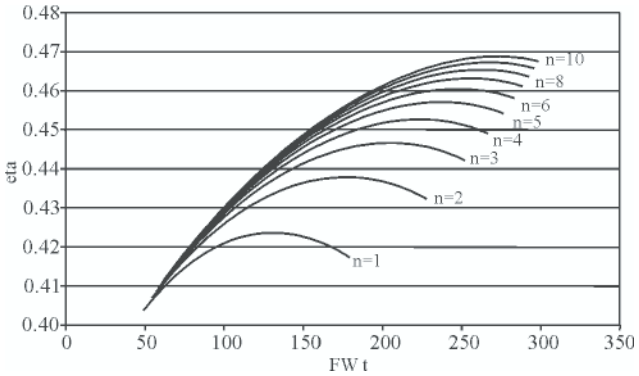

Fig. 9. *CYCLE1 efficiency vs. FW temperature (t_{FW}) and number of preheaters n*

In all analysed cases an optimum feed water temperature for a given preheaters number fulfils the following inequalities:

$$t_{FW,\,CYCLE\,3} > t_{FW,\,CYCLE\,2} > t_{FW,\,CYCLE\,1}$$

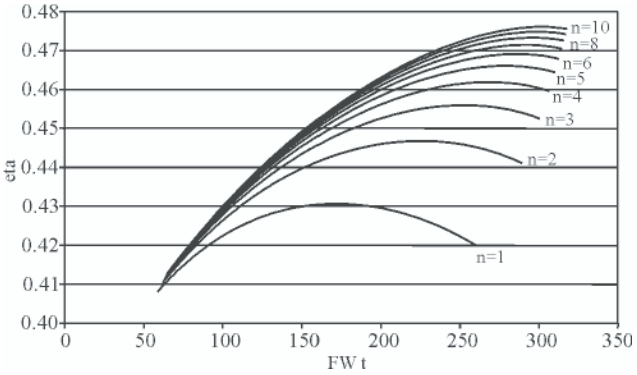

Fig. 10. *CYCLE2 efficiency vs. FW temperature (t_{FW}) and number of preheaters n*

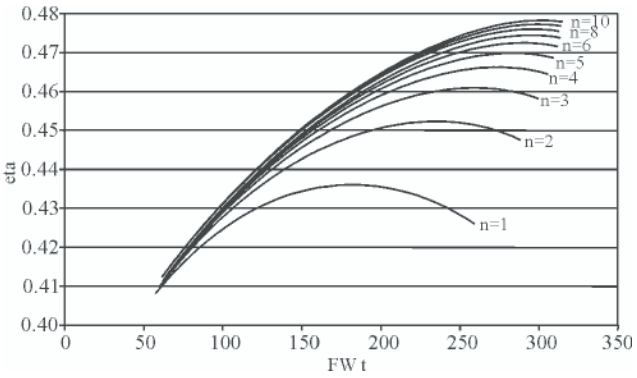

Fig. 11. *CYCLE3 efficiency vs. FW temperature (t_{FW}) and number of preheaters n*

Quantitative relations can be seen on Figs 12 to 14. When preheaters number increases, differences for CYCLE2 and 3 for optimum t_{FW} values are small.

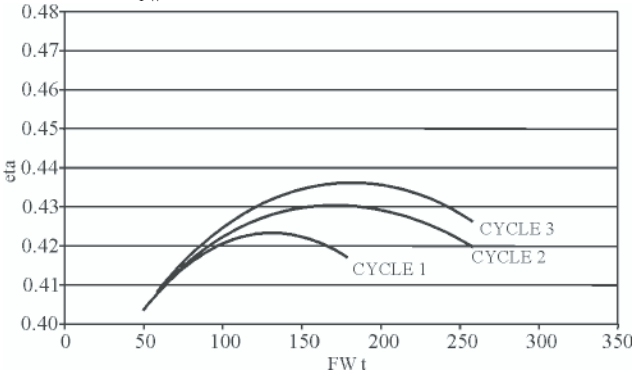

Fig. 12. *CYCLE 1, 2, 3 comparison for preheaters number n = 1*

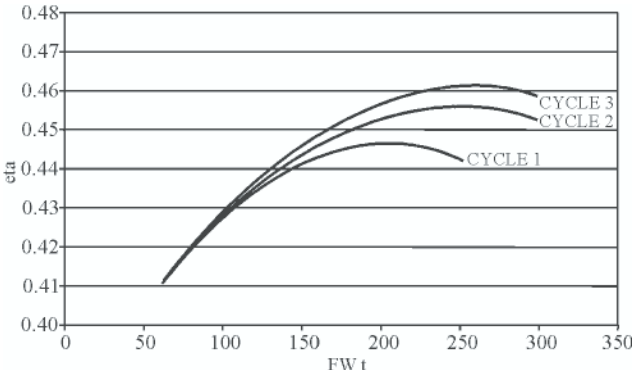

Fig. 13. *CYCLE 1, 2, 3 comparison for preheaters number n = 3*

Max. efficiencies set-up for all three compared cycles is shown on Fig. 16.

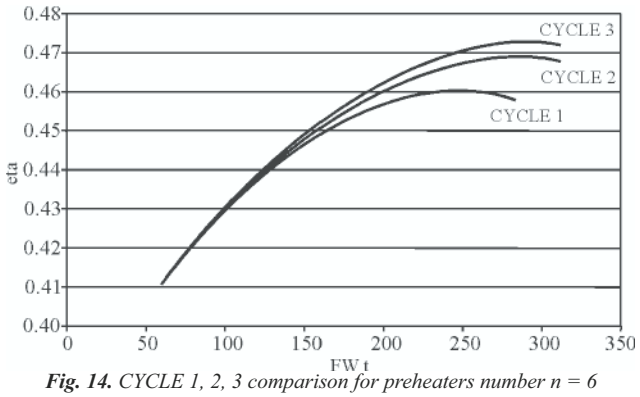

Fig. 14. *CYCLE 1, 2, 3 comparison for preheaters number n = 6*

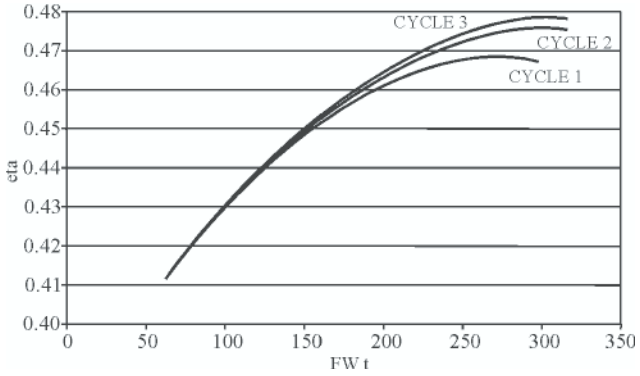

Fig. 15. *CYCLE 1, 2, 3 comparison for preheaters number n = 10*

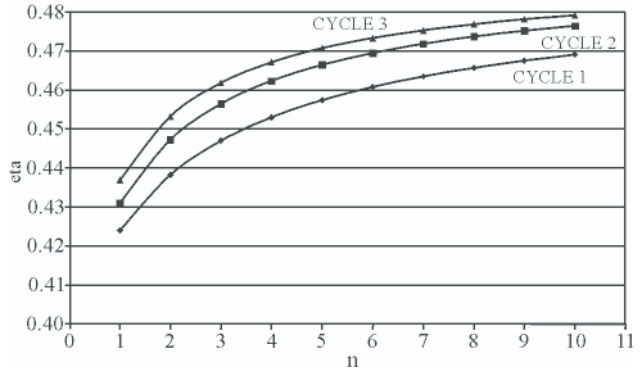

Fig.16. *CYCLE 1, 2, 3 efficiencies vs. preheater number n*

On Fig. 17 differences between CYCLE 3 & CYCLE 1 and between CYCLE 2 & CYCLE 1 are shown. Differences in an optimum of feed water temperature suggests that efficiency differences of the cycles analysed are caused by both a change of an average temperature of heat transfer into a cycle and entropy generation in a heat transfer process in the regeneration system. Using a cycle entropy analysis an identification of such influences was performed.

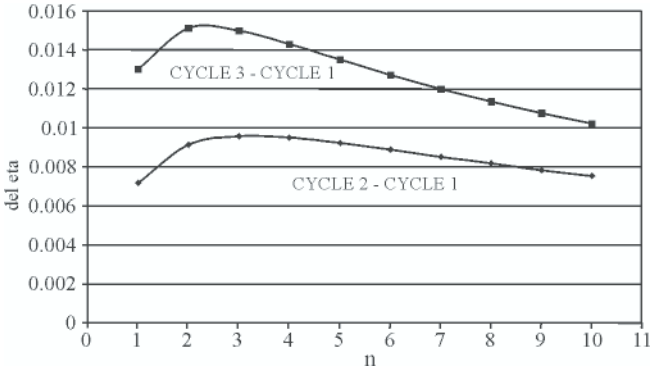

Fig. 17. *Differences between CYCLE 3 & CYCLE 1 and between CYCLE 2 & CYCLE 1.*

ENTROPY ANALYSIS

For the general diagram shown on Fig. 18 that encloses all analysed process structures it can be written as follow [10,11]:

$$Q_{in} - Q_{out} - Q_{amb} = N_b - N_{inneed} = N_{net} \tag{2}$$

$$\frac{Q_{out}}{\overline{T}_{out}} - \frac{Q_{in}}{\overline{T}_{in}} - S_{amb} = S_{sys} \tag{3}$$

where:

Q_{in}, Q_{out} – relevant heat streams into and out of the cycle
N_{inneed} – internal needs within a balance shield
$\overline{T}_{in}$, $\overline{T}_{out}$ [K] – entropy averaged temperature of heat transfer into and out of the cycle
Q_{amb} – heat stream into environment
S_{amb} – entropy generation due to heat transfer with environment
S_{sys} – entropy generation in the system.

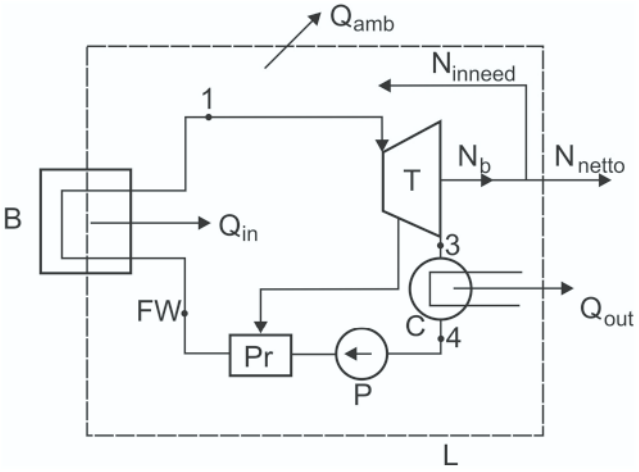

Fig. 18. *Diagram for formulas (1) (2) deriving.*
B *– boiler,* ***Pr*** *– regeneration system,* ***C*** *– condenser,* ***P*** *– pump,* ***T*** *– turbine,* ***FW*** *– feed water,* ***L*** *– balance shield*

The following relates to descriptions given on Fig. 18:

$$\overline{T}_{in} = \frac{Q_{in}}{m_{in}(s_1 - s_{FW})}\ ,\quad Q_{in} = m_{in}(h_1 - h_{FW})$$

$$\overline{T}_{out} = \frac{Q_{out}}{m_3(s_3 - s_4)}\ ,\quad Q_{out} = m_3(h_3 - h_4)$$

Assuming that $Q_{amb} = 0$, then:

$$\eta = \frac{N_b - N_{inneed}}{Q_{out}} = \frac{N_{net}}{Q_{in}} = \frac{\overline{T}_{in} - \overline{T}_{out}}{\overline{T}_{in}}\left(1 - \frac{\overline{T}_{in}\overline{T}_{out}}{\overline{T}_{in} - \overline{T}_{out}}\frac{S_{sys}}{Q_{in}}\right) = \overline{\eta}_c \eta_j \tag{4}$$

where:

$$\overline{\eta}_c = \frac{\overline{T}_{in} - \overline{T}_{out}}{\overline{T}_{in}} \tag{5}$$

$$\eta_j = 1 - \frac{\overline{T}_{in}\overline{T}_{out}}{\overline{T}_{in} - \overline{T}_{out}}\frac{S_{sys}}{Q_{in}} = 1 - \frac{\overline{T}_{out}S_{sys}}{\overline{\eta}_c Q_{in}}$$

m – mass flow rate.

The $\overline{\eta}_c$ efficiency is Carnot machine efficiency that operates between entropy averaged temperatures of heat transfer into and out of the cycle; η_j – is a measure of perfection of equipment in the cycle. In the considered case, when compression and expansion processes are isentropic and heat transfer is isobaric, η_j is a measure of egzergy losses in the heat transfer process as well as in mixing process in regeneration preheaters.

To compare $\overline{\eta}_c$ and η_j for the cycles analysed configurations with four regeneration preheaters and optimum feed water temperature were chosen. The analysis results are shown in table 1.

Tab. 1.

Item	Config.	$\overline{\eta}_c$	S_{sys} [kW/deg]	η_j	$\overline{\eta}_c\eta_j = \eta$	η/η_c
1	CYCLE 1	0.473	0.1163	0.957	0.453	0.928
2	CYCLE 2	0.483	0.1064	0.956	0.462	0.947
3	CYCLE 3	0.485	0.0865	0.963	0.467	0.957

It results from the table that for the considered configurations of the regeneration system, entropy averaged heat inlet temperatures are almost the same for CYCLE 2 and CYCLE 3 (temperatures $\overline{T}_w$ are the same for all appropriate configurations). It is due to small difference between values of feed water optimum temperatures for CYCLE 2 and CYCLE 3 configurations. The first cycle (CYCLE 1) has the highest absolute energy losses in regeneration preheaters whereas CYCLE 2 configuration has the lowest value of η_j efficiency. It comes from different heat amount introduced into CYCLE 1 and CYCLE 2. High efficiency $\overline{\eta}_c$ for that cycle (CYCLE 2) causes that its total efficiency is higher then CYCLE 1 efficiency. In the third cycle both S_g, S_g/Q_d ratio have the smallest values what in connection with high efficiency $\overline{\eta}_c$ leads into the highest efficiency $\eta = \overline{\eta}_c \eta_j$. It should be noted that formulas (1) and (4) give the same values of efficiency.

REMARKS AND CONCLUSIONS

- The most important result of the analysis performed is a statement that for different cycle configurations different efficiencies can be obtained with finite regeneration preheaters number. Whereas for all three analysed cycles a top limit is Carnot cycle efficiency (when preheaters number goes to infinity) that for finite preheaters number considerable differences in efficiency are obtained. Figures from 12 to 15 show that CYCLE 3 configuration is always more efficient than CYCLE 2 or CYCLE 1 within the whole area of feed water into the boiler temperature changes. It comes from Fig. 16 that CYCLE 3 configuration efficiency is 0.46 with only three regeneration & separation preheaters whereas to obtain the same efficiency with CYCLE1 configuration it has to be used six preheaters. It is essential from the turbine flow path point of view. Each turbine extraction is a place where the steam flow is disturbed. Decreasing extractions number without any losses for the cycle allows the turbine efficiency increase.

- As it can be seen from comparison showed on Fig. 17 within the whole range of the analysis (from n = 1 to n = 10 of regeneration preheaters) CYCLE 2 gives 0.7 % efficiency increase in relation to CYCLE 1 whereas CYCLE 3 gives more than 1 % efficiency increase respectively.

- The results obtained encourage to further regeneration & separation preheater analysis. Such a preheater can be used

in both conventional and nuclear power plants although in nuclear plants an area of its application can be much wider. It shall be noted that for CYCLE 3 configuration the highest steam dryness can be obtained, higher than for CYCLE 1 and CYCLE 2.

- The work presented is performed as a theoretical analysis but results obtained show at a necessity to look for both new condenser power plant cycle configurations and new equipment that can make possible to increase efficiency [3, 8]. The analysis is a base for choosing regeneration systems development directions.

- Good characteristics of the regeneration & separation preheater obtained for model conditions have not to be directly transferred to cycles with real processes. Their suitability shall be verified by appropriate thermodynamic and economic analyses.

BIBLIOGRAPHY

1. Chmielniak T., Lewandowski J.: *Rooms for improvement of the thermodynamic imperfection of processes of supplying with the electricity* (in. Analysis of the possibility of reducing the thermodynamic imperfection of processes of supplying the sustainable development of the country in the aspect with the electricity, the warmth and coolness. Ed.: A. Ziębik, J. Szargut, W. Stanek). The IV department of Technological Sciences you, Committee of the Thermodynamics and burning, Warsaw 2006
2. Chmielniak T., Kosman G.: *Problems of the development of steam turbines for high parameters of steam*. Committee of Problems of Energetics you. Set of papers of the Seminar: Essential Problems of Machines and Energy Devices. Jabłonna, 27-28.03.2003
3. Krzyślak P.: *New conceptions of increase in the efficiency of thermal cycles with steam turbines of the great power*. Ed. of the Poznań technical university, series of Trial 401, Poznań 2006
4. Zabłocki W.: *Energy blocks with pots about parameters the nadkrytycznych as the prospect of the future in the modernization and the development of the Polish power industry*. Committee of Problems of Energetics you. Set of papers of the Seminar: Essential Problems of Machines and Energy Devices. Jabłonna, 27-28.03.2003
5. Haywood K.W.: *Analysis Engineering Cycles of*. Pergamon Press, Oxford, New York, Toronto, Sydney, Braunschweig 1975
6. Chmielniak T.: thermodynamic Circulations of heat turbines. Ossolineum, Wrocław 1988
7. Szargut J.: *Thermodynamics*. WNT, Warsaw 2004
8. Application for a patent. *The way and the arrangement of the regeneration of the thermal cycle of the steam turbine*. P 381640, patent office 2007
9. Wagner in., Kruse and.: *Properties of water Steam and* (IFC 97). Springer Verlag, Berlin 1997
10. Chmielniak T.: *Measures of the evaluation of the thermodynamic effectiveness of thermal fitness rooms*. The Warsaw Technical University. Scientific works - z.6 Conferences, 1995
11. Łukowicz H.: *Rates of the decline of elements of thermal fitness rooms based on analysis of the generation of the entropy*. Archive of Energetics, XXXIV volume, 2, 2005.

CONTACT WITH AUTHORS

Piotr Krzyślak, Assoc. Prof.
Faculty of Mechanical Engineering
Gdansk University of Technology
Narutowicza 11/12
80-952 Gdansk, POLAND
e-mail : pkrzysla@pg.gda.pl

Tadeusz Chmielniak, Prof.
Institute of Measurements and Automatic Control
in Electrical Engineering
The Silesian University of Technology
Konarskiego 18
44-100 GLIWICE, POLAND
e-mail: tadeusz.chmielniak@polsl.pl

Photo: Cezary Spigarski

POLISH MARITIME RESEARCH 4(58) 2008 Vol 15; pp. 37-44
10.2478/v10012-007-0095-9

Problems of the starting and operating of hydraulic components and systems in low ambient temperature (Part I)

Ryszard Jasiński, Ph. D.
Gdansk University of Technology

ABSTRACT

Severe winters and sweltering summers which more and more often occur nowadays are the reason why machinery designers face many difficulties when designing devices which will be serviceable in extreme ambient conditions. Hence, defining the principles and conditions of safe operation of hydraulically driven machines and devices is essential for their designers and operators. For this reasons the author did a series of tests of hydraulic component and systems in thermal shock conditions (cooled-down component were supplied with hot working medium). In such conditions, starting parameters of the selected hydraulic component and systems which secured safety of their operation were determined. The experimental tests were carried out in the laboratory of the Chair of Hydraulics and Pneumatics, Gdańsk University of Technology.

Keywords: hydraulic machines, hydraulic drives, diagnostics, hydraulic systems

INTRODUCTION

Hydraulic systems used in numerous machines and devices operating in a given climatic zone should work reliably in various atmospheric conditions characteristic of the zone in question. The influence of low temperature is highly unfavourable for hydraulic system serviceability during the period of machine start-up, especially after its long lasting stand-by.

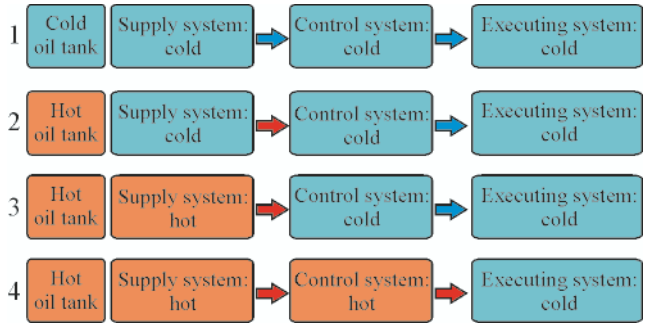

Fig. 1. *Four cases of starting conditions of a hydraulic system at low ambient temperature*

Starting the hydraulic system at low ambient temperature can be performed using either cold or hot working medium, which is usually hydraulic oil.

The following cases of starting the hydraulic system at low temperature are possible (Fig. 1):

1. at the instant of starting, all hydraulic component of the working machine have the same low initial temperature, which means that the working medium flows from the supply system to the cold control and executing component
2. the oil in the tank is heated up, whereas the supply, control, and executing component are cooled down
3. the temperature of the supply system is higher than that of the cooled-down control and executing component
4. the executing component are cooled down, whereas the supply system and control component are of higher temperature.

In the 1st case, at the starting instant the complete hydraulic system together with the oil are of the same temperature as the environment, whereas in the remaining cases of system start-ups (i.e. cases 2, 3, and 4 above) the oil, just before its delivery to the cooled-down unit, is heated up to a temperature much higher than the ambient one. These are the conditions for the appearance of a thermal shock.

On the basis of the provisions of the Polish standard [6] and the rules of Polish Register of Shipping (PRS) [7, 8] on the serviceability of hydraulic component in sub-freezing temperature conditions, the following requirements can be formulated:

- cooled-down hydraulic component (including hydraulic motors and cylinders) should correctly operate when they are supplied, in a stepwise mode, with hot oil of a temperature higher by up to 50 K than that of the unit
- according to the PRS rules, tests of hydraulic component should be performed in the most unfavourable supply conditions. It means for Z-class component operating at the temperature of -25 °C and supplied with the working medium of the temperature of 50 °C, recommended for hydraulic devices, that their operation is to be checked at the temperature difference between the oil and the environment equal to 75 °C.

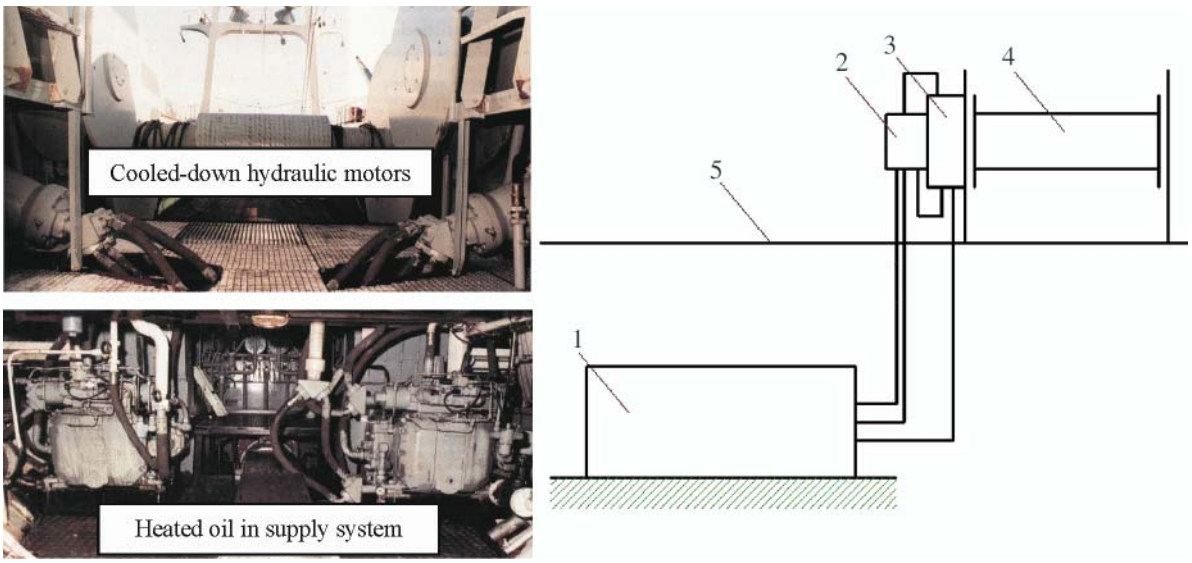

Fig. 2. *Simplified schematic diagram of supplying the hoisting winch:* ***1*** *– ship's central oil supply system,* ***2*** *– set of valves,* ***3*** *– hydraulic motor,* ***4*** *– hoisting winch, 5 – ship's deck*

In extreme conditions of supplying a cooled-down unit with hot working medium, observed in case of shipboard devices, for instance, the difference between the above temperatures may even reach as much as 80 K.

The ship's hydraulic hoisting winch, shown in Fig. 2, contains hydraulic component exposed to thermal shock conditions. Its supply system is situated under the deck and the oil inside it is heated as a result of its earlier work. After switching over the valve placed on the deck, Fig. 1 case 3, the oil will flow from the supply system to the motor, the temperature of which is equal to the ambient temperature. Consequently, dynamic heat transfer from the hot oil to the cooled-down shipboard hydraulic component will take place, changing the temperature of the component. Elements of the hydraulic component will be heated non-uniformly, which may result in the elimination of the clearances between the co-operating elements, and, as a further consequence, may lead to the failure of the hydraulic unit. The hoisting winches are usually driven by hydraulic motors.

In heavy-duty machines, for instance those used for earth work, all cases of hydraulic system start-ups represented in Fig. 1 can happen. The bulldozer, shown in Fig. 3, contains two or more hydraulic systems. One of them is the drive system, responsible for supplying the motors which drive wheels or caterpillars. The other is the working system, which consists of a number of working component. The cooled-down motors (1) of the drive system may be heated up uniformly like the remaining component of the system, as a result of the loss of energy in the system (Case 1 in Fig. 1), or dynamically when supplied with the hot oil heated up in advance in a preliminary supply pump circuit (thermal shock conditions) (Case 4 in Fig. 1). The executing and control component (2) of the hydraulic working system of the bulldozer in question are exposed to thermal shock conditions corresponding to case 3 and 4 in Fig. 1.

The start-up of a system in winter conditions of low ambient temperature is characteristic of decreased efficiency of particular component and the entire machine, in which higher vibrations and noise are produced. In these very unfavourable conditions, shorter lifetimes and more frequent failures of the hydraulic component are observed.

For the above reasons the author performed tests of hydraulic component of various designs in low ambient temperatures. The tests made it possible to detect and describe the phenomena which take place in hydraulic component and systems during their start-ups in such conditions.

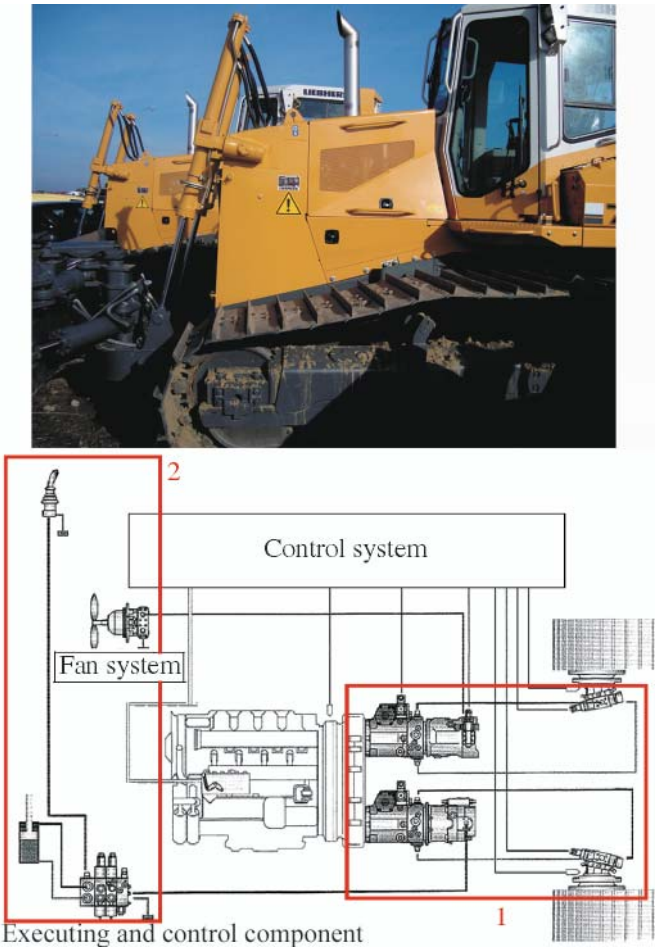

Fig. 3. *Hydraulically driven bulldozer:* ***1*** *– drive system,* ***2*** *– working unit and fan systems [10, 11]*

PHENOMENA WHICH OCCUR IN HYDRAULIC COMPONENT AND SYSTEMS DURING THEIR START-UPS AT LOW AMBIENT TEMPERATURE

During the start-up of the hydraulic unit at low ambient temperature many unfavourable phenomena may occur. One of them is decreased hydraulical - mechanical efficiency, which results in lower overall efficiency of the hydraulic component.

The volumetric efficiency usually increases a little as compared to that in the normal starting conditions if only the cavitation does not occur.

During the start-up of the system in thermal shock conditions, the effective clearance between the co-operating elements changes. When the temperature difference between the working medium and the cooled-down hydraulic unit is too high, the clearance may completely disappear, thus leading to the failure of not only the individual unit but also of the entire system. There are various designs of hydraulic component. Each design includes certain characteristic points (nodes) of co-operation between the elements in which the disappearance of the clearance can happen. Due to a huge variety of the existing design solutions [1, 5], only the most commonly used hydraulic component of heavy-duty machines are presented in the article.

In the axial piston pumps and motors, e.g. those with cam-driven commutation unit (Fig. 4), as well as in the radial ones, the disappearance of the clearance between pistons and cylinders, between slipper and swash plate (in designs with hydrostatic support), as well as between particular elements of the commutation unit can take place. In gear pumps and motors the disappearance of the axial clearance between side surfaces of gear wheels and covers, or that of the radial clearance between tooth crests and the casing raceway can occur (Fig. 5).

DETERMINATION OF THE CLEARANCE BETWEEN CO-OPERATING ELEMENTS OF THE HYDRAULIC UNIT DURING ITS START-UP IN THERMAL SHOCK CONDITIONS

Changes of clearances between co-operating elements of the hydraulic unit during its start-up in the considered conditions depend on many factors : load, ambient temperature, oil temperature, oil flow rate.

Fig. 6 presents the following quantities : l_0 – geometrical clearance, l_m – assembling clearance, l_e – effective clearance. The geometrical clearance l_0 is determined by real dimensions of the co-operating elements. During the assembly of the hydraulic unit, the geometrical clearance l_0 becomes smaller due to elastic deformations of the elements, Δl_m, resulting from the assembling grip.

The effective clearance le depends on the assembling clearance l_m, elastic deformation Δl_p of the hydraulic unit elements, which results from the oil pressure action, as well as on the difference Δl_t in the linear thermal expansion of the elements co-operating within the subsystem.

$$l_e(\tau) = l_m + \Delta l_p(\tau) - \Delta l_t(\tau) \tag{1}$$

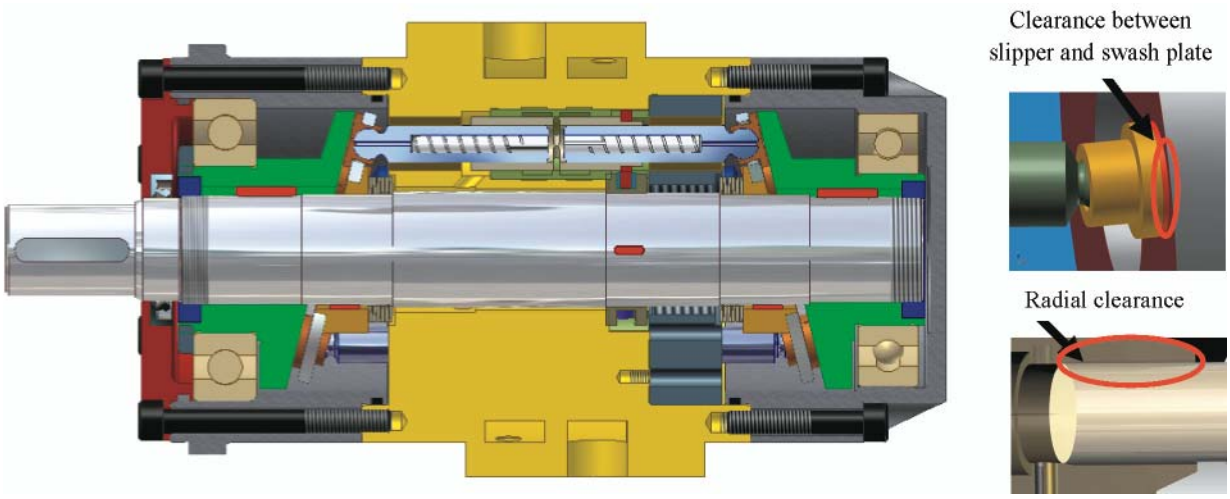

Fig. 4. PWK 27 axial piston pump [5] with indicated places between co-operating elements where the disappearance of the clearance can occur

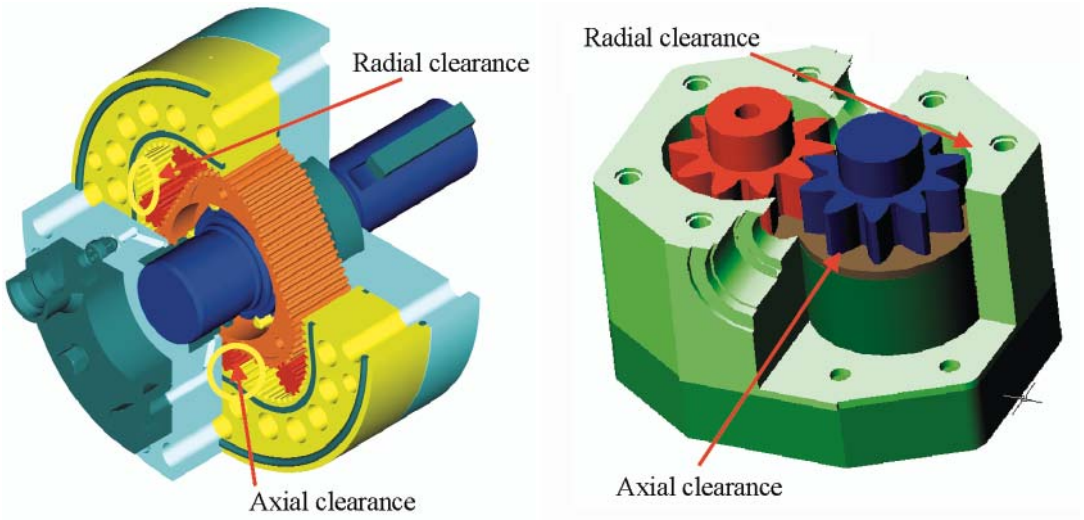

Fig. 5. SOK hydraulic satellite motor [9] with indicated places where the disappearance of axial clearance (between satellites and covers) or radial clearance (between satellite teeth and casing raceways) can take place, as well as a high-speed gear pump (motor) with indicated places which are sensitive to thermal shock conditions

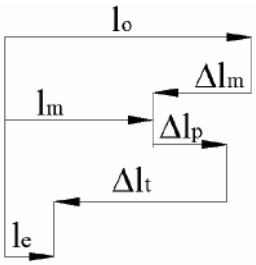

Fig.6. Dimensional analysis for determining the effective clearance between co-operating elements of hydraulic unit under thermal shock conditions

The pressure contributes to the increase of the clearance. The higher the pressure in unit chambers, the greater increase of the effective clearance resulting from the elastic deformation of the elements of the hydraulic unit, $\Delta l_p(\tau)$, when it is supplied with the oil in thermal shock conditions.

The author of the present article has elaborated a method for assessing changes of the clearance l_e in the considered starting conditions [2, 3].

LABORATORY STAND FOR TESTING HYDRAULIC COMPONENT IN THERMAL SHOCK CONDITIONS

Experimental tests have been conducted to detect phenomena taking place during the start-ups of hydraulic component under thermal shock conditions [2, 3, 4].

The Chair's laboratory is equipped with, among other components, multi-pump supply devices fitted with oil temperature stabilization, devices for testing hydraulic component and systems, as well as the system for measuring and recording mechanical, hydraulical and thermal quantities.

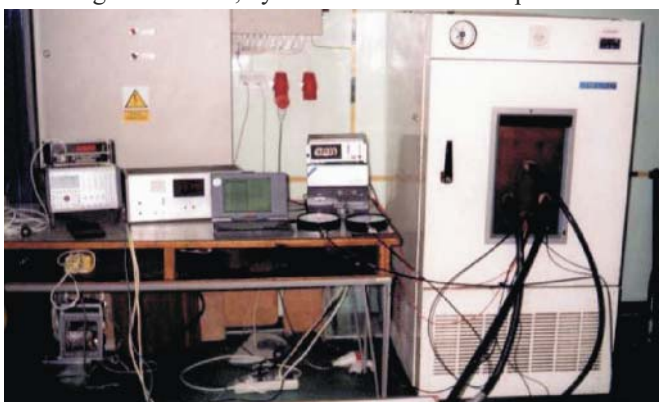

***Fig. 7.** Low-temperature chamber and measuring system installed in the laboratory of the Chair of Hydraulics and Pneumatics*

The component were cooled down to the temperature of –38 °C, the minimum, in the low-temperature chamber (Fig. 7). The tests were carried out without forced air circulation. The temperature T_1 of the oil supplying the motor was maintained within the range from 30 °C to 60 °C (usually at 50 °C) using the oil temperature stabilization system.

During the start-up of the hydraulic unit the following quantities were measured: $p_1(\tau)$ – pressure at hydraulic unit inlet, $p_2(\tau)$ – pressure at hydraulic unit outlet, $Q(\tau)$ – oil flow rate, $n(\tau)$ – rotational speed of pump motor shaft, T_{ot} – temperature in the cold chamber, $T_1(\tau)$ – temperature at hydraulic unit inlet, $T_2(\tau)$ – temperature at hydraulic unit outlet, $T_i(\tau)$ – temperatures at selected points of elements of the tested component, $M(\tau)$ – torque.

The Advantech Visidaq system was used for collecting the measured data in the computer-aided data transmission and recording system (Fig. 8).

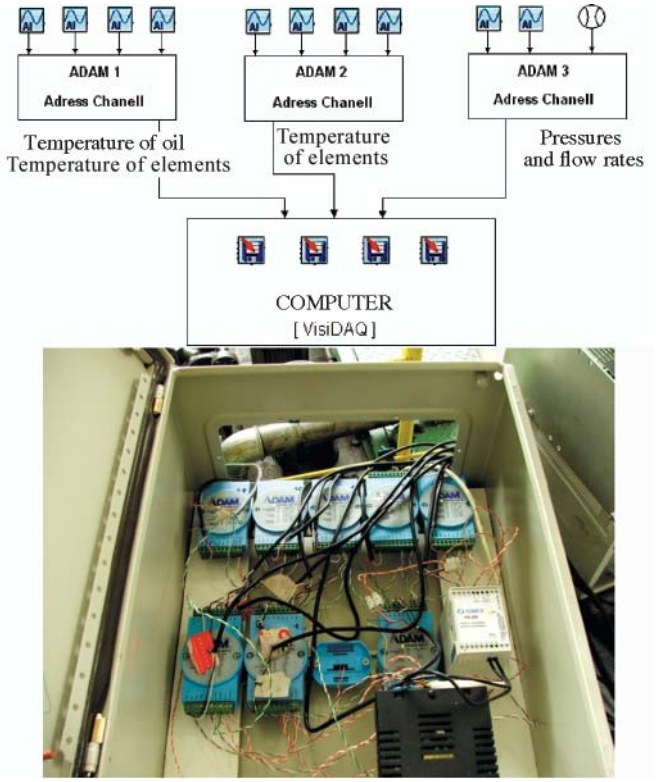

***Fig. 8.** System transmitting and recording the data collected from sensors*

THE HYDRAULIC COMPONENT TESTED AT LOW AMBIENT TEMPERATURE

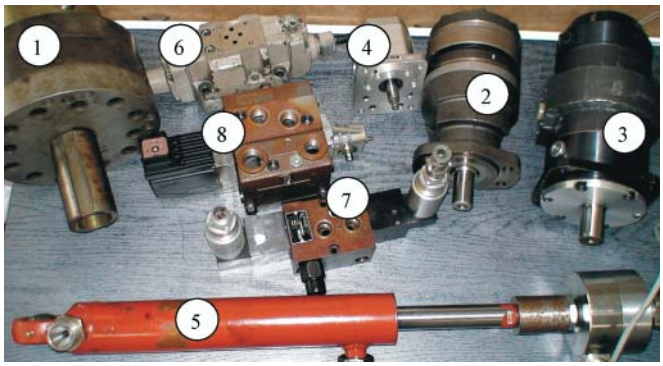

***Fig. 9.** Hydraulic component tested in low ambient temperature: **1** – SOK 100 satellite motor, **2** – TF 170 orbital motor, **3** – axial piston pump PWK 27, **4** – gear pump, **5** – hydraulic cylinder; the valve: **6** – 4WEH16C33/6AW220-50, **7** – RE2510/101 and **8** – PVG 32 proportional valve*

In the laboratory of the Chair of Hydraulics and Pneumatics, a number of hydraulic component were tested in thermal shock conditions [2, 3], including:

- the satellite motors: SOK 100 and SOK 160 made by ZUO HYDROSTER (Fig. 9)
- the orbital motors: GMR 160 made by REXROTH, and TF 170 made by PARKER (Fig. 9)
- PZ-2-K-10 gear pump, which operated as a motor, made by HYDROTOR
- PZ-2-K-6,3 gear pump, made by HYDROTOR (Fig. 9)
- PWK 27 axial piston pump made by HYDROTOR (Fig. 9)
- PV 16 axial piston pump made by PARKER
- RK2-12 radial piston pump made by LUKAS
- CJ2F-50/28/250 hydraulic cylinder made by AGROMET ZEHS, Lubań (Fig. 9)

- CJ2F-50/28/250 hydraulic cylinder made by STALKO
- RE2510/101 electro-hydraulically controlled valve made by HYDROTOR
- 4WEH16C33/6AW220-50 electro-hydraulically operated directional spool valve made by REXROTH (Fig. 9)
- PVG 32 proportional valve made by SAUER DANFOSS (Fig. 9)
- UZPP16 pressure relief valve made by PONAR WADOWICE
- 4WS2EM10 - 45 / 20B2T315Z8EM servovalve made by BOSCH REXROTH.

All these hydraulic component were supplied with the mineral oil Total Azolla 46.

SYMPTOMS WHICH INDICATE CORRECT OR INCORRECT OPERATION OF A HYDRAULIC MOTOR DURING ITS START-UP IN THERMAL SHOCK CONDITIONS ON THE BASIS OF PRESSURE AND ROTATIONAL SPEED TIME-HISTORIES

In the tests of hydraulic unit start-ups in thermal shock conditions three characteristic parameters were changed, which were the oil flow rate, the hot oil temperature, and the initial temperature of the cooled-down motor. Depending on the value of the oil flow rate Q and the temperature difference $\Delta T_{ol\text{-}ot}$ between the hot oil and the cooled-down motor at the initial instant, three areas of starting parameters at which the motor will operate either correctly, or temporarily incorrectly, or completely incorrectly, can be named (Fig. 10).

Figs 11 through 14 show typical time-histories of changes of parameters of hydraulic motor operation during its start-up in thermal shock conditions. On the basis of these time-histories the areas of parameters ($Q, \Delta T_{ol\text{-}ot}$) of correct and incorrect motor operation can be determined.

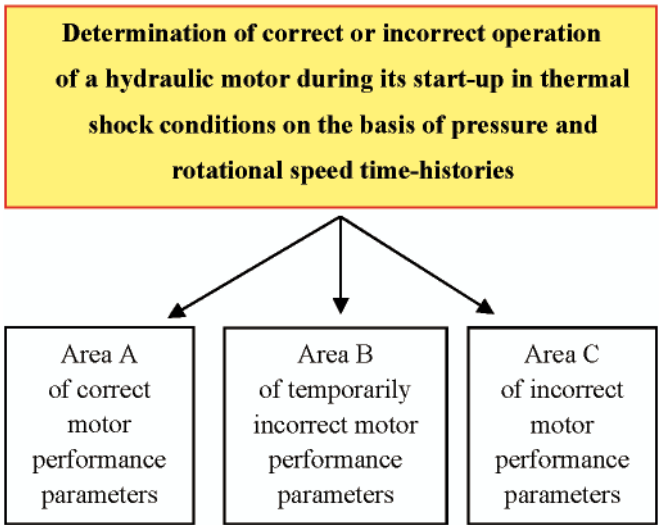

Fig. 10. Areas of starting parameters of hydraulic motor

Fig. 11 shows sample time-histories of correct motor start-ups which represent the area A in Fig. 10. During these start-ups no symptoms of incorrect motor operation, e.g. no pulsating changes of oil pressure or rotational speed, were observed.

The diagrams shown in the next figure, Fig. 12, illustrate the temporarily incorrect start-up of the motor, area B in Fig. 10, during which certain symptoms, such as transient increase of oil pressure at motor inlet, accompanied by imperceptible rotational speed changes, were recorded.

A sample of incorrect motor start-up in the area C is shown in Figs 13 and 14. During this start-up such symptoms as changes of oil pressure and rotational speed appeared for the critical period only, or irreversibly at all. The motor operated incorrectly for some time, i.e. for the critical period only (Fig. 13), as for a number of seconds the clearance between motor elements was reduced to zero, which resulted in pressure

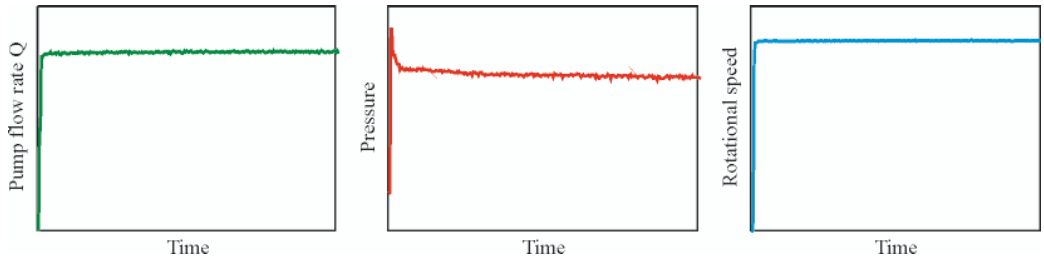

Fig. 11. Time-histories of parameters characteristic for correct motor operation (area A in Fig. 10)

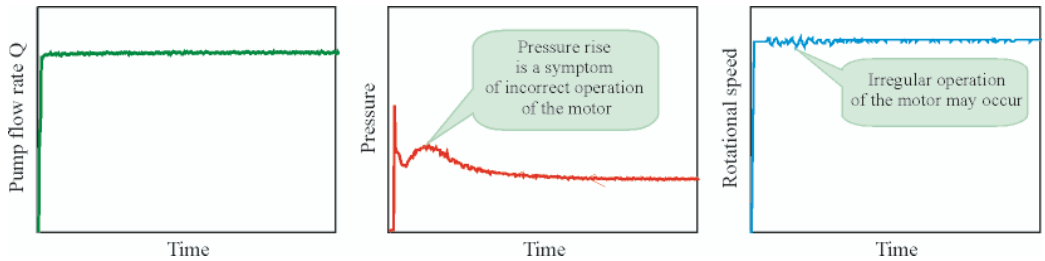

Fig. 12. Time-histories of parameters characteristic for temporarily incorrect motor operation (area B in Fig. 10)

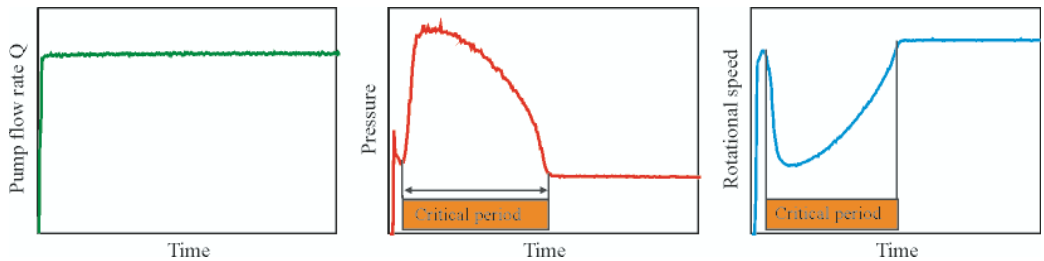

Fig. 13. Time-histories of parameters characteristic for incorrect motor operation (area C in Fig. 10)

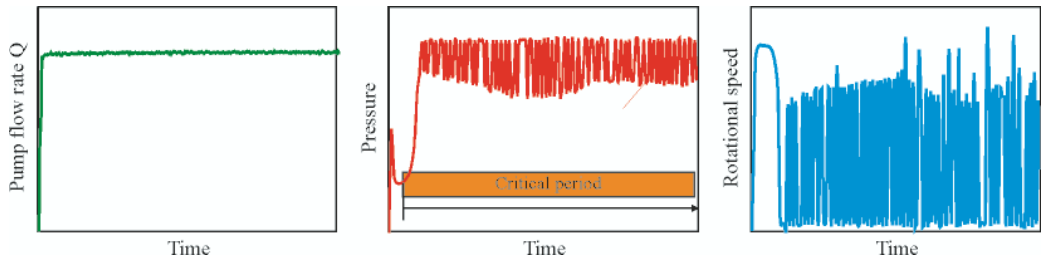

Fig. 14. *Time-histories of parameters characteristic for incorrect motor operation (area C in Fig. 10).*
Note*: in this case only cutting off the oil supply to the motor terminated the critical period of motor operation*

rise and rotational speed drop. After that period the motor returned to correct operation.

Fig. 14 illustrates the situation of permanently incorrect motor operation, including possible motor stop or irregular operation. During the irregular motor operation (Fig. 14), a critical period is observed which lasts until the oil supply to the motor is cut off. During this period stepwise changes of inlet pressure and rotational speed, and short-lasting motor stoppages occur.

SAMPLE SYMPTOMS WHICH INDICATE INCORRECT OPERATION OF THE HYDRAULIC MOTOR

Results of the tests done on the SOK 100 satellite motor (see Fig. 5, item 9) whose working elements move between side plates with the clearance l_e , are presented as a sample case. In several start-up tests with the SOK 100 motor, incorrect motor operation was recorded during which the motor returned, after some time, to its normal (correct) operation. One of such start-ups occurred for the following values of the parameters: Q = 100 dm3/min, initial motor temperature equal to –20 °C, oil temperature equal to 50 °C. Fig. 15 shows the oil pressure time-histories recorded in the supply and outflow manifolds during incorrect operation of the SOK 100 motor.

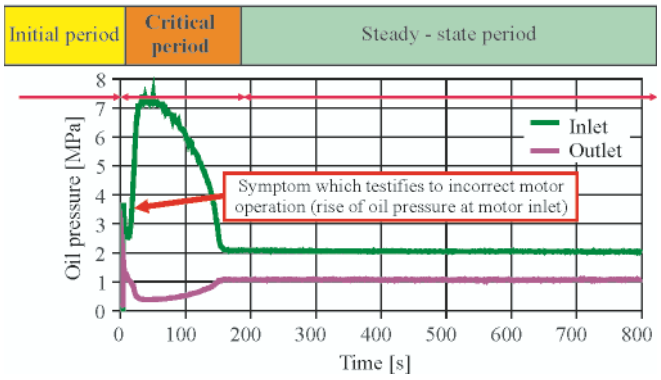

Fig. 15. *Oil pressures at motor inlet and outlet: cold chamber temperature t_{ot} = –20 [°C], oil temperature t_{ol} = 50 [°C], oil flow rate Q = 100 [l/min]*

As results from the oil pressure time-history (Fig. 15), after 18 seconds from the start-up the motor revealed symptoms of incorrect operation: the oil pressure at motor inlet suddenly rose up to 7.2 MPa. The incorrect motor operation lasted for about 150 seconds.

In the start-up time-history of the motor revealing symptoms of incorrect operation the following three periods can be named (Figs. 13 and 15):

- ☆ *initial period*: for a few seconds the motor operation was correct, the motor monotonously speeded up and only after a number of seconds its operation became irregular
- ☆ *critical period*: after ten to twenty seconds the incorrect motor operation was observed (oil pressure rise and rotational speed drop)
- ☆ *steady-state period*: after the critical period the motor operation became stable again, i.e. its rotational speed became steady and the oil pressures at motor inlet and outlet stabilised.

The situation observed during the SOK 100 motor start-up tests performed in the conditions of the ambient temperature t_{ot} = -15 [°C], the oil temperature t_{ol} = 53 [°C], and the oil flow rate Q = 100 [l/min] (Fig. 16), was quite different.

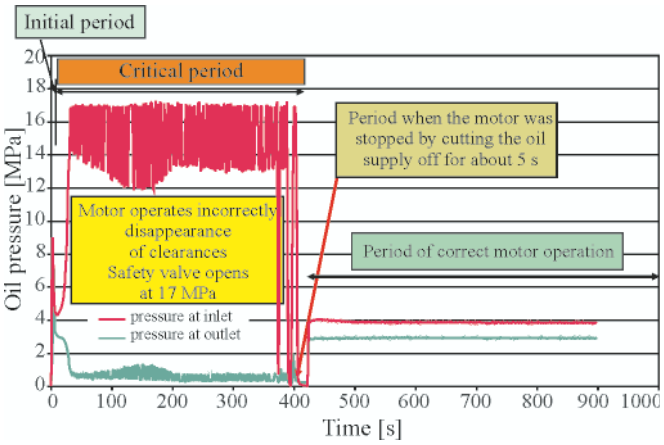

Fig. 16. *Oil pressures at motor inlet and outlet: cold chamber temperature t_{ot} = –15 [°C], oil temperature t_{ol} = 53 [°C], the oil flow rate Q = 100 [l/min]*

In these conditions the operation of the motor was incorrect. During the start-up the motor did not come back to correct operation. As the incorrect operation period could last longer, the oil supply was cut off.

During the initial period (Fig. 16) the oil pressure rises in a stepwise mode up to about 9 MPa, then it drops to 5 MPa for a few seconds and again rises suddenly up to the safety valve opening pressure equal to 17 MPa. Until then the motor operates incorrectly. Sudden pressure changes occur within the range from 13 to 17 MPa. The high pressure (17 MPa) provokes the deformation of covers and increases the axial clearance. In these conditions the moving elements of the motor are free to rotate until the pressure drop, after which the deformation of plates decreases which can lead to complete disappearance of the clearances. The lack of clearance between the co-operating elements increases the friction and, consequently, stops the motor. Then the oil pressure in the working chambers rises and the clearance increases. The above described situation was recorded up to second 406. After this time the oil supply to the motor was cut off. After starting the motor again it began to operate correctly after about 5 s.

The time duration of the above described phenomena is affected by the scale of the stepwise rises of the oil flow rate, and the difference between the ambient temperature and that of motor elements.

In the considered case of incorrect motor operation only two characteristic periods were observed:

⇨ initial period

⇨ critical period.

In the critical period full reduction of clearances took place, accompanied by the increase of the friction between co-operating motor elements. As a consequence, mechanical seizing of motor elements was observed. The temperature difference was so high that particular elements became heated-up after different periods. The safety valve protected the motor against complete damage.

Fig. 17 shows noticeable traces of failures formed during the SOK 100 motor start-up with symptoms of incorrect operation in thermal shock conditions.

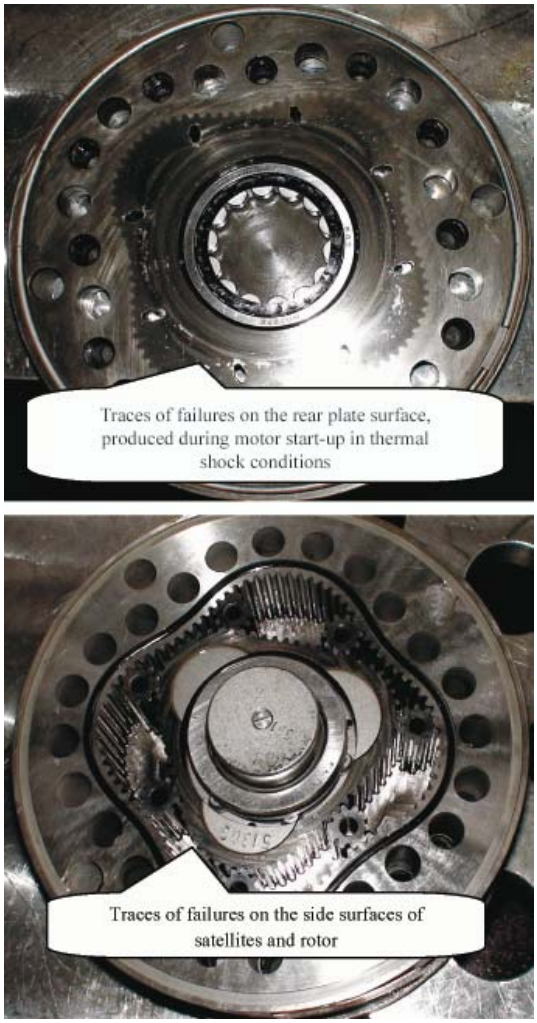

Fig. 17. *Traces of failures formed during SOK 100 motor start-up with symptoms of incorrect operation in thermal shock conditions*

AREAS OF STARTING PARAMETERS OF SELECTED HYDRAULIC COMPONENT IN THERMAL SHOCK CONDITIONS

On the basis of the tests of SOK 100 satellite motor (Fig.18), GMR 160 orbital motor (Fig.19), PWK 27 pump (Fig. 20), and RE2510/101 valve (Fig. 21) the areas of their starting parameters were determined. They are defined by stepwise increase of oil flow rate and difference between oil temperature and that of the hydraulic unit at the initial instant.

It was assessed that the SOK 100 satellite motor (Fig. 5, item 9) having axial clearance of 23 μm can operate correctly (Fig. 18) at the temperature difference between the oil and the cooled-down motor equal to 55 °C and

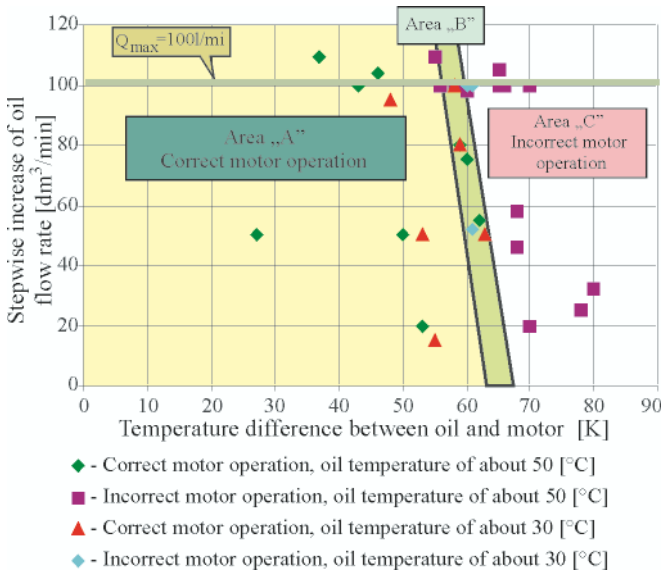

Fig. 18. *Areas of operating parameters of SOK 100 satellite motor in thermal shock conditions*

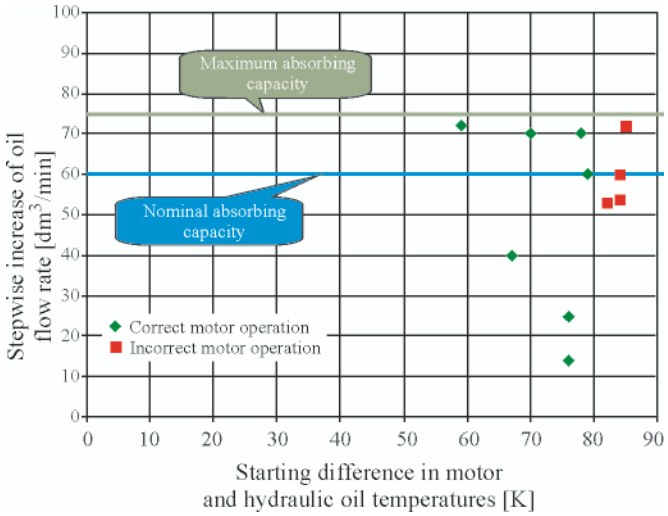

Fig. 19. *Starting parameters of GMR 160 motor in thermal shock conditions*

the maximum oil supply flow rate. Motor start-ups at higher temperature differences may completely reduce the clearance and lead to the failure of the motor and the entire hydraulic device. The transient area „B" (Fig. 18) is inclined by a small angle to the vertical axis. As a result, the smaller the stepwise change of the flow rate, the higher the possible initial difference between oil and motor temperatures (area A) at which the motor is still able to operate correctly.

The GMR 160 orbital motor having the axial clearance of 40 μm and the radial one of 28 μm is more resistant to thermal shock conditions, as it appeared to operate correctly at the temperature difference up to 78 K and nominal oil flow rate (Fig. 19).

The tests of the PWK27 pump have revealed that during the start-up it operated incorrectly in some conditions. It was the case when the start-up was carried out at the pressure on the delivery side of the pump, equal to about 5 MPa, and the rotational speed exceeding 1500 rpm (Fig. 20). During the initial period of the pump start-up its incorrect operation was manifested by instantaneous lack of hydrostatic support in the area of co-operation of the hydrostatic slipper and the swash plate. The incorrect operation of the PWK 27 pump in thermal shock conditions can be avoided by the use of an appropriate valve located behind the pump, in order to raise its pressure up to 5 MPa at least.

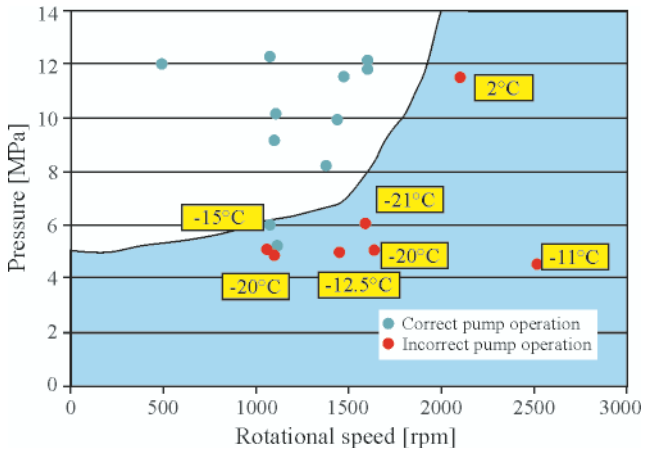

Fig. 20. Starting parameters of PWK27 pump in thermal shock conditions

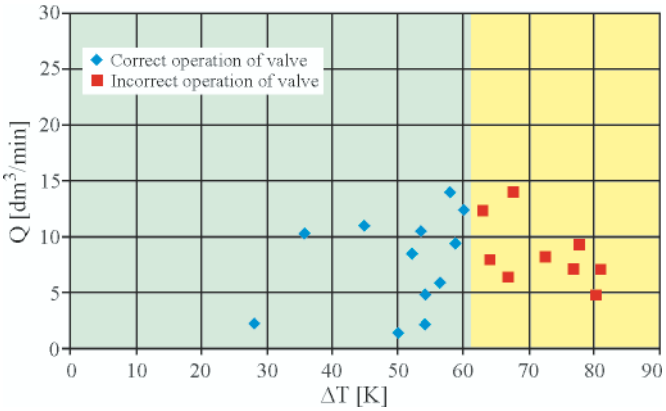

Fig. 21. Range of operation of RE2510/101 directional valve as a function of oil flow rate and temperature difference between oil and valve

The RE2510/101 valve is not resistant to the operation in thermal shock conditions at the temperature difference between oil and valve, $\Delta T_{ol\text{-}ot}$, higher than 62 °C (Fig. 21). The diameter of the valve slider was equal to 18 mm and the initial clearance between the slider and the casing was equal to 6 μm, according to the measurements performed by the Metrology Laboratory, Gdańsk University of Technology.

CONCLUSIONS

- The clearance between the co-operating elements is the main constructional factor which affects the operation of a hydraulic unit in thermal shock conditions. Due to the heat exchange process, moving elements of the unit are heated faster by the flow of hot oil than the casing (motionless element). Different linear deformations of particular elements are the reason why the effective clearance may be reduced to zero during unit heating. The lack of clearance results in the appearance of dry friction between the moving and motionless elements. As a result, the produced heat is directly transferred to the elements. The temperature of the moving elements suddenly increases, which makes their dimensions even bigger. During this time the moving elements rotate irregularly, thus causing permanent failures of both the moving and motionless elements.
- The phenomena which most affect the operation of the component in thermal shock conditions occur during the first two minutes of the start-up process.
- The process of hydraulic motor damage can be prevented by prompt cut-off of the oil supply to the motor.
- The performed tests of hydraulic component in thermal shock conditions showed the way in which a given unit may behave in extreme conditions of operation.
- Some of the tested component turned out to be unserviceable at the temperature differences slightly exceeding 50 °C. It was also stated that the same component, but manufactured with greater clearances, were capable of operating at higher temperature differences. However, the operation of such a unit would be associated with its lower efficiency.
- The parameters of hydraulic motor which are crucial for the appearance of incorrect motor operation include stepwise oil flow rate, oil temperature, and initial temperature of the motor.
- The discussed problems should be taken into account when designing hydraulic component and systems which are to be used for driving devices and machines in low ambient temperatures.

BIBLIOGRAPHY

1. Balawender A.: *Energy analysis and testing methods of low-speed hydraulic motors* (in Polish). Zeszyty naukowe PG (Scientific Bulletins of Gdansk University of Technology), Gdańsk 1988.
2. Jasiński R.: *Operation of low-speed hydraulic motors in thermal shock conditions* (in Polish). Doctoral thesis, Gdańsk 2002.
3. Jasiński R.: *Experimental tests of PWK 27 axial multi-plunger pump of Hydrotor firm in low ambient temperatures* (in Polish), „Napędy i sterowanie" No. 4/2008
4. Jasiński R.: *Methods of determination of correct operation area for hydraulic component in low ambient temperatures.* Developments in Mechanical Engineering, Gdańsk 2008
5. Osiecki A.: *Hydrostatic drive of machines* (in Polish). Wydawnictwo Naukowo-Techniczne (Scientific Technical Publishing House), Warszawa 1998
6. Polish Standardization Office: PN–86/M-73079 - *General conditions of using the uniform hydraulic system* (in Polish)
7. Polish Register of Shipping: *Publication No. 11P* (in Polish), Gdańsk 1994
8. Polish Register of Shipping: *Environmental tests of ship equipment* (in Polish). Gdańsk 1975
9. Hydroster Ship Equipment Works: *Technical information and documentation of SOK 1 hydraulic motors* (in Polish). Gdańsk
10. Bosch Rexroth: *Product catalogues*
11. Liebherr: *Product catalogues*.

CONTACT WITH THE AUTHOR

Ryszard Jasiński, Ph. D.
Faculty of Mechanical Engineering
Gdansk University of Technology
Narutowicza 11/12
80-952 Gdansk, POLAND
e-mail: rjasinsk@pg.gda.pl

POLISH MARITIME RESEARCH 4(58) 2008 Vol 15; pp. 45-51
10.2478/v10012-007-0096-8

Fault detection in measuring systems of power plants

Jerzy Głuch, Assoc. Prof.
Gdansk University of Technology

ABSTRACT

This paper describes possibility of forming diagnostic relations based on application of the artifical neural networks (ANNs), intended for the identifying of degradation of measuring instruments used in developed power systems. As an example a steam turbine high-power plant was used. And, simulative calculations were applied to forming diagnostic neural relations. Both degradation of the measuring instruments and simultaneously occurring degradation of the measuring instruments and thermal cycle component devices, were taken into account. Good quality of diagnostic neural relations was stated. They make it possible to distinguish degradation of measuring instruments from degradation of thermal cycle components. The calculated errors of identification of dergraded devices and measuring instruments in the case of simultaneous occurence of three different degradations were on the level of 0.25 %. Performance of the relations was presented by using an example based on industrial practice.

Keywords: steam turbines, turbines exploitation, power units, efficiency, thermal diagnostics, diagnostic relations

INTRODUCTION

Development of diagnostic methods make it possible to undertake more and more difficult diagnostic tasks. To them belongs the need of diagnosing technical objects and devices in the case of incomplete measurement information and failures of sensors. Thermal-and-flow measurements of sophisticated power object belong to the most difficult. They are always non-stationary. Their results are influenced by many independent operational parameters of object, its size as well as arrangement of sensors and way of their attachment.

The diagnosing of energy conversion processes in ship power plants, both motor and steam turbine driven, is especially difficult because of their complex structure and interdependence of their operational parameters. This paper presents investigations on the problem of recognition of correctness of gathered measurement results. Examples based on characteristics of a land steam power plant are given. Complexity of the power plant makes it possible to draw conclusions which would be valid, at least to a certain extent, also for ship power plants.

For a long time the problem of quality of results of measurements carried out in power plants has been a subject of interest of researchers and practitioners in the field of operation of complex systems [1, 3, 4, 5, 6, 7, 9, 11, 12, 13, 14, 16, 17, 18, 19, 20, 21, 22, 23].

Among the methods intended for solving the problem, it is compensation calculus which plays important role [19].

Measurement information often concerns sum of influence of several devices at once. As showed in [7], in the case of a complex power object in which disturbances in work of one device propagate to other devices, to separate component measurement signals is possible. The observation can be used to identify sensors. Unserviceability of a sensor influences result of measurement of only one quantity and does not find any reflection in indications of other sensors.

The distinguishing of sensor failure from operational degradation of component devices of thermal cycle constitutes one of the most important tasks of thermal-and-flow diagnostics of steam power plants. The results of simulative calculations, given in further part of this paper, answer the following questions:

- how much detailed can be diagnostics of a considered subsystem of devices?
- is it possible to distinguish a sensor failure from degradation of a device?

The answer is of a great importance for designers of measuring systems and for users of diagnostic systems. The investigations on diagnostic relations based on the method of artificial neural networks (ANN), intended for the finding of incorrectness in measurements, are presented in further part of the paper.

Determination of degradation symptoms on the basis of measurements - on the one hand - and a model of correct performance - on the other hand - is one of more important

operations in thermal-and-flow diagnostics. The correct performance is described by the so called reference state. It is a functional model since object-dependent variables determined with its help are functions of independent parameters, i.e.: structure, geometry and independent variables. The functional model makes it possible to determine the reference state for all operational points of the object in question.

It is not possible to perform measurements without errors, whereas erroneously indicated symptoms lead to an erroneous diagnosis. Hence it is important to determine an acceptable level of error, after exceedance of which a given measurement result should be rejected. Methods and procedures for detecting measurement errors and uncertainties are to take into account also varying load conditions of power plant, as it gives chance to distinguish changes in measurement results, caused by a measurement error, from normal changes of parameters resulting from changeable loads, external conditions and actions of operators.

SELECTED SPECIFIC CONDITIONS OF MEASUREMENTS

The author's attention is further focused on the high-power steam turbine cycle shown in Fig. 1. In it can be distinguished several points in which measurement data are ambiguous from the point of view of thermal-and-flow diagnostics [10, 15]. In them for instance the mixing of fluxes of different working media occurs, hence to distinguish influence of degradation of various component devices of the cycle on the basis of measurements of only one quantity, is difficult. Whereas measurement data taken form various measurement points make such differentiation possible. The mutual interaction brings prospects for searching for diagnostic relations in spite of lacking results of certain measurements [10, 15].

The differentiation of degradation causes among those dealing with the thermal cycle devices and those dealing with set of measuring instruments is made additionally difficult due to the overlapping of measurement uncertainty onto measurement results obtained in the above described way.

The investigations, described in the further part, which lead to building a method for detecting degradation of measuring instruments, are based on simulative calculations of degradation of component devices of complex thermal cycles and measuring instruments as well.

RESULTS OF SIMULATION AND IDENTIFICATION OF DEGRADATION BY THE ANN

Computational simulations lead to determination of degradation signature composed of symptoms. Each of the symptoms determines deviation of value of thermal-and-flow parameter corresponding with it (e.g. mass flux, pressure, temperature) or characteristics (of e.g. efficiency, flow capacity of particular component elements) from its reference value characteristic for non-degraded object. In the considered case such degradation signature was selected.

The signature together with relevant cause of degradation was used for training the artificial neural network intended for identifying the causes of degradation. The signature forms input to the network, and combinations of degradations represented by relevant zero-one series (0 – no degradation; 1 – occurrence

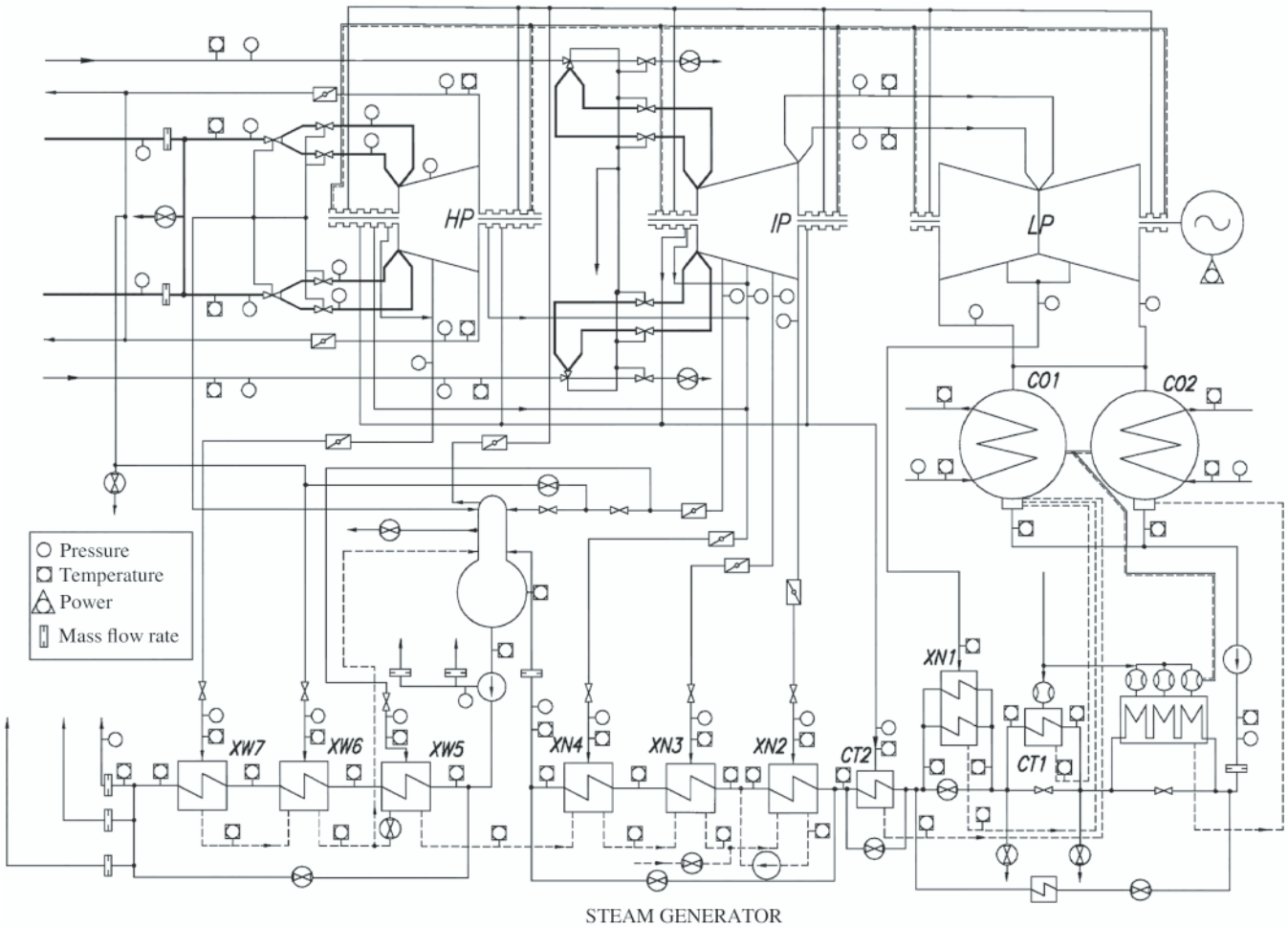

Fig. 1. Schematic thermal cycle diagram of a high-power unit with indicated measurement points

of degradation) form output from the network. Taking into account experience gained from the preceding investigations [8, 10, 15], one assumed that to obtain a better accuracy, several ANNs, each of them focused on identifying only one cause will be applied instead of one ANN intended for identifying all causes of degradation.

The ANN was assumed to have structure of multi-layer perceptron with application of step transition functions [2]. It ensures to get result in the form of „0" or „1", in compliance with the above described nomenclature of degradation causes. Hence, operation error of the ANN consists in incorrect determination of the quantity „0" or „1". For effective operation of such network application of a large number of neurons in intermediate layer of the network is required. Their maximum number results from a number of training samples. In the case in question it was possible to apply a few hundred of neurons.

Operational degradation was simulated by means of calculations with application of appropriate 1-D computational methods adjusted to reliable measurements. In the calculations both degradations of devices and measurement instruments were simulated. And, were taken into account degradations of geometry of blade system and sealing system of groups of HP and IP stages of turbine cylinders as well as degradations of sensors usually placed at extraction pipelines. The set of geometrical quantities taken into account in the simulation is presented in Tab. 1. To them was attached a set of measuring instruments fastened to extractions and subjected to degradation. Finally, the set of 37 units in number, of devices and measuring instruments subjected to degradation, was obtained.

In the simulative calculations the following was assumed:

- unchanged geometry of all devices of the thermal cycle, beyond currently investigated subsystem
- geometry changes represent possible operational failures, either of partial or maximum values, of the devices in question (0 ÷ 100% degree of degradation)
- load conditions of the power unit are represented by 8 independent parameters: mass flow rate of live steam supplying the unit, live steam inlet pressure, live steam inlet temperature, secondary steam inlet temperature, condensation pressure, degasing pressure, primary injection flux, secondary injection flux.
- searching for degradation symptoms is carried out among the following parameters which can be either measured or determined on the basis of measurement:
  - output of the power unit
  - specific heat consumption
  - pressure and temperature values in the extractions marked 1 through 7
  - steam flow capacity coefficients and efficiency indices.

Computational simulations lead to the forming of a degradation signature composed of symptoms. Eeach of the symptoms determines deviation of value of respective thermal-and-flow parameter (mass flow rate, pressure, temperature, or characteristics) from its reference value (i.e. characteristic for non-degraded object). The signatures consisted of 66 symptoms. Description of the quantities comprised in the signature is given in Tab. 2.

For the simulating of degradations of measurement instruments, was used the observation described in [8], which concerns lack of propagation of sensor errors into indications of measurement instruments located in other parts of thermal cycle. This way, sensor's unserviceability is able to change only one symptom in degradation signature. For the simulation it was assumed that sensor's indication error can vary within the range of ± 2%. Fig. 2 shows a fragment of the signature which describes degradation of the sealings in 4-th group of

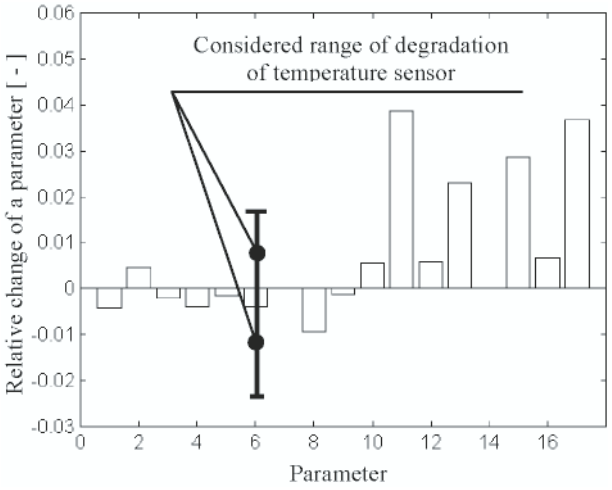

Fig. 2. *An example fragment of signature for twofold degradation concerning the sealings of 4-th group of stages and the temperature measuring instrument at 2-nd extraction. (**Note**: meaning of the successive parameter numbers is in accordance with the signature description given in Tab. 2).*

Tab. 1. *Geometrical parameters of devices and measuring instruments subjected to degradation, selected for simulation*

No	Geometrical parameters and measuring devices subjected to degradation
1	Clearance in nozzle box gland of HP control valves
2	Clearance in external glands of HP cylinder
3	Clearance in glands of 1-st HP stages group
4	Surface roughness of 1-st HP stages group
5	Leading edges destruction of 1-st HP stages group
6	Clearance in glands of 2-nd HP stages group
7	Surface roughness of 2-nd HP stages group
8	Leading edges destruction of 2-nd HP stages group
9	Clearance in nozzle box gland of IP control valves
10	Clearance in external glands of IP cylinder
11	Clearance in glands of 3-rd IP stages group
12	Surface roughness of 3-rd IP stages group
13	Leading edges destruction of 3-rd HP stages group
14	Clearance in glands of 4-th IP stages group
15	Surface roughness of 4-th IP stages group
16	Leading edges destruction of 4-th HP stages group
17	Clearance in glands of 5-th IP stages group
18	Surface roughness of 5-th IP stages group
19	Leading edges destruction of 5-th HP stages group
20	Clearance in glands of 6-th IP stages group
21	Surface roughness of 6-th IP stages group
22	Leading edges destruction of 6-th HP stages group
23 ÷ 37	Temperature and pressure sensors at extractions 1 ÷ 7

turbine stages and is modified by simultaneous occurrence of unserviceability of the temperature sensor located at the extraction 2.

Hence, 37 ANNs, each intended for identifying only one cause of degradation, were trained and tested. It was peliminarily stated that the identification of degradation of particular sensors and geometrical parameters was faultless [7]. The investigations on indentification of this kind have been extended to multiple degradation cases.

Finally, the following degradations were considered in various combinations:

- ⇨ single–time one – one kind of geometry or one degraded sensor
- ⇨ twofold one – all combinations of two simultaneously degraded quantities out of the set of sensors and kinds of geometry of devices
- ⇨ threefold one – all combinations of three simultaneously degraded quantities out of the set of the quantities in question.

Tab. 2. *Description of the quantities used to form symptoms of which full signature of degradation of the flow system of HP and IP turbines in question, is consisted*

No of symptom	Symptom based on:	No of symptom	Symptom based on:
1	Power	**34**	Mass flow rate at the 5-th extraction
2	Specific heat consumption	**35**	Mass flow rate at the 6-th extraction
3	Pressure behind the control stage	**36**	Mass flow rate at the 7-th extraction
4	Steam pressure at the 1-st extraction	**37**	Efficiency of control stage
5	Steam temperature at the 1-st extraction	**38**	Capacity coefficient of control stage
6	Steam pressure at the 2-nd extraction	**39**	Efficiency of the 1-st stages group
7	Steam temperature at the 2-nd extraction	**40**	Capacity coefficient of 1-st stages group
8	Steam pressure at the 3-rd extraction	**41**	Efficiency of the 2-nd stages group
9	Steam temperature at the 3-rd extraction	**42**	Capacity coefficient of 2-nd stages group
10	Steam pressure at the 4-th extraction	**43**	Efficiency of the 3-rd stages group
11	Steam temperature at the 4-th extraction	**44**	Capacity coefficient of 3-rd stages group
12	Steam pressure at the 5-th extraction	**45**	Efficiency of the 4-th stages group
13	Steam temperature at the 5-th extraction	**46**	Capacity coefficient of 4-th stages group
14	Steam pressure at the 6-th extraction	**47**	Efficiency of the 5-th stages group
15	Steam temperature at the 6-th extraction	**48**	Capacity coefficient of 5-th stages group
16	Steam pressure at the 7-th extraction	**49**	Efficiency of the 6-th stages group
17	Steam temperature at the 7-th extraction	**50**	Capacity coefficient of 6-th stages group
18	Live steam mass flow rate	**51**	Capacity coefficient of 1-st stages group for extractions
19	Live steam pressure	**52**	Efficiency of the 2-nd stages group for extractions
20	Live steam temperature	**53**	Capacity coefficient of 2-nd stages group for extractions
21	Secondary steam mass flow rate	**54**	Efficiency of the 3-rd stages group for extractions
22	Secondary steam pressure	**55**	Capacity coefficient of 3-rd stages group for extractions
23	Secondary steam temperature	**56**	Efficiency of the 4-th stages group for extractions
24	Mass flow rate at the 1-st stages group	**57**	Capacity coefficient of 4-th stages group for extractions
25	Mass flow rate at the 2-nd stages group	**58**	Efficiency of the 5-th stages group for extractions
26	Mass flow rate at the 3-rd stages group	**59**	Capacity coefficient of 5-th stages group for extractions
27	Mass flow rate at the 4-th stages group	**60**	Efficiency of the 6-th stages group for extractions
28	Mass flow rate at the 5-th stages group	**61**	Capacity coefficient of 6-th stages group for extractions
29	Mass flow rate at the 6-th stages group	**62**	Capacity coefficient of 1-st stages group for extractions
30	Mass flow rate at the 1-st extraction	**63**	Efficiency of HP cylinder
31	Mass flow rate at the 2-nd extraction	**64**	Capacity coefficient of HP cylinder
32	Mass flow rate at the 3-rd extraction	**65**	Efficiency of IP cylinder
33	Mass flow rate at the 4-th extraction	**66**	Capacity coefficient of IP cylinder

In the case of single-time degradations three intermediate values within the range between zero degradation and maximum one (i.e. 25%, 50% i 75% of its maximum value) were taken into account. In the case of multi-time degradations only maximum values of degradations of particular quantities were considered.

The ordered sets of simulation results were used for training the ANNs in order to made them tought in detecting geometrical degradations.

Size of databases for models

The prepared combinations of single-time, twofold and threefold degradations, associated with 37 geometrical quantities sufferring operational degradation and measuring instruments subjected to degradation, are presented in Tab. 3. Each of them is represented by the vector of 37 components. Number of combinations of possible particular degradations in which only one scale of degradation and one set of independent variables have been taken into account, results from the following combinatorial relations:

- single-time $\binom{37}{1} = 37$
- twofold $\binom{37}{2} = 666$
- threefold $\binom{37}{3} = 7770$.

During planning operations for simulative calculations the sets of data and results were split into the part used for training and that used for testing. Size of the so obtained sets is presented in Tab. 3. It is equal to the number of performed simulative calculations of degradations.

In the database not intended for using in training all the degradation sets contain both full scale of degradation and partial one (of 50 % of its maximum value) of the geometrical quantities.

Tab. 3. *Size of simulation sets – models of degradation of component devices of the thermal cycle within the HP and IP cylinders, obtained for the determined set of independent variables*

Characteristics of partial databases	Database used for training	Database used for testing
Total size of the database	8584	17612
Size of the database for single-time degradations	4 * 37 = 148	2 * 37 = 74
Size of the database for twofold degradations	1 * 666 = 666	3 * 666 = 1998
Size of the database for threefold degradations	1 * 7770 = 7770	2 * 7770 = 15540

IDENTIFICATION OF DEGRADATIONS BY THE ANN TRAINED ON THE BASIS OF SIMULATION RESULTS

To identification of degradations the ANNs of a multi-layer perceptron kind were applied, like e.g. in [8, 10, 13].

In building a diagnostic relation based on the ANN methods one can apply:

- one global network which determines degradation code in the form of vector
- a set of networks each of which identifies only one cause of degradation.

The second solution is more favourable because of a lower demand for computer memory as well as a shorter training period as compared with the first case, at maintained similar accuracy [9]. Hence, 37 ANNs were subjected to investigations on identification of degradations; each of them was intended for the identifying of only one geometrical or measuring cause. The teaching inputs and outputs of the ANNs are presented in Fig. 3.

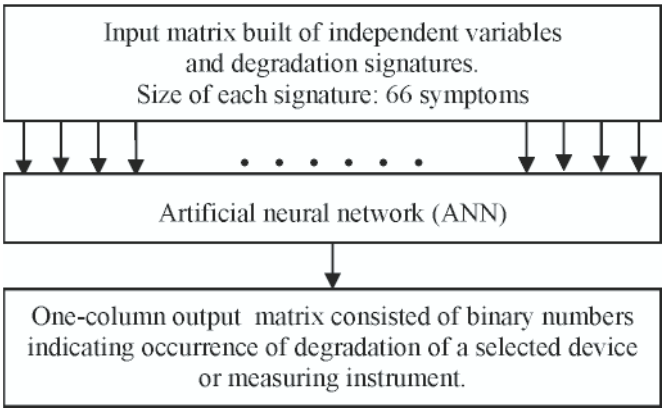

Fig. 3. *Inputs and outputs of one ANN (out of 37 dedicated ANNs) dedicated to fulfil role of a diagnostic relation which identifies degradation of one, out of 22 (see Tab.1), geometrical dimension of component devices of steam power unit or one, out of 15, (see Tab. 1, items No. 23 through 37), measuring instrument located at the cycle's extractions.*

Knowing from simulations, an expected response of the ANN one can assess correctness of neural calculations.

Single-time degradations were identified faultlessly both for the cases used for training and those not used for training, Tab. 4, as obtained also in [7, 10, 15]. Hence in this case it is possible to distinguish, without any trouble, degradations/faults of a measuring instrument from operational degradations of geometry of elements. Identification of multifold degradation cases is more difficult. The results of identification of such degradations, obtained from testing, are presented in Tab. 4. The number of considered cases, given in the denominator of each fraction, shown in Tab. 4, determines number of combinations between degradations beginning from single-time ones to threefold ones.

Identification errors, in consequence, distinctions between faults of measuring instruments and geometry degradations, are small. Hence it is possible to use the ANN methods for the combine diagnosing of devices and measurements of complex power systems. The described ANN can be taken as neural diagnostic relations capable of identifying locations of degradations.

IDENTIFICATION OF DEGRADED MEASURING INSTRUMENTS PRESENTED ON THE EXAMPLE TAKEN FROM OPERATIONAL PRACTICE

The trained, above described, neural networks which identify degradation of devices and measuring instruments, were tested by using a few examples of measurement data obtained from current power unit operation. The set was solely tested of the ANNs each of which identified only one

Tab. 4. Functioning quality of the network intended for the identifying of kind of degradations within HP and IP cylinders of high-power turbine

% contribution of erroneously identified degradation models	Erroneous responses to the test for which the database applied to training, was used	Erroneous responses to the test for which the database not applied to training, was used
Single-time ones	$\Delta_{3.1} = \frac{0}{4 \cdot 37} \cdot 100\% = 0\%$	$\overline{\Delta_{3.1}} = \frac{0}{2 \cdot 37} \cdot 100\% = 0\%$
Twofold ones	$\Delta_{3.2} = \frac{0}{666} \cdot 100\% = 0\%$	$\overline{\Delta_{3.2}} = \frac{4}{3 \cdot 666} \cdot 100\% = 0.202\%$
Threefold ones	$\Delta_{3.3} = \frac{5}{7770} \cdot 100\% = 0.064\%$	$\overline{\Delta_{3.3}} = \frac{39}{2 \cdot 7770} \cdot 100\% = 0.2509\%$

degradation on the basis of the processing of the complete degradation signature.

It concerns results of the measurements whose illustration in the form of the expansion line based on pressure and temperature values recorded at extractions of high-power turbine, has been presented in Fig. 4. Such run of the current state expansion line (the red line in Fig. 4) and its comparison with the run of the reference state line (the blue line in Fig. 4) can be met during the monitoring performed short time after steadying the reference state. This is the case when component devices of thermal cycles are usually not yet degraded but degradations may occur in measuring system. Such graphical presentation makes the assessing of performance of the diagnostic relation elaborated to identify location of degradation, easier. The relation is based on transformation of the complete signature of degradation, that is the measurements possible to be found on the entropic diagram of expansion (Fig. 4) and the remaining quantities which build the degradation signature and are calculated from measured quantities. The result of operation of the neural relation indicates that degradation of the temperature measuring instrument at 3-rd extraction, occurs (see item 9 of Tab.1). It was identified by the ANN no. 31 of the set of neural networks. The calculation results of the remaining ANNs were equal to „0", this means that the degradations attributed to them have not been occurred at all.

SUMMARY

- The performed tests based on the simulations and selected operational measurements showed that the application of artificial neural networks as diagnostic relations which are capable of identifying locations of degradations of component devices of thermal cycles of steam power units and locations of degraded measuring instruments, is rational. The tests based on simulations are characterized by a small value of identification error. The tests making use of current measurement results show that to identify defected measuring instruments is possible. However possible identification of a kind of degradation of component devices of turbine thermal cycles has not been so far confirmed by observations after disassembly of the turbine under repair as until now such operation has not been performed.
- To simulate degradations of a larger size seems to be necessary. However to do it a better computer hardware, especially as regards its greater operation memory, is required. Development of computers provides such prospects.

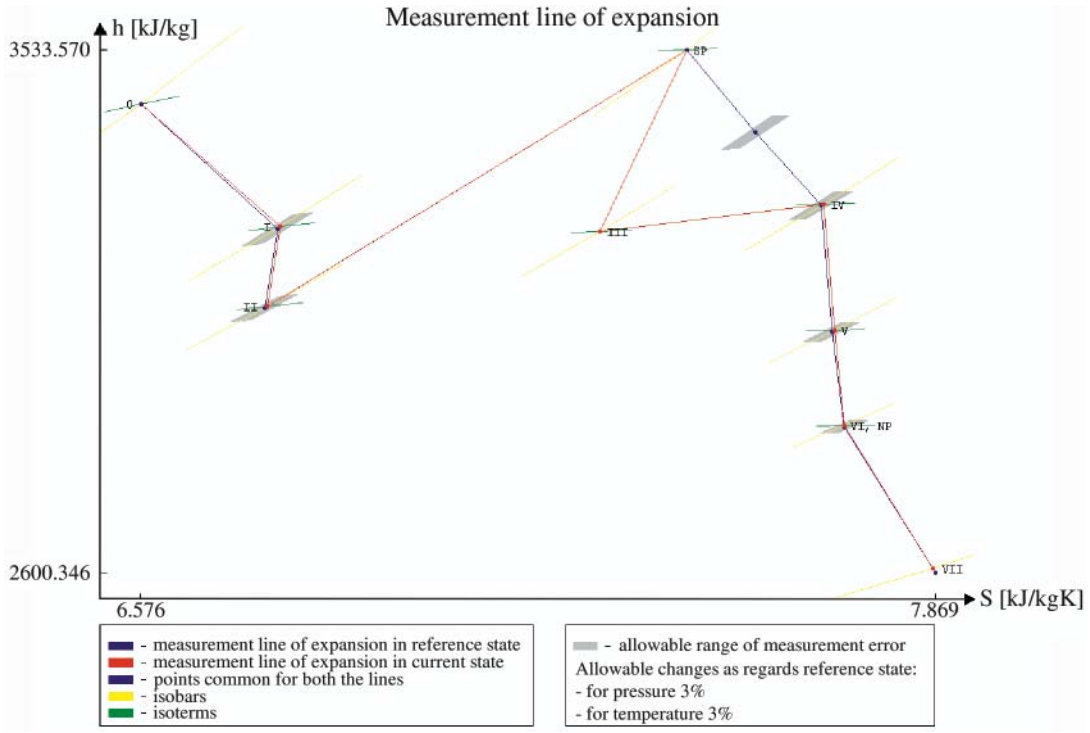

Fig. 4. Illustration of the expansion line determined for the parameters measured at extractions and achieved after a short period of operation of the power unit

BIBLIOGRAPHY

1. Abernethy R. B., Benedict R. P., Dowdell R. B.: *ASME Measurement Uncertainty,* Transactions of ASME, Journal of Fluids Engineering, June 1985, ASME 1985, p. 161-164
2. Demuth H., Beale M.: *Neural Network Toolbox for use with Matlab,* Natick: The Math Works Inc. 1996
3. Dewaleff P., Leonard O.: *On-Line Measurement Validation and Performance Monitoring Using Robust Kalman Filtering Techniques*, W: (In materials of) 5-th European Conference on Turbomachinery, Prague, March 17-21, 2003, p.345-346
4. Doel D. L.: *Sample Analyses Including Interpretation of Residual Error,* VKI Lectures on Gas Turbine Condition Monitoring & Fault Diagnosis, Ed. Sieverding & Mathhioudakis, ISSN0377-8312, January 13-17, Rhode Saint Genese, Belgium, Unit 4
5. Fodemski T. R., *et al*.: *Thermal measurements, Part 1 and 2* (in Polish), WNT (Scientific Technical Publishing House), Warsaw 2001
6. Gardzilewicz A., Głuch J., Bogulicz M., Uziębło W.: *Correctness control of thermal fluid flow measurement data achieved from DCS systems of steam-turbine electric power stations* (in Polish), W: (In materials of) 5th Conference on diagnostics of industrial processes DPP'2003, Władysławowo, 15÷17 September 2003, p. 391-396
7. Głuch J.: *On detection of incorrect measurements in DCS systems of power objects* (in Polish), W: (In materials of) The Scientific Conference MECHANIKA 2005, Gdańsk, 4 February 2005, p. 75-81
8. Głuch J.: *Application of Artificial Neural Networks (ANN) as Multiple Degradation Classifiers in Thermal and Flow Diagnostics,* TASK Quarterly 2005 No. 9, Gdańsk 2005, p. 1001÷1012
9. Głuch J.: *Control of thermal-and-flow measurements in DCS systems of complex power objects* (in Polish), (In materials of) The Conference DPP'05, Rajgród, 12÷14 September 2005, Special Issue of the journal Pomiary Automatyka Kontrola, No. 9/2005, p. 170÷172
10. Głuch J.: *A method of thermal-and-flow diagnostics capable of identifying of location and degree of degradation of turbine power units* (in Polish) Series: Monographs, No. 81, Wydawnictwo Politechniki Gdańskiej (Publishing House of Gdańsk University of Technology), Gdańsk 2007
11. IEC: *IEC International Standard CEI IEC 953-1 i 953-2*, Rules for Steam Turbine Thermal Acceptance Tests, Part 1 and Part 2, First Edition 1990.
12. Kosowski K.: *Some aspects of vibration control; Part I: Active and passive control*, Polish Maritime Research, 4/2004 (42), Vol. 11, Gdańsk, 2004, p. 22-27
13. Kosowski K.: *Some aspects of vibration control; Part II: An optimal active controller*, Polish Maritime Research, 1/2005 (43), Vol. 12, Gdańsk, 2005, p. 28-31
14. Kościelny J. M.: *Directions of development of decentralized control systems (DCS)* (in Polish), Pomiary Automatyka Kontrola No. 6/1998, p. 207÷210
15. Krzyżanowski J., Głuch J.: *Thermal-and-flow diagnostics of power objects* (in Polish), Wydawnictwo Inst. Masz. Przepł. PAN (Publishing House of the Institute of Fluid Flow Machinery, Polish Academy of Sciences),Gdańsk 2004
16. Makal J.: *Measurement uncertainty of multi-channel measuring system* (in Polish), Pomiary Automatyka Kontrola, No. 9/2001, p. 5÷7
17. Michalski L., Eckersdorf K.: *Temperature measurements* (in Polish), WNT (Scientific Technical Publishing House),Warsaw 1986
18. Polish Standards: PR: PN-EN 60953-1: PR: PN-IEC953-1, PR: PN-EN 60953-2: PR: PN-IEC953-2,. *Requirements for thermal performance tests of steam turbines* (in Polish). *Sheet 1 and 2: Methods A and B,* December 1998
19. PTC6: *Performance Test Code 6 on Steam Turbines ASME PTC6-2001, 1996* (Revision of ASME PTC6-1976)
20. Romessis C., Mathioudakis K., *Jet Engine Sensor Validation with Probabilistic Neural Networks*, W: (In materials of) 5-th European Conference on Turbomachinery, Prague March 17÷21, 2003, p. 369-380
21. Rusinowski H., Szega M., Ziębik A., Majchrzak H, Szweda J.: *Operational control system of the power unit No. 4 installed in Opole Power Station, to which compensation calculus methods are applied* (in Polish), (In materials of) The Conference PBEC'2001, Zesz. Nauk. Polit. Warszawskiej(Scientific Bulletins of Warsaw University of Technology) No. 190, 2001, p. 249-260
22. Witoś M.: *Measurement line diagnosing in dispersed control systems* (in Polish), (In materials of:) 5th Domestic Conference DPP'2001, Łagów, 17÷19 September 2001, p. 377-380
23. Żółtowski B., Ćwik Z.: *Lexicon of technical diagnostics* (in Polish), Wydawnictwo Uczelniane Akademii Techniczno-Rolniczej (Publishing House of Technical-Agricultural Academy of Bydgoszcz), Bydgoszcz 1996.

CONTACT WITH THE AUTHOR

Jerzy Głuch, Assoc. Prof.
Faculty of Ocean Engineering
and Ship Technology,
Gdańsk University of Technology
Narutowicza 11/12
80-952 Gdańsk, POLAND
e-mail : jgluch@pg.gda.pl

POLISH MARITIME RESEARCH 4(58) 2008 Vol 15; pp. 52-58
10.2478/v10012-007-0097-7

Modelling of propeller shaft dynamics at pulse load

Andrzej Grządziela, Assoc. Prof.
Polish Naval University

ABSTRACT

The article discusses a method of modelling of propeller shaft dynamics at the presence of virtually introduced underwater detonation effects. The propeller shaft model has four degrees of freedom, which provides opportunities for introducing shaft displacements and rotations similar to those observed in a real object. The equations of motion, taking into account the action of external agents, were implemented to the Matlab SIMULINK environment. The obtained time-histories and their spectra were compared with the experimental results of the tests performed on the marine testing ground. The performed model identification confirmed its sensitivity to changing parameters of motion and external actions.

Keywords :

INTRODUCTION

Modelling of technical machines and devices is nowadays done in the form of mathematical and physical models of canonical equations, or virtual 3D tools. Both methods return comparable results, and selecting one of them is determined by an individual approach to the problem, or past experience and habits of a research worker. A basic goal of modelling for diagnostic purposes is to be able to predict failure symptoms, both of primary and secondary nature. The application of static or dynamic loads makes it possible to shorten considerably the time and reduce significantly the cost of the investigations. An important property of the modelling is the ability to introduce complex virtual damages, which in practice either occur rarely, or their occurrence leads to rapid destruction of the machine or group of machines. The modelling aims at finding a group of sensitive symptoms, which uniquely interpret changes of technical state of the machine. The created set of symptoms, tested on a real object, makes a good basis for fast and easy implementation of the vibration based diagnostic system.

The article analyses modes of free vibration of the propeller shaft in the ANSYS environment, and the model of action of underwater detonation, understood as the right-hand side of the second-type Lagrange equation. The ability to introduce virtual damages, such as shaft line axis misalignment, for instance, makes it possible to obtain a sensitive, diagnostic oriented model of the propeller shaft. The following actions were introduced to the proposed dynamic model [2]:

- main engine driving torque
- screw propeller anti-torque
- axial thrust force
- the action resulting from changes in relative positions of load-carrying bearings and thrust bearings in the shaft line
- the action of the hydrodynamic pressure generated by an underwater detonation.

3D MODELLING

The analysis of the propeller shaft dynamics bases on a 3D model worked out in SOLID Works environment and analysed in the ANSYS environment – see Fig. 1. The performed analyses aimed at obtaining the information on free vibration modes of the shaft, with further identification of possible threats during its operation. The results of the analyses of four initial free vibration modes are collected in Tab. 1. These results confirm an opinion that during the operation of a real propulsion system the propeller shaft, working within the range of $n_{PS} = 150 \div 900$ rev/min, is subject to the appearance of resonances.

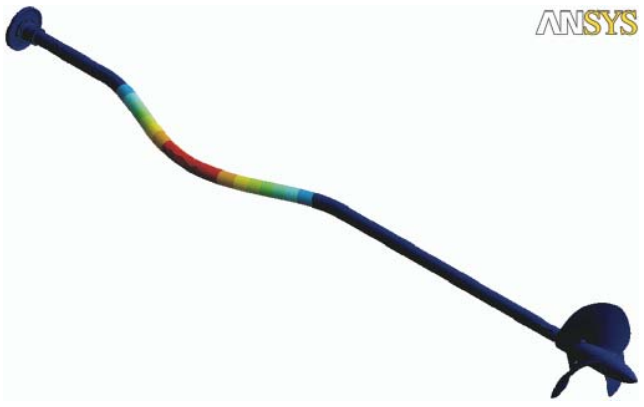

Fig. 1. *Sample free vibration mode observed in the analysed propeller shaft*

Tab. 1. Analysis of four initial free vibration modes of the shaft

Mode (vibration mode number)	Analysed degree of freedom	Frequency [Hz]	Shaft revolutions [rev/min]
1	Axial. torsional - free Axial - fixed	7.8386	470.30
2	Axial. torsional - free Axial - fixed	7.8529	471.17
3	Axial. torsional - free Axial - fixed	23.961	1437.6
4	Axial. torsional - free Axial - fixed	24.023	1441.4

DYNAMIC MODEL OF THE SHAFT LINE

In the propeller shaft model the driving torque of the internal combustion piston engine is transmitted via the reduction gear to the constant-pitch propeller. The model meets the following requirements:

- ★ makes it possible to introduce the action of external agents
- ★ reveals sensitivity to changing parameters of propeller shaft motion
- ★ reveals sensitivity to propeller shaft axis misalignment
- ★ reveals no sensitivity of the coaxiality symptom to disturbances coming from the environment
- ★ preserves the compliance of the spectral structure in the frequency domain with the results of measurements done on a real object.

The propeller shaft model was an object of simulation tests to check its sensitivity to the action of external agents and compliance with the behaviour of the object in the conditions of the simulated environmental action [5]. The proposed model is nonlinear, and an attempt to describe it by linearisation of actions is unacceptable as it may lead to incorrect conclusions resulting from possible superposition of the effects observed in linear systems [3]. Since in the equations of motion the time is represented explicitly, this system is non-autonomous. A scheme of the reactions on supports at the presence of the external actions is given in Fig. 2.

The kinetic energy of the presented system was written as:

$$E_k = \frac{1}{2} I_N \dot{\varphi}_N^2 + \frac{1}{2} I_{SR} \dot{\varphi}_{SR}^2 + \frac{1}{2} m_I (\dot{v}_I^2 + \dot{h}_I^2) + \frac{1}{2} m_{II} (\dot{v}_{II}^2 + \dot{h}_{II}^2) + \frac{1}{2} m_{SR} (\dot{v}_{SR}^2 + \dot{h}_{SR}^2) + \frac{1}{2} m_N (\dot{v}_N^2 + \dot{h}_N^2) \quad (1)$$

Then, the potential energy of the system was written as:

$$E_p = \frac{1}{2} k_{NS} \varphi_N^2 + \frac{1}{2} k_{ws} (\varphi_{SR} - \varphi_N)^2 + \frac{1}{2} k_{Ig} (h_I^2 + v_I^2) + \frac{1}{2} k_{IIg} (h_{II}^2 + v_{II}^2) + \frac{1}{2} k_{IIIg} (h_{III}^2 + v_{III}^2) + \frac{1}{2} k_{IVg} (h_{SR1}^2 + v_{SR1}^2) \quad (2)$$

And, finally, the dispersed energy was written as:

$$E_R = \frac{1}{2} c_{ws} (\dot{\varphi}_{SR} - \dot{\varphi}_N)^2 + \frac{1}{2} c_{Ts} \dot{\varphi}_{SR}^2 + \frac{1}{2} c_{Ig} (\dot{h}_I^2 + \dot{v}_I^2) + \frac{1}{2} c_{IIg} (\dot{h}_{II}^2 + \dot{v}_{II}^2) + \frac{1}{2} c_{IIIg} (\dot{h}_{III}^2 + \dot{v}_{III}^2) + \frac{1}{2} c_{IVg} (\dot{h}_{SR1}^2 + \dot{v}_{SR1}^2) \quad (3)$$

The external actions of the drive, understood as the driving torque and the required propeller torque, were given as:

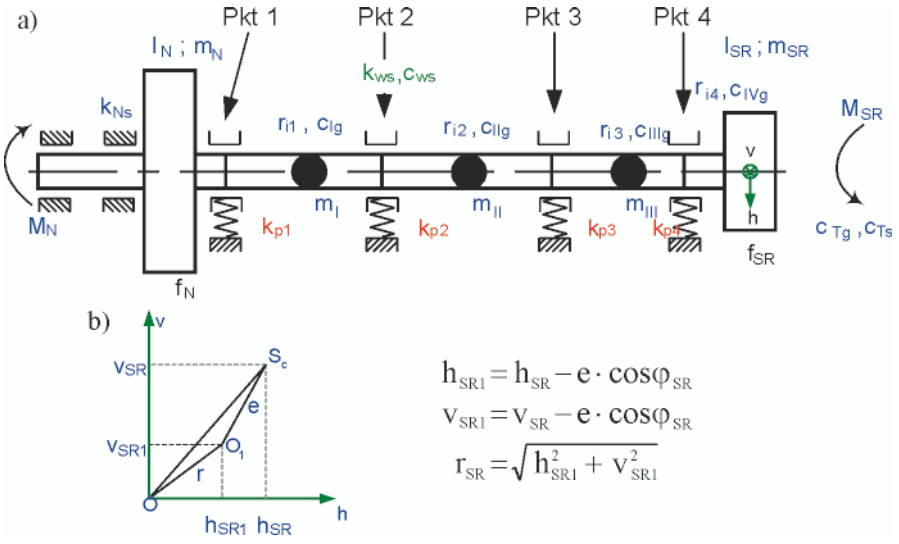

Fig. 2. Scheme of the analysed propeller shaft

where the symbols used in the formulas stand for:

- I_N; m_N – reduced moment of inertia and reduced mass of the driving part
- I_{SR}; m_{SR} – reduced moment of inertia and reduced mass of the driven part (screw)
- M_N; M_{SR} – driving torque and anti-torque (on screw)
- m_I; m_{II}; m_{III} – reduced masses of shaft elements between successive supports
- k_{Ns} – torsional stiffness of the drive
- r_{i1}; r_{i2}; r_{i3}; r_{i4}; – transverse stiffness coefficients of shaft elements between successive supports
- c_{Ig}; c_{IIg}; c_{IIIg}; c_{IVg} – transverse dampings of shaft elements between successive supports
- k_{ws}; c_{ws} – shaft stiffness and torsional damping
- φ_N; φ_{SR} – rotation angles of the drive and the screw, respectively
- h_{SR}; v_{SR} – horizontal and vertical coordinate of the gravity centre S_c (taking into account shaft deflection)
- h_{SR1}; v_{SR1} – horizontal and vertical coordinate of the rotation centre O_1
- h_N; h_I; h_{II}; v_N; v_I; v_{II} – horizontal and vertical coordinates for masses m_N; m_I; m_{II}
- c_{Tg}; c_{Ts} – water damping resistance: transverse (neglected) and torsional.

$$Q = M_N - M_{sr} \tag{4}$$

Calculating the stiffness k requires solving the statically undeterminable system, which was done using the method of impact coefficients α_{ij} (and coefficients $r_{ij} = f(\alpha_{ij})$ depending on them). In the first step, making use of the equation of three moments and the Wierieszczagin method, the impact coefficients were determined in a general form:

$$\alpha_{k-1,k} = \alpha_{k,k-1} = \frac{l_k}{6EJ_k} \tag{5}$$

$$\alpha_{k,k} = \frac{1}{3}\left(\frac{l_k}{EJ_k} + \frac{l_{k+1}}{EJ_{k+1}}\right) \tag{6}$$

$$\alpha_{k+1,k} = \alpha_{k,k+1} = \frac{l_{k+1}}{6EJ_{k+1}} \tag{7}$$

Then, by rearranging the general formula (in the matrix form) $y_j = \alpha_{ij}S_j$ to the form $S_j = r_{ij}y_j$ the coefficient r_{ij} was determined (taking into account that some matrix elements are equal to zero):

$$\begin{bmatrix} S_1 \\ S_2 \\ S_3 \\ S_4 \end{bmatrix} = \begin{bmatrix} a_{11} & a_{12} & 0 & 0 \\ a_{21} & a_{22} & a_{23} & 0 \\ 0 & a_{32} & a_{33} & a_{34} \\ 0 & 0 & a_{43} & a_{44} \end{bmatrix}^{-1} \cdot \begin{bmatrix} y_1 \\ y_2 \\ y_3 \\ y_4 \end{bmatrix} \tag{8}$$

After using the second type Lagrange equations and introducing coefficients r_{ij} to these equations we arrived at Equations (9) which describe the vibrational motion of the propeller shaft. These equations were introduced to the Matlab SIMULINK environment – Fig. 3. Then, the model was complemented by the actions of virtual external agents, which can act individually or in a coupled form. The obtained simulation results refer to the following issues:

- the analysis of propeller shaft vibrations in stationary conditions
- the analysis of the system response to individually introduced external dynamic disturbances, such as changes of parameters of coaxiality and underwater detonation pulse
- the analysis of system response to external dynamic disturbances introduced in a coupled form, for instance for assumed changing coaxiality parameters at the presence of the underwater detonation pulse.

$$\begin{aligned}
&I_N\ddot{\varphi}_N + c_{ws}(\dot{\varphi}_N - \dot{\varphi}_{SR}) + k_{NS}\varphi_N + k_{ws}(\varphi_N - \varphi_{SR}) = M_N \\
&m_I\ddot{h}_I + c_{Ig}\dot{h}_I + r_{11}h_I + r_{12}h_{II} + r_{13}h_{III} + r_{14}h_{SR} = 0 \\
&m_I\ddot{v}_I + c_{Ig}\dot{v}_I + r_{11}v_I + r_{12}v_{II} + r_{13}v_{III} + r_{14}v_{SR} = 0 \\
&m_{II}\ddot{h}_{II} + c_{IIg}\dot{h}_{II} + r_{21}h_I + r_{22}h_{II} + r_{23}h_{III} + r_{24}h_{SR} = 0 \\
&m_{II}\ddot{v}_{II} + c_{IIg}\dot{v}_{II} + r_{21}v_I + r_{22}v_{II} + r_{23}v_{III} + r_{24}v_{SR} = 0 \\
&m_{III}\ddot{h}_{III} + c_{IIIg}\dot{h}_{III} + r_{31}h_I + r_{32}h_{II} + r_{33}h_{III} + r_{34}h_{SR} = 0 \\
&m_{III}\ddot{v}_{III} + c_{IIIg}\dot{v}_{III} + r_{31}v_I + r_{32}v_{II} + r_{33}v_{III} + r_{34}v_{SR} = 0 \\
&I_{SR}\ddot{\varphi}_{SR} + c_{ws}(\dot{\varphi}_{SR} - \dot{\varphi}_N) + c_{Ts}\dot{\varphi}_{SR} + c_{IIIg}(\dot{h}_{SR}e\sin\varphi_{SR} + \\
&- \dot{v}_{SR}e\cos\varphi_{SR} + e^2\dot{\varphi}_{SR}) + k_{ws}(\varphi_{SR} - \varphi_N) + \\
&+ r_{44}(h_{SR}e\sin\varphi_{SR} - v_{SR}e\cos\varphi_{SR}) = M_{SR} \\
&m_{SR}\ddot{h}_{SR} + c_{IVg}(\dot{h}_{SR} + \dot{\varphi}_{SR}e\sin\varphi_{SR}) + r_{41}h_I + r_{42}h_{II} + r_{43}h_{III} + \\
&+ r_{44}(h_{SR} - e\cos\varphi_{SR}) = 0 \\
&m_{SR}\ddot{v}_{SR} + c_{IVg}(\dot{v}_{SR} - \dot{\varphi}_{SR}e\cos\varphi_{SR}) + r_{41}v_I + r_{42}v_{II} + \\
&+ r_{43}v_{III} + r_{44}(v_{SR} - e\sin\varphi_{SR}) = 0
\end{aligned} \tag{9}$$

The calculations performed in the Matlab SIMULINK environment aimed at iterative introduction of changes of dynamic parameters describing the operation of the propeller

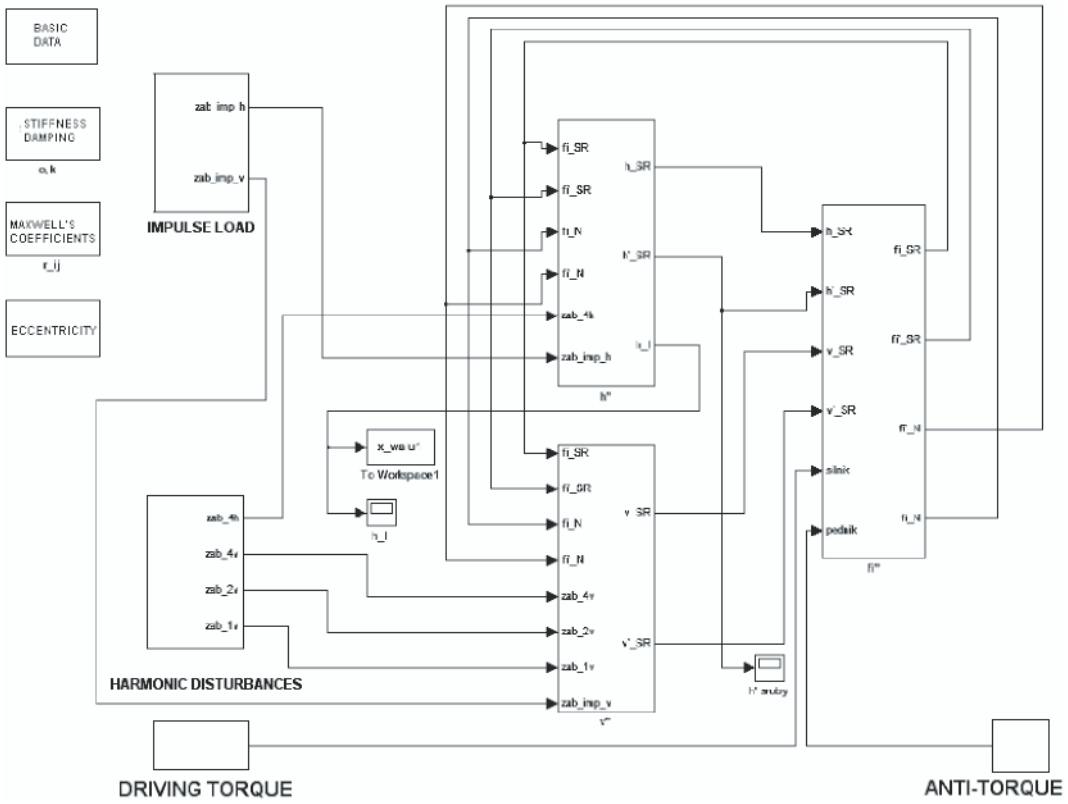

Fig. 3. Starting block of the propeller shaft model in the Matlab SIMULINK environment

shaft model in the simulated real conditions. The model components included the driving torque and anti-torque, changes in the displacement of the propeller shaft axis, and the pulse load coming from an underwater detonation. The underwater detonation model assumed the existence of three successive gas bubble pulses [1,4].

Selected sample simulations of the vibration acceleration spectra recorded at point 2 at the presence of environmental action are given in Fig. 4, while Fig. 5 additionally includes the underwater detonation.

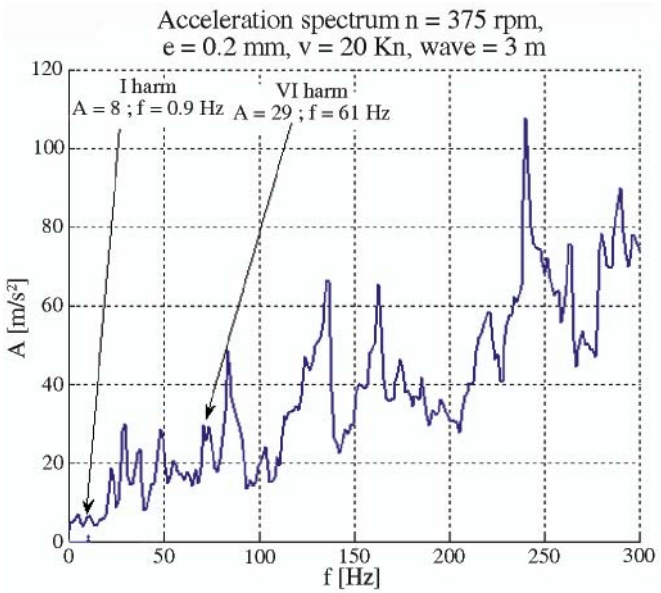

Fig. 4. *Simulated transverse vibration spectrum at point 2 for n_{PS} = 375 rev/min, P = 0.2 mm, ∢ K = 0° and ς = 3m*

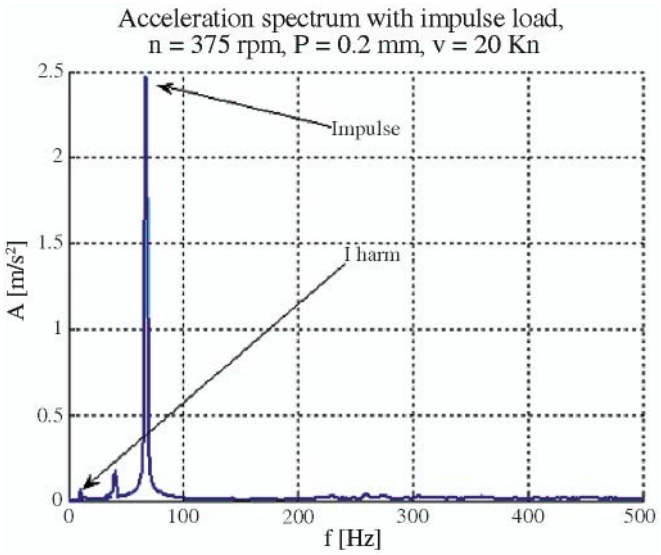

Fig. 5. *Simulated transverse vibration spectrum at point 2 for n_{PS} = 375 rev/min ∢ K = 0°, ς = 5m, and detonation pulse i_D = 50 g*

Fig. 6 shows the simulated action of the underwater detonation at point 1 of the propeller shaft model, done for two distances of the detonation epicentre from the ship hull. The transverse vibration spectra of the propeller shaft loaded with the underwater detonation pulse suggest the existence of a remarkable effect of the distance from the detonation epicentre on the vibration acceleration at the examined point. The nature of the pulse load makes use of the pulse load model [1,4].

In order to illustrate the sensitivity of the model to changes in shaft line misalignment, in Fig. 7 are shown selected spectra of vibration velocities which were recorded at point 2, along V-axis, for course and wave amplitude parameters equal to ∢ K = 0° and ς = 5 m, respectively, and for the propeller shaft rotational speed n_{PS} = 570 rev/min, for shaft axis displacements P = 0.2 mm and P = 0.5 mm.

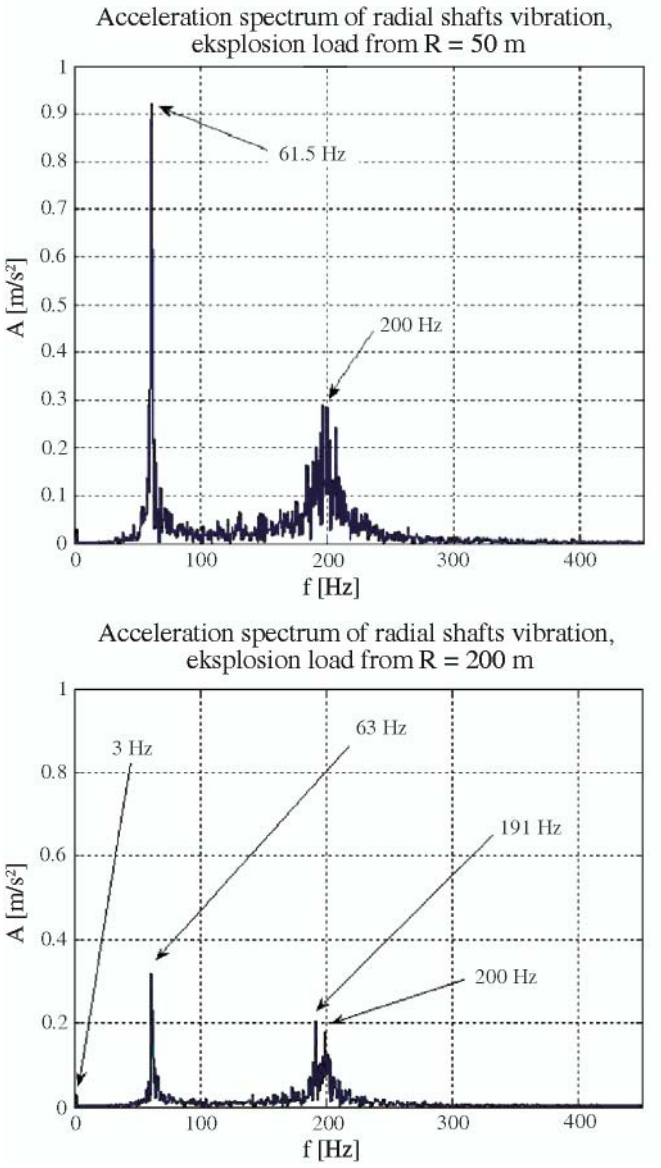

Fig. 6. *Simulated transverse vibration acceleration spectra at point 1 for the charge mass m = 40 kg blowing at a distance R = 50m and R = 200 m*

The obtained results confirm the unique effect of shaft axis displacements on the structure and characteristic parameters of the modelled spectrum.

IDENTIFYING THE PROPELLER SHAFT MODEL

The presented dynamic model of the propeller shaft was loaded with virtual loads, including coupled loads, in order to check model applicability to technical diagnostics purposes. The basic criterion for the model compliance with the real object is the compliance of corresponding spectra in frequency domain for different shaft revolutions in stationary conditions [3]. A sample analysis of the results of simulation is given in Figs. 8a and 8b. Changes in the shaft rotational speed which were assumed in the model have resulted in the increase of frequency of the basic harmonic and the sixth harmonic, being an identified symptom of shaft axis misalignment, like in the investigations of a real object. At the same time, the value of the symptom corresponding to the shaft axis displacement by P = 0.1 mm increases with increasing shaft revolutions.

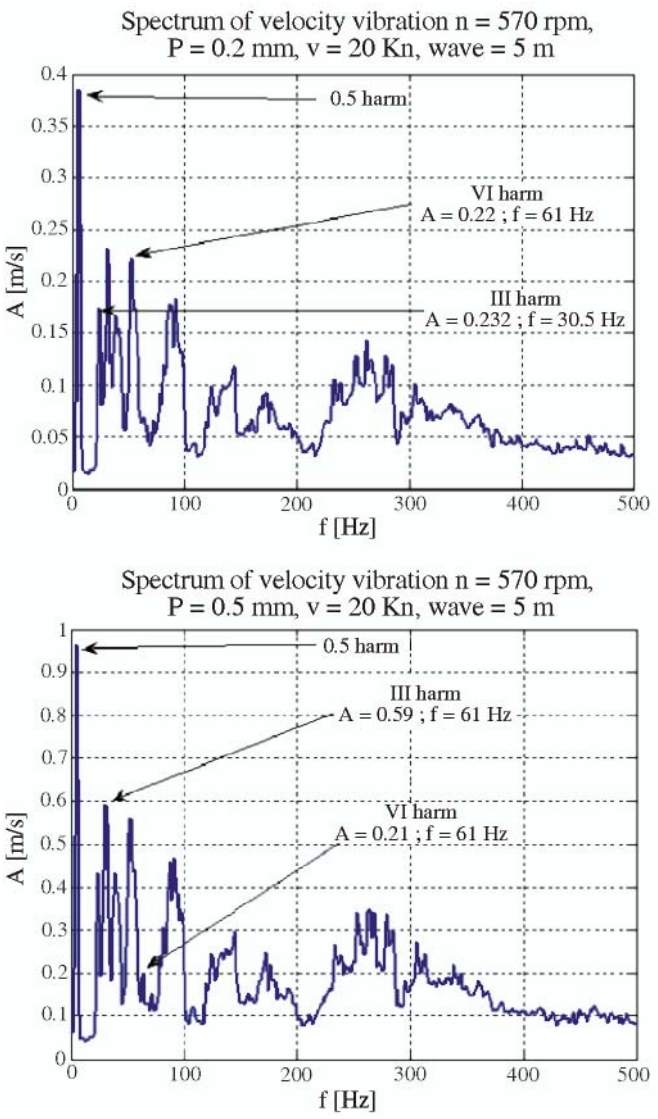

Fig. 7. *Simulated transverse vibration velocity spectra at point 2 for assumed propeller shaft axis displacements equal to P = 0.2 mm and P = 0.5 mm*

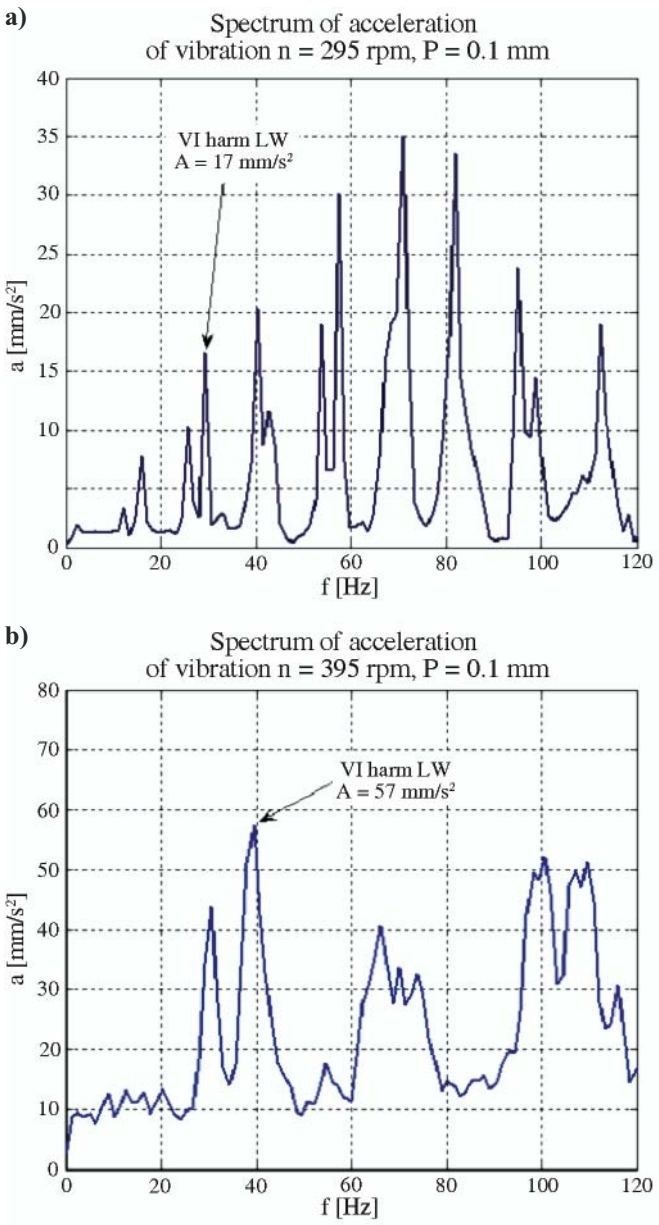

Fig. 8. a) *simulated vibration acceleration spectrum for shaft revolutions n_{PS} = 295 rev/min at axis displacement P = 0.1mm;* ***b)*** *simulated vibration acceleration spectrum for shaft revolutions n_{PS} = 395 rev/min at axis displacement P = 0.1mm*

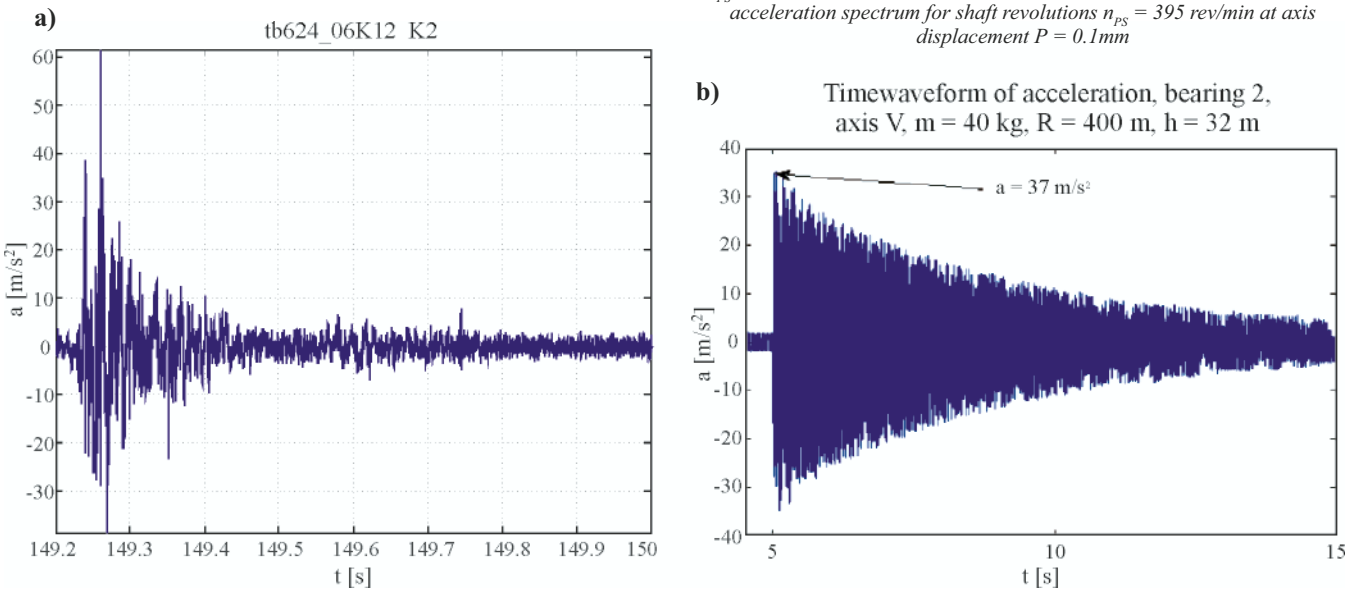

Fig. 9. a) *real vibration acceleration time-history recorded during underwater detonation;* ***b)*** *simulated vibration acceleration time-history during underwater detonation*

The identification of elastic shaft deformations provoked by an underground detonation is shown in Figs. 9a and 9b. The results measured on a real object were obtained on the marine testing ground after detonating the TNT blowing charge of m = 40 kg at a distance of R = 400 m and the depth of h = 32 m [4]. The simulated detonating action which was introduced to the model consisted of 3 successive pulses, according to the Cole relation [1]. The elastic deformation is best visible when comparing the time-histories of vibration accelerations. Like a real curve, the simulated vibration acceleration time-history is intensively damped, which testifies to the self-centring of the propeller shaft and the elastic nature of the deformation.

The next step in model identification consisted in comparing the results of simulations and measurements done on a real object for known shaft misalignment. The levels of the first and sixth vibration velocity harmonics recorded on the reduction gear thrust bearing casing (point 1 in the model) are given in Fig. 10a, while Fig. 10b shows the effect simulated for the assumed axis displacement equal to P = 0.2 mm, the same as on the real object.

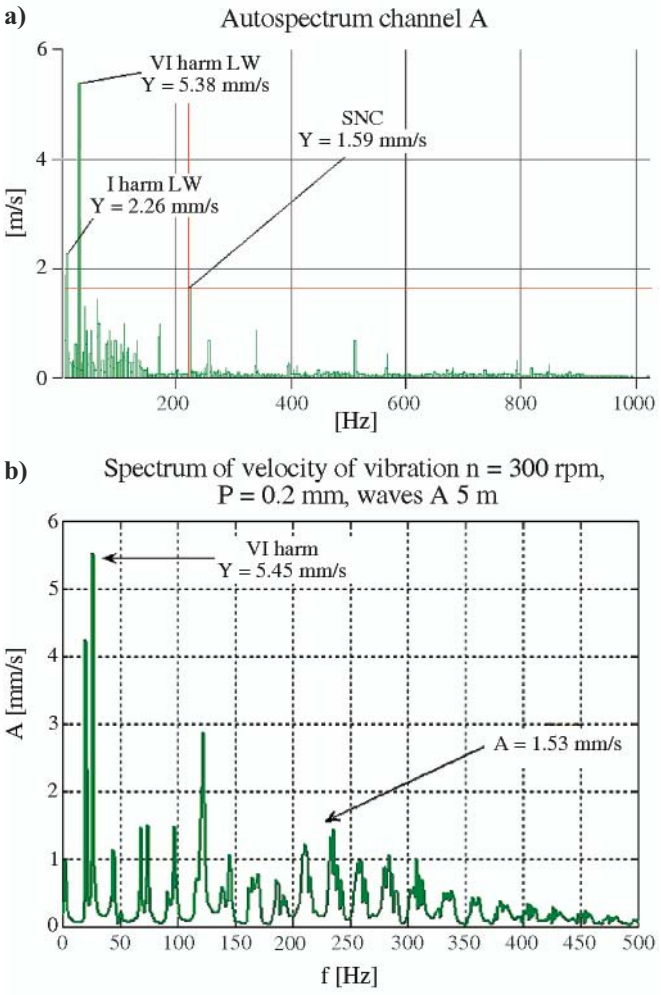

Fig. 10. a) *vibration velocity spectrum measured on a real object;* ***b)*** *vibration velocity spectrum simulated using the proposed model*

The analysis of the vibration velocity spectra shown in Figs. 10a and 10b reveals that the model preserves similarity of the relations between the basic harmonics. Slight differences in the values of basic components result from the need to use a function which matches the effect of strong nonlinear damping of the water environment, in which a large part of the propeller shaft and the propeller screw are immersed. Identifying the mathematical model consists in such selection of a set of coefficients or functions that the model solutions are close, within an assumed error tolerance, to the experimental results [8]. Table 2 collects maximum errors recorded when comparing model symptoms with those observed on the real object.

Tab. 2. *Maximum errors of model symptoms with respect to the measured results*

Symptom	Sixth harmonic of vibration velocity [mm/s]	Sixth harmonic of vibration acceleration [mm/s^2]	Detonation pulse [m/s^2]	First harmonic of vibration velocity [mm/s]
Measured	12.4	5.38	212.2	8.97
Obtained from model	13.6	5.45	206.4	9.78
Maximum relative error	9.67%	1.3%	-2.73%	9.03%

The maximum relative error was assumed not to exceed 10%. Analysing the data collected in Tab. 2 leads to a conclusion that the proposed model is identifiable and sensitive to basic diagnostic parameters.

CONCLUSIONS

A basic goal of modelling is the identification of the diagnostic model. In the reported case, comparing the results of the empirical studies and the simulations has proved good applicability of the proposed model. The obtained results confirmed model sensitivity to changes of the technical state of the object and varying input parameters. A vital property of the model was the insensibility of the axis misalignment symptom to the action of assumed environmental disturbances, such as underwater detonation.

Comparing the measured results with those obtained from the simulations indicates that there is potential space for the use of the results of the simulations in the data base of the on-line monitoring system for propulsion systems used on mine countermeasure vessels. The proposed model is general in nature, which makes it possible to adapt it in similar propeller shaft constructions.

NOMENCLATURE

a	– acceleration
A	– acceleration amplitude
c_{Ig}; c_{IIg}; c_{IIIg}; c_{IVg}	– transverse dampings of shaft elements between successive supports
c_{Tg}; c_{Ts}	– water damping resistance: transverse (neglected) and torsional
h	– depth of detonation
h_{SR1}; v_{SR1}	– horizontal and vertical coordinate of the rotation centre O_1
h_N; h_I; h_{II}; v_N; v_I; v_{II}	– horizontal and vertical coordinates for masses m_N; m_I; m_{II}
h_{SR}; v_{SR}	– horizontal and vertical coordinate of the gravity centre S_c (taking into account shaft deflection)
i_D	– maximum detonation acceleration pulse
I_N; m_N	– reduced moment of inertia and reduced mass of the driving part
I_{SR}; m_{SR}	– reduced moment of inertia and reduced mass of the driven part (screw)
k_{Ns}	– torsional stiffness of the propulsion system

k_{ws}; c_{ws}	–	stiffness and torsional damping of the shaft
m	–	mass
m_I; m_{II}; m_{III}	–	reduced masses of shaft elements between successive supports
M_N; M_{SR}	–	driving torque and anti-torque (on screw)
n_{PS}	–	propeller shaft rotational speed
P	–	axial displacement of the shaft line
r_{i1}; r_{i2}; r_{i3}; r_{i4};	–	transverse stiffness coefficients of shaft elements between successive supports
R	–	distance from detonation epicentre
φ_N ; φ_{SR}	–	rotation angles of the drive and screw, respectively
ς	–	wave amplitude [m]
$\measuredangle K$	–	ship course angle.

BIBLIOGRAPHY

1. Cole R. H.: *Underwater Explosions*. Princeton University Press, Princeton 1948
2. Cudny K.: *Ship shafting. Structures and calculations* (in Polish). Wydawnictwo Morskie. Gdańsk.1990
3. Dąbrowski Z.: *Machine shafts* (in Polish). PWN, Warszawa 1999
4. Grządziela A.: *An analysis of possible assessment of hazards to ship shaft line, resulting from impulse load.* Polish Maritime Research, No. 3/2007, pp. 14 – 17, Gdańsk 2007
5. Grządziela A.: *Dynamic problems of shaftslines*. Diagnostyka No. 4 vol. 44/ 2007 r, pp. 5 – 10, Olsztyn 2007.

CONTACT WITH THE AUTHOR

Andrzej Grządziela, Assoc. Prof.
Mechanic-Electric Faculty,
Polish Naval University
Śmidowicza 69
81-103 Gdynia, POLAND
e-mail : AGrza@amw.gdynia.pl

Photo: Cezary Spigarski

POLISH MARITIME RESEARCH 4(58) 2008 Vol 15; pp. 59-65
10.2478/v10012-007-0098-6

Numerical investigations of the engine cooling system in a small power vessel pod propulsion system

Czesław Dymarski, Prof.
Wojciech Leśniewski, Ms. C.
Gdansk University of Technology

ABSTRACT

The development of electronics and electrotechnology enabled to put electric motors of the alternating current in the pod and to use them for the main drive of ships. A lot of heat which must be picked up from the system is a problem which is turning up at applying the system of this type. Many big ships lately contended with these problems. Building the small propeller for the boat powered with solar power we decided to check the influence of the chilling middle on the temperature of the work of an engine. In the article we are presenting a built propeller and a way, into which an issue of the exchange of the heat was analysed using the Fluent software.

Keywords: azimuthing electric propulsion, pod propeller, heat transfer, cooling system

INTRODUCTION

Nowadays one of most rapidly developing types of ship propulsion systems is the combined diesel-electric system with two or more azipods. Usually this system consists of a number of current generating units, driven by internal combustion piston engines or gas turbines that deliver power to alternating current motors via the central electric switchgear and frequency converters. The motors, which drive directly ship propellers, are mounted in a pod situated in the lower part of a column suspended under the ship hull. As a rule, the column can move around by 360° with respect to the vertical axis, which secures excellent manoeuvring abilities of the ship and eliminates the need for using traditional steering gears. The ability to change smoothly the speed of the electric motors makes it possible to use simple and cheap constant pitch propellers. Other advantages of the discussed propulsion system include: smaller space occupied by the system inside the ship, better spatial arrangement of the main engine room elements, higher reliability secured by the use of two or more propellers, and the reduction of noise. These advantages are the reason why more and more ships, in particular large and luxurious passenger ships, and specialised vessels that require dynamic positioning, are equipped with this type of propulsion. It is noteworthy, however, that this type of propulsion, as compared to the traditional system with low-speed internal combustion engines, reveals also certain disadvantages. It is less efficient, much more expensive, and still some technical problems referring to its operation are to be solved. Lower efficiency of the entire system mainly results from lower efficiency of high- or medium-speed internal-combustion engines and the inevitable double energy conversion: from the mechanical energy to the electric energy and vice versa. High investment cost of the system results from extremely high price of motors with magnets made of rare earths, which are to be used here due to their small dimensions that make it possible to install them in the pod. The operating problems mainly refer to the bearing and sealing systems of the electric motor rotor shaft, which simultaneously plays the role of the propeller shaft, and the cooling system used in this motor. It is noteworthy that the above problems referring to the bearing and sealing systems can originate, among other reasons, from incorrect operation of the motor cooling system, as the conditions for heat absorption from the system are extremely unfavourable. Relatively very high power of the motor, against its extremely small dimensions and small space inside the pod, make the process of absorption of the generated heat extremely difficult.

In order to provide opportunities for correct operation of the propulsion system in various operating conditions, numerous research activities are performed as early as at the ship design stage. Due to extremely high cost of experimental investigations, wherever possible they are substituted with numerical analyses that make it possible to simulate system operation in a vast variety of expected operating conditions.

The article presents results of the numerical analysis of operation of the motor cooling system of the low power pod propulsion system, which is to be used in a small vessel, namely the catamaran ENERGA SOLAR that makes use of the solar energy.

TECHNICAL CONDITIONS AND DESCRIPTION OF THE EXAMINED PROPULSION SYSTEM

Fig. 1 shows a cross-section through the designed propeller. Its construction differs slightly from that used in high-power propellers. The present construction makes use of a toothed planetary reduction gear, mounted coaxially between the motor and the constant pitch propeller. The kinematic scheme of this gear is given in Fig. 2.

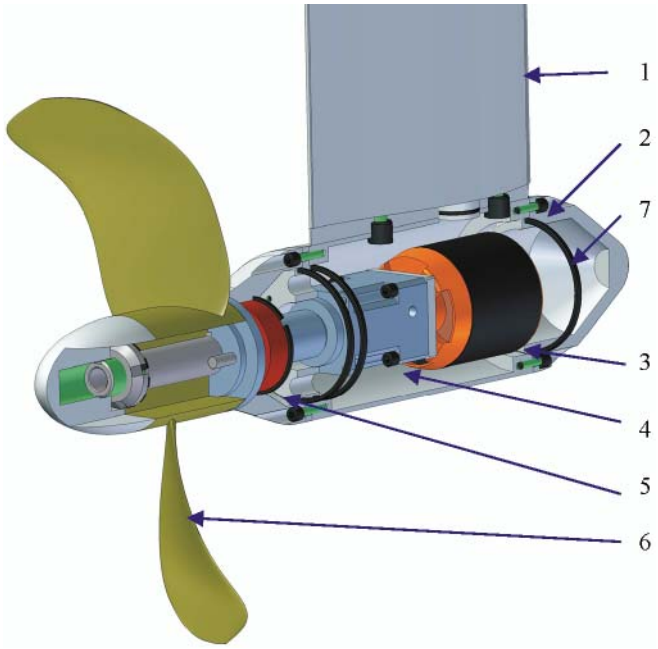

Fig. 1. *Cross section through the propeller:* ***1*** *– rotating column;* ***2*** *– pod;* ***3*** *– electric motor;* ***4*** *– planetary gear;* ***5*** *– rolling bearing;* ***6*** *– constant pitch propeller;* ***7*** *– O-ring*

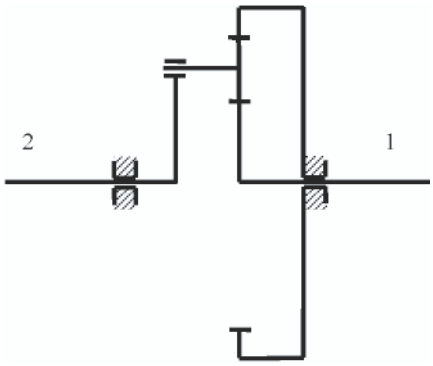

Fig. 2. *Kinematic scheme of the planetary gear with transmission ratio i = 3, made by APEX DYNAMICE, INC.* ***1*** *– input shaft;* ***2****- output shaft*

The presented propeller uses an asynchronous high torque three-phase motor Axi 5345 made by a Czech company MODELMOTORS Ltd. The nominal torque of the motor is Mn = 4.5 Nm, while its outer diameter is only 63 mm. In order to determine the efficiency of the motor working in combination with the frequency converter, it was examined on a specially prepared laboratory research rig. This examination made it possible to determine efficiency characteristics vs. engine load and rotational speed [1]. For instance, for motor revolutions n = 30 rev/s and the torque on shaft M = 1.1 Nm the system efficiency was equal to $\eta = 86.4\%$ and decreased almost linearly with increased load, down to the level of $\eta = 61.8\%$ at M = 4.32 Nm.

The applied constant-pitch propeller with D = 280 mm in diameter was tested in a natural scale in the flow tank of the Ship Design and Research Centre in Gdansk. These tests made it possible to prepare its hydrodynamic characteristics shown in Fig. 3.

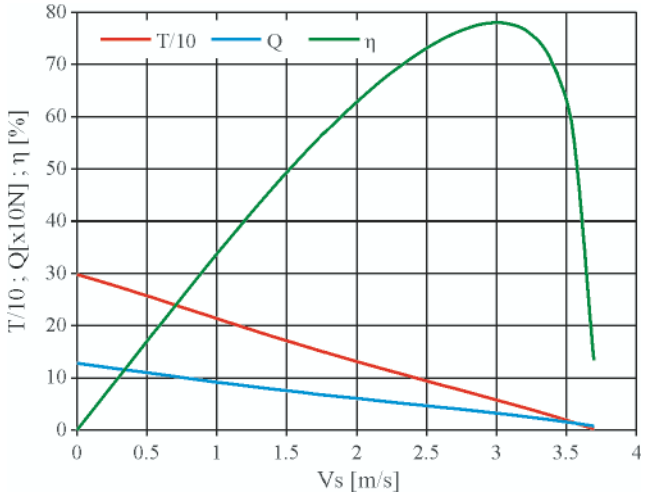

Fig. 3. *Hydrodynamic characteristics of the propeller*

CALCULATING WATER VELOCITY DISTRIBUTION AROUND THE PROPELLER

Modelling the flow over the propeller was significant part of the study of the shape of the pod having the electric motor with the gear and bearings installed inside it. It was also part of preparation for heat transfer calculations. The latter task required preparing the data on the velocity field around the pod. More precise methods of this type of calculations are presented, for instance, in [3] and [4]. Moreover, the information about the water flow velocity field in this area makes it possible to estimate, to some extent, the correctness of the assumed pod shape from the hydrodynamic point of view. The presence of strong disturbances in the flow near propeller would indicate that some corrections in the shape of the pod are necessary. To facilitate the activities oriented on preparing the grid that divides the system into finite elements, necessary for numerical calculations, the axial symmetry of the system was assumed which means neglecting the propeller column. This assumption not only made the preparation for numerical calculations much simpler, it also considerably speeded up the calculations themselves. The calculation domain extended 5 [m] both in front of and behind the propeller, and 3 [m] on each side. For the calculated values to model the reality in the most possible way, the calculation grid was refined in the vicinity of the propeller, and was left coarser in the regions in which no significant flow disturbances were expected. The calculations did not take into account the operation of the propeller screw.

The analysis of the flow over the propeller was performed using the code Fluent, a package belonging to a big family of CFD (Computational Fluid Dynamic) codes. This programme makes it possible to calculate velocity and temperature distributions, pressure and mass fields, and model chemical phenomena. It makes use of numerical methods to solve the equations of momentum, energy, and mass transfer. It is based on the finite element method and the finite volume method, the idea of which consists in integrating the equations describing the problem over each control volume. The code provides opportunities for analysing phenomena in two and three dimensions. Given below are the basic equations which are solved by the code when analysing the flow problem.

Mass conservation equation:

$$\frac{\partial \rho}{\partial t}+\frac{\partial}{\partial x}(\rho \upsilon_x)+\frac{\partial}{\partial r}(\rho \upsilon_r)+\frac{\rho \upsilon_r}{r}=S_m \qquad (1)$$

where:

x – axial coordinate
r – radial coordinate
v_x – axial velocity
v_r – radial velocity
S_m – added mass

Axial and radial momentum conservation equations:

$$\frac{\partial}{\partial t}(\rho \upsilon_x)+\frac{1}{r}\frac{\partial}{\partial x}(r\rho \upsilon_x \upsilon_r)+\frac{1}{r}\frac{\partial}{\partial r}(r\rho \upsilon_x \upsilon_r)=$$

$$=-\frac{\partial p}{\partial x}+\frac{1}{r}\frac{\partial}{\partial x}\left[r\mu\left(2\frac{\partial \upsilon_x}{\partial x}-\frac{2}{3}(\nabla \cdot \vec{\upsilon})\right)\right]+ \qquad (2)$$

$$+\frac{1}{r}\frac{\partial}{\partial r}\left[r\mu\left(\frac{\partial \upsilon_x}{\partial r}+\frac{\partial \upsilon_r}{\partial x}\right)\right]+F_r$$

and:

$$\frac{\partial}{\partial t}(\rho \upsilon_r)+\frac{1}{r}\frac{\partial}{\partial x}(r\rho \upsilon_x \upsilon_r)+\frac{1}{r}\frac{\partial}{\partial r}(r\rho \upsilon_x \upsilon_r)=$$

$$=-\frac{\partial p}{\partial x}+\frac{1}{r}\frac{\partial}{\partial x}\left[r\mu\left(\frac{\partial \upsilon_r}{\partial x}+\frac{\partial \upsilon_x}{\partial r}\right)\right]+$$

$$\frac{1}{r}\frac{\partial}{\partial r}\left[r\mu\left(2\frac{\partial \upsilon_r}{\partial r}-\frac{2}{3}(\nabla \cdot \vec{\upsilon})\right)\right]+ \qquad (3)$$

$$-2\mu\frac{\upsilon_r}{r^2}+\frac{2}{3}\frac{\mu}{r}(\nabla \cdot \vec{\upsilon})+\rho\frac{\upsilon_z^2}{r}+F_r$$

where:

$$\nabla \cdot \vec{\upsilon}=\frac{\partial \upsilon_x}{\partial x}+\frac{\partial \upsilon_r}{\partial r}+\frac{\upsilon_r}{r} \qquad (4)$$

μ – viscosity
F – external force

For the processor, which is the package Fluent, to be able to perform the calculations, it needs preparing a relevant computational grid, using a preprocessor, which takes into account boundary conditions. The calculation grid prepared using the preprocessor Gambit for the presently examined problem is shown in Fig. 4.

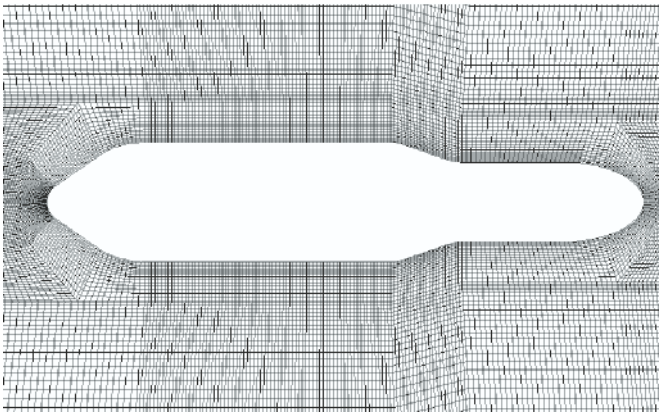

Fig. 4. *2D calculation grid in the vicinity of the propeller*

The calculations were performed using as the boundary condition the water velocity equal to 3 [m/s] at the inlet to the computational domain. The boundaries of this domain were treated as walls without friction generated by the flowing fluid. The distributions of the water velocity magnitude and particular component calculated in the vicinity of the propeller for the above conditions are shown in Fig. 5.

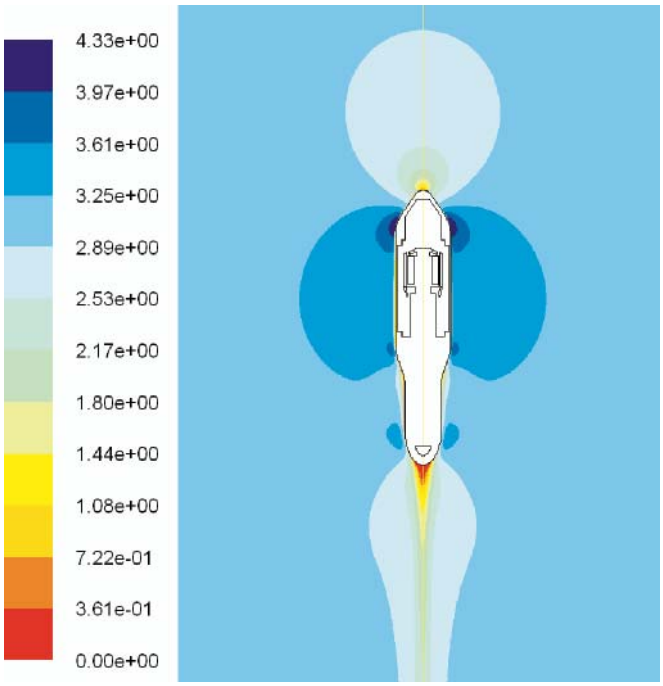

Fig. 5. *Velocity distribution in the vicinity of the propeller. Visible is the wake behind the propeller cone*

The above-presented results of calculations reveal that the water velocity in direct vicinity of the propeller pod increases from zero at its front end to the maximum level of 4.33 [m/s] recorded in the border between the conical and cylindrical part. Along the cylindrical part, initially the velocity decreases rapidly and then is stabilised at the level of 3.35 [m/s], up to the diameter reduction region, where it again increases and decreases below 3 [m/s].

CALCULATING TEMPERATURE DISTRIBUTIONS IN THE PROPELLER AND SURROUNDING WATER

A basic problem in the pod propulsion systems concerns absorption of the heat generated by the engine in operation. The heat is generated due to losses that accompany the energy conversion and due to friction processes. Assessing the volume of this heat was possible by measuring, on the research rig, the electric power supplied to the motor and the effective mechanical power on the output shaft for different loads. For instance, for the propeller filled with oil and the mechanical power output P_e = 500 [W] the power loss, equivalent to the flux of generated heat, was approximately equal to P_{str} = 150 [W].

Finite element method based heat transfer calculations were in this case much more difficult due to the type of the examined motor with rotating case, which required preparation of a 3D calculation grid. In order to decrease the labour consumption and shorten the time of calculations the modelled shape was limited to one fourth of the propeller. It was assumed additionally that the heat generated in the motor is carried away to the water flowing round the propeller only through the cylindrical surface of the pod.

Heat transfer calculations, performed with the aid of the FEM method, were much more complicated in this case due to the type of the examined motor, which was the motor with rotating casing. The basic energy equations solved by the code are given below.

$$\frac{\partial}{\partial t}(\rho E)+\nabla\cdot(\vec{\upsilon}(\rho E+p))= \\ =\nabla\cdot\left(k_{eff}\nabla T-\sum_j h_j\vec{J}_j+(\bar{\bar{\tau}}_{eff}\cdot\vec{\upsilon})\right)+S_h \quad (5)$$

Where: the three first terms on the right-hand side of the equation represent, respectively, the energy transfer due to conduction, diffusion and dissipation. S_h represents chemical reaction heat and any other source of heat.

$$E=h-\frac{p}{\rho}+\frac{\upsilon^2}{2} \quad (6)$$

For a solid body:

$$\frac{\partial}{\partial t}(\rho h)+\nabla\cdot(\vec{v}\rho h)=\nabla\cdot(\vec{\upsilon}\rho h)=\nabla\cdot(k\nabla T)+S_h \quad (7)$$

ρ – density
h – enthalpy
k – conductivity
T – temperature

The calculations required preparing a 3D grid. In order to optimise the labour and time consumption of the calculations, the modelled shape was limited to one fourth of the propeller. Moreover, it was assumed that the heat generated in the motor is transferred to the water flowing by the propeller only through the cylindrical part of the pod.

The calculation grids for the examined flow region and propeller elements are given in Figs. 6 ÷ 9.

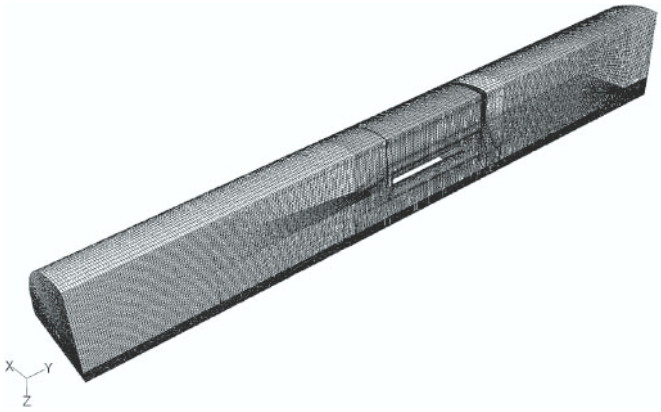

Fig. 6. *3D calculation grid for the examined heat transfer region (without water flowing by the propeller)*

It was assumed that the entire heat is generated in electric motor windings. In the prepared calculating model it was assumed that the heat flux originates on inner walls of the winding, having the surface S = 0.006 [m^2]. For the heat flux generated at effective power output P_e = 500 [W] and equivalent to the power loss $\dot{Q} = P_{str}$ = 150 [W] the heat flux density $\dot{q}$ attributed to the examined quarter of the calculation domain is equal to:

$$\dot{q}=\frac{\dot{Q}}{4\cdot S}=\frac{150}{4\cdot 0.006}=6250\ [W/m^2]$$

The input parameters for the calculation were:

V - velocity of the water flowing by the propeller, calculated in the way presented in Chapter 2
n - rotational speed of the motor
$\dot{Q}$ - heat flux generated by the motor, determined from the efficiency measured on the research rig
T_w - temperature of the water flowing by the propeller.

along with the following properties of the oil used for motor cooling:

ρ - oil density
Cp - oil specific heat
ν - oil kinematic viscosity coefficient
α - overall heat-transfer coefficient.

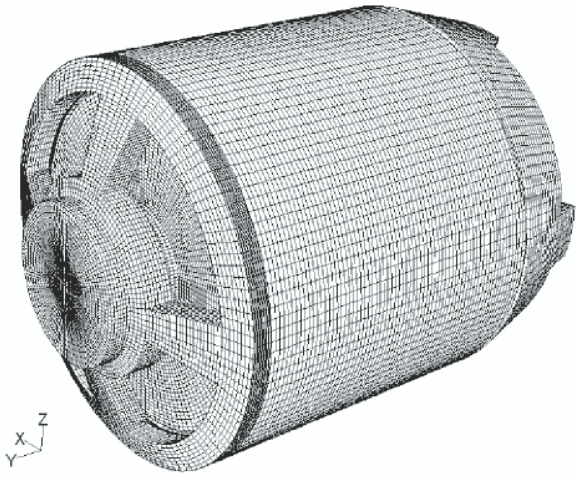

Fig. 7. *3D calculation grid modelling the motor*

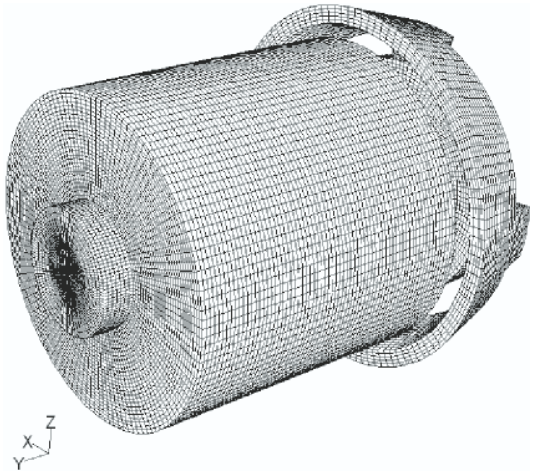

Fig. 8. *3D calculation grid modelling the motor stator*

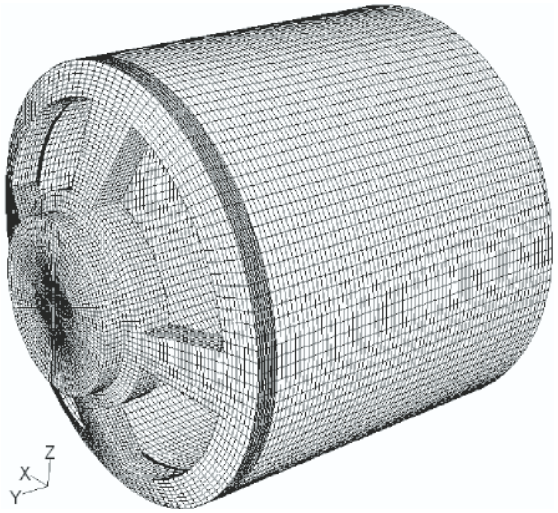

Fig. 9. *3D calculation grid modelling the motor rotor*

Current values of the above parameters which were used in the calculations were the following:

V = 3.35 [m/s]
$\dot{n}$ = 30 [rev/s]
Q = 150 [W]
T_w = 291 [K] (18 [°C])
ρ = 857 [kg/m^3]
Cp = 2160 [J/kgK]
ν = 0.026 [kg/ms]
α = 0.2 [W/mK]

Fig. 10 presents the calculated distributions of linear velocities in selected propeller elements.

Temperature distributions calculated for the above input data in the examined region and in the cylindrical part of the pod are shown in Figs. 11 and 12.

The above presented distributions reveal that the maximum temperature takes place in the motor iron region and is equal to T_{max} = 301 [K] (28 [°C]). The heat from the iron is taken by the gear, rotor and oil. To assess the contribution of the cooling medium which fills the propeller motor and pod, identical calculations were performed for the same conditions when the

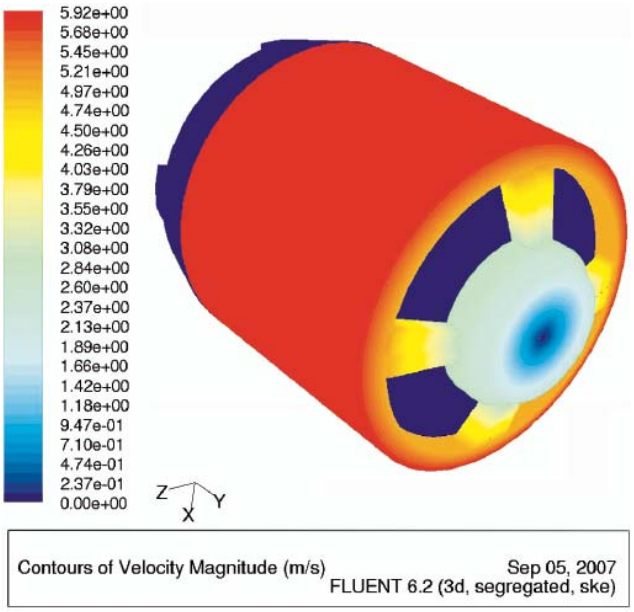

Fig. 10. *Linear velocity distribution in motor elements*

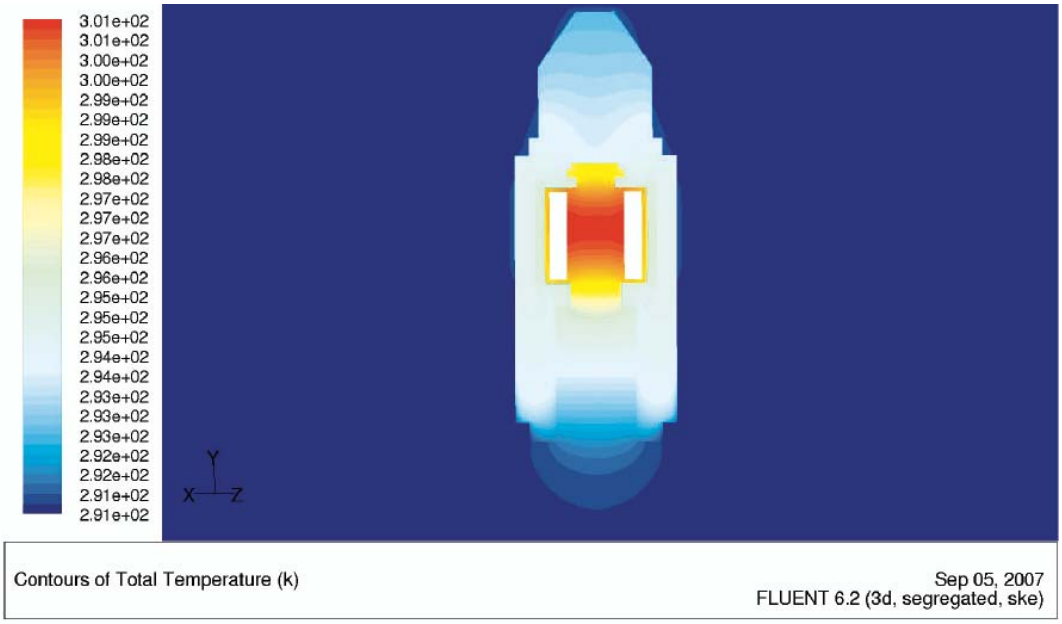

Fig. 11. Temperature distribution inside the propeller filled with oil

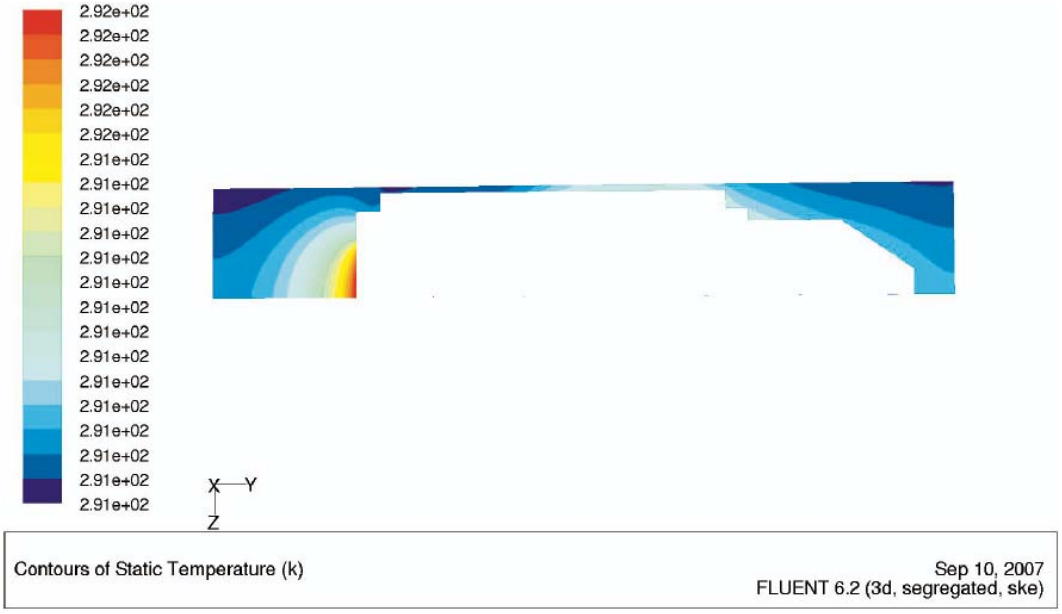

Fig. 12. *Temperature distribution on walls composing the cylindrical part of the propeller pod*

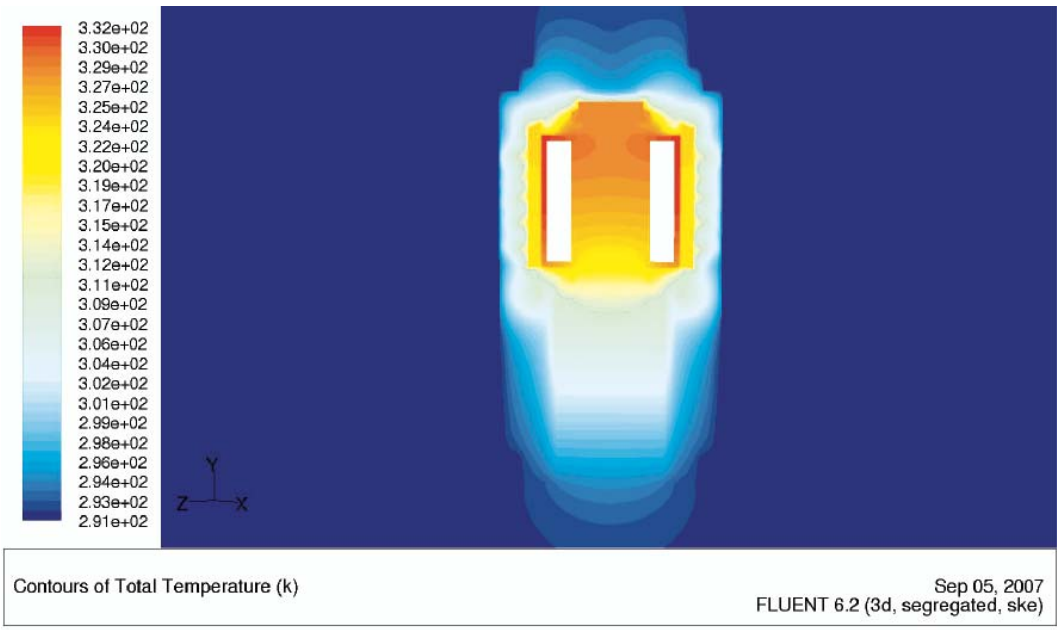

Fig. 13. *Temperature distribution inside the propelled filled with the air*

propeller was filled with the air instead of oil. The results of those calculations are shown in Fig. 13. As could have been expected, the air was not capable of taking over as much heat as the oil. The maximum temperature in this case reached T_{max} = 332 [K] (59 [°C]).

CONCLUSIONS

- The designs of electric propulsion systems for small boats which are available on the market are the attached direct current motors that reveal small overall efficiency. They are used in general as auxiliary propulsion system and could not be used in the constructed racing catamaran driven by solar energy as they cannot work continuously for such a long time. The sailing races for which the boat Energa Solar was designed provide opportunities for presenting own technical solutions and comparing them with those presented by leading teams from all over the world. Energa Solar is the only boat to have the propulsion system based on such a small three-phase motor, which makes it possible to enter upon competition with strong teams from all over the world.
- The performed investigations of the propeller screw and motor allowed a relevant planetary gear to be selected. The determined characteristics have proved that the motor can operate in a direct drive system. However, power losses recorded in such a design are many times as high as those generated by the planetary gear. In this case the motor operating at the rotational speed 11 [rev/s] should be loaded with a torque three times as high as that recorded in the proposed design. The losses recorded in the motor working in combination with an inverter would reach as much as 70%. The presently produced planetary gears are precise machines, the efficiency of which reaches 97% even at very small power levels.
- Manoeuvring such a small vessel on the water forces frequent changes of operating parameters of the propulsion system. Instantaneous losses can be higher than those assessed during the investigations. Consequently, the oil temperature in the propeller can also rise higher. The use of oil as a cooling medium results from experience gained during the racings.
- The temperature determined in the numerical analysis is verisimilar taking into account the results of temperature measurements performed on the motor working in oil.
- The next step in the research will be the measurement of temperature distributions on a real object. The designed propeller, shown in Fig. 14, will also be examined in respect of the effect of the propeller screw position on the overall efficiency of the propulsion system.

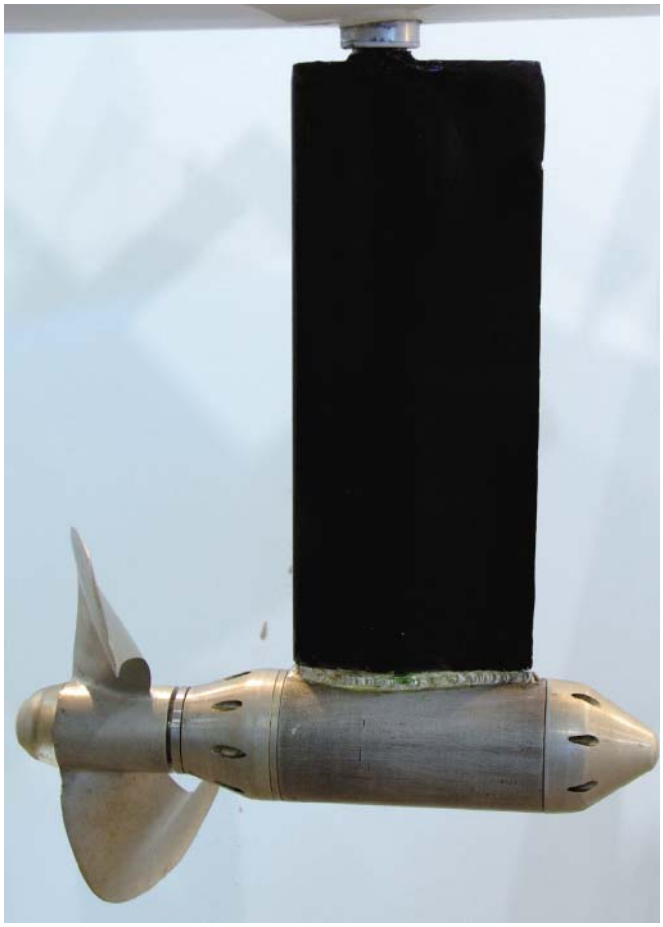

Fig. 14. *The designed propeller in the arrangement with the pulling screw*

❍ Due to permanent increase of oil prices, the electric drive becomes an alternative for internal combustion engines. Studying problems concerning ecological propulsion systems is very popular and frequent nowadays. More and more companies assign large sums for developing initiatives promoting the use of renewable energy resources.

BIBLIOGRAPHY

1. Chachulski Kazimierz: *Fundamentals of ship propulsion* (in Polish), Wydawnictwo Morskie, Gdańsk 1988
2. Dudziak J.: *Theory of ship* (in Polish), Foundation for the Promotion of Maritime Industry. Second issue, updated, Gdańsk 2008
3. Dymarski P., Dymarski Cz.: *Curvilinear Panels and Higher Order Dipole Distribution Method for Ducted Propeller Flow Calculations*. Marine Technology Transaction, Technika Morska, Polish Academy of Sciences - Branch in Gdańsk, Marine Technology Committee. Vol. 12, 2001 r.
4. Dymarski P.: *Numerical simulation of viscid flow around hydrofoil,* Polish Maritime Research, No 1/2006
5. Collective work edited by M. Dietrich: *Fundamentals of machine construction.* Third edition, Wydawnictwa Naukowo Techniczne Warszawa 2007
6. Niezgodziński M. E., Niezgodziński T.: *Resistance formulas, diagrams and tables,* Wydawnictwa Naukowo Techniczne Warszawa 1996 (in Polish)
7. SKF catalogues of products
8. APEX DYNAMICS, INC catalogues of products
9. MODELMOTORS LTD catalogues of products
10. SHOTTEL catalogues of products
11. WARTSILA catalogues of products
12. ROLLS-ROYCE catalogues of products
13. FLUENT 6.0 Documentation.

CONTACT WITH THE AUTHORS

Czesław Dymarski, Prof.
Wojciech Leśniewski, Ms. C.
Faculty of Ocean Engineering
and Ship Technology,
Gdańsk University of Technology
Narutowicza 11/12
80-952 Gdańsk, POLAND
e-mail : cpdymars@pg.gda.pl

Photo: Cezary Spigarski

POLISH MARITIME RESEARCH 4(58) 2008 Vol 15; pp. 66-71
10.2478/v10012-007-0099-5

The effect of heat treatment on the structure and corrosion resistance of Al-Zn-Mg alloys

Wojciech Jurczak, Ph. D.
Polish Naval Academy

ABSTRACT

The parameters of heat treatment of Al-Zn-Mg alloys subjected to precipitation hardening have a substantial impact on mechanical and corrosion resistance. The rate of cooling after supersaturation, along with the ageing temperature and time, affect significantly mechanical properties of these alloys. The type of ageing (artificial or natural) after saturation implies corrosion resistance in seawater. Being a modification of the AlZn5Mg1 alloy, denoted as PA47, the AlZn5Mg2CrZr alloy reveals best mechanical properties among all aluminium alloys in shipbuilding [1]. However, the higher level of precipitation hardening, the higher susceptibility to corrosion, in particular to stress corrosion cracking (SCC). Describing the structure of Al-Zn-Mg alloys by identifying the precipitation free zone (PFZ) and the Guinier-Preston (G-P) zones provides the information on the corrosion resistance of these alloys.

Keywords: Aluminium alloys, structure**,** corrosion resistance, precipitation hardening

INTRODUCTION

Al-Zn-Mg alloys for heat treatment which are used in shipbuilding are hardened by fine-dispersion precipitation products. Effective hardening of the aluminium alloys consists in the introduction of strange atoms and dislocations to the basic metal lattice, an effect of thermal processing, and in the creation of a sufficient number of fine-dispersion coherent phase or intermetallic compound precipitation products having the form of small particles. In order to secure high volumetric contribution of the precipitation products, they should form in the lattice of the basic metal and, if possible, beyond the grain boundaries and other defects of the crystal structure, as these defect decrease the potential barrier of nucleation, this way becoming the privileged places for precipitation of secondary heterogeneous phases [2, 3].

Heat treatment of Al-Zn-Mg alloys comprises supersaturation and ageing processes. The supersaturation, which consists in soaking the alloy in the solid-solution phase (within the solubility limit range) in a well-defined time, is the first stage, after which fast cooling takes place. Unlike Al-Mg alloys, the Al-Zn-Mg alloys are subjected to the process of ageing (natural or artificial), which is possible due to the presence of Zn or Mg atoms in the solid solution lattice. Zinc reveals varying, temperature dependent solubility in solid state, and the rate of precipitation of phases of $MgZn_2$, Al_3Mg_2, $Al_2Mg_3Zn_3$ type should be selected in such a way that they remain in the solid solution in the form of fine phases during the cooling process. The temperature of ageing determines the type and structure of the precipitated phases [4].

In practice, however, the stability of properties of Al-Zn-Mg alloys, including their corrosion and tribological resistance, strongly differs from sample to sample, as it depends on the technological production and processing time-history and the conditions in which particular machine and construction elements are used and operated.

Taking this into account, the effect of heat treatment parameters on the structure of the AlZn5Mg2CrZr alloy, and, consequently, its mechanical properties and corrosion resistance were examined experimentally. The article reports the results of this examination.

CHARACTERISTICS OF THE EXAMINED MATERIAL

The objects of examination were hot-rolled sheets of a new alloy AlZn5Mg2CrZr. The sheets were 6 and 12 mm thick and they were taken from two industrial melts 507. The chemical composition, heat treatment, and mechanical properties characteristic for four lots of sheets are given in Table 1. Ingots, having dimensions of 145x450 mm, were produced using the method of semi-continuous casting in the temperature of ~700 °C. The ingots were cut into parts 750 mm long and homogenised in the temperature of 480 °C during 12 hours. The temperature in which the ingots were heated before rolling was 440-460 °C. 12-14 roll passes were done for sheets of g = 12 mm, while for sheets of g = 6 mm the number of roll passes was equal to 20-24. The rolled sheets were cut to the dimension and passed to tb-type heat treatment.

Tab. 1. Chemical composition of AlZn5Mg2CrZr tb alloy /certif. IMN-OML no. 4550/91.336 OML/91/

No. of	Chemical composition [%]											No. of lot and
alloy	Zn	Mg	Cr	Zr	Ti	Fe	Si	Cu	Mn	Ni	Al	certificate
507	5.13	1.9	0.16	0.15	0.071	0.27	0.15	0.08	0.057	0.006	remaining	1085
tb - **supersaturation** - heating to 480 °C during 50 min., cooling with hot water of min. 70 °C **natural ageing** 0-4 days in 20 °C, **two-stage artificial ageing** - 95 °C/8h + 150 °C/ 8h												

The properties of the examined AlZn5Mg2CrZr alloy were compared with those revealed by the PA47 alloy [5]*, whose chemical composition, given by the metallurgical certificate no. 2945/485/4, is the following: 1.24% Mg, 5.3% Zn, 0.18% Mn, 0.034% Ti, 0.14% Cr, 0.16% Si, 0.32% Fe, 0.05% Cu, and the remaining Al.

Tab. 2. Heat treatment parameters of AlZn5Mg2CrZr and PA47 alloys

No.	Alloy symbol	Melt	Al-Zn-Mg alloy heat treatment parameters			State symbol
			Solution heat treatment		Ageing type	
			Temperature and time	Cooling after solution heat treatment		
1	**AlZn5Mg2CrZr** AlZn5Mg1*	507	**450 °C/1.5h** 430 °C/45 min	**air 20 °C**	**natural** 100 days	**ta**
2	**AlZn5Mg2CrZr** AlZn5Mg1*	507	**450 °C/1.5h** 430 °C/45 min	**water 20 °C**	20 °C/6 days + artificial ageing: 95 °C/15h + 150 °C/10h	**tb_{21}**
3	**AlZn5Mg2CrZr** AlZn5Mg1*	507	**450 °C/1.5h** 430 °C/45 min	**air 20 °C**	20 °C/6 days + artificial ageing: 95 °C/15h + 150 °C/10h	**tb_{23}**
4	**AlZn5Mg2CrZr** AlZn5Mg1*	507	**450 °C/1.5h** 430 °C/45 min	**water 80 °C**	20 °C/6 days + artificial ageing: 95 °C/15h + 150 °C/10h	**tb_{22}**

* reference alloy PA47

Homogeneous distribution of Zn and Mg atoms in the aluminium matrix lattice, an effect of the supersaturation, leads to the creation of vacancies in the lattice, the number of which depends on temperature. During the ageing, these vacancies provide opportunities for diffusion of Zn and Mg atoms which occupy points in the three-dimensional lattice of aluminium.

THE EFFECT OF HEAT TREATMENT ON MECHANICAL PROPERTIES OF AL-ZN-MG ALLOYS

Comparing the results obtained for a series of examined samples made it possible to recognise to which extent the modification of chemical composition of the AlZn5Mg2CrZr alloy, which consisted in increasing the contents of Cr, Zr, Ti and reducing the contents of Mn with respect to the PA47 alloy, along with properly selected heat treatment, affects the mechanical properties of the alloy. At the increased total contents of Zn + Mg, the modification aimed at reducing the effect of the degree of dispersion of the selected phases on grain boundaries (GZ) and in the surrounding precipitation free zones (SWW), which in case of PA47 provoked a tendency to intensive corrosion.

For identical ageing conditions, it is the cooling method after supersaturation (cooling in cold water of 20°C) which secures the highest mechanical properties of the examined AlZn5Mg2CrZr alloy.

Tab. 3. Mechanical properties of AlZn5Mg2CrZr and AlZn5Mg1 alloys by various type of heat treatment

Alloy symbol Type of heat treatment	Mechanical properties		
	R_m [MPa]	$R_{0.2}$ [MPa]	A_5 [%]
AlZn5Mg2CrZr	423	379	14.3
ta	418	258	14.0
tb_{21}	480	438	9.2
tb_{22}	465	418	9.8
tb_{23}	381	310	11.5
AlZn5Mg1*	310	240	13.1
ta	386	242	22.3
tb_{21}	401	354	17.9
tb_{22}	376	319	17.8
tb_{23}	358	293	14.3

* reference alloy PA47

THE EFFECT OF HEAT TREATMENT ON THE STRUCTURE OF THE ALZN5MG2CRZR ALLOY

Figure 1a shows the structure of the non-recrystallized sheet after cold rolling All Al-Zn-Mg sheet samples reveal

a typical fibrous texture, parallel to the rolling direction. Precise observation could also make it possible to notice separate recrystallized grains on the surfaces parallel and perpendicular to the rolling direction, better visible on the former surfaces, Fig. 1b, included as reference for comparison, shows the structure of the AlZn5Mg2CrZr alloy after annealing and rolling in relatively low temperatures [6].

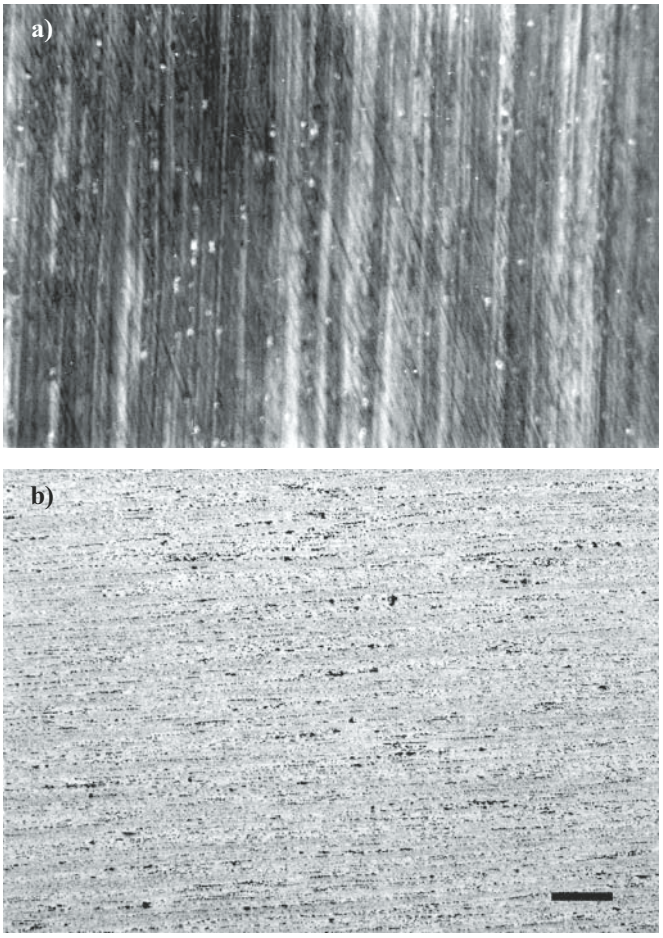

Fig. 1. *Structure of the alloy:* ***a****- AlZn5Mg2CrZr-T sheets g = 12 mm in tb state, additionally oxidised in Backer's reagent, 100x enlargement, and sample* ***b****- AlZn5Mg2CrZr -O annealed by heat treating at 426°C for 3 hours, cooled at 20°C down to 232°C for 3 hours, then held at 232°C for 6 hours, and finally air cooled to room temperature. Etched with Keller's solution. Micron bar length was 100 mm. The microstructure consists of random distribution of* $Mg(Zn,Al,)_2$ *, and insoluble* $FeAl_3$

In Al-Zn-Mg alloys the following types of precipitation products are observed: large products randomly distributed in the metallic matrix, and G-P zones having the form of tweed structure. Beside the G-P zones, solid solution zones (SWW) are observed in direct vicinity of the boundaries of grains and subgrains. Larger products of $MgZn_2$ precipitation are also observed at the grain boundaries.

The fibrous structure, characteristic for rolled products, is not homogeneous, as the degree to which alternately located fibres are enriched with Cr and Ti peritectics components is different. The origin of this heterogeneity is connected with the peritectic reactions of Cr and Ti taking place when the alloy solidifies. The products of the peritectic reaction, referred to as Ti and Cr atoms in the literature, collect in the centre of the dendritic cell, while peripheral parts of this cell clearly are visibly poorer in those elements [6,9]. Plastic working results in the appearance of separate bands which have more or less Cr and Ti atoms - bands which are richer and poorer in those elements lie alternately one on the other. If the differences in the concentration of those elements in adjacent bands are large and Cr and Ti are in the solid solution and not as finely dissipated separation particles connected with the peritectic reaction, then in case of corrosion attack the bands which are damaged first are those which are poor in Cr and Ti, while the rich bands remain free of corrosion. The poor bands work as cathodes and the rich bands as anodes in the electrochemical micro corrosion cells. The corrosion takes an intercrystalline course along the bands which are parallel to the direction of plastic working. If the differences in the concentration of Ti and Cr elements are small, then the appearance of corrosion is limited, and it happens when 0,12-0.16 % of zirconium is added to the alloy. The favourable structure is the structure with small dissipated products of Cr and Ti precipitation, which can be obtained by annealing the sheets in temperatures over 500°C for Cr and much higher for Ti. Thus the effect of Ti is clearly negative form the point of view of alloy sensitivity to interlayer corrosion. The precipitated Mn and Fe eutectics elements do not provoke corrosion themselves, but accelerate it in the presence of Cr and Ti atoms.

Figs 2-5 show the microstructures of the AlZn5Mg2CrZr alloy in heat treatment states ta, tb_{21} , tb_{22} , tb_{23} .

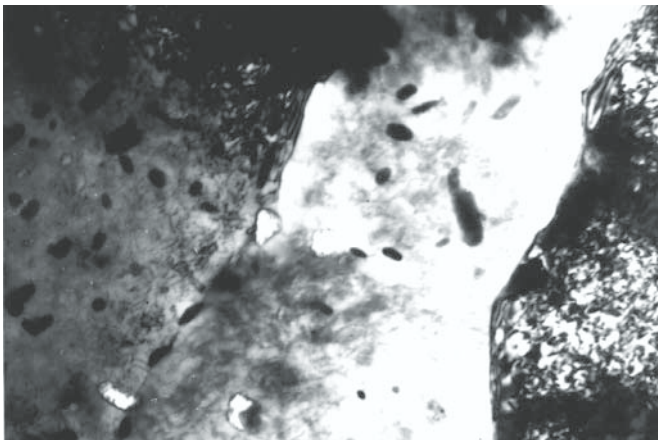

Fig. 2. *Microstructure of AlZn5Mg2CrZr alloy, state ta, TEM, thin foils. 47000x enlargement*

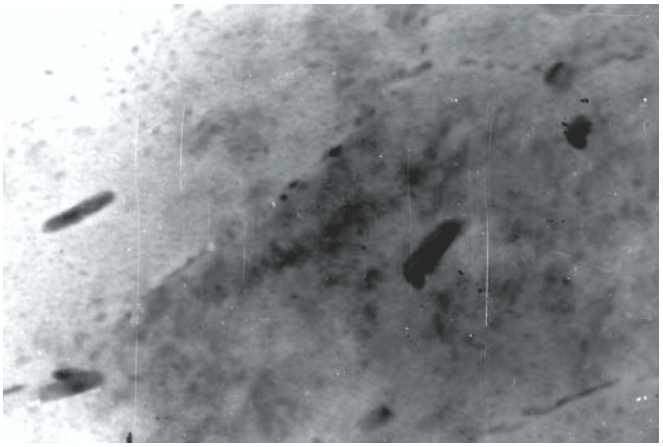

Fig. 3. *Microstructure of AlZn5Mg2CrZr alloy, state* tb_{21} *,TEM, thin foil. 47000x enlargement*

Tab. 4 collects SWW widths for the AlZn5Mg2CrZr alloy in different heat treatment states.

Tab. 4. *SWW widths for AlZn5Mg2CrZr alloy in different heat treatment states*

Heat treatment state	tb_{23}	tb_{22}	tb_{21}	ta
SWW [nm]	400	180	95	60

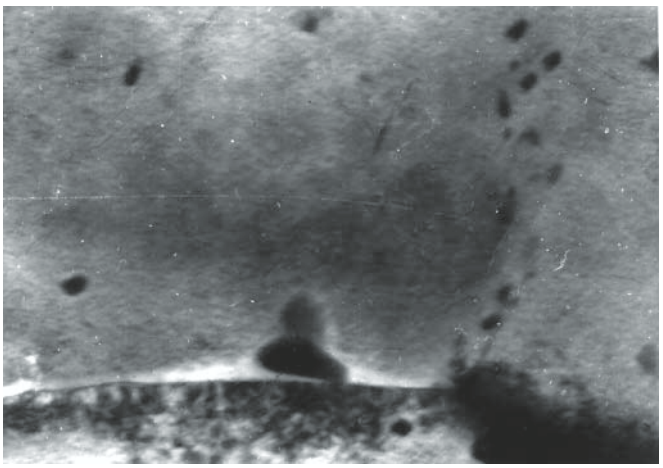

Fig. 4. *Microstructure of AlZn5Mg2CrZr alloy, state tb_{22}, TEM, thin foil. 47.000x enlargement*

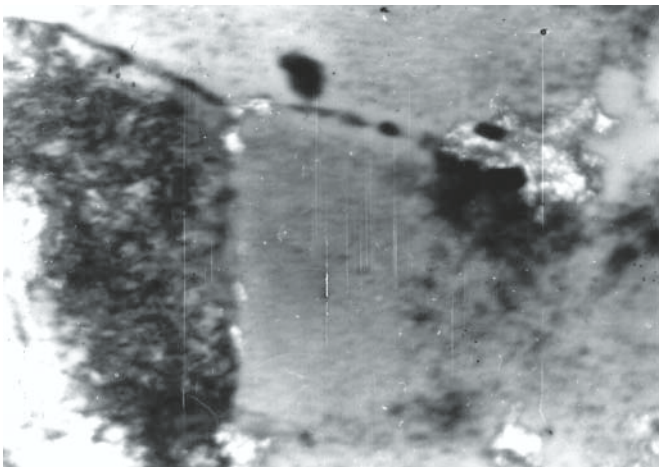

Fig. 5. *Microstructure of AlZn5Mg2CrZr alloy, state tb_{23}, TEM, thin foils. 47.000x enlargement*

The performed research has made it possible to detect clear dependence of the structure and mechanical properties of the AlZn5Mg2CrZr alloy on the heat treatment state. The AlZn5Mg2CrZr alloy in tb_{21} state revealed higher mechanical properties than in tb_{22} or tb_{23} state.

In the structure of the alloy obtained via rapid cooling in cold water after supersaturation and further artificial two-stage ageing, /state tb_{21}/ the precipitation of G-P zones was observed. Identifying the G-P zones was done using selective electron diffraction and the material presented in [7]. The conclusion about their presence was drawn based on the so-called "tweed structure", which is the effect of the first decomposition of the solid solution. The observed precipitation free zones (SWW) are adjacent to grain boundaries of 50-80 nm in width. The factors which most affect the dimension of the SWW zones are the temperature and time of artificial ageing.

On the grain boundaries more intensive precipitation of the $MgZn_2$ phase is observed. On the other hand, in samples cooled in the air after supersaturation /state tb_{23}/ the decomposition of the solid solution was more advanced. Small amounts of transient phase η' and equilibrium phase T precipitation products were observed. The latter phase most likely precipitated directly from the solid solution during slow cooling after supersaturation. The SWW zones of 340-420 nm in width were observed as well.

Fig. 6 shows the relation between the mechanical properties of the AlZn5Mg2CrZr alloy and the width of the SWW zone, when three types of cooling after supersaturation were used /cold water 20°C, hot water 80°C, air/. Increasing the rate of cooling after supersaturation results in the decrease of the SWW zone, accompanied by the increase of mechanical properties /R_m, $R_{0,2}$/.

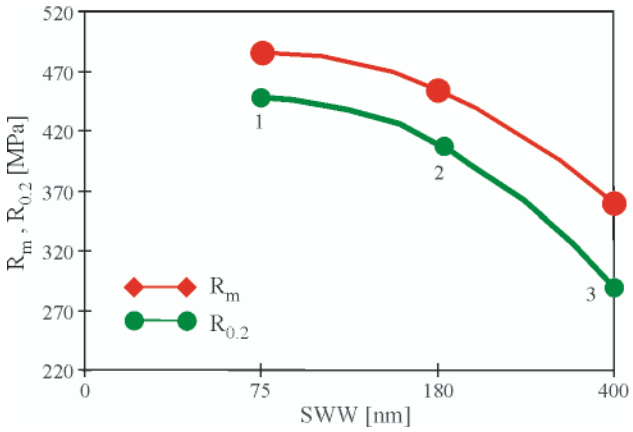

Fig. 6. *Relation between SWW zone width and mechanical properties of the AlZn5Mg2CrZr alloy, which after supersaturation was subjected to:*
1 *- slow cooling in cold water /T = 20°C/-tb_{21},*
2 *- cooling in hot water/T = 80°C/tb_{22},*
3 *- cooling in air - tb_{23} and then subjected to two-stage ageing - 90°C/8h + 145°C/16h*

Tab. 5. Description of AlZn5Mg2CrZr alloy microstructure in different heat treatment states

No.	AlZn5Mg2CrZr alloy heat treatment state	Microstructure description
1	t_a	Phase η precipitation products visible on grain boundaries
2	tb_{21}	Precipitation free zone adjacent to grain boundaries is 60-100 nm wide, and larger $MgZn_2$ phase precipitation products are observed on grain boundaries
3	tb_{22}	Small products of transient phase η 'precipitation are observed inside the grains. Phase η ($MgZn_2$) precipitation products, arranged in a number of rows, are observed on grain boundaries.
4	tb_{23}	Small products of transient phase η ' and equilibrium phase T precipitation are observed inside the grains. Individual phase η precipitation products observed on grain boundaries

The above phases were identified using electron diffraction

CORROSION-AND-STRESS RESISTANCE OF THE ALZN5MG2CRZR ALLOY

Despite still existing numerous controversies, the literature overview makes it possible to describe mechanisms responsible for the process of crack incubation and propagation in Al-Zn-Mg alloys subjected to stress corrosion. The process

of corrosion crack is, as a rule, intercrystalline in nature. This testifies to special role of changes taking place on grain boundaries and the areas adjacent to them (as a result of microstructure changes connected with chemical composition and heat treatment).

Fig. 7 presents mean percentage decrease of mechanical properties of the examined alloy AlZn5Mg2CrZr and the reference alloy PA47.

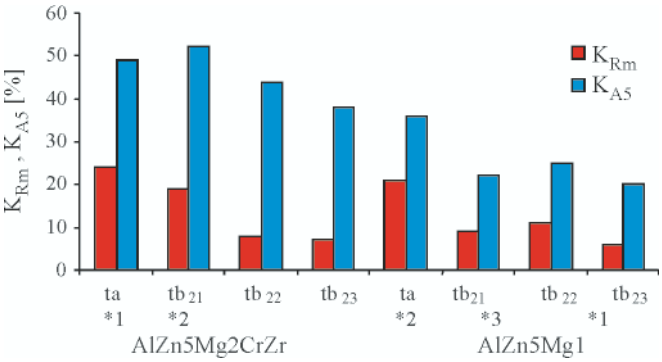

Fig. 7. *Mean percentage reduction of the tensile strength K_{Rm} and plasticity K_{A5} of the AlZn5Mg2CrZr alloy and AlZn5Mg1 alloy, subjected to heat treatment after corrosion stress exposure in 3% water solution of NaCl during 1500 h, where: *X - number of samples, which were destroyed in time shorter than 1500h.*

K_{Rm} and K_{A5} coefficients were calculated using formulas 1 and 2 .

$$K_{R_m} = \frac{1}{n}\sum \frac{R_{mo} - R_{mk}}{R_{mo}} 100\% \quad (1)$$

$$K_{A_5} = \frac{1}{n}\sum \frac{A_0 - A_k}{A_0} 100\% \quad (2)$$

where:

R_{mo} - ultimate tensile strength, before corrosion exposure
R_{mk} - ultimate tensile strength, after corrosion exposure
n - number of samples
A_0 - plastic elongation of the tested material before corrosion exposure
A_k - plastic elongation of the tested material after corrosion exposure
K_{Rm} - mean percentage of the reduction of the ultimate tensile strength after corrosion exposure
K_{A5} - mean percentage of the reduction of the plastic elongation after corrosion exposure determined on test samples of 5xg gauge length.

ANALYSIS OF THE EXAMINATION RESULTS

The description of the AlZn5Mg2CrZr alloy microstructure in states ta, tb_{21}, tb_{22}, tb_{23} is given in Table 5, which that referring to the SWW zone width is collected in Table 4. The structure of the alloys was observed on thin foils in a transmission electron microscope Tesla-100Bs-500

The essence of Al-Zn-Mg alloy hardening consists in transferring the maximum possible number of zinc and magnesium atoms to the solid solution, and then collecting these atoms as precipitation products in the form of G-P zones. These (coherent) clusters have common matrix with the mother liquor. As the process of ageing continues, these clusters become partially or totally separated from the mother liquor, thus creating precipitation products having their own stoichiometric formula:

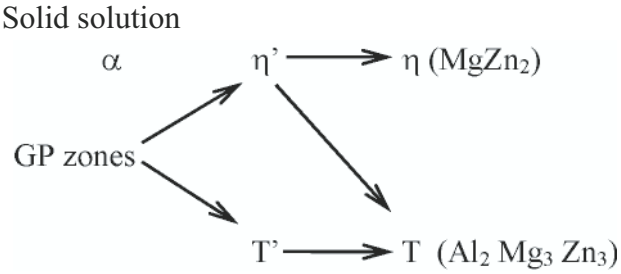

The rate of transformation of the G-P zones into transient phases η' and T' depends on the temperature of ageing. During this process the G-P zones cross over the critical point, i.e. the point, starting from which a GP zone either keeps increasing or, when it is not sufficiently large, dissolves in the matrix. The presence of the vacancies acts towards the increase of the G-P zones. Therefore the GP zones grow most slowly in the vicinity of grain boundaries, which act as vacancy traps [6,8]. During further ageing, the G-P zones which are situated near the boundaries and are smaller than the critical ones, dissolve in the matrix. As a result, the precipitation free zone (SWW) is formed near the boundary. This zone is often referred to as the solid solution zone (RS).

The natural ageing after supersaturation leads to the creation of a narrow RS zone, or to its complete absence. The longer the time of natural ageing, the narrower the RS zone.

The research activities confirmed the existence of a relation between the width of the RS zone and the resistance to stress corrosion. When the width of the RS zone increases, the resistance of the alloy to stress corrosion increases as well. The above analysis makes it possible to formulate the following general conclusions that (1) the heat treatment of the examined AlZn5Mg2CrZr alloy considerably affects its structure, and (2) the rate of cooling after supersaturation is a decisive factor determining the width of the SWW zone and the resultant resistance of the AlZn5Mg2CrZr alloy to stress corrosion.

CONCLUSIONS

As a result of the experiments we can conclude that the AlZn5Mg2CrZr alloy in **tb** state reveals better resistance to stress corrosion than in **ta** state, and therefore can be successfully used in shipbuilding. Moreover:

- in the **tb** state, decreasing the cooling rate after solution heat treatment results in better stress corrosion cracking resistance
- in the **ta** state, increasing the load results in significant strength reduction, to a lower level than in the **tb** state. This suggests that after heat treatment up to **ta** state the AlZn5Mg2CrZr alloy can be only employed in ship constructions which do not work under heavy stress corrosion cracking conditions.

The analysis of the results of examination of mechanical properties and corrosion resistance of the AlZn5Mg2CrZr alloy, and comparison with those of the AlZn5Mg1 alloy lead to the following conclusions:

- Mechanical properties of Al-Zn-Mg alloys depend on (see Tab. 3):
  - Chemical composition of the alloy. With increasing content of Zn + Mg the mechanical properties become higher, while the plastic properties - slightly lower.
  - Heat treatment of the alloy. The **ta** state reveals worse strength parameters (R_m in particular) than the **tb** state.

After comparing the **tb$_{21}$** and **tb$_{23}$** states it was found that the former leads to ΔR_m = 20.6%; $\Delta R_{0.2}$ = 29.2% and ΔA_5 = -25%, while, compared to the **tb$_{22}$** state, the **tb$_{21}$** state gives ΔR_m = 3.1%, $\Delta R_{0.2}$ = 4.6% and ΔA_5 = -6.5%. From the above we can conclude that increasing the cooling rate after solution heat treatment (**tb$_{21}$** - 20°C water cooling) results in the increase of strength parameters and in some reduction of plastic qualities.

- The resistance of Al-Zn-Mg alloys to stress corrosion cracking depends on:
  - Chemical composition of the alloy. With increasing content of Zn + Mg the stress corrosion cracking resistance decreases.
  - Heat treatment. In particular:
    - In the **ta** state the AlZn5Mg2CrZr and AlZn5Mg1 alloys show poor resistance to stress corrosion cracking and are prone to layer corrosion;
    - Artificial ageing after supersaturation heat treatment (**tb** state) increases the resistance of the Al-Zn-Mg alloys to layer corrosion;
    - Introduction of artificial ageing after supersaturation heat treatment (**tb** state), when accompanied by the reduction of the cooling rate, improves the resistance of the Al-Zn-Mg alloys to the stress corrosion cracking;
    - Heat treatment up to the **tb$_{22}$** and **tb$_{23}$** states improves the stress corrosion cracking resistance of the AlZn5Mg2CrZr and AlZn5Mg1 alloys.

The AlZn5Mg2CrZr alloy reveals better properties, as far as its application in shipbuilding is concerned, than the AlZn5Mg1 alloy.

The microductility of the examined Al-Zn-Mg alloys strongly depends of chemical composition and metallurgical-and technological aspects, which are decisive upon the degree of their hardening by low-dispersion secondary-phase precipitation products.

BIBLIOGRAPHY

1. Jurczak W.: *The effect of chemical composition and heat treatment on mechanical properties of Al-Zn-Mg alloys used in welded ship structures, and their resistance to stress corrosion*. Ph.D. thesis, Gdansk University of Technology 1998 (in Polish)
2. Łagin I.: Struktura i swojstwa spłwow sistemy Al-Zn-Mg. W-wa 1982.
3. Gorczyca S. et al.: *The effect of solid solution hardening and precipitation products action*. Metalurgia 29, Proc. of Conference on Metallurgy and Founding 1981 (in Polish)
4. Kawabata T. Izumi O.: *Acta Metall*, Vol. 24, pp. 817-825, 2006
5. Bugłacki H.: *The effect of heat treatment and chemical composition of binding materials on mechanical properties and stress corrosion of the AlZn5Mg1 alloy in welded ship structures*. Ph. D. thesis. Gdansk University of Technology 1981 (in Polish).
6. George F, Vander Voort: . *Atlas of aluminium microstructures*. 2005
7. George F. Vander Voort: *Atlas of aluminium microstructures*. 2006 by Taylor & Francis Group, LLC
8. Łagin et. al: *Struktura i swojstwa spłwow sistemy Al-Zn-Mg*. W-wa 1982
9. Davis J.R.: *Aluminium and aluminium alloys*. Ohio 2004

CONTACT WITH THE AUTHOR

Wojciech Jurczak, Ph. D.
Faculty of Mechanics and Electrics
Polish Naval Academy
Śmidowicza 69
81-103 Gdynia POLAND
e-mail: W.Jurczak@amw.gdynia.pl

Photo: Cezary Spigarski

POLISH MARITIME RESEARCH 4(58) 2008 Vol 15; pp. 72-84
10.2478/v10012-007-0100-3

Principles of work of different types of underwater breathing apparatus

Ryszard Kłos, Assoc. Prof.
Polish Naval Academy

ABSTRACT

*This paper is continuation the diving apparatuses classification method (**Polish Maritime Research, No 1/2008**), depend on three criteria: the kind of the breathing gas, the operational depth range of the diving apparatus, and the principle of operation. There are presented principle of work particular class of apparatuses.*

Keywords: diving apparatus, principle of work

INTRODUCTION

Design of underwater breathing apparatus is determined primarily by type of circuit of the breathing medium, hence discussed here are the principles of operation of general types of engineering solutions (not of any model in particular), according to following division:

- open circuit apparatus
- semi-closed circuit apparatus
- closed circuit apparatus.

METHODS

Open circuit UBA

Open circuit UBA is basically known as air breathing apparatus. Engineering variations of this type of apparatus are many. Apart into hose and SCUBA types they can be also divided according to number of stages of pressure reduction to be obtained at the demand valve:

- single-stage pressure reduction regulator
- two-stage pressure reduction regulator.

Systems of a higher number of pressure reduction stages are not met (although, installation of the so called pilot valves is claimed to serve as an additional reduction stage by some). The two-stage reduction systems may be divided into:

- designs with separated stages of reduction
- designs with combined stages of reduction.

Recommended for diving works is hose apparatus with two-stages pressure reduction. Regardless of the type of the automatic pressure reduction allowing for the ambient depth of diving, general principle of the open circuit apparatus is similar. It has been generally displayed in Fig. 1 (demand valve of two separate pressure reduction stages).

SCUBA (used as escaping apparatus) consits exclusively of the B equipment as marked in the Fig. 1. In its version with hose it contains additionally external supply unit A and supply line C. The major interest of the construction of UBA is the demand valve which reduces the pressure in the supply hose (or in integral set of pressure cylinders 15) to the ambient pressure of the diving depth. The demand system is divided into:

- water space 4 with the escape valve 5
- gaseous area 7 containing the pressure reduction unit 8 (second stage of pressure reduction)
- first stage of pressure reduction unit 10 (for self-contained version).

First stage reduction unit 10 (for SCUBA) is controlled by the hydrostatic pressure via the diaphragm it cooperates with. Thanks to it the breathing medium remains under a constant overpressure in relation to the hydrostatic pressure of a given diving depth. The reduction unit of the second stage 8 is controlled by hydrostatic pressure via the diaphragm 6. As a result it can deliver the breathing medium into the diver's lungs at a pressure equal to the hydrostatic pressure on the depth of diving. In order to diminish the inhalation resistance this unit is often equipped with a device aiding suction (not shown in

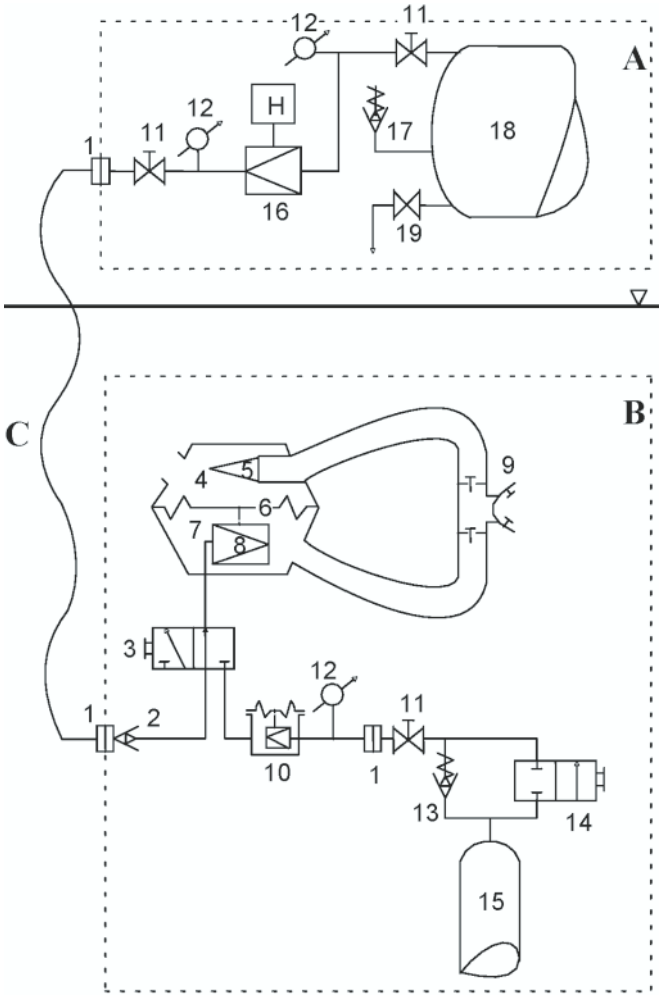

Fig. 1. *Open circuit UBA.* ***A****. External supply of hose version UBA with open circuit of breathing medium.* ***B****. SCUBA with open circuit of breathing medium.* ***C****. Supply line.* ***1)*** *function,* ***2)*** *non-return valve,* ***3)*** *selector valve,* ***4)*** *water space of demand valve,* ***5)*** *non-return escape valve,* ***6)*** *diaphragm,* ***7)*** *gaseous space of demand valve,* ***8)*** *unit of breathing medium pressure reduction cooperating with the diaphragm - second stage pressure reduction (second stage regulator),* ***9)*** *mouthpiece device with valves and hoses,* ***10)*** *reducer holding overpressure of breathing medium constant relative to hydrostatic pressure (first stage pressure reduction – first stage regulator),* ***11)*** *cut-off valve,* ***12)*** *manometer,* ***13)*** *throttle-stop valve of the reserve unit,* ***14)*** *valve actuating reserve of the breathing medium,* ***15)*** *unit self-contained holders,* ***16)*** *manually controlled reducer,* ***17)*** *safety valve,* ***18)*** *external holders with the breathing medium stored,* ***19)*** *drainage valve*

the Fig. 1). As to ensure emergency supply of the breathing gas the external supply unit should also include reserve holders. For self-contained version cylinders set 15 should also have pressure valve of the breathing medium reserve marked in the Fig. 1 as 13. During regular work the diver receives breathing medium from the external supply unit A (distribution valve 3 is set as indicated in the Fig. 1, the valve 11 from the autonomous cylinder set 15, open).

It is recommended for the breathing medium to be administered at a pressure preliminary reduced (reducer 16), but allowing for a proper work of the second stage of the demand valve. Owing to it, the hoses resistant to lower pressure may be used. The self-contained cylinders set 15 together with its software when cut off with the distribution valve 3 serves as emergency reserve of the breathing medium. The moment the breathing medium from the external supply unit has been cut off, the user switches the valve 3 triggering autonomous supply. The reserve of the breathing medium should be sufficient to let the diver leave the working site safely and his surfacing or reaching a safe place (e.g.: diving bell).

The circuit of the breathing gas at work with external supply is a simplified version of what happens to it at SCUBA; hence it is discussed taking the latter case as a model. During a regular work of SCUBA version the reserve valve 14 (in position as in Fig. 1) is shut.

From the cylinder set 15 the breathing medium is pushed through the throttle-stop valve of the reserve device 13, through the first reduction stage 10 to the reduction unit of the demand valve 8 (the selector valve 3 is now positioned differently than shown in the Fig. 1) where from, through a hose, the inhale valve and a mouthpiece device 9 right into the diver's lungs. Than, from the lungs through the exhale valve of the mouthpiece, hose and non-return escape valve 5, through the water section of the demand valve 4 into the water. The moment the pressure in the cylinders set 15 has fallen to the value at which the valve 13 gets cut off, the diver feels the inhalation resistance rising, and then short of the breathing medium. This is a signal that the reserve of the breathing medium (indicated by the manufacturer of the apparatus) has been cut off. To trigger this supply the user must switch the reserve valve 14. Description of the types of open circuit apparatus is presented in Table 4. Examples of the open circuit apparatuses detailed in Table 3 are shown in Photos 12÷17.

Table 4. *Basic features of open circuit UBA*

Open circuit UBA	
This type diving apparatus is known primarily as air UBA. For recreational and sports purposes most commonly used in self-contained (SCUBA), air version. For commercial diving recommended exclusively is the hose version with two, separate-stage pressure reduction regulator.	
Disadvantages:	- Limited maximum diving depth (at air as breathing medium) not allowing for the continental shelf exploration and exploitation. - At artificial breathing media the system unacceptable out of economic considerations, at helium mixtures, in particular. - Relatively short time of protective action of the autonomous version, and at air as breathing gas also long decompression time and long time needed for relaxation afterwards. - Complicated construction of the regulators (comparing to technical other solutions) affecting reliability of operation and imposing requirement of specialistic qualified personnel.
Advantages:	- The breathing medium used does not get mixed with the fresh one. - Unexpensive and readily available breathing medium in the air is used. - Diving depth, at the air as breathing medium, sufficient to carry out harbour underwater works, protection against damages to ships, and at majority works involved in the maintenance of hydro-engineering objects.

Photo 12. *PA-38/3600 type SCUBA*

Photo 13. *Diving apparatus PR-27 type SCUBA*

Photo 14. *AGA Mk II SCUBA*

Photo 15. *PL-70 UBA*

SEMI-CLOSED CIRCUIT OF BREATHING MEDIUM UBA (SCR)

In UBA with semi-closed (semi-pen) circuit of breathing medium (SCR) exclusively artificial breathing media are used:

- ★ SCR using ready breathing medium (premix-SCR)
- ★ SCR producing breathing medium during diving (automix-SCR).

The automix SCR offers possibility of:

- ✶ producing breathing medium during diving at a constant ratio of content of oxygen and inert gases
- ✶ producing breathing medium during diving at changeable ratio of content between oxygen and inert gases according to depth.

Taking mode of supply as division criterion we can distinguish between:

- ✸ self-contained SCR (SC-SCR)
- ✸ external (hose) supply SCR.

In SCR the role of system supplying breathing medium under the ambient pressure of diving depth has been taken over by elastic bags or breathing bellows. In this aspect SCR can be into designs equipped with:

- ✹ one-bag SCR
- ✹ two-bags SCR.

Any bigger number of bags is seldom to be met. Again, considering the mutual arrangement of the bags, the two-bags can be classified into designs with:

- ☆ separate-bags
- ☆ one bag contained in the other.

Characteristic for diving systems which use premix is that they administer breathing gas at constant volume or actuated to the breathing rhythm of the user. The technical design of the metering device allows grouping them as follows:

- SCR with nozzle reduction-metering system
- SCR taking advantage of evacuation of the metering cylinder
- SCR with system of breathing gas metering by means of set of bags arranged one in the other.

The classification of various technical designs of SCR in regard of the breathing bags construction is contained in Table 5.

Premix-SCR

General principle of two-bag premix-SCR (separate bags) with nozzle reductive-metering system is shown in Fig. 2. The SC-SCR part of one-bag SCR is illustrated in Fig. 3. Their principles of work being so much alike it is the SCR presented in Fig. 2 that will be discussed in details. When discussing the principles of operation of the SCRs term "metering" will be used, i.e. mass flow per time unit passing through the bore of a nozzle of SCR.

The part which is crossed and marked as B represents SCUBA version of SCR. Again, connecting the parts A and B with supply hose C creates hose supply SCR version (house-SCR), where breathing gas supply stored in unit 15 is emergency (escape) supply. In hose-SCR version gas from the cylinder 17 is passed via reducer 12 and selector valve 4, metering nozzle 11, inner supply unit into supply hose C. Through supply unit, return valve 2, valve selecting mode of supply 3, into inhalation bag 10. In the autonomous version breathing medium from the unit of cylinders 15 passes through cut-off valve 14 and manometric pressure control 13 to finally reach reductor 12. Then through the selector valve 3 (set differently than show in the Fig. 2) and the nozzle 11, which was selected with nozzles selector valve 4, into the breathing bag 10. Breathing bags are made of an elastic, gas-tight fabric, therefore the pressure in the bags approximates summaric value of the ambient hydrostatic pressure at the given depth and the overpressure opening relief valve (certain fluctuations of the pressure in the breathing area should be expected according to the positioning the apparatus on the diver's body and his very position in the water). The breathing medium from the inhalation bag 10 is lost through the hose and inhalation valve of the mouthpiece device 9 into the diver's lungs. Exhalation runs through exhalation valve and exhalation hose into exhalation bag 8, wherefrom the breathed out gas passes into carbon dioxide absorbent 7. The relief

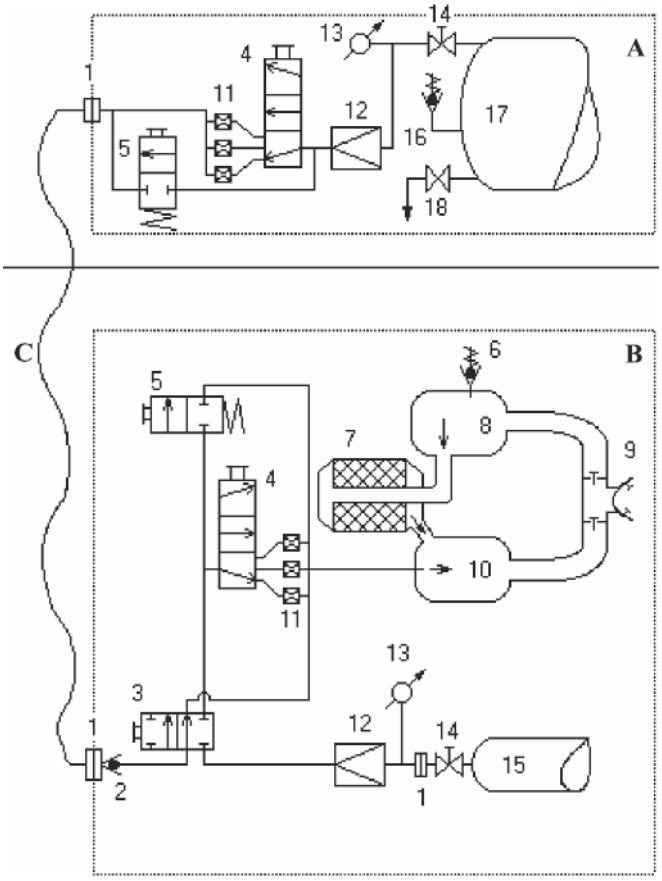

Fig. 2. *Two-bag version of the premixSCR.* ***A****. External supply unit of hose version of premix-SCR,* ***B****. SC-premix-SCR,* ***C****. Supply hose,* ***1)*** *coupling,* ***2)*** *return valve,* ***3)*** *supply mode selector valve,* ***4)*** *metering nozzles selector valve,* ***5)*** *by-pass valve,* ***6)*** *relief valve,* ***7)*** *carbon dioxide absorbent,* ***8)*** *exhalation bag,* ***9)*** *mouthpiece device with valves and hoses,* ***10)*** *inhalation bag,* ***11)*** *metering nozzles,* ***12)*** *reducer,* ***13)*** *manometer,* ***14)*** *cut-off valve,* ***15)*** *autonomous set of cylinders,* ***16)*** *safety valve,* ***17)*** *external cylinders with breathing medium stored,* ***18)*** *drainer valve*

Table 5. *Classification of SCRs in view of type of construction of the breathing bags*

Classification of SCR		
One-bag SCR	**Two-bag SCR**	
	with separate bags	**with bags arranged one in the other**
Disadvantages:	- In one-breathing-bag SCR breathing medium designed for rebreathing is partly lost. - All the designs are less hygienic than the open circuit of breathing medium due to partly closing of the breathing medium circuit. - All constructions of SCR are less economical in use than diving apparatus of closed circuit of breathing medium. - The complex construction of breathing bags in SCR with the bags one in the other may result in less reliability of the device.	
Advantages:	- In two-breathing-bag solution the losses to come about involve only the breathing medium which has not been purified from carbon dioxide, thus economizing on filling of the absorbent and prolonges duration of its protective action (vital for the hose version). - In the SCR with separate bags it is easier to arrange the bags in the casing, making the whole unit more compact. - With the SCR with bags contained one in the other, we are able to precisely determine the ratio between the amount of the breathing medium removed and the total amount of this medium in the circuit. Metering the breathing gas is carried out on periodical basis and adjusted to the breathing rhythm of the diver. To set the overpressure of opening the relief valve for this type apparatus turns less important than for other systems with semi-closed circuit of the breathing medium.	

valve 6 which is mounted on exhalation bag is meant to lose the excess of the exhaled gas into the water.

The expired medium running through the absorbent gets purified from carbon dioxide and joins the clean breathing medium circuit entering inspiration bag 10, mixing here with fresh breathing medium. Worth of notice, the value of the reduced pressure of breathing medium should remain at a level permitting the selected nozzle to work within the range of its supercritical flows, maintaining it for the whole of the diving depths allowed, what means that its mass expenditure is kept at a constant level with an assumed tolerance.

This type of hose supply premix SCR is equipped with special by pass valves 5, designed for filling and washout (ventilation) of the breathing area. In the hose supply SCR version, by-pass valve (for the design described above) is steered by an external supply A team - holding intercourse with the diver by means of technical aids. A basic feature of premix SCR is contained in Table 6. Apart from the nozzle metering system, the other solutions are also to be met. They operate on principle that ventilation of the diver's lungs is the function of the oxygen stream consumed. The solution applied in Swedish ACSC type SC-SCR (Alternatively Closed/Semiclosed Demand Breathing Apparatus – Photo 19) lies in evacuation of the special metering cylinder. In French FENZY-68 type SC-SCR (Photo 23) and DC-55 (Photo 24) metering of fresh breathing medium is regulated by set of bags contained one in the other.

Metering system performed by evacuation of the metering cylinder is presented in Fig. 4. Every slight movement of the breathing bellow 1 induced by breathing is counted by the pawl mechanism of the system regulating the metering valves 2. Filling and evacuation of the metering cylinder 4 is carried out by switching valve 3 by the steering system 2.

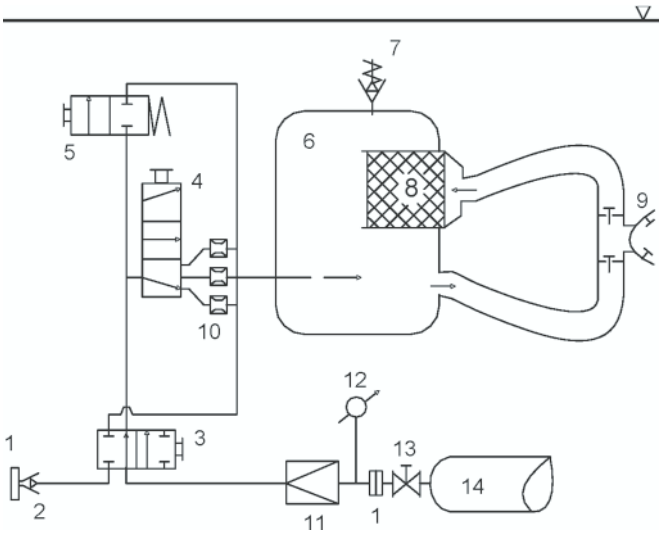

Fig. 3. *One-bag SC-premix-SCR.* ***1)*** *coupling,* ***2)*** *return valve,* ***3)*** *selector valve,* ***4)*** *selector valve of metering nozzles,* ***5)*** *by pass valve,* ***6)*** *breathing bag,* ***7)*** *relief valve,* ***8)*** *carbon dioxide absorbent,* ***9)*** *mouthpiece unit with valves and hoses,* ***10)*** *metering nozzles,* ***11)*** *reducer,* ***12)*** *manometer,* ***13)*** *cut-off valve,* ***14)*** *autonomous set of cylinders*

Photo 18. *SC-premix-SCR APW-6M type*

Table 6. *Characteristic of premix SCR*

Apparatus of semi-closed circuit of ready breathing medium (Premix SCR)	
Premix SCR is known as system designed for gas mixtures as breathing medium (oxygen is possible). Among the breathing media used most frequently one may find the mixtures: helium-oxygen (Heliox), helium-nitrogen-oxygen (Trimix) or nitrogen-oxygen (Nitrox).	
Disadvantages:	- The choice of breathing medium as to its composition and metering confined to a relatively narrow range of depth. - Relatively complicated preparation of apparatus for work (preparing breathing mixture, checking its composition, checking correctness of the absorbent's filling, checking metering and positioning of the relief valve, checking leak tightness etc.). - Technical difficulties resulting from a proloned storing of the breathing medium (likehood of stratification of the components, with helium-oxygen mixtures, in particular). - Despite a partial reuse of the exhaled medium it gets wasted through relief valve, what adversely affects worthwileness of the very diving, especially at high costs of the breathing medium components. - Technical problems connected with manufacturing of metering nozzles and changes in their characteristics with elapse of time (decalibration of the nozzles). - High sensitivity to of the breathing medium to dust contamination likely to cause chocking of the metering nozzles. - Due to a partial closure of the breathing medium circuit all semi-closed designs are less hygienic than open circuit systems.
Advantages:	- Simplicity of the design providing its reliability. - Partial reuse of the exhaled breathing gas allows for expansion of the protection period of the apparatus thus econimizing the process of diving related to diving with open-circuit diving apparatus. - In majority cases it offers a choice of parameters of work allowing for effectiveness of diving operations and shortening diver's decompression time by selecting range of oxygen partial pressures, reduction of breathing medium density - by application of light gases etc.

Photo 19. *SC-premix-SCR ACSC type*

Photo 20. *Premix house-premix-SCR FGG III type*

Photo 21. *Premix house-premix-SCR GAN-87 type*

Photo 22. *SCR applied in SealabIII [4]*

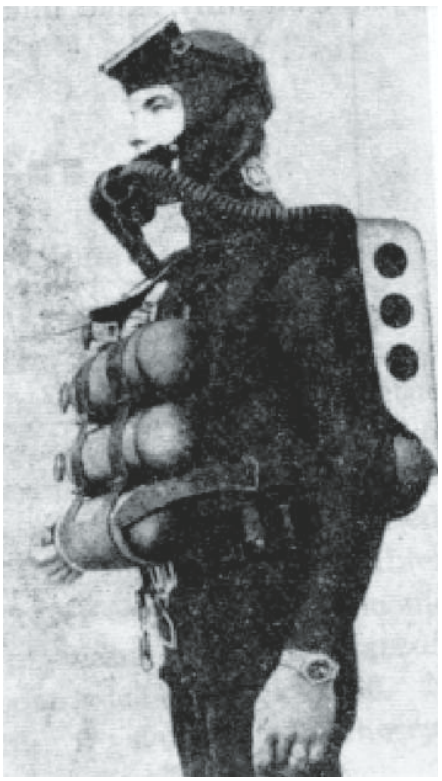

Photo 23. *SC-premix-SCR Fenzy-68 type [4]*

Photo 24. *SC-premix-SCR DC-55 type*

In Fig. 4 the valves 3 are shown in position of evacuation of the metering cylinder 4. To maintain the constant mass rate of the fresh medium metered, the supply overpressure of the cylinder 4 is kept at a constant level by the pressure reducer 5. This system can sense the outer pressure via an

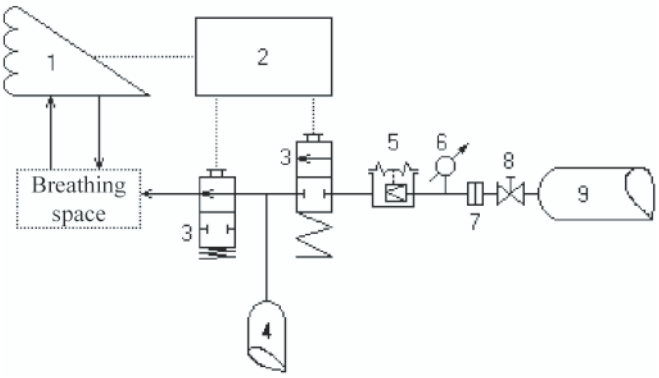

*Fig. 4. Metering system in the premix-SCR taking advantage of evacuation of a constant capacity holder and constant over-pressure of loading. **1)** breathing bellow, **2)** system regulating metering valves, **3)** metering valves, **4)** metering cylinder, **5)** reducer maintaining constant overpressure of breathing medium supply relative to ambient pressure, **6)** manometer, **7)** coupling, **8)** valve, **9)** supply cylinder*

elastic diaphragm. When the sum of the bellow's motions achieves the certain definite number valves 3 get switched and the content of the cylinder 4 is then forced through into the breathing space of SCR. This solution gives the possibility of economical management of the fresh breathing gas stock, as its metering is carried out on demand due breathing rate. It also allows for a precise development of decompression procedures, as any changes in the composition of the breathing medium are only in a slight degree dependent on the actual exertion input of the diver. For the designs with a constant metering of fresh breathing medium this relationship is much more distinct. ACSC apparatus is equipped with a number of very complicated mechanical safety devices, among them: emergency supply of breathing medium, a device preventing from subsidence of breathing bellow during a rapid submersion etc. For this reason it turns a very complicated and a delicate design, first costs and operating costs are high. This apparatus is know only in nitrox version, although there have been undertaken several attmepts to use it at deep diving as well. This type of SCR is employed exclusively for military purposes oading operations. It is an element of mine clearance diving system. In this aim it is made of non-magnetic material and is equipped with a device diffusing breathing medium released through the relief valve into the water.

In French SCRs FENZY-68 and DC-55 metering of the fresh breathing medium is solved by means of a special unit of bellows (bags) arranged one in the other (Fig. 5). When discussing operating priniciples of this system one must make a clear distinction between exhale and inhale phase. One-way circuit of the breathing medium is maintained with non-return valves 1. During exhale phase (Fig. 5a) escape valve of the mouthpiece device gets open. The exhaled gas is let through the mouthpiece 12, exhale hose and escape valve into CO_2 absorbent 11 and then to the large bag 2, therefrom, via non-return valve into the small bag 3. On inhalation (Fig. 5b), escape valve is closed. In turn, the inhale valve opens. From the large bag 2 the breathing medium is issued into the lungs-through the inhale valve, inhale hose and mouthpiece device 12. On inspiration the capacity of the bag 2 diminishes. When collapsing the large bag 2 is pressing the metering valve 5 lever triggering it. It causes the fresh breathing gas from the cylinder 10 to flow passing the cut-off valve 9, coupling 8, reducer 6 and metering valve 5, into the large bag 2 to get mixed with the recycled breathing medium. And now via non-return valve, breathing hose and the mouthpiece device 12 right into the lungs. This solution is very economical because breathing medium is administered on demand, actuated by the breathing action and the capacity relation between the large and the small bags.

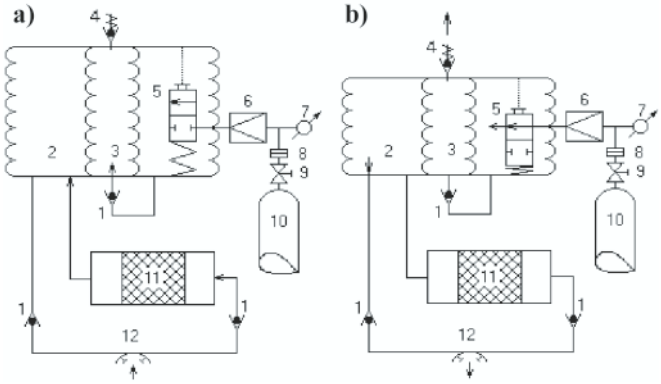

*Fig. 5. Engineering principles of SCR, with breathing bags arranged one in the other. **A**. Exhalation phase, **B**. Inhalation phase, **1)** non-return valve, **2)** large bag (outer), **3)** small bag (inner), **4)** relief valve, **5)** metering valve, **6)** reducer, **7)** manometer, **8)** coupling, **9)** valve, **10)** cylinder with breathing medium, **11)** CO_2 absorbent canister, **12)** mouthpiece device*

Such a system however, does not provide a sufficient metering at larger diving depths. For this reason at depths greater than 25 m it must be supported by a nozzle system of constant metering. SCRs FENZY-68 and DC-55 type are as much as ACSC are used only in the navy, in nitrox version to about 50 m H_2O.

Automix-SCR

Operation principle of one-bag breathing automix-SCR is illustrated in Fig. 6. The system produces breathing medium characterised by a constant ratio of contents between oxygen and inert gases. Designs of this type (Fig. 6) in hose-SCR

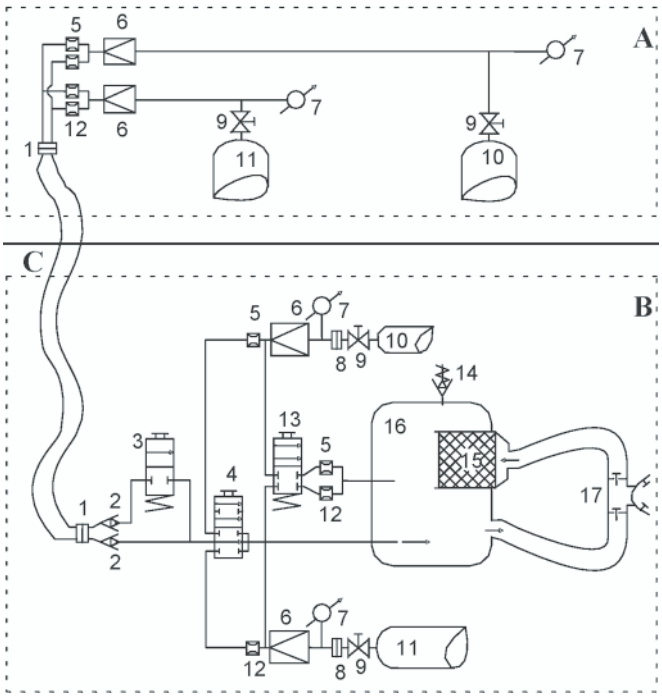

*Fig. 6. One-bag version of automix-SCR. **A**. External supply unit of hose automix-SCR, **B**. SC-automix-SCR, **C**. Group of supply wires and pipes (umbilical). **1)** coupling, **2)** non-return valve, **3)** by-pass valve cooperating with the external supply unit A, **4)** selector valve, **5)** oxygen metering valve, **6)** reducer, **7)** manometer, **8)** cylinder coupling, **9)** cut-off valve, **10)** cylinder of oxygen, **11)** cylinder of inert gas, **12)** metering nozzle of inert gas (e.g. helium), **13)** by-passvalve cooperating with independent supply unit, **14)** relief valve, **15)** carbon dioxide absorbent, **16)** counterlung, **17)** mouthpiece device with valves and hoses*

version are equipped with installations meant for mixing breathing medium outside the system (external supply unit marked as A). The entire system producing the breathing mixture is localised on the diving station or diving bell. It may additionally be fitted with e.g. sensors of oxygen content (partial pressure). In its hose-SCR version the apparatus may consist of a combination of several units engaged in automix-SCR and another premix-SCR (SC emergency supply). The SC-SCR, marked as B is showed in Fig. 6, is the automix-SCR. The SC-SCR version B is made of breathing bag (bags) 16, carbon dioxide absorbent canister 15, gas cylinders 10 and 11, and finally of a unit generating breathing medium. The production of the breathing medium consists in mixing a stream of oxygen and a stream of inert gas. The metering of the gases is carried out by means of nozzles metering within their supercritical ranges (this issue will be discussed in Chapter 4). Appropriate reduced overpressure of gases is maintained by the pressure reducers 6. Fullness of the cylinder is controlled by manometers 7.

Oxygen and inert gas get mixed in the supply hose and enter counterlung 16, wherefrom via inhale hose of the mouthpiece the ready mixture is directed into the diver's lungs. The exhale is released through the mouthpiece 17, through its valve and exhale hose, passing carbon dioxide absorbent 15, into the counterlung. The surplus of the breathing medium escapes from the bag through the relief valve 14 into the water. Just like in the case of the apparatus discussed above, the breathing medium is also administered into the lungs of diver at a pressure which value equals the sum of ambient hydrostatic pressure of the given diving depth and the overpressure of opening the relief valve. To preliminary fill the breathing space and to wash it out with fresh breathing medium a by-pass unit 3 is used - at work with hose supply or 13 - at independent operations. Fundamental features of automix-SCR are summarized in Table 7. Example of automix-SCR discussed in Table 3 is presented in Photos 25÷27.

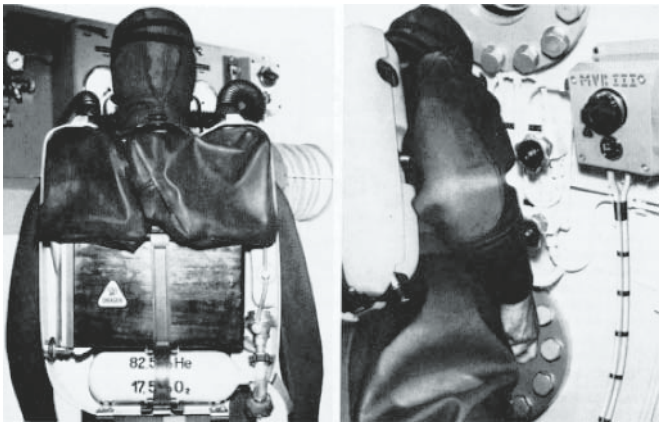

Photo 25. *House-automix-SCR SMS-III type*

Photo 26. *SC-automix- SCR APW-3 type*

Table 7. *Basic features of automix-SCR*

Breathing apparatus of semi-closed circuit of breathing medium mixed during diving (Automix-SCR)	
Automix-SCR has never been in a wide use due to the problems with their manufacturing and exploitation. It is know only in experimental or in a limited run	
Disadvantages:	- Homogeneity and stability of the breathing medium contained in the bag much more difficult to maintain than in the designs using a premixed breathing medium. - In case of apparatus producing breathing medium of a constant ratio of content between oxygen and inert gas each time the composition of the breathing medium as well as the mode of metering must be carefully selected sufficing only to a relatively narrow range of diving depth. - Prior to each dive the apparatus must be subjected to a quite troublesome procedure of preparation and checking. - Despite a partial reuse of the breathing medium it gets wasted at relief valve what affects economical rate of diving with breathing mixture made of expensive components. - High sensitivity to dust pollution likely to chock metering nozzles. - Due to a partial closure of the breathing medium circuit all these designs are less hygieninc than the open circuit systems.
Advantages:	*Such as of apparatus of semi-closed circuit of premixed breathing medium, and:* - Potential for operating on clean gases instead of their mixtures. This allows avoid problems connected with production and storing of precisely composed breathing mixtures. It enhances the economical rate of exploitation of this apparatus in comparison with the diving apparatus using a premixed breathing medium. - A change of breathing medium for a selected range of depth involves a mere change of the metering nozzles. - In case of apparatus producing breathing medium of variable ratio of oxygen to inert gas the potential dynamic change of the ratio between oxygen and inert gas making the breathing medium according to the depth of diving.

Photo 27. *SC-automix-SCR APW-6 type*

CLOSED CIRCUIT BREATHING APPARATUS (CCR)

The designs of closed circuit breathing apparatus (CCR) can be divided into:

- oxygen CCR (oxy-CCR)
- breathing mixtures CCR (mix-CCR).

Oxygen CCR

Oxygen is the most often specified group of the closed circuit breathing medium [7]. In oxy- CCR the breathing cycle is as follows: oxygen is inhaled from the breathing space of CCR. As it is exhaled, the gas passes through canister with carbon dioxide absorber to the breathing space. Oxygen consumption during diving is not large, not the diving depth affected but dependent only upon the work performed.

When compared to open circuit UBA, oxy-CCR doesn't require large supply of the breathing gas and offer an enrange action radius range. Therefore, construction of oxy-CCR enables extended operating duration, however due to oxygen toxicity it can be used only at the shallow depths. As there is no need for a periodical release of the breathing medium, there are no escaping bubbles to the water and oxy-CCR can be used for special diving covered warfare. During normal work that system requires only periodical washout of the breathing space to eliminate accumulating contaminants and wash out of nitrogen that saturates human body under normal conditions. There is also need for release of the breathing medium excess during ascend of the diver. Due to oxygen toxicity, an oxygen dive is limited by the depth and exposure time. Moreover, an oxygen diver should satisfy special physical and psychical predisposition. For these reasons an oxygen dive is prohibited in many countries, however, is possible to carry out in civil underwater operations.

Oxy-CCR constructions have been developed in two main directions. The first is an improvement of traditional construction of the Fleuss CCR. It consists of the breathing bag connected with carbon dioxide absorbent canister. The canister may be filled with carbon dioxide absorbent (different forms of soda lime are most often used) or with various oxygen generating masses (sodium, potassium or lithium superoxides). These apparatuses may have manual or constant oxygen metering system (the latter aided with manual or automatic periodical adding of oxygen). Example of oxy-UBA is presented in Fig. 7. Improvement of this oxy-CCR design consists in the use of patents leading to its better tactical-technical properties. Elimination of buoayancy change effects due to breathing rate and the changes in the depth of dive, application of the constructional solutions leading to reduced breathing resistance, application of compact designs, elimination of the magnetic field generated by the oxy-CCR, elimination of the noise generated during breathing and oxy-CCR work, application of the oxy-CCR equipment that enables camouflage during transport and covered storage, application of constructions that not require special tools at daily servicing, corrosion and trying conditions resistant materials, water temperature change resistant constructional and exploitation materials, maximisation of the apparatus mass to its action radius range, application of streamline shapes of low resistance during swimming etc.

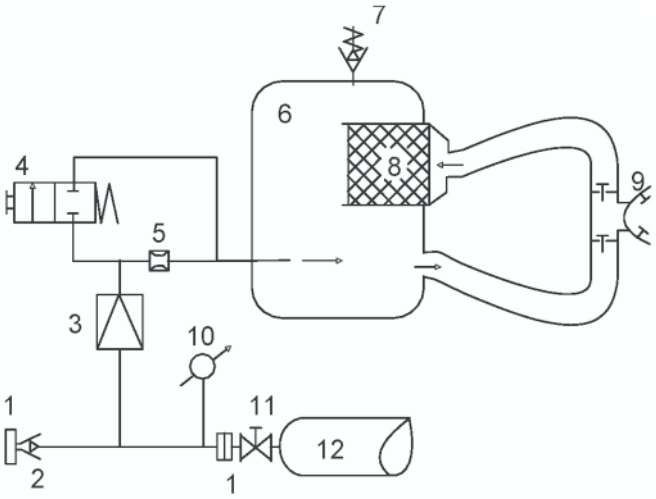

Fig. 7. *SC-CCR of the constant oxygen metering.* ***1)*** *joint,* ***2)*** *non-return valve,* ***3)*** *reducer,* ***4)*** *by pass valve,* ***5)*** *oxygen metering nozzle,* ***6)*** *the breathing bag,* ***7)*** *relief valve,* ***8)*** *cylinder coupling,* ***9)*** *mouthpiece assembly with valves and hoses,* ***10)*** *manometer,* ***11)*** *cut-off valve,* ***12)*** *oxygen cylinder*

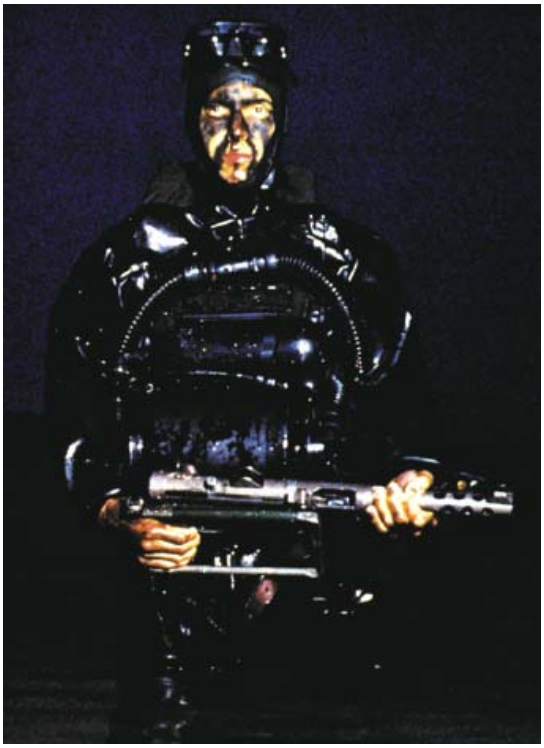

Photo 28. *Oxy-CCR AGA-Oxydive type*

Photo 29. *Oxy-CCR LT II type*

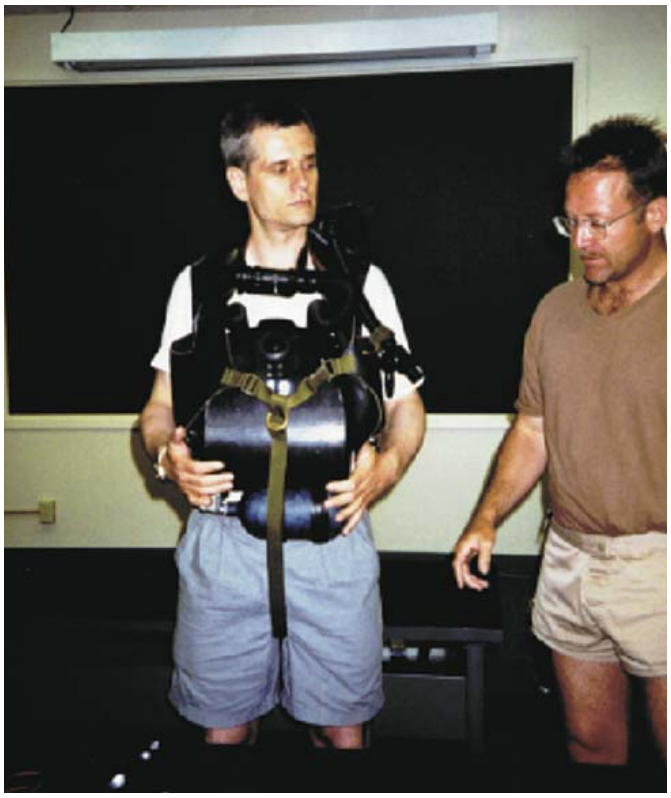

Photo 30. *The author and oxy-CCR LAR V type*

Photo 31. *Oxy-CCR LAR VII type*

Photo 32. *The author and oxy-CCR S-10 type*

Swedish oxy-CCR AGA-Oxydive type (Photo 28), German oxy-CCR LT II type (Photo 29) or later version LAR V (Photo 30) and LAR VI (Photo. 31), or Canadian S-10 (Photo 32) represent this group of oxy-CCR.

Another group consists of oxy-CCRs, where instead of the breathing bag a large rubber diaphragm is used, arranged on the top of the shallow box, with the lever of by-pass valve on its bottom. If oxygen volume in the breathing space falls below a certain established minimum, the diaphragm will press the lever triggering oxygen by-pass valve. The diaphragm is strapped with the limiters adjusting maximum breathing space volume to the diver's preferences and mass of his equipment. Solutions of oxy-CCR are employed in American Cobra (Photo 33) or French OXY-NG (Photo 34).

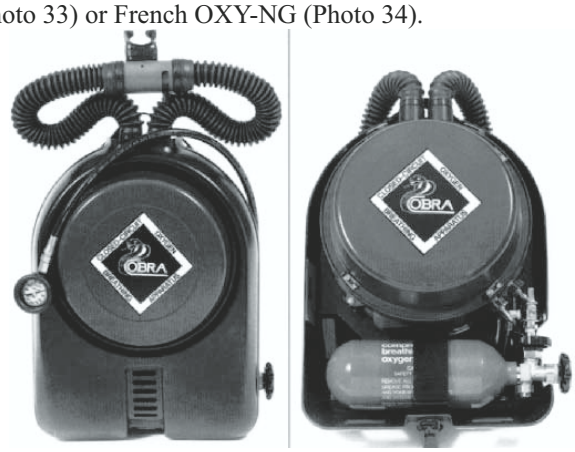

Photo 33. *Oxy-CCR Cobra type*

Photo 34. *oxy-CCR Oxy-NG type.* ***a)*** *during sea tests (the own photo),* ***b)*** *the author during trials in the harbour basin of Marseill*

Mix-CCR

Closed-circuit gas mixture UBA (mix-CCR) can be groped as follows:

- ❖ small circuit mix-CCR
- ❖ increased (enlarged) circuit d mix-CCR
- ❖ large circuit CCR.

Small circuit mix-CCR are called the SC-mix-CCR, e.g.: Mk 15/16 – Photo 35. increased (enlarged) circuit mix-CCR denotes a circuit between the apparatus and the diving bell (or other submersibles) equipped with measuring instruments, systems of regeneration and enrichment the breathing gas with oxygen and so on, e.g.: Dolphin 7, Photo 36. A large circuit of mix-CCR is the circuit between the surface (via e.g.: the diving bell) and the diver. The measuring equipment, systems of regeneration and enrichment the breathing gas with oxygen are placed on the surface, e.g.: CCBS 450 with the surface system GAK 600, the diver's equipment and the main table of the system (Photo 37).

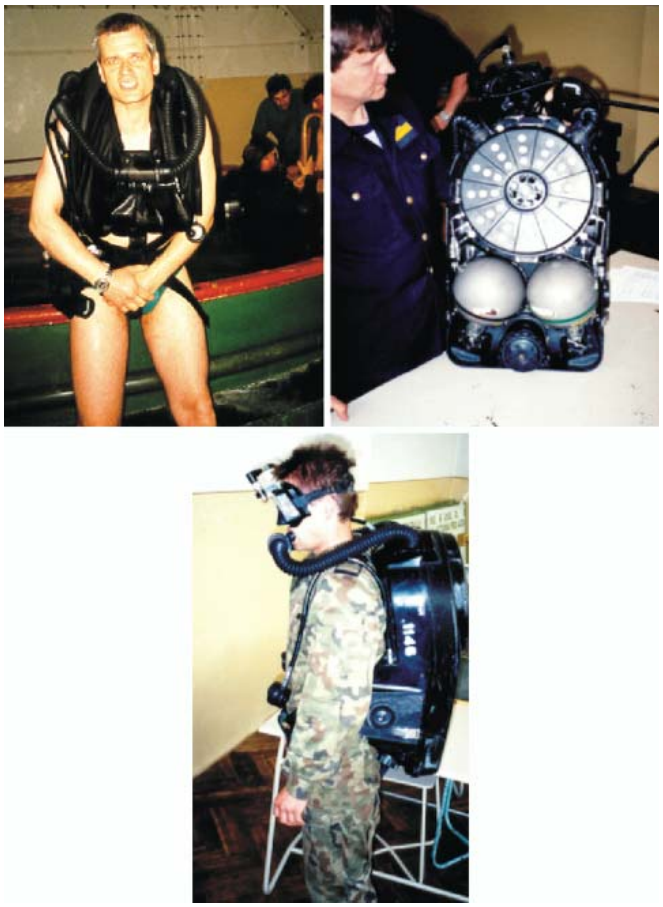

Photo 35. *The author before diving with use Mk-15/16 and views of SC-mix-CCR Mk-15/16 type*

General principle of the SC- mix-CCR operation is presented in Fig. 8. Elektrolung, popular name of this design comes from the apparatus manufactured by Oceanic Equipment Co. (Photo 38).

The breathing bag (Fig. 8) together with the carbon dioxide absorbent canister is connected with the mouthpiece assembly by means of the breathing hoses. The breathing medium circulates within as with the direction arrows in the Fig. 8. Inhale and exhale valves ensure one-way direction. These constructional junctions operate in exactly the same way as SCRs discussed above. From the cylinder 1 via cut-off valve 2 inert gas flows into the breathing bag, passing on its way:

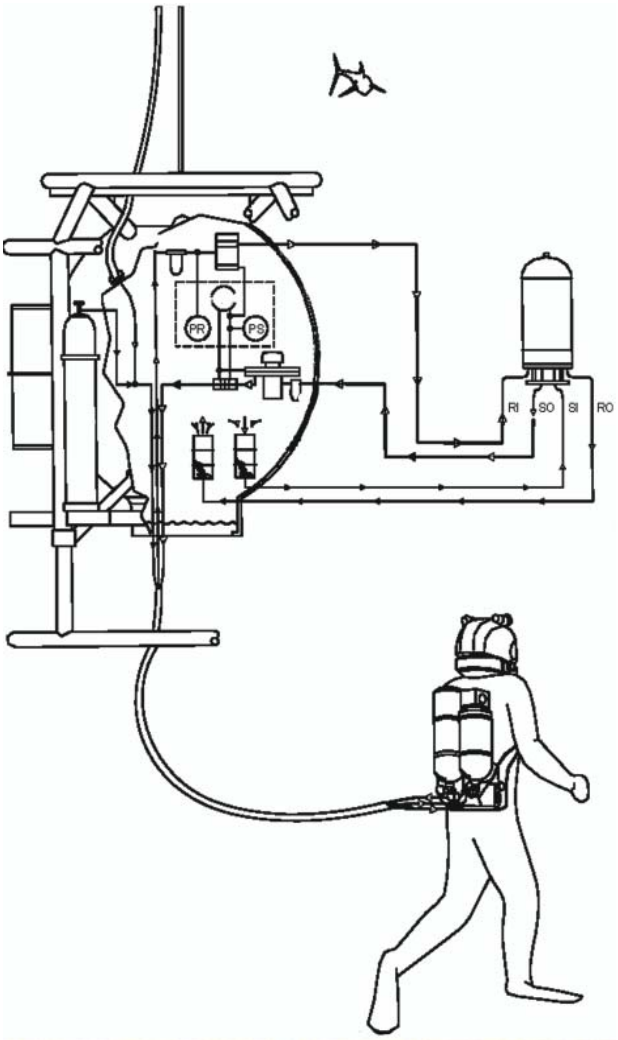

Photo 36. *The diving mix-CCR system and diving helmet Dolphin 7 type*

manometric pressure control 4, and the automatic assembly allowing for ambient hydrostatic pressure at the depth of diving 5. Oxygen from oxygen cylinder 16 runs through cut-off valve 2, manometric control 4, through the oxygen reducer 15 and flow controlling valve 13 into the breathing bag. The oxygen sensor 9 placed in the breathing bag, constantly measures the oxygen partial pressure. The signal is simultaneously displayed

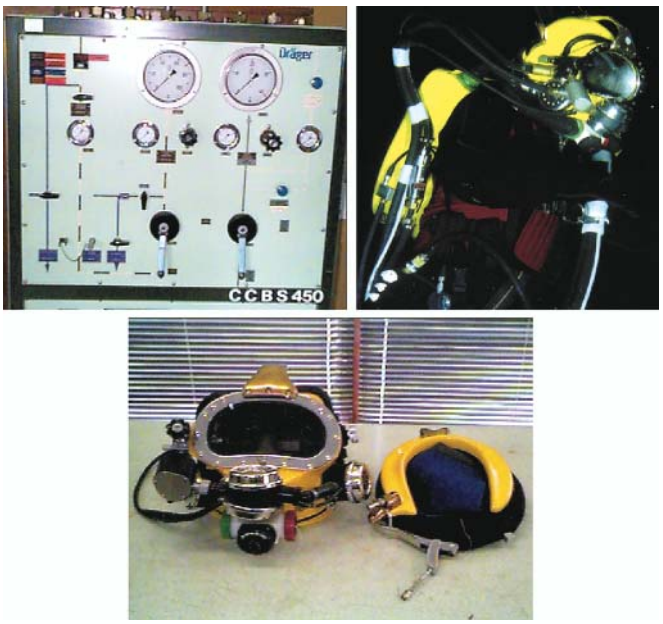

Photo 37. *Main board and the diver's hose-mix-CCR system CCBS type*

Photo 38. *Elektrolung SC-mix-CCR manufactured by Oceanic Equipment Co [1]*

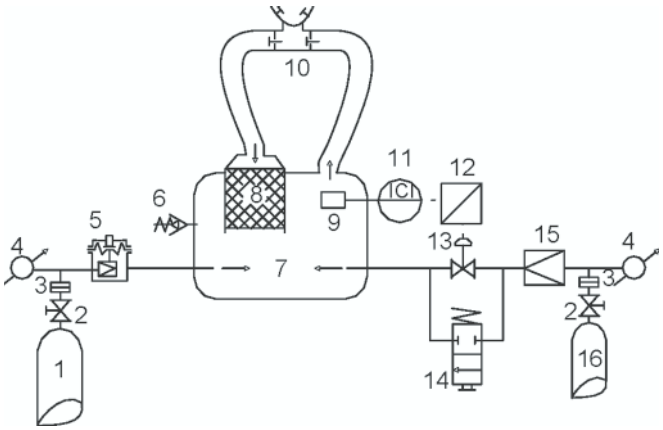

Fig. 8. *SC-mix-CCR.* ***1)*** *inert gas cylinder (e.g. helium),* ***2)*** *cut-off valve,* ***3)*** *coupling,* ***4)*** *manometer,* ***5)*** *reduction unit maintaining the filling of the breathing bag at the demanded level,* ***6)*** *relief valve,* ***7)*** *breathing bag,* ***8)*** *carbon dioxide absorbent,* ***9)*** *sensor of oxygen partial pressure,* ***10)*** *mouthpiece device with valves and hoses,* ***11)*** *measuring-controlling unit of oxygen partial pressure,* ***12)*** *converter of electric signal into pressure response,* ***13)*** *valve with pneumatic servo,* ***14)*** *oxygen by-pass valve,* ***15)*** *oxygen reducer,* ***16)*** *oxygen cylinder*

on the diver's control desk and is transmitted to current-pressure transducer 12. The transducer uses the oxygen line to perform supply the executive element regulating opening of the valve 13. If the oxygen partial pressure is too small, the valve 13 will be opened by the executive pneumatic element. Additional by-pass valve 14 is used for a preliminary filling of the breathing bag and its washout during oxygen compression. There were three sensors instead one of the oxygen partial pressure applied in this type of CCR (similar to Mk15/16 mix-CCR). The indications of each one were displayed on the diver's control board. Additional sensors not shown in Fig. 8 served as also as sensors of low or high partial pressure signal in the breathing bag. They were specifically calibrated so that their sensitivity should be maximal at the established maximum oxygen partial pressure (IIAH) and the established minimum oxygen partial pressure (IIAL). They signalled any exceeding of these values. Apart from measuring and transmitting the signal on the diver's board, main sensor 9 controlled opening of the oxygen valve.

Enlarged and large circuit mix-CCR are complete systems supporting dives. An example of such a system is presented in Fig. 9. The UBA (the diver's helmet) is equipped with a switch of operation mode that can be set on operation either in closed or open system. It can be also set in the position of the SC-mix-CCR (bail-out UBA) provided the system has one. In case of the system failure, bail-out UBA cannot be used if the diver switch on the diver's helmet emergency valve to the open circuit system, being supplied then with emergency breathing medium.

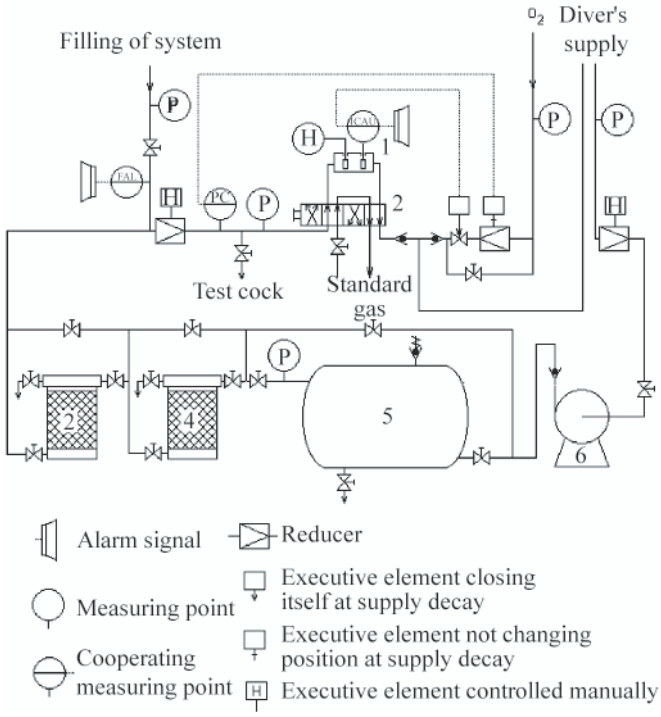

Fig. 9. *Supply unit of large closed circuit of breathing medium mix-CCR.* ***1)*** *unit for measuring oxygen partial pressure and breathing medium humidity,* ***2)*** *group of selecting valves for control of measuring unit in operation,* ***3)*** *drier,* ***4)*** *carbon dioxide absorbent,* ***5)*** *storage reservoir,* ***6)*** *compressor unit.* ***P*** *– point of measuring pressure,* ***PC*** *– point of measuring pressure and automatic control,* ***H*** *– measuring point of humidity or manual control,* ***ICAU*** *– measuring of sensor current and automatic control with a signalling of low and high level,* ***FAL*** *– flow indicator*

Breathing medium is stored in the surface store-room or in gas cylinders placed on the diving bell. The breathing medium circuit exemplary system (Fig. 10, PMR 1/2008) is forced with pump 6. The pump sucks the exhaled gas through manually operated reducer that is being set on sucking. Then gas

Table 8. *Characteristic of mix-CCR*

Closed-circuit breathing gas mix underwater breathing apparatus (Mix-CCR)	
Mix-CCR can be classified in two groups that differ with the breathing medium applied. There are two types oxy-CCR and mix-CCR. Oxy-CCR is primarily used for military purposes. Mix-CCR is mostly used in large (or enlarged) circuit version in saturation diving operations.	
Disadvantages:	- Large circuit mix-CCR requires an extensive and technically complicated system of gas-supply operated by highly skilled personnel. - Small circuit mix-CCR is very complicated construction and requires expert personnel. Due to the lack of good oxygen partial pressure sensors mix-CCR can be unreliable. - Oxy-CCR should be used by specially trained divers of special presidposition due to the possibility of carbon dioxide poisoning. - Due to closure of the breathing gas circuit in all CCR type constructions accumulation of contaminants can occur.
Advantages:	- Due to economy of the CCR are the most economical types of UBA. - CCR offers the possibility of rapid and optimum adjustment of its working parameters to each of the diving depth.

is pumped to the system, where from after purification is repeatedly pumped to the diver through the pump reducer (supply reducer). The settings of the reducers on the sucking and pumping line are connected with each other and depend upon the range of the diving depth and ventilation rate required. Together with the valves of the mouthpiece assembly they ensure a proper circulation of the breathing medium. They prevent the pump from sucking out the whole breathing gas form the circuit and the breathing gas being not all suddenly pumped into the diver's helmet, at too large pressure. The breathing medium when sucked by the pump passes through the storage reservoir 5, carbon dioxide 4 and dryer 3 and earlier mentioned reducer to the measurement chamber1. In the measurement chamber arranged on the gas line the breathing medium humidity is measured (H) and the oxygen contents (ICAU). The oxygen by-pass valve is controlled by the measurement. In case of failure the oxygen adding can be manually operated and the supply unit is fit to work in a mode of emergency supply of the breathing medium-through the valve that enables to fill the system. In this situation gas exhaled by the diver is directed into the water (open circuit work- after the appropriate switch of the valves in the diver's helmet). The rate of breathing gas dehumidification is operated manually by the dyer by-pass valve. Appropriate positioning of this valve with the dryer inlet valve separates stream of breathing gas that enables control of flowing breathing gas dehumidification. The system must offer a possibility of calibrating its measuring instruments with standard gases (valve 2) and periodical breathing gas sampling (test cock) for gas analysis. Characteristic of closed circuit apparatus is given in Table 8.

CONCLUSIONS

- Beyond any doubt air-UBA are the most often used construction among other that have been described earlier. Intensive development of these constructions has led to highly reliable UBA despite its relative complexity.
- Other described types of UBA exemplify the elementary production of specialised companies. Some types of UBA have never been implemented or were manufactured occasionally and are not in common use. Undoubtedly, except air-UBA, constant metering premix-SCR (used during dives beyond saturation zone, especially dedicated for M|CM divers), mix-CCR (used during saturation deep-diving), and oxy-CCR (military application) are the most often used UBA.
- Despite of their unquestionable disadvantages premix-SCR are relatively simple designs. It makes that SCR are technically reliable. Recently great interest is focused on special construction diving apparatuses. Premix-SCR is employed for independent deep diving operations. "Technical diving" is the special hazardous kind of diving that attracts from all over the world the wide groups of divers looking for strong sensations.

BIBLIOGRAPHY

1. Bachrach A.J., Desiderati B.M., Matzen M.M.: *A pictorial history of diving*. Best Publishing Co. 1988
2. Clarke D.W.: The history of breathing apparatus and current state of the art ‡z:‡ *Lung and physiology and divers breathing apparatus*. Proceedings from the International Workshop Ballater, Scotland, 1÷4 Nov. 1991: Department of Biomedical Sciences Marshal College Aberdeen 1992
3. Diving Manual: Ministry of Defence (Navy), B.R.2805 (Army Code No 61231) March 1982
4. Gussman J.: *The man is getting depths*. Wydawnictwo Morskie Gdańsk 1984
5. Mer & Océan - *Spécial Cousteau* 1997
6. Underwater works: Wydawnictwo Morskie Gdańsk 1971
7. Przylipiak M., Torbus J.: *The equipment and diving works - guide*. WMON Warszawa 1981
8. Rawlis J.: *The history of commercial, military and sport diving*. Trans. IMarE 101(1989)161÷170
9. *The five methods for professional diving*. Announcement Drägerwerk AG Lübeck (Oct.1987)
10. Shilling C. W., Werts M. F., Schandelmeier N. R.: *The underwater handbook*. Plenum Press New York and London
11. *US Navy diving manual*. Best Publishing Co. Carson California 1980
12. *US Navy diving manual (revision 3)*. The Direction of Commander, Naval Sea Systems Command 1993

CONTACT WITH THE AUTHOR
Ryszard Kłos, Assoc. Prof.
Department of Diving Technology
and Underwater Activities
Polish Naval Academy
Śmidowicza 69
81-103 Gdynia POLAND
e-mail: skrzyn@wp.pl

POLISH MARITIME RESEARCH 4(58) 2008 Vol 15; pp. 85-95
10.2478/v10012-008-0001-0

The multidimensional approach to development strategy of marine industry

Part II.
Multifaceted analysis of the development outlook for the Polish marine industry

Iouri N. Semenov, Prof.
Szczecin University of Technology

ABSTACT

Today the Polish marine industry demands multi-step conversion of its companies into future-oriented enterprises. The article presents some results of the multifaceted analysis of this branch of the Polish economy. Main attention is devoted to identification of the critical barriers to its modernization. It is shown that such purpose as increase of competitiveness requires the correct assessment of various obstacles to innovative changes. Moreover, it is recommended the scenarios approach to the risk minimization of quantitative transformations and qualitative changes in the Polish marine industry. Various scenarios forecasting obstacles impacts are presented. Special attention is focused as on the decision-makers willingness to innovative changes, as on eventual techniques for fruitful overcoming the barriers to accelerated development of the Polish marine industry. Proposals are illustrated by numerous results of fulfilled investigation.

Keywords: Polish marine industry, obstacles to innovative change, maritime transport, risk assessment

INTRODUCTION

The Polish marine industry had significant growth over the past 60 years, evolving from small regional shipping companies and shipbuilding/shiprepair enterprises into a recognized branch serving international clientele. The first deep-sea ship built in postwar Poland was the small steamship, the 2,540 DWT, which have been launched in the Gdansk shipyard in November, 1948. In 1965, the rate of ships' production for the Poland shipyards reached of peak value, and placed Poland shipbuilding as eighth on the worldwide list of producers.

Rapid development of the Polish marine industry takes place in the beginning of XXI century. So, growth in this sector of the Polish economy has been estimated at between 5.5% and 6.0% annually. In 1993-2003 the total number of productive, co-operative, associated and affiliated enterprises was increased from approx. 3790 to more than 8500; however workplaces number was decreased from 120,000 to 100,000. Last six years, the Poland has a significant presence in such branch of the marine industry as yachting. Now the Polish shipbuilding differs by high exporting possibilities. The exports share of this industry accounts for over 90% of gross output [12]. Therefore, the Polish construction and repair shipyards employ approx. 20 thousand persons, while the entire shipbuilding industry provides work for nearly 70 thousand persons. Today's development of the Poland's shipping companies are directed to specialized services through timely deliveries, skill management and disciplined crews, as the Poland's shipyards have gained prominence through quality productions of top-class chemical tankers, containerships, super yachts and recreation boats. The key ways of contemporary development of the Polish economy are [15, 17]:

- ⇨ The competitive growth of domestic market which focused on seven major segments of the marine industry, including the shipbuilding, maritime transport, fishing, inland navigation, yachting, ships' service and logistic assistance.
- ⇨ Support of innovative activity which is concentrated on expansion of scientific and engineering researches. This area includes also training of enterprises personnel.
- ⇨ Progress of legislative activity which focused on stable perfection of the Polish legal system for comprehensive development of the marine industry.

Unfortunately cyclical character of development of market-oriented economy with its peaks and troughs periods is distinctive feature also for the Polish shipyards and the shipping companies. It occurs for the most part because of absence systemic innovative strategies of management of these segments of the marine industry.

From 2004 the Poland is Member-State of the EU, and has chances for rapid development. In-process adaptation of some Polish companies to the market changes (especially to the recession stage), not enough use of the European experience, as well as the retarded technologies reduces their competitiveness on domestic and foreign markets, and in

consequence, their chances for commercial success. The main reasons are [8, 12]:

- financial problems, e.g. the increasing prices of metallurgical products and energy supplies, incorrect economical forecast when a contracts on delivery of new-building ships were signed without taking exchange rate risk, just as high labour costs;
- administrative problems, e.g. insufficient support of innovative activity, as a consequence of incorrect guidelines and the marketing forecast for development ways;
- unsatisfactory production environment, and as result low labour productivity;
- risk-averse culture and lack of entrepreneurial spirit of top-managers.

In turn, the Polish maritime transport is facing some more problems, namely insufficient competitiveness and low operational flexibility. For example, during periods between 1991 and 2000, the Polish shipping companies has tended to drastic limitation of investment program on new ships and sophisticated transshipment equipment. High intellectual potential of the Polish specialists manifested in furtherance to effective adoption of competitive maritime technologies has numerous and varied supporting evidences, including creation of internal regulatory systems and navigation guidelines, permanent monitoring of market forces, designing of successful onshore management systems, and other incentive solutions. At the same time, error-free choice of prevailing investment strategy is one of the major problems for the Polish shipping companies to solving. In addition to lack of investments into innovative activity there are also other external barriers which hamper both modernizations of a ship equipment, and renovation of the Polish fleet's structure as a whole [3, 13].

First of all, relatively high incompatibility between the Polish production environment and advanced technologies may be important barrier to successful modernizations of any enterprises. This takes place when technology is „bundled" into complex systems, i.e. one systemic component cannot be replaced or upgraded without necessitating changes in the whole system [4, 10]. This bundling of technology hampers the production's modernization in some Polish enterprises (e.g. the Polish shipyards, H.Cegielski – Poznań SA. etc.) and the transportation process' improvement in some shipping companies. Principal cause is excessively expensive investments, which are required for purchase and implantation of the bundled technologies. As have shown researches of the author, the Polish enterprises willingly implant the unbundled technologies as more accessible to them because financial and organizational barriers to their performance are considerably smaller, not paying attention to low efficiency of such modernizations.

Furthermore, one of the most common problems is unsatisfactory relationships between scientific communities on the one hand, and business environment on the other hand.

1	**Task** – Generalization of foreign experience in innovations implantation.
	The objective – Analysis of the modernization practice in the worldwide marine industry.
2	**Task** – Collection and data generalization for the current situation of the Polish marine industry.
	The objective – Identification of development trends for the Polish marine industry.
3	**Task** – The investigation of development dynamics of the Polish marine industry.
	The objective – Determination of critical points in the Polish marine industry development.
4	**Task** – Systematization of the causes, entailing generation of obstacles to development.
	The objective – Identification of the obstacles to industry innovative development.
5	**Task** – Decomposition and grouping of likely obstacles to development.
	The objective – Structurization of probable obstacles to development of the RP marine industry.
6	**Task** – Investigation of probable obstacles to the innovative process by each-to-each technique
	The objective – Identification of the critical and minor obstacles to industry development.
7	**Task** – Forecasting of possible obstacles for the sustainable development of marine industry.
	The objective – Qualitative assessment of possible scenarios of the RP industry development
8	**Task** – Mapping of risk distribution for sustainable development of the Polish marine industry.
	The objective –Risk assessment of eventual innovative projects.
9	**Task** – Stratification of forecast's results for innovative transformations within the marine industry.
	The objective – Choice of the best development strategy for the Polish marine industry up to 2040 through multilevel analysis.

Fig. 1. *Sequential analysis of transformation outlooks for the Polish marine industry up to 2040*

According to the Community Innovation Survey, the Polish innovation rate decreased from 37.6% in the years 1994-1996 to 17.6% in 1998-2000. In turn in the years 2002-2004 the share of innovative enterprises increased to 25.6%. For comparison, this ratio for the UE Member-States increased to 51% on average. Hence, for the Polish marine industry is more and more important to take part in Community programme named Leadership 2015. This programme assumes a competitive growth in this economic sector through innovation, knowledge and entrepreneurship for the European shipbuilding and shiprepair industry [6]. Despite the actions taken by the Polish shipyards, their economic and financial situation in the last years was still difficult. At present, negotiations for the sale of this business sector being reorganized are under way with private investors. It will allow re-structuring the Polish sea industry. Author recommends analyzing of development outlooks for the Polish marine industry prior to innovations implantation (Fig. 1).

This analysis will help successful modernization of the Polish marine industry as includes both identification of eventual barriers to innovative changes, and simulation of their pernicious impact on reorganization of this industry as whole. The Step 1 of the sequential analysis (Fig. 1) is presented in the Part I of the paper. A basic sketch of the Step 2 and the Step 3 is shown in Introduction. Let's pass to the next steps of our investigations taking into account documents shown in the Table 1.

OBSTACLES TO REORGANIZATION OF THE POLISH MARINE INDUSTRY

Identification of the obstacles to innovative development of marine industry (Step 4, Fig. 1) plays decisive role so as to take timely steps and to not lose the chances to temper the impact of eventual obstacles. Various inventions as well as innovations play a vital part in technological advancement of the Polish marine industry though the industrial reorganizations in the Polish conditions are sufficiently sophisticated. As result, the maritime transport meets with strong mechanisms creating various barriers to innovative activity. Usually, this is due to the obsoleteness of the industrial environment, and financial or legislative reasons [8, 11]. In author's opinion take place wider spectrum of the so-called barriers to reorganization of the Polish marine industry.

Let's consider in details the main obstacles to the progress of this business segment, since financial problems as critical "bottleneck".

1. Financial obstacles include:
   - lack of investment funds, as consequence of a hindered access to external finance
   - competing business priorities, in particular, the pressure for short- term profits
   - a high expenses of innovative projects
   - a high level of the inflation risk, as well as credit risk and exchange rate risk
   - a high cost as raw materials, and energy resources.

   In 2006-2007, wide researches of a business environment in the Polish economy have begun. The findings indicate that the high tax rates and overly complication of legal regulation are main barriers to business development. For example, more than 10% of all entrepreneurs have opinion that the Polish legal system isn't friendly for business activity.

2. Regulative obstacles include:
   - deep-rooted traditions of local authority and regional legislative practice
   - a low flexibility of obligations under a contract to cargo deliver for various service forms
   - enormous number of restrictive laws and government regulations
   - complicated and long-term deciding procedures
   - scantiness of pre-starting procedures to effective implantation of new ideas.

   Other several barriers also hamper innovative development. Since this problem is not enough studied in the Polish literature [8, 15, 16]. Therefore, let's it analyze, taking into account foreign experience [2, 5]. Some of obstacles have subjective nature. This type of barriers to innovative activity includes individual obstacles, which evolved from mental features of decision-makers, and team obstacles, which developed from the intra-staff relation.

Table 1. *Documents used for the problem study*

№	Title	Author	Date
1	*Poland and the Knowledge Economy: Enhancing Poland's Competitiveness in the European Union*	World Bank, Washington	2004
2	*Strategic Evaluation on Innovation and the Knowledge–based Economy in relation to the Structural and Cohesion Funds for the programming 2007-2013*. Report to the EC and Additionally. Country Report: Poland	Polish Ministry of Economy, Warsaw	4. 09. 2006
3	*Strategy for Increasing the Innovativeness of the Economy for the years 2007-2013*	Technopolis: Walendowski J, Brussels.	7.07. 2006
4	*Defining the Future European Shipbuilding and Shiprepair industry-Competitiveness through Excellence*. COM (2007) 220 final	LeaderSHIP 2015, Brussels	25.4. 2007.
5	*Policy mix for innovation in Poland – key issues and policy recommendations*. DSTI/STR/TIP(2006)	OECD, Directorate for Science, Technology and Industry , Warsaw	27.06.2007
	Panorama of transport, KS-DA-07-001-EN-C	Eurostat and EC, Luxembourg	28.06.2007
6	*Analyses and Forecasting Department*. Report Economy	Polish Ministry of Economy, Warsaw	2007
7	*Statistical Yearbook of Maritime Economy*	Central statistical Office. Statistical office in Szczecin, Warsaw-Szczecin	2007
8	*Competitiveness of the SME sector 2007*	Lewiatan, Warsaw	2007

3. Subjective barriers include:
   a) *Individual obstacles*:
   - top management unawareness of support importance of new ideas
   - lack of entrepreneurial spirit
   - top management unwillingness to risk
   - incorrect guidelines hampering conversion of new initiatives into new product
   - a low level of personal liability and motivation to innovative changes
   - lack of task awareness, as consequence of poor creativity
   - prejudice against innovative changes
   - low awareness of environmental issues.

   b) *Team obstacles, as result of intracompany features*:
   - a high-level of intra-staff conflicts
   - disconnect between first-line managers and personnel
   - erroneous actions as a result of unclear explanation of innovative task
   - unconvincing or improper motivations of personnel
   - a low level of personnel's skills and proficiency.

   Besides, the author identified other three problems in development of the Polish enterprises.

   Composition of such problems includes:
4. Labor obstacles:
   - emigration processes
   - lack of job rotation as consequence of difficulty to attract qualified human resources
   - skills shortages of the working personnel
   - passivity of personnel to innovative changes in connection with possible impact on existing social relationships and personal threat to lose one's work.

5. Industrial obstacles, as result of reformative changes of the Polish economy:
   - bundling (systemic interdependency) of manufacturing technologies
   - informational, structural and evolutional complexities of innovative changes
   - the peculiar environment of eu's enterprises from convergence and phasing–in regions
   - a high level of incompatibility of outdated and innovative manufacturing processes
   - a high level of the risk of production excess under limited market potential
   - a low level of use of nonwaste technologies and as result high production costs
   - a high level risk arising from force external to the industry
   - a conflict of claims on raw materials and other resources.

6. Operational obstacles, as consequence of delayed access the Poland to the EU:
   - a unsatisfactory state of transport infrastructure, e.g. insufficient number of access roads
   - a low labour productivity
   - a high level of coordination problems, as result of poor experience in logistical activity.

   Administrative obstacles play a substantial role in innovative process. The dominant causes of these barriers can be exorbitant bureaucracy and disinclination to meet any innovation, as well as organizational reasons and business motives. Let's analyze administrative obstacles according the Step 5, Fig. 1. First of all, we should formulate definition of structurization process. Structurization is the comprehensive process of information ordering through full division of collected data into separate items, and secondly assembling these items into the hierarchical connected coalition by attributes of causal relations. This process begins on poorly structured informational sets, and has finish on well-structured hierarchical connected coalition. Such well-structured coalition of information attributes relating to administrative barriers is shown in Fig. 2.

7. Administrative barriers:
   7.1. *Administrative obstacles as result of exorbitant bureaucracy:*
   7.1.1. scrupulous control of innovative process even if risk-factors have moderate level

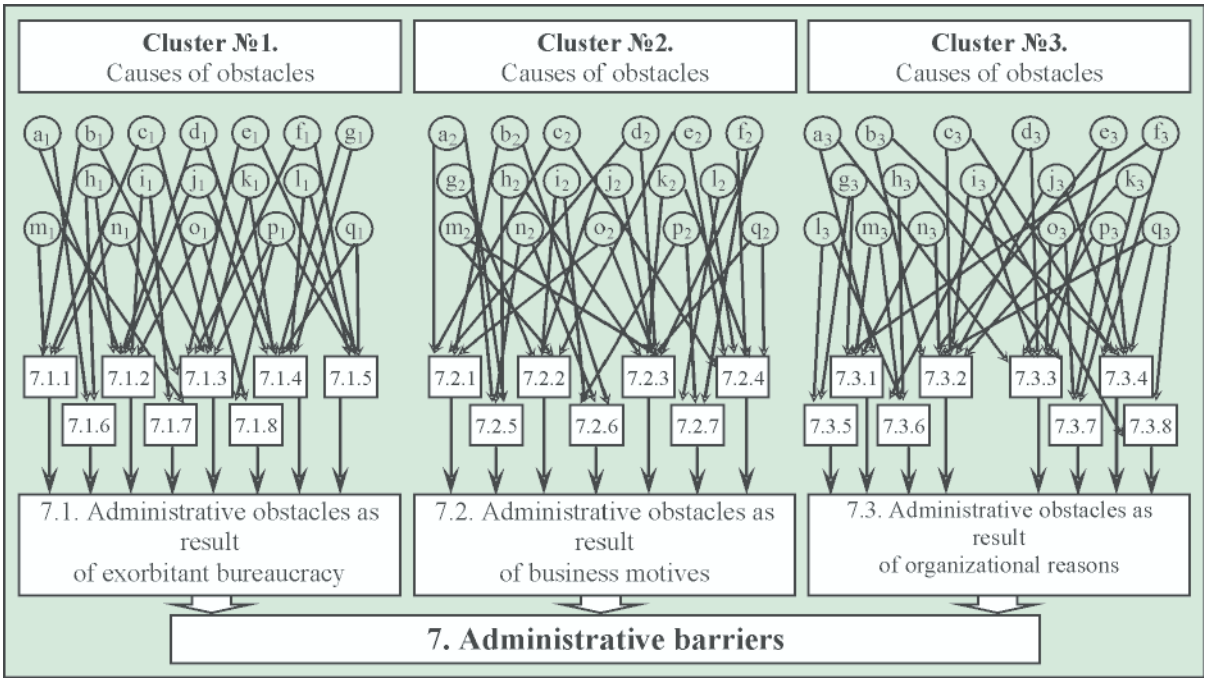

Fig. 2. *Structurization of collected data about administrative barriers to innovative development of the Polish marine industry*

7.1.2. inflexibility of management
7.1.3. inconsistent decision-making system
7.1.4. long-term verification of documentations and intricate process of decision-making
7.1.5. insufficient horizontal interoperations in management scheme
7.1.6. a high risk of stoppage of innovative process
7.1.7. the widespread delaying of decision-making
7.1.8. redundant requirements to novelty document feed.

Causes of these administrative obstacles:
a_1 – formalism and subjective interpretation of transformation results
b_1 – voluntarism and frequently changeable priority systems
c_1 – preference of overall uniformity
d_1 – excessive level of decision-makers' doubt
e_1 – nonacceptance of active debate devoted to the analysis of an innovative policy
f_1 – low psychological adaptation of decision-makers to new conditions
g_1 – excessively level of uncertainty and doubtfulness of decision-makers
h_1 – redundant informational feedbacks
i_1 – extra-formalized schemes of management
j_1 – strict hierarchical subordination
k_1 – stiff stratified structure of authority and extraordinary centralization of decision-making
l_1 – communication gaps
m_1 – overall normalization of regulations
n_1 – nonflexible approach to business planning
o_1 – rejection of full responsibility for business results
p_1 – overcautious decision-makers
q_1 – overcritical approach to new ideas.

7.2. *Administrative obstacles as result of business motives*:
7.2.1. excessive corporate spirit
7.2.2. distorted business priorities, e.g. choice of priority "short-term profits" as main
7.2.3. uncertain outcome of transformation process
7.2.4. minor public-private cooperation
7.2.5. strong business competition
7.2.6. limited business prospects for new market segments
7.2.7. predominantly aspirations for the status quo in business relations.

Causes of these administrative obstacles:
a_2 – lack of a perspicacity and vision of development
b_2 – lack of well-defined goals and implantation strategies
c_2 – insufficient attention on competitors' business strategies
d_2 – doubts about possible profitability of innovative project
e_2 – adverse results of marketing research
f_2 – growing signs of business recession
g_2 – disregard of clientele preferences and owners' wishes
h_2 – poor knowledge of business brainpower
i_2 – shortage of skillful and experienced employees
j_2 – lack of clientele's demands
k_2 – pessimistic trends of business cycle, as result of business slowdown
l_2 – business corruption and fraud
m_2 – overstocked market
n_2 – panicky prices
o_2 – unwillingness to acknowledge own errors and learn from past business defeats
p_2 – lack of business acumen
q_2 – more than strong traditionalism encouraging conservative business techniques.

7.3. *Administrative obstacles as result of organizational reasons*:
7.3.1. overstraining criteria of acceptance for innovative risk
7.3.2. overlong period of decision-makings
7.3.3. preferred of overcautious management strategy
7.3.4. overcomplicate procedures of accepting innovative projects
7.3.5. unawareness of development importance of cooperation about new ideas
7.3.6. stiff structure of implementation procedures for innovative projects
7.3.7. deficient system of recognition programs of new ideas and tangible rewards
7.3.8. underestimate of offered innovative decisions.

Causes of these administrative obstacles:
a_3 – shortage of time for innovative transformations
b_3 – a high risk of undecidability of coordination problems
c_3 – lack of profitability evidence
d_3 – inability of use of crisis management techniques
e_3 – unenviable reputation of inventor-firm
f_3 – lack of will-power to gather and combine resources in the large innovative project
g_3 – incorrect or unconvincing business-plan of innovative project
h_3 – inability to use of modern techniques for analysis of lead development strategies
i_3 – lack of pressure from legislative authorities
j_3 – insufficient marketing endeavor
k_3 – overanxious by an overmastering force
l_3 – over-simplify understanding of innovative problems
m_3 – a low level of implementation control
n_3 – fastidiousness of top-managers at reviews of new ideas
o_3 – unwillingness to acknowledge own errors and learn from past
p_3 – overchoice of innovative offers
q_3 – overclaiming to new idea.

In remote times, the unfriendliness of a natural environment (the so-called natural barriers to changes) was the major insurmountable obstacles to any transformations. In modern conditions such the natural obstacles include:
8. Natural barriers:
- topographical aspects of the ports;
- hydrological features of the south baltic coastline
- meteorological conditions of offshore zone.

Identification of the critical and minor obstacles to development (Step 6, Fig. 1) is performed through comparison of statistical information [7, 9, 11, 12]. Result of data handling for the Polish innovative activity presents Fig. 3.

Financial barriers hold the first place, but administrative barriers and industrial barriers are significant obstacles too. The contradiction between development and obstacles

may be short-term, long-term or permanent. Barriers to activity evolve by multilevel hierarchy:

- barriers hampering the innovative changes in system of mini-level, usually have personal or technological (industrial) nature
- barriers hampering the innovative changes in system of middle-level, e.g., operational obstacles by way of required navigation depth for super-large ship
- barriers hampering the innovative changes in system of meta-level, e.g., legal obstacles to ocean-going navigation of single hull tankers.

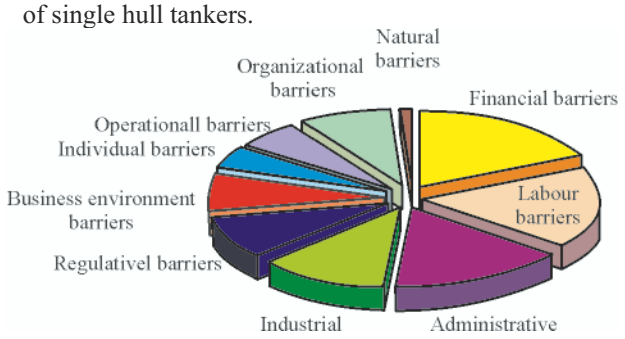

Fig. 3. *Comparing shares of main obstacles to development of the Polish marine industry*

Let's discuss this statement in next section.

FORECASTING OF THE POLISH MARINE INDUSTRY DEVELOPMENT

The marine industry as multilevel branch of Polish economy

Mobility as result of progressive evolution always was remaining key prerequisite for a well-functioning society. Long before the industrial revolution, our civilization have evolved thanks to innovative changes. Such alterations have moved from a propulsive force of wind & sail or animal power & wheel to a propulsive plant basing on coal & steam engine, as well as later to petroleum & diesel engine. Therefore, transformations of shipping systems occur more than 5500 years from scattered, uncoordinated, and rather homogeneous (monomodal) structures, e.g., mail-coaches or sailing fleet into very oriented, networked, coordinated and heterogeneous structures, e.g. multimodal transport systems distinguishing by high development potential. Today innovative changes in transportation systems excite particular interest as 21st century marks a new stage in their development. As a result, the main goals of the EU transport policy for each Member State are mobility improvement of civilian population and various freight, "bottlenecks" elimination, and optimization of each individual mode of transport both in monomodal and multimodal use, as well as rapid implantation of fault-tolerant vehicles, energy-efficient and greener shipping systems [1, 16].

In the Polish conditions these problems should be solved considering insufficient compatibility of the overland and waterborne infrastructure, as well as high degree of an openness of the Polish transport systems. According to the last parameter, the Polish marine industry includes two groups of transport systems:

- The first group consolidates the so-called "closed transport systems". Any system is closed composition if it has stable structure, unchangeable during life-cycle, allowing preventive or repair work only. According to the system approach, the closed systems are the isolated objects, which must be designed as high-reliability constructions. E.g. the Polish pipeline systems for transportation of crude oil and gas have numerous the advantages, namely they are an environment-friendly and user-friendliness, as well as differs by stable transport process and the minor transport risk. Closed transport systems have higher assurance factor and survival value. But they are ill-adapted both to the current transformational tendencies and to new ideas, in view of a presence of most if not all obstacles to modernization, and as a consequence, lack of investors' motivations.
- The second group consolidates the so-called "open transport systems". For example, the Polish fleet is open system, because it has flexible structure that can adapt and change according with market demands. Therefore, the modernization realizability of the Polish fleet depends from financial obstacles, just as a place of its components in the functional hierarchy.

Let's reflect on history and modern innovative transformations within the Polish maritime transport. For this purpose, we shall consider some transformations mapping at the various levels of functional hierarchy, namely at the mini-, the middle-, and at the meta-level.

The mini-level. Let's explains this level on one representative illustration e.g., a ship engine. Its one consists from various components, including the combustor, compressor, the gearbox, or piston assembly etc. as well as based on different principles of their assemblage. As have shown author's investigations, the mini-level of the Polish fleet is characterized by high level of innovative activity, in view of practical lack of any obstacles.

The middle-level. Various ships operating within the Polish shipping companies are characteristic example the middle-level for the Polish marine industry. Improvement of these ships implies modification of numerous ship subsystems, namely architecture of ship hull, arrangement of superstructure, layout of an engine-room or placing of a steering mechanism, and others, including generators, pumps etc. The improvement of any such subsystems leads, as a rule, to corresponding alterations in the other subsystems. All this creates numerous obstacles to a continuity and synchronization of innovative process. Up until now, the maritime transport novelties are developed and implemented with a view to the traditional preferences declared by the majority of shipowners, as well as freighters. Unfortunately, often enough the satisfaction of such wishes can be achieved only by a refusal from radical innovations and, as a result, apply the outdated solutions e.g., use of noncompetitive but inexpensive onboard equipment. The contrary situation takes place, when the EU directives or/and business interest requires an advanced environment protection, survivable onboard equipment and high-reliability hull frames, just as improved operational safety or higher comfort of modern vessels. In this situation, the probability of generating of new barriers is very high. Any innovative transformation have the tendency to drastic complication of the day-to-day operations of maritime transport, and increases the costly damages risk as consequence of decision-makers' errors. All this stimulates search of solutions aimed at reduction of total number of eventual obstacles through usability of new solutions.

The meta-level. The regional network of the Polish harbours is one from examples of meta-level. The Polish ports as maritime nodes developed during last 2000 years. For this period their complexity has increased hundredfold. There are two tendencies in seaports development. On the one hand number increase of special-purpose handling terminals (e.g. LNG terminal planning in Świnoujście), and on the other hand broadening of cargoes spectrum, which are simultaneously

handled on universal terminals. The modern Polish seaports are complex systems, which includes both unmovable installations, namely mooring facilities, fairways, composite breakwaters, warehouses, etc., and mobile equipment including such cargo-handling equipment as the portal cranes and wheel loaders. Therefore, their modernization take time and long-term funds allocated to overcoming various obstacles. One more example of the Polish meta-level systems is the fast-developing multimodal transport which has combined various types of overland and waterborne transport.

Investigation of development trends for the Polish marine industry through scenarios approach

Neglect of barriers identification, as well as, untimely, belated counteractive steps are the critical causes of a failure, which in worst case can lead to bankruptcy of the enterprise. Investigations have been concentrated on modeling the influence of eventual barriers to innovative changes into the Polish marine industry enterprises through three probable scenarios, namely: green, yellow and black (Step 7, Fig. 1.):

The black scenario considers the most complicated situation, when unfavorable concatenation of circumstances leads to generating of unexpected negative system effects at forming of barriers to the innovative development of the Polish marine industry, and as result, timely steps on overcoming barriers are not undertaken.

The yellow scenario considers the situation, when dynamics of forming of barriers to innovative development of the Polish marine industry will be similar to current dynamics, and as result, some timely steps on overcoming barriers are undertaken.

The green scenario considers the situation, when favorable concatenation of circumstances leads to generating of positive system effects at forming of barriers to the innovative development of the Polish marine industry, and as result, significant efforts to overcoming barriers are not required.

At the same time, necessary to take into account that:

- ✦ the current situation about chances and obstacles to stable development of the Polish marine industry were calculated using the numerous information including reviews of the separate Polish enterprises, and annual reports of the Polish government illustrating transformation processes in the Polish economy (see Introduction);
- ✦ the barriers' type, their frequency and amplitude were categorized according to analysis of various statistical data. During investigations take into account that any obstacle preliminarily classified as low probable, can change the status and will be transformed into critical barrier under a circuit of possible events, and at last
- ✦ barriers to steady development of the Polish marine industry should be investigated on the mini-level, the middle-level, and at last the meta-level. For example on the mini-level of the Polish marine industry, innovative project of new-building ship should be study according ability to overcoming barriers to perform such key functions as propulsion, capacity and safety. The specific targets of detailed investigations are determined by levels of informational and logical certainty for three scenarios of possible events.

Researches included four phases:

1. Simulation of negative impacts on the innovative project environment (Fig. 4).

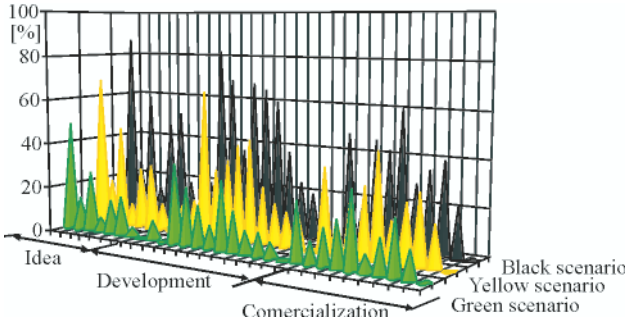

Fig. 4. Simulation of frequency and amplitude of negative impacts on the innovative project environment

2. The forecast of the barriers' impact hampering the successful implementation of an averaged capital-intensive project for the mini-level of the Polish marine industry (Fig. 5).

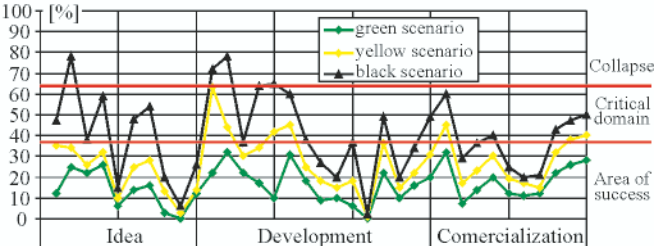

Fig. 5. The forecast of the barriers' impact hampering the successful implementation of an averaged capital-intensive project. Simulation result for the mini-level of the Polish marine industry

3. The forecast of probable barriers to innovative development of the Polish marine industry up to 2040 (Fig. 6).

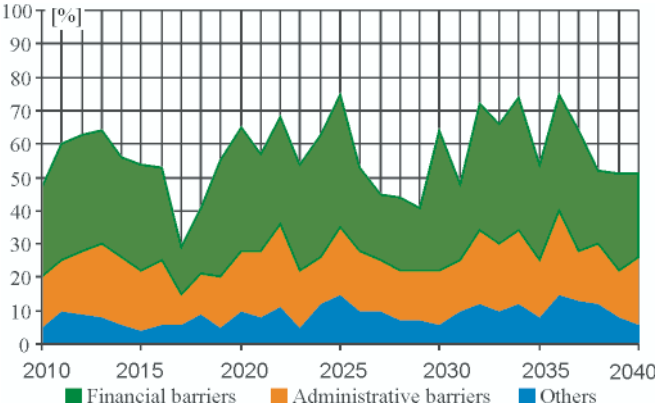

Fig. 6. The forecast of probable obstacles to innovative development of the Polish marine industry up to 2040. Simulation of generating possible barriers to innovative activity

4. Estimation results of multi-step conversion of its companies into future-oriented enterprises of the Polish marine industry up to 2040 (Fig. 7).

RISK ANALYSIS OF INNOVATIVE TRANSFORMATIONS

The modern business world is opened to various social and technological changes through implantation of new investing projects. In many aspects such projects focuses on either increase of volume of freight traffic, or transportation safety, as well as feeling of high comfort for first-class passengers. The each enterprise of the Polish marine industry has different capability for solution of described problems. Success depends from next factors:

- ✧ professionalism level of all groups of decision-makers

- ✧ accuracy of marketing researches and forecast precision of European development trend
- ✧ correctness and opportuneness of organizational changes
- ✧ strong personal motivation to innovative renovations.

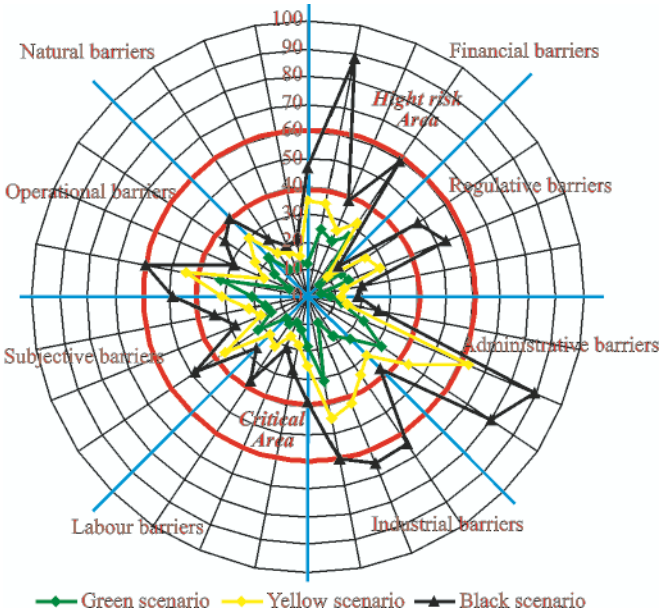

Fig. 7. Estimation of modernization risks for meta-level of the Polish marine industry up to 2040

Several conclusions from the results of risk investigation for an averaged capital-intensive project relating to Fig. 5:

- ◆ According to the black scenario the most risky are the first stage and the second stage of an innovative project's implementation, so they have approximately equal probability of a premature stoppage of the project (the first and second peaks of a collapse domain) as a consequence of impact from regulative, financial and administrative obstacles.
- ◆ The most of the raised risk peaks situated in critical domain is typical for the first stage and the last stage of the project implementation. It can be connected with impacts of financial and operational barriers.
- ◆ According to the most realistic scenario (yellow) the first stage of the innovative project is favorable. That is connected with a high intellectual potential of innovators and the scientists working for the marine industry. The most risky is the second stage according to the yellow scenario. It can be explained by synergetic effects from cumulative impacts of industrial, subjective, financial obstacles.

For the purpose of impact minimization from various obstacles to the sustainable development of the Polish marine industry it is necessary to concentrate attention to overcoming subjective barriers through various trainings of the personnel of the enterprise and to search of new stimulus. Training should focus on the opportunities to improve quality and profitableness of the Polish transport system through the study of best examples of the advantage of the European shipping companies. Under these circumstances should be taking into account, on the one hand the current world trends of shipbuilding development and the specificity of the coastal Regions, and on the other hand the eventual barriers to successful implementation of new solutions and methods of their overcoming.

The main inference from performed researches: It concludes that integration of the above mentioned barriers and fatal decision-making logic can cause loss of competitiveness of the Polish marine industry within the next 15-20 years.

The very important are the following actions to overcoming operational barriers to modernization the middle-level the Polish marine industry:

- ➡ to investigate evolution both shipbuilding products and advanced service technologies relative to critical factors of success, with purpose of early verification of a selected innovations with the additional control of compatibility between this ones and standard shipbuilding products implanted into large-scale commercialization earlier;
- ➡ to determine of all interested actors and their involving in the innovative process with the purpose of compatibility improvement within the limits of circuits "idea-product" through effective transfer of RDI-results (advanced technologies, new techniques of management etc.) into shipbuilding, and shipping services;
- ➡ to put into practice a pilot projects within the marine cluster for deep verification as actual necessity of these projects in the authentic conditions of the Polish market, as well as practical serviceableness and profitability of the new techniques and technologies,
- ➡ to liven up business contacts with stable and eventual clientele (shipowners, freighters etc.) for information about new potentialities of the future-oriented enterprise, and at last
- ➡ to carry out monitoring changes of rivalry on targeted sector of the market with the purpose of permanent analysis of the current vulnerabilities of the enterprise and weaknesses of the developed innovative project, to predict a basic kinds positive synergies effects, just as negative revenge effects. The assembled diagram of attenuations and intensifications of barriers to quick development of the Polish marine industry shown on Fig. 6.

As laid down by [11, 12, 16] success of the Polish marine industry depends on the long-term policy of regional development, and ability of decision-makers to use such Polish values, just as introduction into the EU, creative potential of the Polish scientists and skills of domestic workers. Therefore, innovative changes on meta-level must meets five objective, including market demands; significant competitiveness; proven technological supremacy and reliability; environment-friendly, and at last compatibility with technological surrounding.

In the resume, let's enumerate the basic opportunities and threats of innovative transformations (Fig. 7). One of the most unexpected results is the litany of development factors of the Polish marine industry on meta-level which haven't any improving effects, or cover minor influences on investors' solutions. These factors include:

- ⇨ specifics of exploiting the polish fleet (operational barriers)
- ⇨ the climate in location points of the polish seaports (natural barriers)
- ⇨ experience and education level of the polish seafarers (labour barriers)
- ⇨ number of marine agencies contributory with the polish seaports (subjective barriers).

The second inference from attained results. It concludes that introduction of the advanced innovations in the Polish seaports, feeder transport or assisting fleet can leads to extraordinary increase in competitiveness of the Polish maritime transport as the whole, even when other components of this transport have not been modernized simultaneously. This conclusion proves by high mastery and wide knowledge of the Polish managers.

The third result from achieved investigations. It concludes that takes place six factors which directly impact on risk

magnitude for multistage conversion of the Polish maritime transport, namely:

- current market situation
- availability of investing funds
- positive trends of economical index for best innovative practice
- readiness of a shipowners, freighters etc., to innovative changes
- eligibility and compatibility of a new solutions relates to loading/unloading operations
- operational efficiency of feeder modes associated to maritime transport.

According to these appraisals for the Polish fleet have possibilities first of all, to entry on new sectors of market e.g., LNG transportation or marine tourism, as rapid extension of the commercial market on the ferries sector of the short-sea shipping within the Baltic Sea [1].

The most productive are the following ways of stimulation of an innovative activity on all levels of the Polish marine industry:

- increasing of legal support for relationships between the inventors and authorities, in purpose of strengthening co-operations within the "knowledge and innovativeness triangles"
- expanding of informational and financial support of the innovative clusters as a basis for flexible public-private cooperation within framework of the Polish marine transport
- painstaking identification and a strict control of political, marketable and social risk-factors, for overcoming the usual and atypical obstacles to innovative activity; Fig. 8 and Fig. 9 present a forecast of changes of barriers and frequency of their development
- indicating the new ways for large-scale commercialization of innovative ideas.

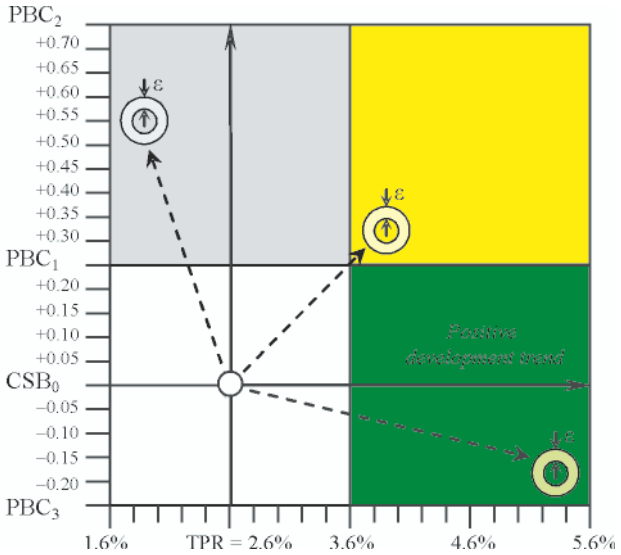

*Fig. 8. Simulation results of probable changes of barriers impacts up to 2015. **ε** – possible calculation error; **PBC** – Possible Barriers Change; **CSB** – Current State of Barriers to development of the Polish marine industry; **PBC**$_1$ – the lower border of possible increase of barriers for black and yellow scenarios; **PBC**$_2$ – the highest border of possible increase of barriers for black and yellow scenarios; **PBC**$_3$ – the lower border of possible reduction of barriers for green scenario; **TPR** – Turnover Profitability Rate*

Therefore, the Polish top-managers always should be amicable to new ideas, and able to take risk; the Polish middle-

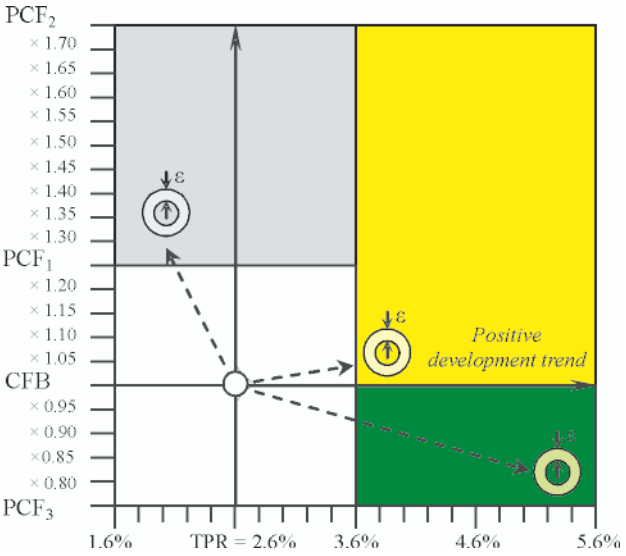

*Fig. 9. Simulation results of probable frequency of barriers development up to 2015. **ε** – possible calculation error; **PCF** – Possible Change of barriers development Frequency; **CFB** – Current Frequency of Barriers development; **PCF**$_1$ – the lower border of possible increase of barriers for black and yellow scenarios; **PCF**$_2$ – the highest border of possible increase of barriers for black and yellow scenarios; **PCF**$_3$ – the lower border of possible reduction of barriers for green scenario; **TPR** – Turnover Profitability Rate*

managers sometimes should have chance to fail; the Polish first-line managers should be focused on achievement of hopeful results during all realization of an innovative project, and at last all managers should be able to draw correct conclusions as from successes, as and defeats.

In the finale, some recommendations for successful transformation of the Polish marine industry, considering on the one hand the strengths and the opportunities basing on high creative potential of the Polish managers, and on the other hand the weakness and the threats connected to various obstacles to development of this sector of the Polish economy, taking into account [6, 11, 12, 17]:

1. The Polish decision-makers should more focus their effort and attention on the maritime transport development as main mode of European multimodal transport system. Success depend on improvement program of various types of overland and waterborne transport, and serving the Poland's gateways, inland waterways and seaports i.e. correct choice of development strategy either "*Expansion of the market through increase in competitiveness of the current offer*", or the radical ones – **"***Capture a market through innovative spurt***"**.
2. The Polish marine industry can be more competitive through orientation to the co-evolution principle, when all components of this industry are simple in designing, proved by practice and compatible each-to-each at all hierarchical levels.
3. In conditions of demand-based business relationships, the Polish maritime transport through high quality and efficiency become the key part of the Polish marine industry.
4. In order to be usable, the Polish transport system integrating overland and waterborne modes must reach a *critical mass* of innovative solutions, be based on the principle of maximization of risk- free that can be received through flexibility, reliability and economical efficiency. This critical mass must answer to two requirements:
   - *sufficiency,* i.e. improved maritime transport should be widely available for competitive use by forwarding agents, as well as regular and irregular passengers

- *not overstrain,* i.e. improved maritime transport should guarantee such possible profit which is high proportionally in comparison with transportation risks.

5. For any shipping company, any part of the Polish transport infrastructure should be usable, and all parts of that transport infrastructure should be usable. Its requirement is very important especially at make-ready to EURO 2012 for full and integrated service of fans, as well as foreign tourists and domestic travelers.
6. In the renovation of the Polish maritime transport, every change is an opportunity for performance improvement. Such improvement must be supported:
   - by adequate marketing and error-free managing solutions
   - by conflict-free organizational changes within the Polish marine industry
   - by obstacles-free frameworks which first of all, should be focused on preservation of clientele's trust, and secondly not to depend from longstanding familiarity of governing body anyone shipping company or anyone shipyard with authorities.

FINAL CONCLUSIONS

- The common goals of the EU transport policy for each Member State are mobility improvement of inhabitants and various freight, "bottlenecks" elimination, and optimization of each individual mode of transport both in monomodal and multimodal use, as well as rapid implantation of fault-tolerant vehicles, energy-efficient and greener maritime transport.

- Transformation of the Polish marine industry should be performed in some steps, beginning from identification of eventual barriers to innovative changes, and simulation their pernicious influence on reorganization of this industry as whole.

- Up to 2040 year the Polish marine industry can meet with three waves of strong mechanisms creating various barriers to innovative activity. The first wave will occupy the period 2012-2014, next amplification of barriers to development will take place between 2022 and 2025, and third wave package will occupy period 2034-2037. Traditionally, this phenomenon explains either by obsoleteness the Polish industrial environment, or by financial or legislative reasons. As follow from performed investigations, each enumerated wave will be creating under strong synergetic mechanisms.

- Any innovative transformation have the tendency to drastic complication of the day-to-day operations of maritime transport, and increases the costly damages risk as consequence of decision-makers' errors. All this stimulates search of solutions aimed at reduction of total number of obstacles through rise both reliability and usability of new solutions. At the green scenario of innovative activity, the size of barriers can be on the average reduced by 15-18%.

- Innovative solutions should be analyzed in three-level space, on the mini-, the middle-, and at last the meta-levels. For example, innovative projects for merchant ships can be analyzed according to key functions including propulsion, equipment and safety system. The degree of detail needed in simulation was determined by level of informational certainty.

- On the mini-level of the Polish marine industry main attention should be focused to training of enterprise personnel. Training be supposed to concentrate on the opportunities to improve quality and profitableness of the Polish transport system through the analysis of best examples of the first-rate European shipping companies, taking into account the current world trends of shipbuilding development, the specificity of the coastal Regions, and the eventual barriers to successful implantation of new solutions, as and methods of their overcoming.

- The middle-level of the Polish marine industry is the most promising to fast development. The very important are the few following actions to overcoming operational barriers to modernization, namely detailed screening of selected innovations and service technologies in relation to critical marketable factors, their verification and the additional control of compatibility between these ones and market demands, and at last, preparatory measures activities for earlier large-scale commercialization of new product.

- For acceleration of overcoming usual and atypical obstacles to the realization of innovative projects at all levels of the Polish marine industry is necessary to increase legal support co-operations within the "knowledge triangle"; to reinforce partnership the inventors and regional authorities, as well as to expand informational and financial support of the innovative clusters through elasticity of public-private cooperation; carefully to identify and strictly to supervise of political, social and marketable risk-factors, and at last to search the new pathways of successful innovations implantation and their large-scale commercialization. In this case, at the green scenario of innovative activity, the barriers frequency to the Polish marine industry development can be on the average reduced by 22-25%.

- The error-free choice of development strategy of the Polish marine industry and end-to-end advancement of the innovative transformations are able to give fruitful results consisting in 10-14 % decrease of revenge effects, and in 8-10% increase of such effects as competitiveness, profitability and safety of improved transport system.

Acknowledgment

This paper was supported by the Polish State Committee for Scientific Research. 2008.

BIBLIOGRAPHY

1. Arndt M., Pauli A. Trans-European Transport Networks (TEN-T) in the Baltic Sea Region, Policy Recommendations, Erkner, 22 December 2005
2. Bass, H.-H., Ernst-Siebert, R. SME in Germany's maritime industry: innovation, internalization and employment; *International Journal of Globalization and small Busin*ess, Vol. 2, Number 1, 24 June 2007 pp.15-33
3. Birla M. FedEx: How the World's leading Shipping Company keeps innovating and Outperforming the Competition, Wiley, John & Sons, 2005
4. Boutellier, R., Gassmann, O., and von Zedtwitz, M.: *Managing Global Innovation: Uncovering the Secrets of Future Competitiveness*, 2end ed., Springer, Berlin, 2000
5. Evangelista R., Sirilli G. *Innovation in the service sector. Results from the Italian Statistical Survey*, Technological Forecasting and Social Change, 58, 1998
6. European Commission. LeaderSHIP 2015: Defining the Future European Shipbuilding and Shiprepair industry-Competitiveness through Excellence. COM (2007) 220 final, 25.4. 2007

7. Eurostat. *Panorama of transport.* Eurostat and European Commission, 2007
8. Kajenska I., Adamowicz E., Kurzydlowski K. *Barriers in Innovation and Technology Transfer in Poland*. 5th triple Helix paper, Turin, Italy, 18-21 May 2005
9. Niedbalska G. Innovation Activities in Polish Industry in 1998-2000: Main Results from the GUS 2001, Innovation Survey, Working Paper № 25, SSEEC, UCL, London, 22 p
10. Pearce R.: *Globalization of R&D: key features and the role of TNCs,* Proceedings of the Expert Meeting *Globalization of R&D and Developing Countries*, United Nations Conference on Trade and Development, Geneva, pp.29-42, 2005
11. Polish Ministry of Economy. *Strategy for Increasing the Innovativeness of the Economy for the years 2007-2013*. Warsaw, 4 September 2006
12. Polish Ministry of Economy: Analyses and Forecasting Department. *Report Economy: Poland 2007*, Warsaw 2007
13. Roe M.S. *The commercialization of East European liner shipping: the experience of Poland Maritime Policy & Management*, vol. 26, Issue 1, January 1999, p 69-79
14. Statistical Yearbook of Maritime Economy, Central statistical Office, Statistical office in Szczecin, Warszawa-Szczecin, 2007
15. Walendowski J. *Strategic Evaluation on Innovation and the Knowledge–based Economy in relation to the Structural and Cohesion Funds for the programming period 2007-2013*. Report to the European Commission, Directorate-General Regional Policy Evaluation and Additionally. County Report: Poland, Brussels, 7 July, 2006
16. Wojnicka E., Rot P., Tamowicz P. *Regional Innovation System in Pomeranian Province of Poland*. 6th International Conference on Technology Policy and Innovation. Kansai Science City, 12-15 August, 2002
17. World Bank. *Poland and the Knowledge Economy: Enhancing Poland's Competitiveness in the European Union*. ISBN 83-89188-21-X. Washington D.C., 2004.

CONTACT WITH THE AUTHOR

Prof. Iouri N. Semenov
Faculty of Marine Technology
Szczecin University of Technology
AL. Piastów 41,
71-065 Szczecin, POLAND
e-mail: jusiem@ps.pl

Photo: Cezary Spigarski

POLISH MARITIME RESEARCH 4(58) 2008 Vol 15; pp. 96-102
10.2478/v10012-008-0002-z

An analysis of influence of lack of the electricity supply to reefer containers serviced at sea ports on storing conditions of cargoes contained in them

Lyudmyla Filina, Ph. D.
Sergiy Filin, Prof.
Szczecin University of Technology

ABSTRACT

Servicing the reefer containers at sea ports requires more reliability and precision than servicing the conventional ones because of specificity of perishable cargoes shipped in them. This paper is aimed at making analysis of way of servicing the reefer containers stored at sea port and at investigating its influence on storing conditions of refrigerated cargoes contained in them. Lack of the electricity supply to refrigerating unit of reefer container is one of the most common extraordinary situations in port area, which may lead to loss of quality of cargo contained in the container. On the basis of scenarios of possible progress of such situations, elaborated by means of calculations, rate of change of temperature of cargo in reefer containers cut-off from electricity supply source was determined and relevant recommendations as to organization of sevicing such containers at sea port, were elaborated.

Keywords: sea port, reefer container, refrigerated cargo, risk factors

INTRODUCTION

The observed rise of living standards of people results in growing consumption of perishable food products, e.g. tropical fruits [13]. Most of such goods is transported in reefer containers to Europe from different countries of Asia, Africa, South America, etc.

Containerization which has been spread over worldwide cargo shipping, has contributed to increased share of sea shipping in cargo turnover in sea ports, including that of containerized cargo, a.o. in Polish ports. Reefer containers constitute about 7 - 15 % of total number of containers handled by Polish sea ports [7].

Among commonly known merits of shipping the goods in containers, as compared with bulk and general cargo shipping, the following can be numbered: shorter period of transport, cost reduction and increased level of safety [2, 3]. For shipping the perishable cargoes to ensure an appropriate level of cargo safety is of crucial importance.

Cold chain of perishable cargoes shipped in containers consists of various links of moving and servicing the containers, located along the route ranging from place of collection or production of goods to consumer site. Sea ports play an important role in the chain; they should be adjusted to servicing the growing number of reefer containers, that will result in rising level of complexity of cargo servicing technology in ports. Although cost of cargo shipping in reefer containers is higher as compared with that in reefer ship holds [10], experts predict that the trend of increasing amount of shipping of the kind will be maintained at least up to the the year 2020 [9].

Such goods as meat, fishes, butter are as a rule transported in the frozen state at the temperature from -18 ºC to -30 ºC, whereas vegetables and fruits in the state of chilling at the temperature from 0 ºC to +15 ºC. In the subject-matter literature cargoes which require constant storing temperature are called *refrigerated cargoes* [9, 13]. Unkeeping the conditions of shipping and storing such cargoes leads to loss of their quality features.

Reefer containers are intended for shipping the cargoes which require determined conditions of shipping, such as the maintaining of cargo storing temperature, humidity and rate of air exchange, etc, constant [1]. As cargoes in reefer containers are very valuable and have a limited period of validity the servicing of such containers should be done fast and reliably. As compared with the servicing of conventional cargoes the servicing of containerized refrigerated cargoes requires additional operations, a.o.: permanent connection of reefer container to an electicity supply source, regular control of its technical state etc.

In Poland the existing container terminals and those presently built as well, are modernized [3,7]. However infrastructure of sea ports undergoes changes slower than structure of cargoes handled in the ports, that results in generating new problems. If the phenomenon is additionally accompanied by lack of experience or insufficient qualifications of port personnel (port management, operators, distributors etc, i.e. strong impact of human factor) or disregarding valid regulations, then risk level of loss of quality of the cargoes dramatically increases. If it exceeds an acceptable level the refrigerated cargo can lose its business value. If quality features of refrigerated cargo are

lost through port's fault, the port should pay compensation to the cargo's owner. Occurrence of such situations results in a damage to reputation of the port, that is associated with possible resignation from services of the port by its clients. This paper is aimed at making analysis of the way the reefer containers are serviced in port and at investigating its influence on conditions of storing the cargoes contained in them.

RISK FACTORS WHICH OCCUR DURING SERVICING THE REEFER CONTAINERS IN SEA PORTS

Depending on size of a port and its organization of cargo servicing, reefer container stays in port for a few hours or several days at most. During this time it is moved from one to another element of port's infrastructure, such as ship, quay, temporary storing place, veterinary border checkpoint (GPKW) and/or custom checkpoint, in/out - gateway to port area. Moreover, on store place the containers are stored in two (rarely in three) layers where they are rearranged in the case of necessity to manipulate containers placed in lower layers. Every operation of handling and rearranging a container is associated with cuttin-off it from the electicity supply source. Number and duration time of the operations depends on a given servicing chain of the containers.

The schematic diagram shown in Fig. 1 constitutes a basis for building rational servicing chains of container during its dislocation over port area with taking into account a current state of infra- and supra-structure of the port. This is an example scheme which is typical for many European ports, that does not prevent it from its possible extension or simplification. In fact, before starting the servicing process of reefer containers it is difficult to precisely determine chain of its servicing as occurrence of risk factors may result in changing sequence and way of realization of its particular links.

Occurrence of risk factors concerning loss of quality features of containerized refrigerated cargoes in port area can be caused by:

- ★ incorrect functioning the reefer container due to a.o. unserviceability of elements of its refrigerating unit or failures of its box structure
- ★ incorrect servicing the container and its cargo in port, resulting from negative impact of human factor etc.

The risk factors can be classified in a few ways [5, 8]. These authors propose to distinguish the following (Tab. 1):

- ➢ human factors (CL) – subjective risk factors
- ➢ technical and technological factors (CTT) – objective-subjective risk factors which are most difficult to be analyzed
- ➢ natural and climatic factors (CPK) – objective risk factors.

Range of development scenarios of extraordinary situations during servicing the reefer container is relatively broad as in sea ports various combinations of risk factors can happen [4, 7]. For instance, such situations may be associated with exceedance of permissible period of disconnection of the container from the electicity supply source, failure of its refrigerating unit or mechanical failures of its box structure, incorrect cargo storing conditions etc. And, such situations may also arise a.o. from a high level of uncertainty of information obtained by port personnel from its management. Among various hazardous situations one of the most often met is lack of the electicity supply to the container being on port store place.

LACK OF THE ELECTICITY SUPPLY TO THE CONTAINER STORED ON PORT STORE PLACE

During its transport the reefer container is to be connected with an electicity supply source. In road transport the reefer containers are sometimes supplied from the truck's electric network or (often) by means of portable electric generators of GENSET type, however such generators are not moved together with the containers along its entire shipping route. During sea voyage the containers are supplied from ship's electric power network, and at container terminal – from electric power network of a given port. Certain sea ports are equipped with own GENSET generators, then the container can be connected with the GENSET unit in the case of lack of free electicity supply terminals on store place [5].

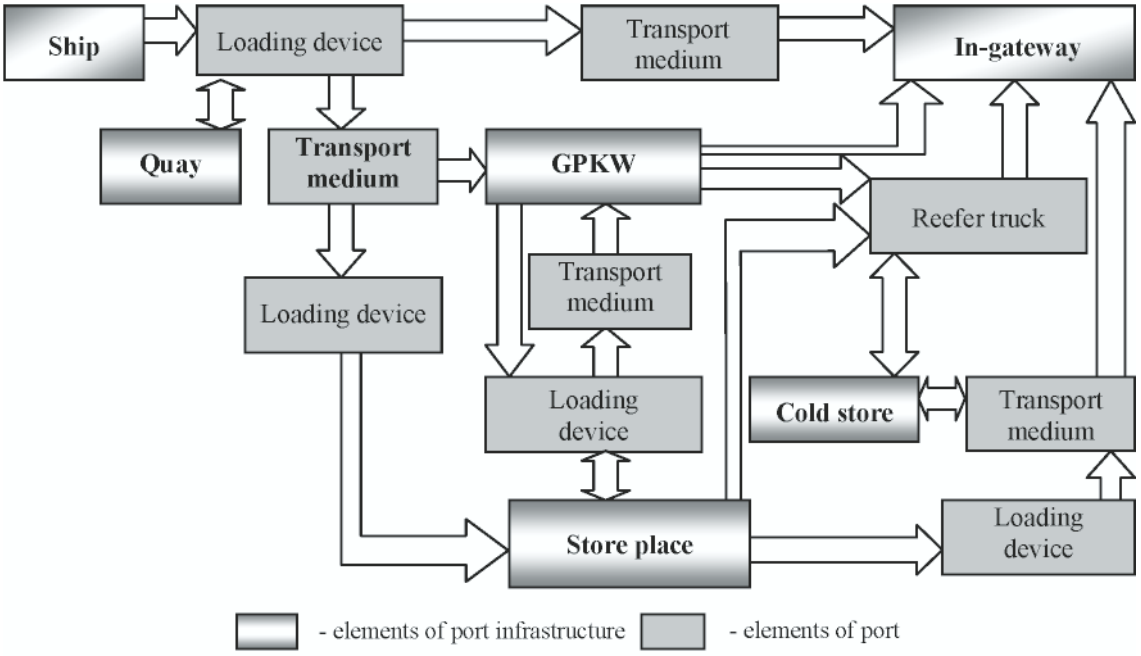

Fig.1. Dislocations of reefer containers over port area in the frame of various schemes of their servicing

Tab. 1. *Examples of occurrence of extraordinary situations acc. to the groups of risk factors*

Group of factors	Selected examples of occurrence of extraordinary situations	Illustrations
Human factors (CL)	➢ Incompetent servicing the container, that leads to a failure of its cooling unit or its cutting-off from the electicity supply source. ➢ Incompetent servicing the container, that leads to a longer period of technological cutting-off the container from the electicity supply source. ➢ Faults in setting the cargo storing temperature ➢ Non-tight closing the container's doors ➢ Long period of opening the container's doors ➢ Burglary of content of the container etc.	
Technical and technological factors (CTT)	➢ Failure of the container's box resulting from material ageing process ➢ Failure of the container's refrigerating unit ➢ Failure of the electicity supply socket to the container ➢ Failure of cargo loading device ➢ Failure of platform truck etc.	
Natural and climatic factors (CPK)	➢ Shorting in the terminal's electicity supply network, resulting from peneration of water ➢ Overrun period of container servicing in port because of unfavourable atmospheric conditions ➢ Change in spatial position of the container leading to shift of cargo contained in it etc.	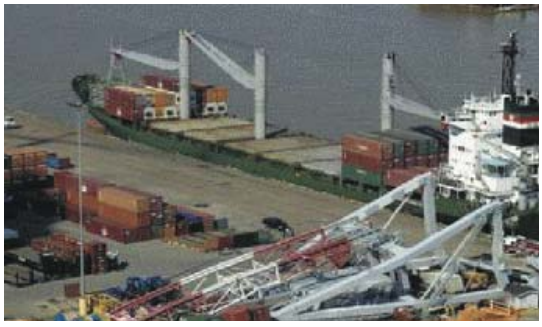

As showed by a functioning analysis of container terminals at Polish and Ukrainian sea ports, container's disconnection from the electicity supply source can last from 2 h to 4 h even in the case of standard unloading operation of the container from ship to quay. Sometimes it happens that containers prepared to be unloaded out of the ship are disconnected from supply source a few hours before the ship's arrival to the port. Disconnection of container from supply source before loading is a necessary technological operation (Fig. 2) and it is not taken as extraordinary one if only an allowable period of lack of the electicity supply is not exceeded. However similar situation may result form breaking the shipping regulations and official duties. For instance, operator resigns from connecting the container with port's electric power network in order to make some financial savings, knowing that within several hours the container will be removed from store place and reloaded onto a receiver's transport medium. The receiver's truck may be delayed due to a traffic jam on the roads leading to port and in consequence the period of lack of the electicity supply to the container may increase to 6÷8 h. The classification of causes of container's cutting-off from the electicity supply source is given in Tab. 2. Technological disconnections of containers are short-lasting and expectable, however random disconnections may last long time and thus be hazardous.

Fig. 2. *Reefer containers cut-off from the electicity supply source on store place*

Tab. 2. Classification of causes of cutting-off loaded reefer container from the electicity supply source during its servicing at port

Types of container disconnections	Causes of container disconnection (cutting-off)
Technological	1. Loading / unloading operation of container to/from the ship 2. Dislocation of container over port area 3. Change of container's position on store place 4. Custom control (veterinary one)* 5. Reloading the container's content 6. Loading operation of container onto a truck or railway platform
Random and forced	1. Lack of electricity in port electric power network 2. Lack of electric sockets to connect containers on store place 3. Failure of electric power network on store place (bay or cable) 4. Repair of container's refrigerating unit
Random but not forced	1. Negligence of official duties by port personnel (they have forgotten or not wanted to connect) 2. Random cut-off the electicity supply cable due to vibration or catching the cable by a vehicle or person.

* In certain ports the GPKW is fitted with electric sockets for connecting reefer containers. It is assumed that the above given, bold marked, situations are associated with lack of possible use of a GENSET electric generating set.

Let us consider a few examples of scenarios of developing the extraordinary situations connected with lack of the electicity supply to the reefer container on port store place.

Example 1. *Failure of electric cable supplying the container*

During servicing process of containers in a port a container hoisting vehicle caught electric cable supplying the reefer container stored on store place. It resulted in mechanical failure of the cable and cutting-off the container from the electicity supply source (Fig. 3).

Example 2. *Lack of free bays on store place*

In a sea port turnover of reefer containers has increased. The port's infrastructure is not adjusted to cope with the increasing number of containers. After unloading the containers from the ship it appeared that all bays fitted with electric sockets to connect the containers on store place were occupied since a receiver did not take away on schedule the preceding batch of containers. Several containers were not connected with the electicity supply source for 10 h.

As observed from the above presented examples, most extraordinary situations result from human factors.

COMPUTATIONAL ANALYSIS OF RATE OF TEMPERATURE CHANGES INSIDE THE DISCONNECTED REEFER CONTAINER

In order to assess quantitatively rate of temperature changes of cargo contained in the disconnected reefer container the software „Kontener chłodniczy" (Reefer container) written in QBASIC language, was elaborated. A mathematical model realized by the software is based on the heat balance method. As showed in [5], in the container disconnected from the electricity source only three heat fluxes are present[1)]: Q_1 – heat flux flowing through container's insulation, Q_5 – heat flux resulting from cargo breathing (it concerns fruits and vegetables only) oraz Q_4 – heat flux for heating or cooling the cargo and its package. If to simplify and disregard the „cold" accumulated in evaporator

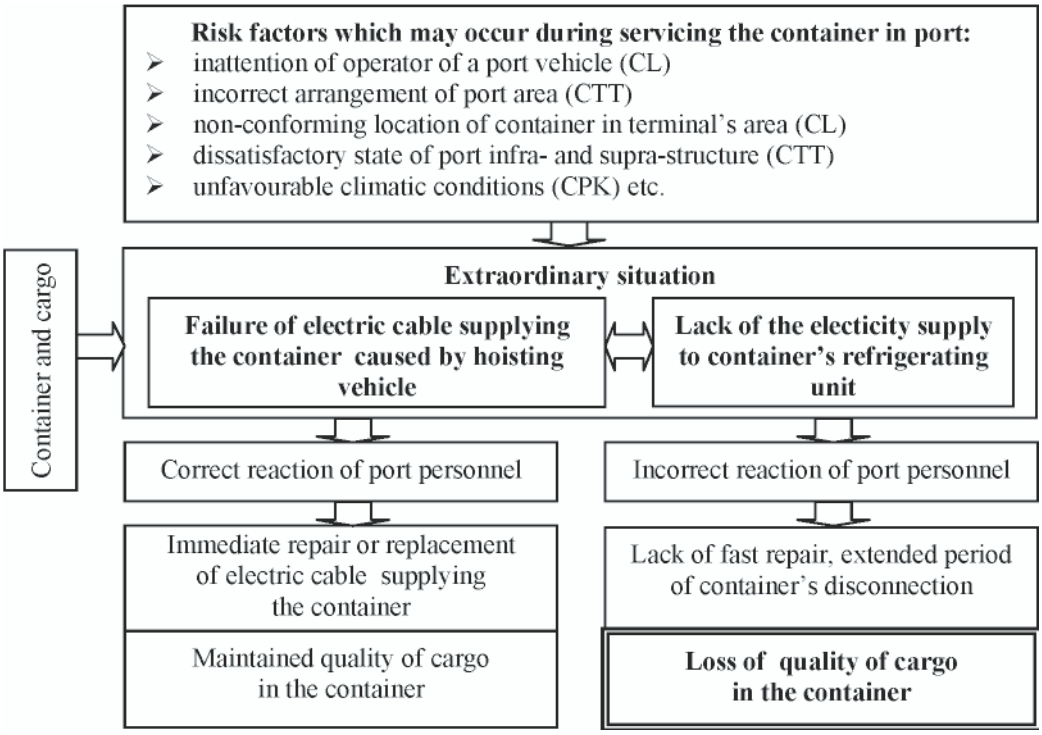

Fig. 3. Model of development scenario of an extraordinary situation during storing the container in port area (concerning failure of electric cable supplying the container)

[1)] In container under work up to ten heat balance components may appear.

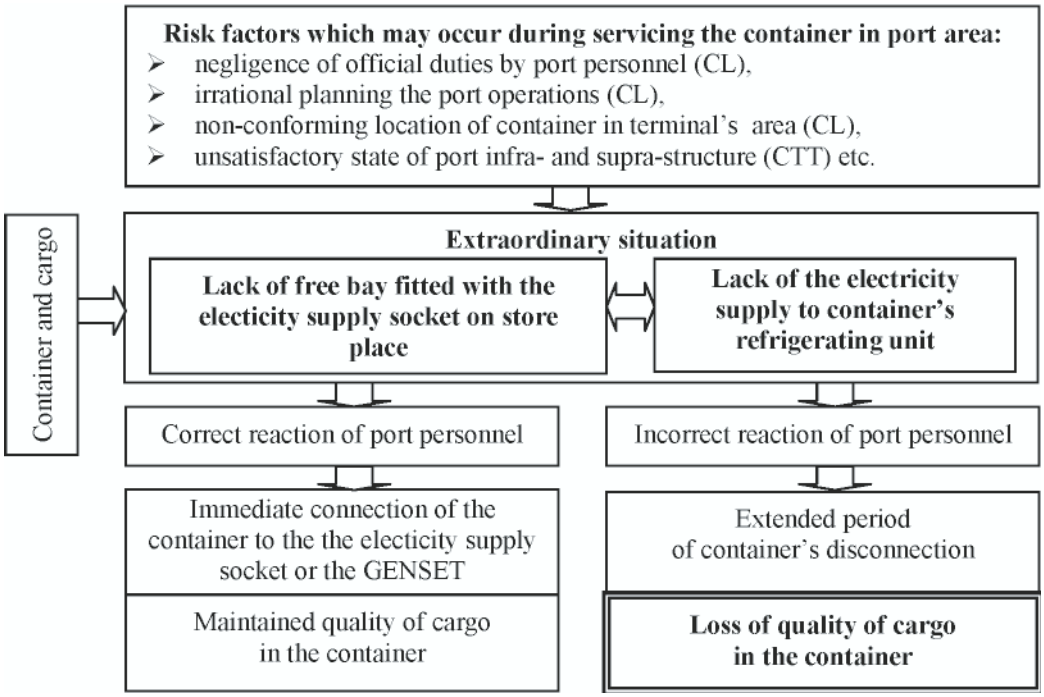

Fig. 4. *Model of development scenario of an extraordinary situation during storing the container in port area (the situation dealing with lack of free bays fitted with the electicity supply socket on store place)*

of refrigerating unit, the container's heat balance during the period of its disconnection will be as follows:

$$Q_1 + Q_5 = Q_4 \tag{1}$$

where:

$$Q_1 = KF[t_{ot} - t_w(\tau)] \tag{2}$$

$$Q_5 = m_{lad} q_{od} e^{k[t_w(\tau)-273]} \tag{3}$$

$$Q_4 = \frac{(m_{lad}c_{lad} + m_{op}c_{op})[(t_w(\tau) - t_p]}{\tau} \tag{4}$$

K – overall heat-transfer coefficient of a container
F – heat exchange area
t_{ot} – ambient temperature
t_w – temperature inside a container, which is assumed equal to mean temperature of cargo
t_p – set temperature of cargo storing (transporting), which is equal to mean temperature of cargo in the instant of cutting off the container from the electricity supply source
m_{lad} ; m_{op} – mass of cargo and its package, respectively
c_{lad} ; c_{op} – specific heat capacity of cargo and its package, respectively
q_{od} – specific heat of breathing
k – coefficient in the relation between breathing heat and temperature
τ – running time counted from the instant of cutting off the container from the electricity supply source.

By solving Eq. (1) with respect to t_w, the relations of changes of temperature inside the cut-off container in function of time, were obtained.

The elaborated software makes it posssible to introduce various kinds of cargoes and packages, various types of containers, as well as to take into account different conditions of heat exchange through particular walls of container, resulting from e.g. their insolation.

Some results obtained by means of the computational relations are graphically presented in Fig. 5÷7. The diagrams of Fig. 5 show that after cutting-off the 20' container from electricity supply source the period of reaching the critical temperature by the cooled cargo (bananas) changes from 21 h in the case of favourable conditions (moderate ambient temperature of +25 ºC, no insolation, state of container's insulation complies with the relevant standards (K= 0.4 W/m²·K) as well as the container is full of cargo) down to 6 h in the case of unfavourable conditions {high ambient temperature, insolation, bad state of container's insulation (K= 0.7 W/m²·K)[2)] as well as the container is half- filled with cargo with respect to its maximum load capacity[3)]}.

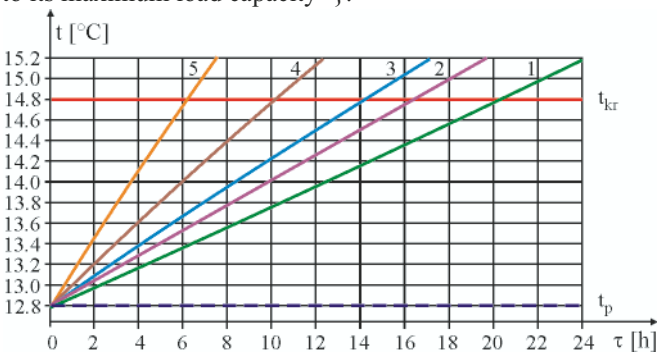

1 – t_{ot} = +25ºC ; K = 0.4 W/m² K ; m = 10 t ; no insolation
2 – t_{ot} = +35ºC ; K = 0.4 W/m² K ; m = 10 t ; no insolation
3 – t_{ot} = +35ºC ; K = 0.4 W/m² K ; m = 10 t ; insolation
4 – t_{ot} = +35ºC ; K = 0.7 W/m² K ; m = 10 t ; insolation
5 – t_{ot} = +35ºC ; K = 0.7 W/m² K ; m = 5 t ; insolation

Fig. 5. *Rate of rise of temperature of the cargo (bananas) contained in the reefer container cut-off from electricity supply source during its storage on sea port store place.* ***t*** *– mean temperature of cargo (bananas) in the reefer container [ºC],* ***τ*** *- period of cutting-off the container from electricity supply source [h],* t_{ot} *– ambient temperature of the container [ºC],* ***K*** *– overall heat-transfer coefficient of the container [W/m²·K],* ***m*** *– mass of cargo inside the container [t],* t_{kr} *– critical temperature at which ripening process of bananas starts [ºC], acc. [14],* t_p *– recommended temperature for transport of bananas [ºC]*

[2)] e.g. as a result of its getting damp.

[3)] it is typical for cargoes which require intensive ventilation.

For short periods of lack of the electricity supply the temperature rise function is almost linear, however in a longer time scale it can be observed that the temperature rise curve is an exponential function in compliance with [6, 11, 15] and as clearly seen in Fig. 6.

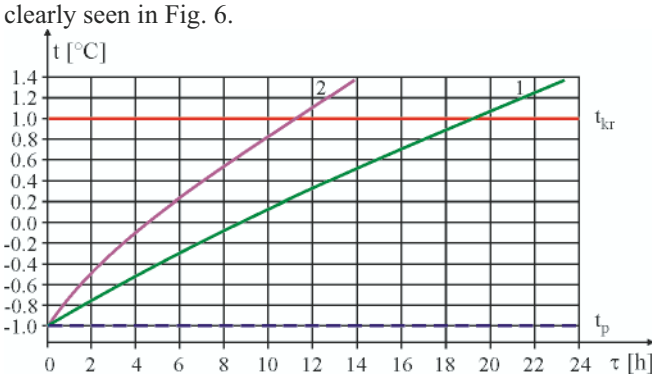

1 – t_{ot} = +30 ºC ; K = 0.4 W/m² K ; m = 14.9 t ; insolation
2 – t_{ot} = +30 ºC ; K = 0.4 W/m² K ; m = 7.45 t ; insolation

Fig. 6. *Rate of rise of temperature of the cargo (pears) contained in the reefer container cutt-off from electricity supply source during its storage on sea port store place.* ***t*** *– mean temperature of cargo (pears) in the reefer container [ºC],* ***τ*** *- period of cutting-off the container from electricity supply source [h],* t_{ot} *–ambient temperature of the container [ºC],* ***K*** *– overall heat-transfer coefficient of the container [W/m²·K],* ***m*** *– mass of cargo inside the container[t],* t_{kr} *– critical temperature[ºC],* t_p *– recommended temperature for transport of pears [ºC], acc. [9]*

In the case of 40' container rate of cargo temperature rise is somewhat lower because of a greater mass of cargo. In Fig. 6 are presented results of calculations of rise of temperature of pears contained in the 40' container cut-off from the electricity supply source.

Similar situation can be observed in the case of cargo cooling process at a very low ambient temperature (Fig. 7). The container filled with grapes, left without electricity supply in the ambient temperature of -20 ºC, is very fast cooled down. Just after 12÷24 h the cargo may appear frozen through. Moreover, in contrast to the case of bananas, consequences of the situation are disastrous as frozen grapes leave their commercial merits [6]. In the case of opening the gate of the container the above mentioned periods would be even shorter, i.e. risk level of cargo quality loss rises even more.

The results presented in Fig. 5, 6, and 7, were obtained under the simplifying assumption on uniformity of temperature

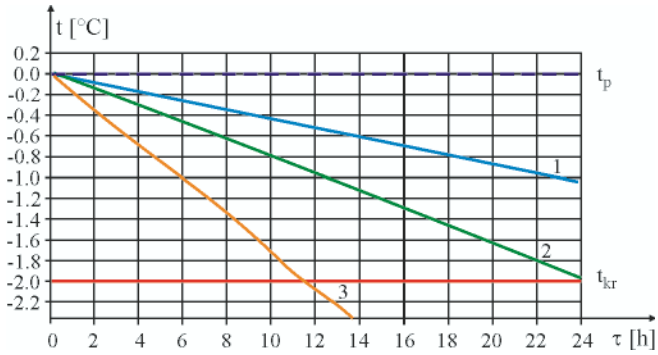

1 – t_{ot} = -20 ºC ; K =0.4 W/m² K ; m = 10 t ; no insolation
2 – t_{ot} = -20 ºC ; K =0.7 W/m² K ; m = 10 t ; no insolation
3 – t_{ot} = -20 ºC ; K =0.7 W/m² K ; m = 5 t ; no insolation

Fig. 7. *Rate of rise of temperature of the cargo (grapes) contained in the reefer container cutt-off from electricity supply source during its storage on sea port store place.* ***t*** *– mean temperature of cargo (grapes) in the reefer container [ºC],* ***τ*** *- period of cutting-off the container from electricity supply source [h],* t_{ot} *– ambient temperature of the container [ºC],* ***K*** *– overall heat-transfer coefficient of the container [W/m²·K],* ***m*** *– mass of cargo inside the container [t]* t_{kr} *– freezing temperature of grapes (critical temperature) [ºC],* t_p *– recommended temperature for transport of grapes [ºC]*

distribution over whole volume of the container. When the container is cut-off from the electricity supply source the fans which have to ensure the above mentioned uniformity, are also switched off, hence the temperature field inside the container becomes very non-uniform, especially in the case of rise of temperature of cargo, i.e. when $t_{ot} > t_p$. Heating the container from the top by sunshine makes natural convection of the air through the gaps between stocks of cartboard boxes placed on pallets, difficult (Fig. 8). As a result, the outer layers of cartboard boxes full of cargo (e.g. bananas), marked red and orange, have a higher temperature than those placed in the middle, and the calculated delay of heating the inner cartboard boxes as compared with the outer ones amounts from 4 h to 8 h. Taking into account the phenomenon, one can assume, for doing more precise calculations, that during the first 6 ÷ 10 h after cut-off the container from the electricity supply the whole outer heat flux is absorbed by the outer layers of cartboard boxes and does not reach their inner layers.

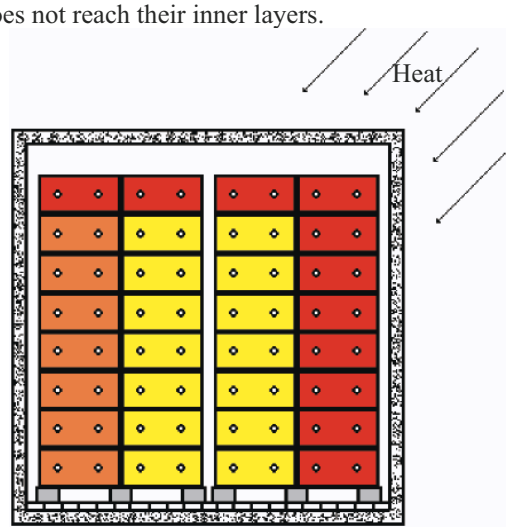

Fig. 8. *Schematic diagram of arrangement of cartboard boxes filled with bananas in the reefer container, to be used in calculations of heat balance with taking into account non-uniformity of temperature inside the container*

The calculation results where the temperature non-uniformity inside the container has been taken into account, are presented in Fig. 9. Like previously, for the calculations the standard stowage of 20' container: 10 pallets each loaded

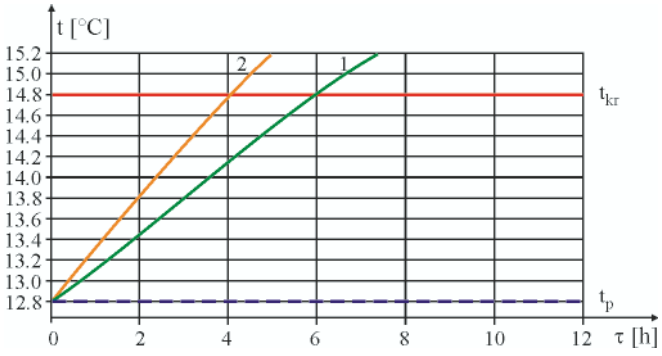

1 – t_{ot} = +35ºC ; K = 0.4 W/m² K ; m = 8.64 t ; no insolation
2 – t_{ot} = +35ºC ; K = 0.7 W/m² K ; m = 8.64 t ; no insolation

Fig. 9. *Rate of rise of temperature of the cargo (bananas) in the upper layer of cartboard boxes (marked red in Fig. 8) inside the reefer container cutt-off from electricity supply source, with taking into account temperature non-uniformity in its interior.* ***t*** *– mean temperature of the cargo (bananas) in a selected layer of cartboard boxes in the reefer container [ºC],* ***τ*** *- period of cutting-off the container from electricity supply source [h],* t_{ot} *– ambient temperature of the container [ºC],* ***K*** *– overall heat-transfer coefficient of the container [W/m²·K],* ***m*** *– mass of cargo inside the container [t],* t_{kr} *– critical temperature at which ripening process of bananas starts [ºC],* t_p *– recommended temperature for transport of bananas [ºC]*

with 48 cartboard boxes filled with 18 kg of bananas each,was assumed. Already within 4 ÷ 6 h after cutting-off the container from the electricity supply, temperature of bananas in the outer cartboard boxes was higher than allowable. Hence, to avoid loss of cargo quality the period of cutting-off the container from the electricity supply source should be not greater than 4 h. The presented results are convergent with the results of experiments on cooling non-uniformity of bananas in ship's hold [12].

In the remaining calculation examples the taking into account of the temperature non-uniformity inside the container led to the period of reaching the critical temperature by outer layers of cartboard boxes 2 ÷ 2.5 times shorter as compared with that obtained in the preceding calculations.

SUMMARY

The cutting-off of reefer container from electricity supply source, independing on its cause, should be considered a serious extraordinary situation which can quickly lead to loss of quality merits of refrigerated cargoes. On number and period of the cutting-offs an essential influence has a way of servicing the reefer container and sequence of servicing operations realized in sea port.

Below, a few recommendations for the servicing of reefer containers in sea ports are proposed:

- Sensitivity of refrigerated cargo to temeperature changes should be crucial criterion in designing its servicing chains. It should be tried to shorten the periods of cutting-off the container from electricity supply source, as much as possible.
- To the servicing of loaded reefer containers in ports to apply the following servicing chain is not recommended: unloading, storing on quay, and next loading it onto a transport vehicle, transporting over port area, veterinary control, and moving it at least onto a store place. The so designed chain is characteristic of an extended period of container's cutting-off from electricity supply source.
- If the servicing of reefer containers is carried out in summer (container's refrigerating unit operates according to refrigeration mode) then the port servicing chain should be designed and realized so as the operations associated with cutting-off the container from electricity supply source to be realized during the hours of the daily lowest ambient temperature.
- If the servicing of reefer containers is carried out in winter at mean ambient temperature lower by more than 10 ºC from transport temperature (container's refrigerating unit operates according to heating mode) then the operations associated with cutting-off the container from electricity supply source should be realized during the hours of the daily highest ambient temperature, and any control of the container, associated with opening its gate on store place, should be avoided.
- At lack of the electricity supply to the container filled with non-ventilated *frozen* cargo, only the temperature inside the container changes and in consequence that of cargo too. And, in the case of *refrigerated* cargoes, namely fruits and vegetables, apart from temperature changes, air exchange becomes impossible (external and internal ventilation), that leads to a higher risk level of loss of cargo quality. Containers filled with such cargoes should be specially carefully serviced by port personnel.
- Reefer containers and their port terminals should be equipped with devices for remote transmission / reception and processing of current information on climatic conditions inside the containers.

This paper presents only certain typical situations which may lead to loss of quality of refrigerated cargo transported in reefer containers. In order to perform a comprehensive analysis of simultaneous influence of various risk factors in particular servicing chains of the reefer container in port, to apply appropriate mathematical tools is necessary. In the Chair of Logistics and Transport Economy, Szczecin University of Technology, reserch is carried out on application of fuzzy logic to the problem in question; their results will be published in the future. The taking into account of all risk factors in planning the operations of servicing the refrigerated cargoes in port will make it possible to minimize probability of occurrence of extraordinary situations and this way to improve quality of functioning the cold chain.

BIBLIOGRAPHY

1. Bonca Z., Dziubek R.: *Construction and operation of reefer containers* (in Polish), WSM (Gdynia Maritime University), Gdynia, 1994
2. *Container Handbook. Cargo loss prevention - information from German marine insurers*, GDV, Berlin, 2007
3. The journal „*Magazyn portowy*" (Port store), Szczecin, 2000 ÷ 2007
4. Filina L., Filin S.: *Some problems of overload and storage of refrigeration containers in the port territory*, Archives of Transport, vol. 16, issue 1, Warsaw, 2004
5. Filina L.: *Methods of rationalization of servicing the containerized refrigerated cargoes in sea ports with application of fuzzy logic theory* (in Polish), Doctor's thesis, Szczecin, 2007
6. Gruda Z., Postolski J.: *Freezing the food products* (in Polish), WNT (Scientific Technical Publishing House), Warszawa, 2000
7. Internal materials of ports Szczecin-Świnoujście, Gdańsk, Gdynia
8. Semenov I. N.: *Risk management in maritime economy* (in Polish), Vol. I, Szczecin 2003
9. Studziński A.: *Operation of refrigerated ships* (in Polish), Trademar, Gdynia, 2005
10. Zakrzewski B., Filin S., Konieczny P.: *An analysis of energy consumption in refrigerated cargo sea transport.* Polish Maritime Research, no. 4, 2000, Gdańsk
11. Алмаши Э., Эрдели Л., Шарой Т.: *Быстрое замораживание пищевых продуктов* (in Russian). Лег. и пищ. промышленность, 1981
12. Стефанович В.В., Комарницкий Б.В.: *Системы охлаждения судовых рефрижераторных помещений* (in Russian). Судостроение, Ленинград, 1984
13. *Транспортировка и хранение тропических плодов* (in Russian), Под ред. И.Г.Чумака. ДП «Рефпринтинфо», Одесса, 2004
14. Филина Л.С. Филин С.О.: *Организация дозревания и транспортировки бананов на конечных стадиях холодильной цепи*, Холодильный бизнес, № 2, 2002, с.20-22
15. Чижов Г.Б.: *Теплофизические процессы в холодильной технологии пищевых продуктов* (in Russian). М.: Пищевая промышленность, 1979.

CONTACT WITH THE AUTHORS

Lyudmyla Filina, Ph. D.
Sergiy Filin, Prof.
Faculty of Marine Technology
Szczecin University of Technology
AL. Piastów 41,
71-065 Szczecin, POLAND
e-mail: lufilina@ps.pl

The Ship Handling Research and Training Centre at Ilawa is owned by the Foundation for Safety of Navigation and Environment Protection, which is a joint venture between the Gdynia Maritime University, the Gdansk University of Technology and the City of Ilawa.

Two main fields of activity of the Foundation are:

- Training on ship handling. Since 1980 more than 2500 ship masters and pilots from 35 countries were trained at Iława Centre. The Foundation for Safety of Navigation and Environment Protection, being non-profit organisation is reinvesting all spare funds in new facilities and each year to the existing facilities new models and new training areas were added. Existing training models each year are also modernised, that's why at present the Centre represents a modern facility perfectly capable to perform training on ship handling of shipmasters, pilots and tug masters.

- Research on ship's manoeuvrability. Many experimental and theoretical research programmes covering different problems of manoeuvrability (including human effect, harbour and waterway design) are successfully realised at the Centre.

The Foundation possesses ISO 9001 quality certificate.

Why training on ship handling?

The safe handling of ships depends on many factors - on ship's manoeuvring characteristics, human factor (operator experience and skill, his behaviour in stressed situation, etc.), actual environmental conditions, and degree of water area restriction.

Results of analysis of CRG (collisions, rammings and groundings) casualties show that in one third of all the human error is involved, and the same amount of CRG casualties is attributed to the poor controllability of ships. Training on ship handling is largely recommended by IMO as one of the most effective method for improving the safety at sea. The goal of the above training is to gain theoretical and practical knowledge on ship handling in a wide number of different situations met in practice at sea.

For further information please contact:
The Foundation for Safety of Navigation and Environment Protection

Head office:
36, Chrzanowskiego street
80-278 GDAŃSK, POLAND
tel./fax: +48 (0) 58 341 59 19

Ship Handling Centre:
14-200 IŁAWA-KAMIONKA, POLAND
tel./fax: +48 (0) 89 648 74 90
e-mail: office@ilawashiphandling.com.pl
e-mail: office@portilawa.com

GDANSK UNIVERSITY OF TECHNOLOGY

is the oldest and largest scientific and technological academic institution in the Pomeranian region. The history of Gdansk University of Technology is marked by two basic dates, namely: October 6, 1904 and May 24, 1945.

The first date is connected with the beginning of the technical education at academic level in Gdansk. The second date is connected with establishing of Gdansk University of Technology, Polish state academic university. Gdansk University of Technology employ 2,500 staff, 1,200 whom are academics. The number of students approximates 20,000, most of them studying full-time. Their career choices vary from Architecture to Business and Management, from Mathematics and Computer Science to Biotechnology and Environmental Engineering, from Applied Chemistry to Geodesics and Transport, from Ocean Engineering to Mechanical Engineering and Ship Technology, from Civil Engineering to Telecommunication, Electrical and Control Engineering. Their life goals, however, are much the same - to meet the challenge of the changing world. The educational opportunities offered by our faculties are much wider than those of other Polish Technical universities, and the scientific research areas include all of 21st Century technology. We are one of the best schools in Poland and one of the best known schools in Europe – one that educates specialists excelling in the programming technology and computer methods used in solving complicated scientific, engineering, organizational and economic problems.

THE FACULTY OF OCEAN ENGINEERING AND SHIP TECHNOLOGY

The Faculty of Ocean Engineering and Ship Technology (FOEST) as the only faculty in Poland since the beginning of 1945 has continuously been educating engineers and doctors in the field of Naval Architecture and Marine Technology.

The educational and training activities of FOEST are supported by cooperation with Polish and foreign universities, membership in different international organizations and associations, as well as participation in scientific conferences and symposia. Hosting young scientists and students from different countries is also a usual practice in FOEST.

The activities of Faculty departments are related to: mechanics and strength of structures, hydromechanics, manufacturing, materials and system quality, power plants, equipment and systems of automatic control, mostly in shipbuilding, marine engineering and energetic systems.

FOEST is a member of such organizations like WEGEMT; The Association of Polish Maritime Industries and the co-operation between Nordic Maritime Universities and Det Norske Veritas. The intensive teaching is complemented and supported by extensive research activities, the core of which is performed in close collaboration between FOEST staff and industry. We take great care to ensure that the applied research meet both the long term and short term needs of Polish maritime industry. FOEST collaborates with almost all Polish shipyards. Close links are maintained with other research organizations and research institutions supporting the Polish maritime industry, such as Ship Design and Research Centre and Polish Register of Shipping, where several members of the Faculty are also members of the Technical Board.

The Faculty of Ocean Engineering and Ship Technology is a unique academic structure, which possesses numerous highly qualified and experienced staff in all above mentioned specific research areas. Moreover, the staff is used to effective co-operation and exchange of ideas between specialists of different detailed areas. This enables a more integrated and comprehensive treatment of research and practical problems encountered in such a complicated field of activity as naval architecture, shipbuilding and marine engineering.

The staff of the Faculty has strong international links worldwide, being members or cooperating with international organizations like International Maritime Organization IMO, International Towing Tank Conference ITTC, International Ship and Offshore Structures Congress ISSC, International Conference on Practical Design of Ship and other floating Structures PRADS just to name a few.

GDANSK UNIVERSITY OF TECHNOLOGY
Faculty of Ocean Engineering and Ship Technology
11/12 Narutowicza Street, 80-952 Gdansk, Poland
Tel (+48) 58 347 1548 ; Fax (+48) 58 341 4712
e-mail: sekoce@pg.gda.pl

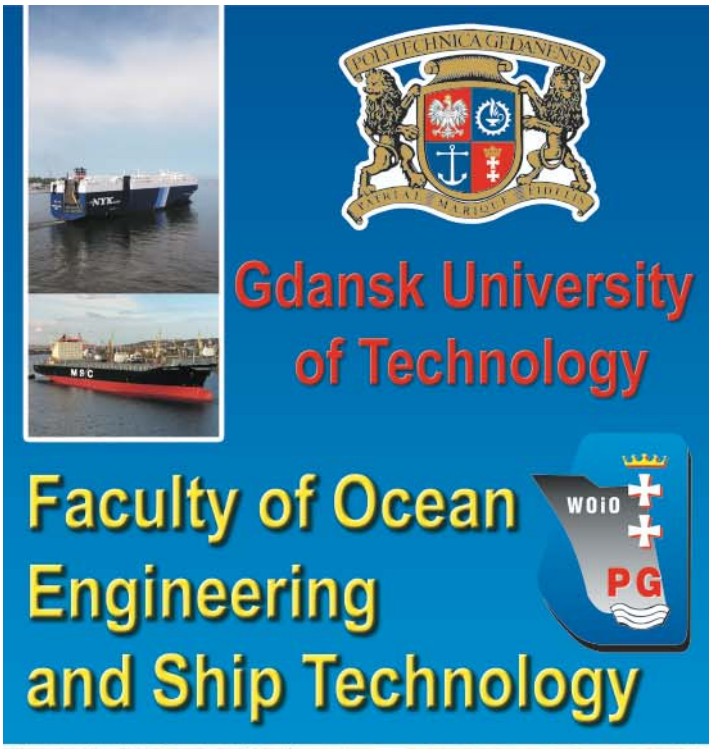

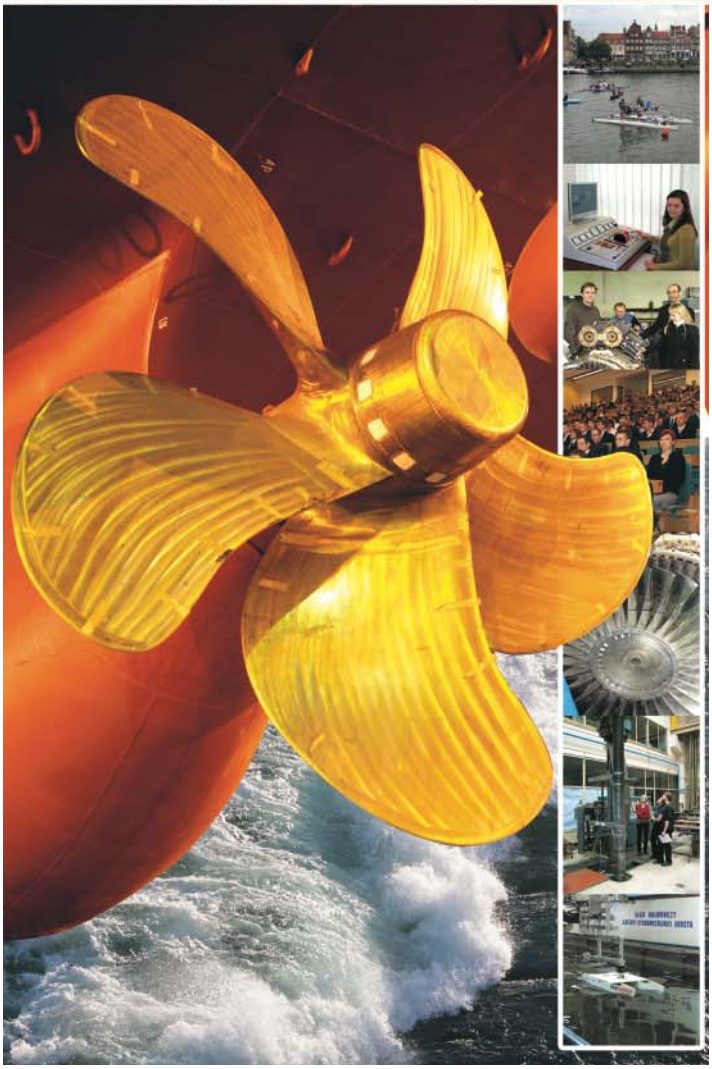

www.oce.pg.gda.pl